INFORMATION TO USERS

This manuscript has been reproduced from the microfilm master. UMI films the text directly from the original or copy submitted. Thus, some thesis and dissertation copies are in typewriter face, while others may be from any type of computer printer.

The quality of this reproduction is dependent upon the quality of the copy submitted. Broken or indistinct print, colored or poor quality illustrations and photographs, print bleedthrough, substandard margins, and improper alignment can adversely affect reproduction.

In the unlikely event that the author did not send UMI a complete manuscript and there are missing pages, these will be noted. Also, if unauthorized copyright material had to be removed, a note will indicate the deletion.

Oversize materials (e.g., maps, drawings, charts) are reproduced by sectioning the original, beginning at the upper left-hand corner and continuing from left to right in equal sections with small overlaps.

Photographs included in the original manuscript have been reproduced xerographically in this copy. Higher quality 6" x 9" black and white photographic prints are available for any photographs or illustrations appearing in this copy for an additional charge. Contact UMI directly to order.

Bell & Howell Information and Learning
300 North Zeeb Road, Ann Arbor, MI 48106-1346 USA

UMI®
800-521-0600

SAFETY CHARACTERISTICS OF A SUSPENDED-PELLET FISSION REACTOR SYSTEM

By

DAVID ROSS KINGDON, B.Eng., M.Eng.

A Thesis

Submitted to the School of Graduate Studies

in Partial Fulfilment of the Requirements

for the Degree

Doctor of Philosophy

McMaster University

SAFETY CHARACTERISTICS OF A SUSPENDED-PELLET FISSION SYSTEM

DOCTOR OF PHILOSOPHY (1998) McMaster University
(Engineering Physics) Hamilton, Ontario

TITLE: Safety Characteristics of a Suspended-Pellet Fission Reactor System

AUTHOR: David Ross Kingdon, B.Eng., M.Eng. (McMaster University)

SUPERVISOR: Professor A.A. Harms

NUMBER OF PAGES: xxv, 197

ABSTRACT

A new fission reactor system with passive safety characteristics to eliminate the occurrence of loss-of-coolant accidents, reduce reactivity excursion effects, and which also provides for closure of the nuclear fuel cycle through on-site spent fuel management is examined. The concept uses multi-coated fuel pellets which are suspended by an upward moving coolant in vertical columns of the reactor core and electro-refining elemental separation to remove selected fission products prior to actinide recycling.

The possibility of fuel melt following a loss-of-coolant is avoided as a decrease in coolant flow results in the removal of fuel from the core through the action of gravity alone. Average fluid velocities in the columns which are necessary to suspend the pellets are calculated and found to be consistent with the necessary heat extraction to yield ~1-10 MW_{th} per column. The total output power of such suspended pellet-type reactors is compared to the power necessary to provide the suspending fluid flow, yielding favourable ratios of ~10^2 - 10^3.

The reduction of reactivity excursion tendencies is envisaged through an ablative layer of material in the pellets which sublimates at temperatures above normal operating conditions. In the event of a power or temperature increase the particles fragment and thereby change their hydrodynamic drag characteristics, thus leading to fuel removal from the core by elutriation. Comparison of nuclear-to-thermal response times and elutriation rates for limiting power transients indicate that the present design assists in reactivity excursion mitigation.

Abstract

Closure of the nuclear fuel cycle is attained through a spent fuel management strategy which requires only on-site storage of a fraction of the fission products produced during reactor operation. Electro-refining separation of selected fission products combined with complete actinide recycling yields no isolation of plutonium or highly enriched uranium during the procedure. The out-of-core waste stream has a significantly reduced radioactivity, volume and lifetime compared to the once-through waste management strategy and thus provides an alternative to long-term geological disposal of fission reactor wastes.

The Pellet Suspension Reactor concept possesses some unique operating characteristics and, additionally, is shown to be similar to conventional fission reactors in terms of common performance features.

ACKNOWLEDGEMENTS

This work arose, in part, from a 1992-93 graduate course given in the Department of Engineering Physics at McMaster University by Dr. A.A. Harms. The initial efforts of the other graduate students in the course, in particular J. Whitlock and W. Fundamenski, are gratefully acknowledged, as is Dr. Harms' subsequent direction and encouragement as my Ph.D. supervisor. Fellow researchers Dr. A.N. Kornilovsky and Dr. V.A. Khotylev provided valuable assistance and suggestions, as did the members of my Ph.D. supervisory committee, Dr. W.J. Garland and Dr. J. Vlachopoulos. Advice on ablative materials and their temperature dependence has been provided by Dr. G.P. Johari and is also gratefully acknowledged.

Financial assistance from the Natural Science and Engineering Research Council, Ontario Ministry of Education and Training, National Chapter of Canada IODE, Canadian Fusion Fuels Technology Project, and McMaster University is sincerely appreciated.

To the few family and friends who,
despite claiming ignorance to
most of this, trusted me
to do it nonetheless.

TABLE OF CONTENTS

LIST OF FIGURES

List of Figures

List of Figures

LIST OF TABLES

LIST OF SYMBOLS

a	subscript to designate the ablator layer in a three-layer pellet
a_{He}	speed of sound in helium gas *[l t^{-1}]* *
A	cross-sectional area *[l^2]*; ampere; isotope mass number
A_s	surface area *[l^2]*
A_{total}	total isotopic mass of a fuel compound
Ac	actinium
Ag	silver
Al	aluminum
AlF_3	aluminum trifluoride
Am	americium
Ar	argon
As	arsenic
At	astatine
Ba	barium
Be	beryllium
Bi	bismuth
Bk	berkelium
Bq	Becquerel
Br	bromine
BISO	Bi-ISOtropic coating structure on a spherical fuel particle
BWR	Boiling (light) Water Reactor
c	subscript to designate the collision-resistant layer in a three-layer pellet
cm	centimetre
C	carbon; dimensionless measure of the degree of particulate or aggregative fluidization
C_i , i = 1-7	constants in the derivation of the Ergun Equation
C_p	specific heat capacity at constant pressure *[l^2 t^{-2} T^{-1}]*
$C_{p,He}$	specific heat capacity of helium at constant pressure *[l^2 t^{-2} T^{-1}]*
C_D	drag co-efficient for spheres
Ca	calcium
Cd	cadmium
Ce	cerium
Cf	californium
Cl	chlorine
Cm	curium
Cs	cesium
CANDU	CANada Deuterium Uranium (pressurized heavy water reactor)

*for relevant quantities, unit follow the definition *[italicized and in square brackets]*

CO_2 carbon dioxide
°C degree Celsius

d effective pellet diameter *[l]*
d_p mean outer pellet diameter *[l]*
$d_{p,x}$ diameter at outer edge of layer x *[l]*
$d_{p,0}$ non-fissile inner core (in pellets) diameter *[l]*
$d_{p,1}$ fissile material (in pellets) outer diameter *[l]*
$d_{p,2}$ ablator layer (in pellets) outer diameter *[l]*
D_c column diameter *[l]*
$D_{c,in}$ column diameter at the base of the core region *[l]*
$D_{c,lower}$ column diameter below the lower constriction boundary *[l]*
$D_{c,upper}$ column diameter above the upper expansion boundary *[l]*
$D_{c,x}$ column diameter at position x *[l]*
Dy dysprosium
D_2O heavy water
DBA Design Basis Accidents

eV electron-volt (1.6×10^{-19} J)
E_n neutron energy $[m\ l^2\ t^{-2}]$
E_{pump} pump energy $[m\ l^2\ t^{-2}]$
Er erbium
Es einsteinium
Eu europium
ECC Emergency Core Coolant
EPRI Electric Power Research Institute

f subscript to designate the fuel core in a three-layer pellet
f_p friction factor in a pipe containing fluidized particles
fi fissile nucleus
F fluorine
F_D drag force $[m\ l\ t^{-2}]$
Fm fermium
Fr francium
Fr_{mf} Froude number at the minimum fluidization velocity (inertial force / gravitational force = $U^2_{mf} / g \cdot d_p \cdot \phi_s$)
FLUBER FLUidized Bed Experimental Reactor
FP Fission Product

g acceleration due to gravity $[l\ t^{-2}]$; gram
Ga Galileo Number ($d^3 \cdot \rho_f^2 \cdot g / \mu_f^2$); gallium
Gd gadolinium
Ge germanium
GCFR Gas-Cooled Fast (breeder) Reactor
GW_e gigawatts-electrical

h heat transfer coefficient $[m\ t^{-3}\ T^{-1}]$
hr hour
H column height *[l]*; hydrogen

He	helium
Ho	holmium
H_2O	light water
HEU	Highly Enriched Uranium
HTGR	High Temperature Gas(-cooled) Reactor
ΔH_L	change in fluid head or fluid head loss *[l]*
i	counting index; *electric current*
I	iodine
In	indium
IAEA	International Atomic Energy Agency
J	joule
k, k(r)	neutron multiplication factor; thermal conductivity (constant or radially dependent) *[m l t^{-3} T^{-1}]*
k_{eff}	effective neutron multiplication factor (including neutron leakage)
k_{He}	thermal conductivity of helium *[m l t^{-3} T^{-1}]*
$k_1=k_f$	thermal conductivity of fuel material *[m l t^{-3} T^{-1}]*
$k_2=k_a$	thermal conductivity of ablator material *[m l t^{-3} T^{-1}]*
$k_3=k_c$	thermal conductivity of collision-resistant material *[m l t^{-3} T^{-1}]*
kg	kilogram
kW	kilowatt
K	kelvin; potassium
$K_{i,e}^*$	elutriation constant *[m l^{-2} t^{-1}]*
Kr	krypton
KCl	potassium chloride
Δk_{eff}	change in the effective neutron multiplication factor
l	*length*
ℓ	effective neutron lifetime *[t]*
L	length *[l]*; litre
L_{mf}	packed or fluidized bed height at the minimum fluidization velocity *[l]*
La	lanthanum
Li	lithium
LiCl	lithium chloride
Lr	lawrencium
Lu	lutetium
LMFR	Liquid Metal Fast (breeder) Reactor
LOCA	Loss-Of-Coolant Accident
LWR	Light Water Reactor
m	*mass*; metre
$\dot{m}$	mass flow rate *[m t^{-1}]*
$m_{atom,i}$	mass of an i-type atom *[m]*
m_b	total mass of pellets in a bed or column *[m]*
m_c	mass of coolant associated with one pellet in power ratio analyses *[m]*
m_i	mass of i-type material *[m]*
mm	millimetre

Md mendelevium
MeV mega-electron-volt
Mg magnesium
Mo molybdenum
Mv density ratio $(\rho_s - \rho_f) / \rho_f$
MOX Mixed-Oxide Fuel
MPa megapascal
MW_{th} megawatts-thermal

n neutron
$N_{f,p}$ fissile material (in pellets) atom density $[l^{-3}]$
N_i i-type material atom density $[l^{-3}]$
N_i^* total number of i-type atoms
$N_{i,max}$ maximum i-type material atom density (for pure i-type medium) $[l^{-3}]$
N_n neutron number density $[l^{-3}]$
N_p number of pellets per column
Na sodium
Nb niobium
NbC niobium carbide
Nd neodymium
No nobelium
Np neptunium
^{239}Np neptunium-239
Nu Nusselt number (hL / k)
$N(A_i)$ number of atoms of species i with isotopic mass number A
NERVA Nuclear Engine for Rocket Vehicle Application
NRC Nuclear Regulatory Commission

ORIGEN Oak Ridge Isotope GENeration

p pressure $[m\ l^{-1}\ t^{-2}]$
p_{in} pressure at the bottom or inlet of a core column $[m\ l^{-1}\ t^{-2}]$
p_{out} pressure at the top or outlet of a core column $[m\ l^{-1}\ t^{-2}]$
p_1, p_2 pressure at points 1 and 2 $[m\ l^{-1}\ t^{-2}]$
P power $[m\ l^2\ t^{-3}]$
P_{fi} fission power $[m\ l^2\ t^{-3}]$
P_{in} input power $[m\ l^2\ t^{-3}]$
P_{out} output power $[m\ l^2\ t^{-3}]$
P_{pump} pumping power $[m\ l^2\ t^{-3}]$
P_{th} thermal power $[m\ l^2\ t^{-3}]$
P_1, P_2 fission products
Pa protactinium
Pb lead
Pd palladium
Pm promethium
Pr Prandtl number; praseodymium
Pr_{He} Prandtl number of helium
Pu plutonium
^{239}Pu plutonium-239

PuO_2 plutonium dioxide
PyC pyrolytic carbide
PHWR Pressurized Heavy Water Reactor
PSR Pellet Suspension Reactor
PUREX Plutonium URanium EXtraction
PWR Pressurized (light) Water Reactor
Δp pressure change

Q_{fi} average energy release per fission event *[m l² t⁻²]*
Q_{fi}^{*} recoverable energy per fission event *[m l² t⁻²]*

r radius *[l]*; radial direction
r_1 fissile material outer radius *[l]*
r_2 ablator layer outer radius *[l]*
r_3 outer pellet radius *[l]*
R column radius *[l]*
R_i removal rate of particles of size i *[m t⁻¹]*
Ra radium
Rb rubidium
Re Reynolds number (inertial force / viscous force = $\rho UL / \mu$)
Re_{mf} Reynolds number of a particle at U_{mf} ($\rho_f U_{mf} d / \mu_f$)
Re_D Reynolds number for fluid flow in a column of diameter D_c ($\rho_f U D_c / \mu_f$)
Rh rhodium
Ru ruthenium
RE Rare-Earth
RSICC Radiation Safety Information and Computational Centre

s second
Sb antimony
Se selenium
Si silicon
SiC silicon carbide
Sm samarium
Sn tin
Sr strontium
SAS Safety Analysis Sequence
SCALE Standardized Computer Analyses for Licensing Evaluation

t *time*
T, T(r), T(r,t) *temperature* (constant, radially, or radially and time dependent)
T_{in} coolant temperature at the core inlet *[T]*
T_{melt} melting temperature *[T]*
T_{out} coolant temperature at the core outlet *[T]*
T_s surface temperature of a pellet *[T]*
T_{He} helium temperature *[T]*
$T_{He}(z)$ helium temperature at height z *[T]*
$T_{He}(0)$ helium temperature at height z = 0 *[T]*
T_∞ temperature of a fluid well beyond the boundary layer *[T]*
$T_1=T_f$ fuel temperature *[T]*

$T_2=T_a$ ablator temperature *[T]*
$T_3=T_c$ collision-resistant material temperature *[T]*
Ta tantalum
Tb terbium
Tc technetium
Te tellurium
Th thorium
ThC_2 thorium dicarbide
ThO_2 thorium dioxide
Tm thulium
TDH Transport Disengagement Height *[l]*
TMI Three Mile Island
TRISO TRi-ISOtropic coating structure on a spherical fuel particle
TRU TRans-Uranic
ΔT temperature change *[T]*
ΔT_{He} change in helium temperature *[T]*

U uranium; superficial fluid velocity *[l t^{-1}]*
U_{in} superficial fluid velocity at the bottom of the core region *[l t^{-1}]*
U_{lower} superficial fluid velocity below the lower constriction boundary *[l t^{-1}]*
U_{mf} minimum fluidization velocity *[l t^{-1}]*
U_{out} superficial fluid velocity at the top of the core region *[l t^{-1}]*
U_{ter} terminal velocity *[l t^{-1}]*
$U_{ter,i}$ terminal velocity of particles of size i *[l t^{-1}]*
U_{upper} superficial fluid velocity above the upper expansion boundary *[l t^{-1}]*
U_x superficial fluid velocity at location x *[l t^{-1}]*
U_{He} helium velocity *[l t^{-1}]*
^{234}U uranium-234
^{235}U uranium-235
^{238}U uranium-238
^{239}U uranium-239
UC uranium carbide
UC_2 uranium dicarbide
UO_2 uranium dioxide

v_n neutron speed *[l t^{-1}]*
v_n' energy dependent neutron speed *[l t^{-1}]*
V volume *[l^3]*; volt *[m l^2 t^{-3} I^{-1}]*
V_c column volume *[l^3]*
$V_{f,p}$ volume of fissile material in a particle *[l^3]*
V_i volume of i-type material *[l^3]*
V_o initial volume *[l^3]*
V_p pellet volume *[l^3]*

w, w(t), w(r,t) fission power density (constant, time, or radially and time dependent) *[m l^{-1} t^{-3}]*
w(z) axially dependent power density *[m l^{-1} t^{-3}]*
w(0) fission power density at time t = 0 *[m l^{-1} t^{-3}]*
W watt; peak value of axially dependent power density profiles *[m l^{-1} t^{-3}]*

List of Symbols

x_i	mass fraction of particles of size i in a particle bed or column
$x_{i,l}$	mass fraction of particles of size i leaving a particle bed through elutriation
$x_{i,o}$	initial mass fraction of particles of size i in a particle bed or column (at t = 0)
$x_{i,r}$	mass fraction of particles of size i remaining in a particle bed following losses due to elutriation
Xe	xenon
Y	yttrium
Yb	ytterbium
z	height in a column above the lower boundary *[l]*
z_1, z_2	height of points 1 and 2 *[l]*
Zn	zinc
Zr	zirconium
ZrC	zirconium carbide
ZrF_3	zirconium trifluoride
ZrF_4	zirconium tetrafluoride
ϵ	void fraction
ϵ_{mf}	void fraction at minimum fluidization velocity
η_{in}	input efficiency
η_{out}	output efficiency
μ	viscosity $[m\ l^{-1}\ t^{-1}]$
μ_f	fluid viscosity $[m\ l^{-1}\ t^{-1}]$
μ_{He}	helium viscosity $[m\ l^{-1}\ t^{-1}]$
μm	micrometre
ν	average number of neutrons released per fission event
ξ	fissile enrichment fraction
ρ	reactivity; mass density $[m\ l^{-3}]$
ρ_{eff}	effective mass density of a multi-layer pellet $[m\ l^{-3}]$
ρ_f	mass density of fluid $[m\ l^{-3}]$
ρ_i	mass density of pure i-type material $[m\ l^{-3}]$
ρ_s	mass density of solid $[m\ l^{-3}]$
ρ_{He}	helium mass density $[m\ l^{-3}]$
σ_{fi}	microscopic fission cross section $[l^2]$
σ_{fi}'	energy dependent microscopic fission cross section $[s^2\ m^{-1}]$
τ	reactor period *[t]*
ϕ_n	neutron flux $[l^{-2}\ s^{-1}]$
ϕ_s	pellet sphericity

Chapter 1

Introduction and Context

The generation of electrical and thermal energy for civilian use through the fissioning of heavy nuclei such as uranium-235 (^{235}U) has existed for approximately 40 years. During the past few decades, however, a number of events have occurred which have substantially inhibited the original projections for the expansion of the fission energy enterprise. In fact, the view often adopted is that the global nuclear power industry may not be able to continue to grow, or even maintain its present size, without significant change. This introductory chapter sketches some of the reasons for these circumstances and places into context one potential path that could be pursued in the future -- a new reactor core concept and fuel management strategy. Selected considerations of this reactor system constitute the focus of this work.

1.1 Fission Energy Fundamentals

The fissioning, or splitting, of selected heavy nuclei was first reported by Otto Hahn and Fritz Strassman late in 1938. A few weeks later, the correct theoretical explanation -- and the naming of the process -- was provided by Lise Meitner and Otto Frisch (Kovan 1992). Fission can occur spontaneously in some nuclides, or is the result of an interaction between the nuclide and a neutron. The dominant process in most of today's nuclear power plants is fission induced by a thermal neutron,

conveniently represented by

$$n + fi \rightarrow \nu n + P_1 + P_2 + \ldots + Q_{fi} \,. \qquad (1.1)$$

Depending upon the energy of the incident neutron, n, and the type of fissile nucleus, fi, the average number of neutrons released per fission, ν, varies from approximately two to three. The resulting fission products or fragments, P_1 and P_2, along with neutrinos, gamma rays, and occasionally others are the important products from each event. The reaction Q-value, Q_{fi}, also depends upon the type of fissile nucleus and incident neutron energy, but typically varies from 190-200 MeV.

The neutrons emitted are of a much higher energy than those which commonly induce such fission and hence are slowed down with the use of a neutron moderating medium. Collisions between the high-energy neutrons and the nuclei of moderator materials, such as water or graphite, cause a reduction in neutron energies to thermal values. During this slowing down process some neutrons are inevitably lost from the fission domain due to leakage from the system and by parasitic capture in other nuclides. However, on average, one of the emitted neutrons remains to act as a chain carrier -- a neutron that induces another fission event in a properly configured reactor core so that the fission chain reaction continues as long as there is sufficient fuel present and the reaction is desired.

A fissile fuel arrangement in which the chain reaction continues unchanged is said to be critical. An assembly in which the neutron population decays over time is referred to as subcritical, while one in which it increases -- potentially without bound -- is termed supercritical. The neutron multiplication factor, k, is used for such neutron accounting, and is defined as the ratio of the number of neutrons in one "generation" to the number in the preceding "generation". Thus, a critical system has $k = 1$, while in a subcritical system $k < 1$ and in a supercritical system $k > 1$. A related quantity

is the reactivity, ρ, used to describe the relative deviation from criticality and defined by

$$\rho = \frac{k - 1}{k} . \qquad (1.2)$$

A further quantity of common utility in nuclear fission systems is the neutron flux, ϕ_n, which is the energy integrated product of the neutron number density, N_n, and the neutron speed, v_n.

The most common fissile isotope used in reactors today is ^{235}U. Uranium, as found in nature, consists of $\approx$ 0.7% ^{235}U, $\approx$ 99.3% ^{238}U and trace quantities of ^{234}U. Since ^{238}U is fissionable by high energy neutrons but acts primarily as a parasitic capturer of neutrons at thermal energies, this low fissile isotopic ratio is sufficient for only a few reactor systems to achieve criticality. It is often necessary to use higher ratios of ^{235}U to ^{238}U in which case it is increased through isotopic separation techniques. Uranium with its fissile content increased with respect to its natural form is said to be enriched, the enrichment, ξ, being the fraction of uranium atoms which are thermally fissile -- i.e. ^{235}U.

The two fission product nuclei P_1 and P_2 differ from one fission event to the next but have well established mass distributions for each fissile isotope (Duderstadt and Hamilton 1976). Some of these fission products, along with their radioactive decay daughters, are highly radioactive and are one of the main reasons for the need for stringent safety systems in nuclear facilities. Such systems are all ultimately designed to prevent the release of potentially dangerous fission products and other radioactive species to the biosphere by a series of barriers know collectively as containment.

These fission products, however, also carry the bulk of the energy released in nuclear fission in the form of kinetic energy, which manifests itself in the heating of

the nuclear fuel. The heat produced is generally conducted through the fuel elements to their surface where it is transported by convection into a liquid or gas primary coolant. Following transfer to a secondary coolant system, the heat is used to generate steam -- the end product in some systems -- which turns a turbine. Subsequently, the turbine is connected to an electrical generator to produce electricity.

Over time, the number of fissile nuclei in the core will decrease due to fuel burnup. This places limits on the length of time a reactor may operate between refuelling operations, depending also on the amount of fuel breeding which may occur. Fuel breeding is the transmutation of fertile nuclei in the reactor core, such as ^{238}U, into fissile nuclei like ^{239}Pu through neutron capture and subsequent radioactive decay, i.e.

$$n + {}^{238}U \rightarrow {}^{239}U \rightarrow {}^{239}Np \rightarrow {}^{239}Pu \,. \qquad (1.3)$$

Control and shutdown capabilities in nuclear reactors are often achieved through the use of control rods. These rods are composed of highly-neutron absorbing materials and when inserted into a reactor core reduce the number of neutrons available to propagate the chain reaction, thereby reducing the reaction rate or shutting down the reactor altogether. However, even when shut down, the fissile fuel continues to generate heat -- initially at a rate approximately 6-8% of the previous operating power immediately following a shutdown, and decreasing thereafter -- due to the radioactive decay of the many fission products produced while the reactor was operating. This decay heat must continue to be removed from the core to prevent the fissile material from overheating and possibly melting. Such a requirement will be referred to many times in subsequent chapters for if fuel melt occurs, the first and one of the most effective barriers to fission product release, i.e. the fuel compound itself, will have been breeched.

More detailed information about nuclear fission and power plants can be found in nuclear reactor textbooks such as Duderstadt and Hamilton (1976), Glasstone and Sesonske (1981), or Henry (1975).

1.2 Global Nuclear Power

At the end of 1997 there were approximately 430 operating nuclear power reactors in the world generating ≈350 GW_e, with about another 35 more units (≈30 GW_e) under construction (Nuclear News, March 1998). This amounts to approximately 6% of the globally installed commercial power generating capacity and about 17% of the world's electrical power, the remainder being supplied primarily by fossil fuels (coal, oil, and natural gas) and hydro-electric facilities. Despite its relatively rapid growth onto the global scene, nuclear fission's installed capacity -- and corresponding market share -- has levelled off in the past few years, Figure 1.1. With few new reactors being ordered or under construction, some projections indicate that the fraction of global electrical energy generated by nuclear fission plants may start to decrease shortly after the turn of the century.

The declining fortune of the civilian nuclear power industry has occurred for a variety of complex reasons. However, there are many arguments which suggest that nuclear fission should remain a part of the global power generation mix. The drawbacks of burning fossil fuels -- including the release of gases to the atmosphere which contribute to acid rain and the greenhouse effect -- are generally well known. Additionally, there are a limited number of sites for new hydro-electric facilities, commercial power production by nuclear fusion will not likely be realized until well into the next century, and other methods such as solar energy, wind or biomass appear unsuited to supply large base loads of electricity. It also appears that even with

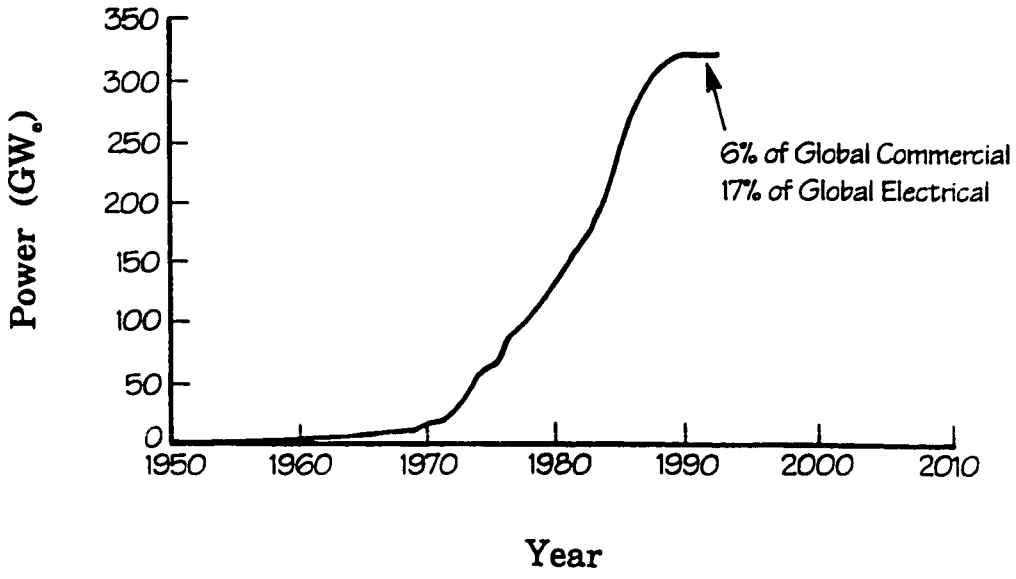

Figure 1.1: Time-history of the total installed electrical generating capacity of the world's nuclear power plants. (Based on data from Nuclear News.)

energy conservation measures, world-wide energy consumption will continue to grow -- primarily in developing nations as they industrialize -- necessitating that an effort be made to retain fission power as a portion of the world's future supply of electricity (Kugeler and Phlippen 1996). It will certainly not be the sole component of a global energy strategy, but can be a justifiable and important part of one. However, as mentioned, the declining interest in -- and public acceptability of -- nuclear power will likely continue to hamper such an effort.

1.3 Declining Acceptability

No attempt will be made here to completely explain the various factors that have contributed to the reduced support for nuclear fission as a means of civilian power generation or even to itemize them all; that task in itself is beyond the scope of this investigation. However, as a consequence of such reduced support, the nuclear power industry has undergone -- and continues to undergo -- significant changes since its beginnings years ago.

Civilian nuclear power emerged out of the Atoms-for-Peace initiative. At the First International Conference on Peaceful Uses of Atomic Energy in Geneva in 1955, approximately 100 proposed reactor types were judged "not obviously impractical" (Cowan 1990; United Nations 1956). Three years later, following the creation of the International Atomic Energy Agency (IAEA), there remained at least 12 reactor systems still being considered (United Nations 1958), including a Dutch proposal for a powder-in-suspension-type reactor (Kreyger et. al. 1958). However, political influences surrounding the Cold War, including the 1958 Euratom Accord which brought U.S. light water-moderated reactor technology to Europe, accelerated civilian nuclear power development such that it may have occurred too rapidly. There was

early recognition that gas-graphite and homogeneous reactor types being developed in England, France and other countries may have been better suited for civilian power production than the military-favoured light water types (Cowan 1990; Felix 1997), but generally there was insufficient time and effort devoted to all the reactor concepts initially identified before an optimal one was selected for the required task.

More recent influences on fission power include the lack of resolution of a waste storage or disposal strategy for spent nuclear fuel, and the view of some that there has been insufficient diligence in the implementation of the defence-in-depth approach to reactor safety. The defence-in-depth approach itself has also come under increased scrutiny from the "normal accidents" school of thought. Heightening regulatory requirements over the years have resulted in an increased number of engineered safety systems being a part of fission reactors. While intended to raise the level of safety at nuclear power plants, this increased redundancy can also increase the likelihood of an unforseen accident (Perrow 1984; Sagan 1993). The added interactive complexity between a system's components -- since redundant systems are often less independent than expected -- and the resulting more opaque safety setup increase the chances of a minor component failure causing a major system disruption in a previously unforseen manner. In addition, such systems tend to be operated "harder and faster", or in more adverse conditions due to the perception of enhanced safety. Both the Three Mile Island (TMI) and Chernobyl accidents can be characterized by the above, and are often cited as examples of "normal accidents" in complex, tightly coupled technological systems such as nuclear reactors (Perrow 1984; Sagan 1993).

Further, such interactive complexity can make testing of individual system components difficult, or can compromise other components during the tests. Complex safety systems are also prone to inadvertent or malicious operator error -- such as shutting one or more parts of the system off -- and are generally quite expensive to

install and maintain. This has contributed to the recognition that while nuclear energy has become more cost-competitive with other types of power generation, it is certainly more expensive than originally touted. Increased capital costs have also occurred due to lengthy siting procedures and thus longer construction times. The inclusion of indirect costs such as environmental effects could possibly help the nuclear fission option, especially when compared to fossil fuel burning, but no consensus has yet been reached on how to incorporate such factors.

Nuclear power plants operating in the world today all use rigid fuel elements bound within the reactor core, a concept which generally evolved from the military submarine programs of the 1940's and 1950's amidst the Cold War. The world's first power reactors were simply scaled-up versions of those originally designed for naval applications. This meant that characteristics crucial for submarine operation but unnecessary for terrestrial power plants -- such as being sufficiently compact to fit into the restrictive size of a submarine's hull, being able to deliver power for all orientations and movements, and being able to operate remotely for long periods of time -- were a part of the early designs, while others such as optimal configurations to avoid or eliminate possible accident scenarios were deemed less paramount. Thus, while safety was certainly a concern throughout the design and operation of all nuclear power systems, many of the fundamental concepts for today's reactors were not those demanded from a civilian safety perspective (Harms 1996). Since then, many safety systems and features have been added, first to render the reactors useful for civilian power production, and subsequently to comply with heightening safety regulations. However, concepts and designs centred on ensuring safe and reliable operation from the outset may have conceivably led to better choices for the industry.

Public opinion of the nuclear power industry has developed into a very powerful force of its own. It has been able to cancel plans, delay and stop construction,

and even remove plants from service (i.e. in Italy, Juhn and Kupitz 1996). Accidents like TMI and Chernobyl have also forced governments and utilities to fear the financial risks and economic consequences following such events. These are in addition to the potential human and environmental dangers not befitting what was initially touted as a cheap, safe and clean energy source. Above all, the perceived lack of sufficient safety at nuclear power plants by the general public appears to be the major stumbling block facing the nuclear industry today.

1.4 Evolution of a Technology

The evolution of nuclear power follows a fairly unique path when compared to other high-tech industries. For most advances in the technological realm -- which must be emphasized as being distinct from purely scientific cases -- changes and developments are brought about in response to a specific need. These needs today are rarely of a fundamental survival nature, but they must be satisfied if a greater level of comfort is to be achieved in a society's lifestyle. A simple example of necessity bringing about technological change is the invention of the wheel to improve the transportation of people and goods centuries ago (Basalla 1988).

Once the necessity has been identified, an optimal solution -- as perceived at the time -- is selected from a diverse set of options, perhaps distinguished by a novel or revolutionary approach. However, equally often it is merely a continual set of minor changes to an existing product or system -- in a sense an evolutionary process -- which brings about the new technology. Nuclear generating stations, however, did not follow either the evolutionary or revolutionary paths alone.

For nearly every nation involved with nuclear reactors, the first considerations were military -- propulsion systems and in some cases the supply of weapons-grade

material (Cowan 1990). The first interest accelerated the development of light water-moderated reactors. There was initially little need for electricity generation by nuclear means, but there was considerable political influence and pressure to demonstrate a peaceful use of atomic energy following the atomic bombing of Hiroshima and Nagasaki in 1945. This was despite the common view that energy generation requirements could easily be satisfied by other fuels available at the time. While the U.S. military and civilian programs were considering several nuclear reactor types for future power needs, national prestige and security -- eg. the race to beat the Soviets -- also spurred rapid development in the area. The head start given to light water reactors by the military propulsion systems made them the obvious choice for a civilian nuclear power program which demanded rapid implementation and high reliability. This rush to a politically-motivated demonstration did not allow for the natural selection of the best candidate -- from both a safety and economic perspective -- for this application.

Without question, the United States' military effort involving nuclear power accelerated technological development by many years, perhaps even decades. The choice of a rigid-fuel, pressurized water reactor configuration from amongst many alternatives was logically conservative for naval propulsion systems, as water was the most well-known fluid at the time. However, the same cannot be said for civilian nuclear power stations. The introduction of a 60 MW_e power reactor at Shippingport, Pennsylvania, was merely a scaled-up version of a reactor originally designed to propel and power an aircraft carrier. Its configuration was not primarily based on selection criteria relevant for a civilian electrical generating plant, as the safe and reliable operation of the system were not the fundamental considerations used to choose the best technological solution to the problem. This reactor subsequently became the prototype for approximately 70% of the fission reactors in the world today, and the

uniqueness of the evolution of this technology was perpetuated as the former Soviet Union, France, Japan and many other countries followed suit with similar nuclear power programs. Canada developed a unique heavy water-moderated natural uranium-fuelled reactor system know as CANDU (Canada Deuterium Uranium).

Another aspect to consider is the conduct of reactor operators. The military could exercise strict control over its personnel, often in environments totally separated from the civilian world, and thus could rely on disciplined and highly trained human performance for part of a reactor's safety characteristics. Such strict control, however, is inconsistent with several democratic values (Perrow 1984; Sagan 1993) and thus civilian nuclear power plants could not be as reliant on human action. In the early 1980's, utility leaders in the United States told the Electric Power Research Institute (EPRI) that future nuclear reactors should be simpler in design and to operate, and ten times safer than the current generation (Sweet 1997). "Advanced" light water reactor designs (Nuclear News, September 1992) have been proposed in an attempt to achieve this level of increased safety. However, the intent of this work is to follow an approach more suited to selecting a core configuration for civilian nuclear power generation -- one with safety as the foremost criterion. This is done by following a path parallel to the powder-in-suspension idea which was conceived of in the earliest stages of reactor design -- but was discarded in favour of the more expedient military-developed option (Went and de Bruyn 1954; Kreyger et. al. 1958; Went and Hermans 1972) -- specifically a reactor core using the concept of pellet suspension.

1.5 Component Substitution

The reactor core concept which is discussed in subsequent chapters is envisaged to be used as a replacement for existing fission reactor cores which, of

course, are just one component of a given power plant. Research and development involving such component substitution is, however, useful for at least two reasons: it may provide unique innovations and may provide complementary contributions to the evolution of existing reactor types.

The practise of renewing a technology by replacing one of its components with an improved alternative is not new. Such component substitutions have also occurred several times during the development of other well known technologies, resulting in a drastic improvement in -- or increased use of -- that device or process (Harms 1996). For example, the introduction of diesel-electric locomotives to replace steam driven engines led to a significant increase in the amount and speed of train traffic in Britain in the late 1800's. Similarly, the substitution of jet engines for propeller or piston engines in aircraft led to a dramatic increase in trans-Atlantic air traffic which continues today. The advantages of electronic micro-chips over vacuum tubes in the construction of computers is another obvious example of this developmental strategy. It is, in part, through substitution of the fission reactor core in nuclear power plants -- the component of such systems which is one of the main hazards and source of negative public perception of the industry -- that this work attempts to address and improve the prospects for nuclear power.

1.6 Conditions For Renewal

In order for the nuclear power industry to invoke significant change that may result in a more positive view from the general public and a possible ensuing renewal of fission power plant development, several considerations are important. Without question, the technical and economic performance of existing reactors must not only be maintained at current levels, but must be improved to provide the public with

positive experiences associated with nuclear power. In addition, reactor safety, waste disposal and non-proliferation concerns must be better addressed, perhaps through a more fundamental strategy as was articulated recently by C. Starr (1997) and previously by K. Hannerz:

> "Most of the present objections to the use of [the] nuclear option have their roots in the reactor safety issue. The approach taken to satisfy the escalating safety concerns has resulted in excessively complex and expensive plant designs [which] still have not succeeded to create public confidence. There are many proposals made to remedy the problem that presently nuclear energy is facing, but the one and the most direct way out of the difficulties is surprisingly absent among these suggestions; namely, a new reactor concept."

As alluded to previously, the global nuclear power industry currently faces many aging reactors which will soon require significant upgrading, retro-fitting, or decommissioning, as well as minimal new construction and orders for additional plants. Even the more recently designed "advanced" reactors are not faring significantly better in the global power production market (Nuclear News, March 1998). However, a possible resurgence of fission power -- based on a "second generation" of nuclear reactors -- could rest with those that are not only much safer and reliable than the present generation, but which also provide these characteristics through the use of natural and passive processes as opposed to an improved quality or increased number of active safety systems alone. Such a simplification would reduce the need for technological add-ons, lower the complexity and cost of the plant, and de-emphasize a reliance on human performance for its safe operation. Tailoring the design to avoid rather than just mitigate the consequences of accident conditions would further improve the economics of the system by permitting a "walk-back" approach where the reactor could be restarted soon after an abnormal incident (Lidsky 1984).

The majority of safety systems -- as distinct from containment systems which

for the most part are based on passive processes -- in today's fission reactors are based on feedback. That is, in the event of a deviation from normal operation, a sensor detects the perturbation and a signal is sent to a control system which tries to adjust parameters to return the system to normal operating conditions, or demands action by an operator. Such systems are an example of active safety (IAEA 1991). An obvious improvement over such schemes is one which does not rely on active systems in the event of a failure of one or several subsystems within the plant while still ensuring safe operation. For that to be possible, the design must be such that in the event of a deviation from normal operation the system autonomously adjusts itself -- even with no external influence, i.e. passively and inherently -- to return to its original state.

Passive safety is sometimes also referred to as "level one" safety, and is exhibited in a variety of everyday devices such as car seatbelts and fire sprinkler systems. The former rely on mechanical principles alone, while the latter also use thermal effects to initiate responses and remedies to abnormal conditions, thus not relying on active components or systems as are common in most other engineered safety systems.

A concept or design which can provide such passive safety against potentially hazardous deviations from standard reactor operation would be a logical next-step in the development of nuclear power. In fact, had nuclear power evolved without the external influences it was subjected to, similar principles may have guided the first reactors ever built. Such improved reactors would best rely solely on natural processes for safely returning the reactor to normal operation (or to shut it down entirely, if necessary) if they are to be accepted by the general public (Kirchsteiger, Reusens and Böck 1995). In addition, these natural processes, such as gravity or thermodynamics, should be transparently obvious and understandable -- even to the non-specialist.

The distinction between these revolutionary -- as opposed to evolutionary --

concepts is that they do not necessarily make mere refinements to an existing reactor system to provide improvements, as is the case for most of the "advanced" reactors under development today. Rather, they make significant changes to the system -- or a major component thereof -- sometimes seemingly returning to very basic considerations (Kugeler and Phlippen 1996). Indeed, in many cases revolutionary concepts are derived from older ideas that were abandoned but can now be modified to provide the much desired attributes of "conceived of" safety. While these new concepts do not have the benefits of extended operating experience like that of the present evolutionary designs (IAEA 1993), new revolutionary fission reactor core concepts which possess passive safety characteristics against potentially dangerous reactor accidents represent one avenue to possibly bolstering the nuclear power industry. Such a renewal is necessary in order that the benefits of fission power over the alternative means of power generation may continue to be realized. One such reactor concept -- the Pellet Suspension Reactor, or PSR -- is the topic of this work.

1.7 Design Process and Interactions

The conceptual design of the PSR presented and analysed here follows a traditional design process in many ways (Ertas and Jones 1996). The project began with the identification of a need for such a new system. Recognition that currently operating fission reactors and advanced reactors presently being designed are inadequate to successfully address all the concerns associated with nuclear energy (Section 1.3), that continued reliance on fossil fuels will not be acceptable for several reasons (Section 1.2), and that no new means of base-load electricity generation appears feasible for many decades into the future, led to the conceptualization of a fission reactor system which addresses three major issues of concern facing nuclear

reactors today:

1. loss-of-coolant accidents (LOCAs) (Chapter 3),
2. reactivity excursion accidents (Chapter 4), and
3. closure of the nuclear fuel cycle (Chapter 5).

In an ideal case, the optimal design of a new product or system is sought before continuing its development. For nuclear power stations, however, political and military influences prevented this to some extent (Section 1.4), and thus the PSR is intended to possess characteristics more suited to being an optimal choice for solely civilian electricity-generating fission reactors. However, as there are many similar research efforts throughout the world (Section 2.2), it is certainly too early to determine which, if any, of these reactor systems are the best choice for a "second generation" of fission reactors.

Despite this, the exploration of one such reactor at the conceptual stage provides valuable comparisons between the many options being considered. For the PSR, the switch from rigid fuel to pellet fuel, and the suspension of such fuel by an upward moving fluid (Section 2.3) were effectively pre-determined requirements. Many alternatives to the pellet catchment system, fuel reprocessing procedures, and other components of the design were looked at throughout, many conceived of through related experience or brainstorming exercises. Most of the design options considered, and their interactions with one another, are discussed in the corresponding sections of Chapters 2-5.

The three main design requirements were clear from the beginning -- to autonomously eliminate LOCAs, to limit reactivity excursion tendancies, and to close the fissile fuel cycle using available or attainable technology. The conceptualization of an overall system layout (Figure 2.5) allowed for the breakdown of the work into several components. Chapter 2 presents the overall concept, some similar designs, and

a variety of options with respect to some of the most unique features of the accident-avoidance systems. The three subsequent chapters deal with each of the major issues mentioned above in turn. For each, the options considered for that aspect of the system, any selections made and reasons therefore, the resulting design, its success or failure to date, and finally the current status of that component are presented.

Chapter 2

Reactor Concept

Fission reactor concepts possessing the goal of improved safety have been proposed for many years. Several of those specifically related to the concept which is the focus of this work are briefly outlined here for comparison and context. Subsequently, an overall description of the proposed fission reactor concept -- several analyses of which are undertaken in Chapters 3-5 -- is presented along with the general means by which it may address some of the problems faced by the nuclear power industry.

2.1 Safety Terminology

Most new fission reactor designs include provisions for greater safety measures when compared to reactors operating today. Many of these rely on what is known as inherent safety -- that which is a consequence of the system design and the materials used, rather than being provided by an additional engineered system. Such an approach has also been referred to as intrinsic, deterministic, conclusive, or absolute safety (IAEA 1991), or the reactor can be said to be passively stable (Taylor 1989). Inherent safety cannot generally be used to describe a reactor system as a whole, but rather only with reference to the failure of one component or the development of a particular accident scenario, such as melting of the fuel material. It should also be

noted that if there are components of a reactor which are passive in nature, that alone does not necessarily render the entire system passive.

As mentioned in the previous chapter, inherent safety characteristics would best be such that they are transparently recognisable and easily demonstrable. Of course, there should also be no dependence on, or possible interference from, safety devices which have a finite -- albeit generally very small -- probability of failure or susceptibility to operator misaction. One of the primary features of the inherently safe reactors examined here is an incapability for melting of the fuel in the core through a scheme which is forgiving enough to tolerate human and mechanical failures, some even being walk-away-safe, i.e. requiring no human intervention for a given length of time -- the grace period. However, one must not overlook the fact that such concepts will only perform as well as they are designed, constructed and maintained, and in limiting cases a poorly designed and built passively safe reactor may be less desirable than one with a well designed, built and maintained active safety system. While conceptual designs are the starting points, in practice, operation and maintenance of reactor components and systems play an equally important role in retaining the safety characteristics of any power plant.

2.2 Similar Concepts

Present-day reactors and most advanced reactors being designed rely on a system which replenishes lost primary coolant with a similar auxiliary coolant in the event of a loss-of-coolant accident (LOCA). This is to prevent melting of the fuel which could lead to the release of radioactive fission products. The decay heat generated in a reactor -- typically ≈6-8% of full power and decreasing after shutdown -- is significant enough that it must be transported away to prevent fuel melt (Kugeler and Phlippen

1996). The revolutionary concepts outlined below -- including the one which forms the basis of this work -- generally do not require this replacement of coolant. Rather, they rely, at least in part, on gravity to remove the fuel from its neutronically critical arrangement -- in some cases from the core altogether -- and to have it re-assemble in a new geometry such that forced auxiliary cooling is not necessary to prevent its melt in the event of a LOCA.

Fission reactor core concepts other than the presently common rigid-fuel designs have been investigated from the earliest days of the fission enterprise. Those based on fuel pellets, and in particular on fuel pellets in suspension, continue to be of interest. These reactor core concepts generally feature suitably coated spheres of fissile fuel suspended in a critical arrangement by an upward flowing liquid or gas coolant. Upon disruption of this coolant flow, the fuel pellets in suspension will descend autonomously under the force of gravity into a subcritical and perpetually cooled arrangement, thus eliminating the likelihood of fuel melting.

A variety of these reactor concepts utilizing pellet fuel in suspension have been proposed or revived in the last decade or two. One such project is that of a fluidized bed nuclear reactor (Sefidvash 1985, 1996). In this design, slightly enriched uranium dioxide (UO_2) fuel pellets are fluidized[1] by an upward moving light water coolant (H_2O). Other fuels such as thorium (Th) and natural uranium, and different coolants such as heavy water (D_2O) or organic materials have also been considered. A sieve at the core's upper boundary is required to prevent the transport of fuel spheres out the top of the reactor by the heated pressurized coolant. Its location may be adjusted to provide an optimal fuel-to-moderator ratio via the void fraction, ϵ, in the fluidized bed. In the event of a LOCA, or merely a reduction of the coolant flow rate, the particles

[1]Fluidization and related concepts are discussed in Chapter 3.

collapse to a packed bed where the smaller moderator-to-fuel ratio renders the system sub-critical and permits sufficient cooling without the flow of primary coolant to ensure that no fuel melt occurs. Similar sub-criticality is achieved if the coolant flow is too great and the fuel is packed against the upper sieve. However, in this design such passive cooling conditions are only maintained for a finite grace period, and thus external intervention in the event of a LOCA is required at some later time. This is typically several hours or days from the LOCA initiation. The reactor's modular design and small power output per unit, Table 2.1, makes many reactor sizes possible, and the resulting reduction in licensing costs from duplicity and high reliability -- including on-line refuelling -- add to its attractiveness. Seismic events would not cause the breakup of any individual fuel elements and thus could not damage the first barrier to fission product release -- namely the fuel compound itself.

A somewhat different concept has been proposed by a Swiss group (Taube et. al. 1986) which uses upward flowing liquid lead coolant to hold uranium carbide (UC) spheres against an upper boundary. The superficial fluid velocity is thus required to be greater than the terminal velocity[2] of the fuel spheres to retain them against the upper bounds of the channels, otherwise gravity disperses the fuel to a subcritical arrangement. This can be either within the channels or on catchment trays below the core in the event of a significant reduction or even total loss of coolant flow. During normal operation, the fluid velocity below the core region is small enough so as not to transport any fuel elements residing on the catchment trays into the channels which eliminates the possibility of an unforseen fuel or reactivity insertion to the critical system. In the event of a LOCA, removal of fuel from the core and its collection on the trays below provides a fuel dispersal action that ensures subcriticality and sufficient

[2]Terminal velocity is discussed with regards to pellet suspension in Chapter 3.

Table 2.1: Representative characteristics of some suspended pellet-type fission reactor core concepts.

	Sefidvash (1986, 1996)	Taube[a] (1986)	Mizuno[a] (1990)	Watanabe[a] (1991)	Seifritz (1992)	van Dam[a] (1996)
enrichment of fuel, ξ (%)	2.2	3	natural (0.7)	2	4.5	16.76[b]
mean pellet diameter, d_p (mm)	8	20	10	1[c]	15	1
cladding thickness (mm) & type	0.5 Zr	0.1 SiC	0.5 Zr	no cladding	0.5 Zr	0.37 TRISO[d]
column diameter, D_c (cm)	25	3.3	30 (hexagonal)	220	8	116
column height, H (m)	1.4	5	2	1	0.75	6
coolant temperature, T (°C)	308 (average)	400-600	270-286	327-727		250-750
coolant pressure, p (MPa)	15.8	3.1		1.8	1.5	6
coolant velocity, U (m/s)	0.51	0.56	0.6	14	2.6	4
void fraction, ϵ (%)	70		75	70	62	80
power, P_{th} (MW_{th})	4.5 - 5 per column	360	9 per channel	300	10	40

[a]only one name of each research group is used to identify the different reactor concepts (the complete list is included in the corresponding reference).

[b]by weight.

[c]including a 0.02 mm diameter inner ferro-magnetic core.

[d]TRISO (tri-isotropic) coating structures of fuel pellets are discussed in Chapter 4.

fuel cooling so that no intervention is needed for 24 hours. Subsequently, spray cooling is required to dissipate the decay heat. The channels are made of appropriate size (Table 2.1) to ensure no choking or clogging will occur if the pellets are required to descend out the bottom of the core in the event of a deviation from normal operation.

Taube et. al. also suggest several features which should be incorporated into any new fission reactor design to eliminate as many potential hazards as possible. These include using an inert coolant and moderator to eliminate all chances of chemical reactions or phase changes, even if either comes into contact with one another, the fuel, structural materials, the atmosphere, or other media. In addition, they recommend the use of low pressure in all fluids such as coolants or moderators, but appear to contradict themselves by employing liquid lead at over 3 MPa in their proposal.

Another concept, somewhat akin to Sefidvash's, is that of Mizuno and co-workers (Mizuno, Ito and Ohta 1990). Their work uses UO_2 spheres which are fluidized by light water in hexagonal columns. An upper sieve provides the core's top boundary, while a density lock mechanism which opens in the event of coolant flow reduction forms the base of the bed. When this lower "trap-door" (see Figure 2.6(a)) opens, the fuel pellets descend into a lower cavity where the fuel arrangement is subcritical and there is sufficient cooling of the pellets to avoid fuel melt.

There are other variations of the fuel-in-suspension concept, including one in which UO_2 fuel spheres are suspended by helium (He) gas in a large diameter column (Watanabe and Appelbaum 1991). Because of the larger gas velocities (Table 2.1 and Chapter 3) necessary for suspending pellets with He instead of water, and the resulting density variations of fissile fuel pellets in such a large diameter core, an additional system is incorporated to attempt to achieve some stabilization of the pellet

distribution. Each pellet contains a core of ferromagnetic material surrounded by the uranium fuel, and externally generated magnetic fields are used to assist in holding the pellets in place within the columns during normal operation.

An additional reactor concept which fluidizes UO_2 spheres in water (Seifritz 1992; Seifritz and Sefidvash 1997) also utilizes a movable upper sieve to control the fuel-to-moderator ratio and thus, along with the flow rate of water coolant, provides a control mechanism for the reactor. Also proposed is the use of hollow pellets to reduce the mass of each -- and thus the fluid velocity required to suspend them.

A final reactor concept based on the suspension of fissile fuel pellets by the coolant that will be mentioned here is that of van Dam and co-workers (van Dam et. al. 1996). In the FLUBER, as they have labelled it, UC spheres are fluidized by He gas, a critical system only achieved when the proper void fraction in the fluidized bed is attained. All other configurations are sub-critical -- rendering it inherently safe against flow-induced reactivity insertions; the provision of decay heat removal exists if the coolant flow is lost or reduced. Neutronics calculations have been performed assuming a uniform fuel density distribution. Calculations involving non-uniform conditions are underway, but the dynamics of the system are expected to have only minor effects on the reactivity due to the slow neutron kinetics characteristics of a graphite moderated reactor. In addition, the large thermal feedback resulting from the excellent mixing properties of fluidized beds will further reduce the effects (van Dam et. al. 1996). This concept makes use of these and other beneficial safety characteristics found in present-day HTGRs (Cameron 1982).

The variety of designs and concepts -- due to configurations, materials, etc. -- summarized above are collectively, however, all reactors of the suspended pellet-type: those which suspend small, spherical pellets of suitably coated fissile fuel in a neutronically critical arrangement between upper and lower bounds of a reactor core

by a vertically flowing liquid or gas. Their passive and inherent safety characteristics against loss-of-coolant accidents, and the primary means through which they are obtained, are the links to the reactor concept which is the focus of this work.

2.3 PSR Core Concept

Suspended pellet-type reactors have evolved in part through the progression from packed or particle beds to fluidized beds, and for greater fluid velocities, suspension arrangements. What has become known as the Pellet Suspension Reactor -- abbreviated PSR here to avoid the potential confusion between such a name and the more general class of suspended pellet-type reactors -- is a specific example of a revolutionary reactor concept. The fundamental distinction between it and conventional fission reactors is that the fissile fuel is not in large fuel elements rigidly constrained within the core. Rather, the fuel takes the form of small spherical pellets composed of a carbide or oxide based nuclear fuel (eg. UC or UO_2) surrounded by several thin protective layers which provide retention of the energetic fission products and long-term structural integrity for the pellets, Figure 2.1 (Harms 1993; Harms and Kingdon 1993). Of the order of 10^7 of such pellets -- whose diameter is ~1 mm -- are needed for such a reactor, however the production and reliable performance of such fuel elements is well established[3]. These fuel pellets have been shown to exhibit excellent fission product retention and high temperature durability, and are based on technology developed in connection with high temperature gas reactors (HTGRs) and particle bed reactors.

In the PSR, the micro-fuel pellets are hydrodynamically suspended in upward flowing helium gas within cylindrical columns. The neutronically-transparent tubes

[3]Fuel pellets are discussed in Chapter 4.

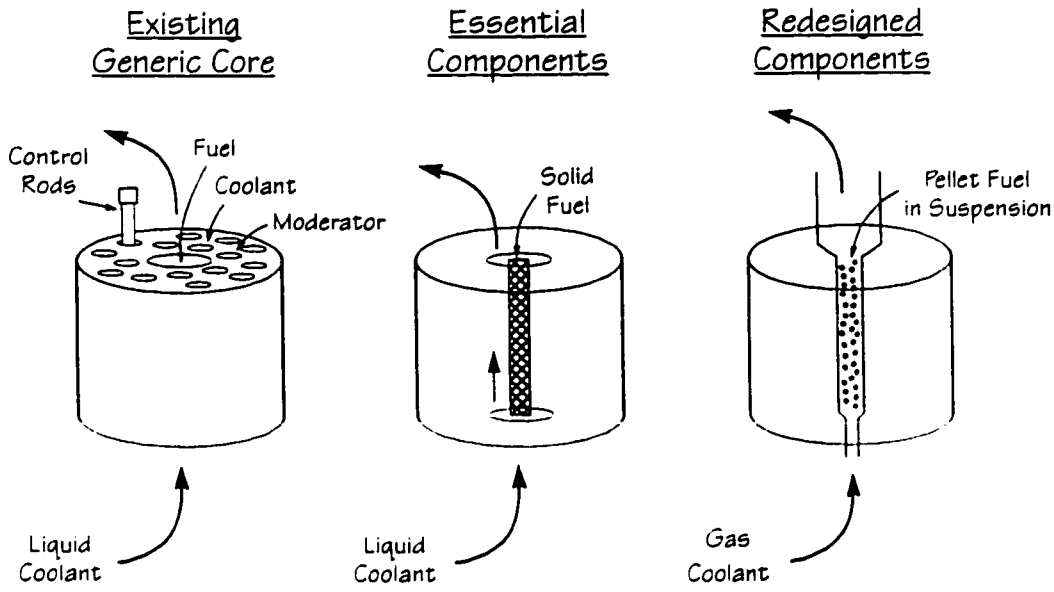

Figure 2.1: Replacement of rigid-fuel elements in a conventional reactor core with pellet fuel suspended by an upward moving liquid or gas coolant.

are approximately 20 cm in diameter and contain only enough particles to occupy about 10% of the column volume. This latter value was selected following criticality searches so as to yield, as near as possible, the maximum reactivity possible through adjustment of the void fraction. During normal operation, the particles are maintained above a lower constriction in the column -- below which the superficial gas velocity is greater than the terminal velocity of the pellets thus transporting any which fall below it back to the main column -- and below an upper expansion of the tube -- above which the fluid velocity drops below that capable of suspending the particles[4] so that any carried above the boundary fall back into the central region -- which form the bounds of the reactor core, Figure 2.2(a) (Kingdon and Harms 1996). The height of the columns is of the order of a few metres, and several, perhaps even one hundred such vertical columns -- separated by an appropriate moderating material such as graphite or low pressure D_2O into which conventional control rods may be inserted for use in reactor start-up, control, operation and shutdown, as in CANDU reactors -- form the reactor core. The total diameter of such a system, including a surrounding reflector, is several metres. Two possible variations of the suspension column which are distinguished by solid upper boundaries are shown in Figure 2.2(b). These alternatives are motivated by the need to maintain a stable fuel distribution in each column from a reactivity point of view, which can be achieved by having the fuel particles motionless or moving about only minimally during reactor operation.

In the event of gas coolant flow reduction or complete coolant pump failure the fuel pellets autonomously descend under the force of gravity out of the core columns and into a dry, divergent, gas-filled conical annulus where they form a packed bed of particles in which the fissile fuel takes on a sub-critical arrangement (Harms and

[4]This is known as the minimum fluidization velocity U_{mf} -- discussed in Chapter 3.

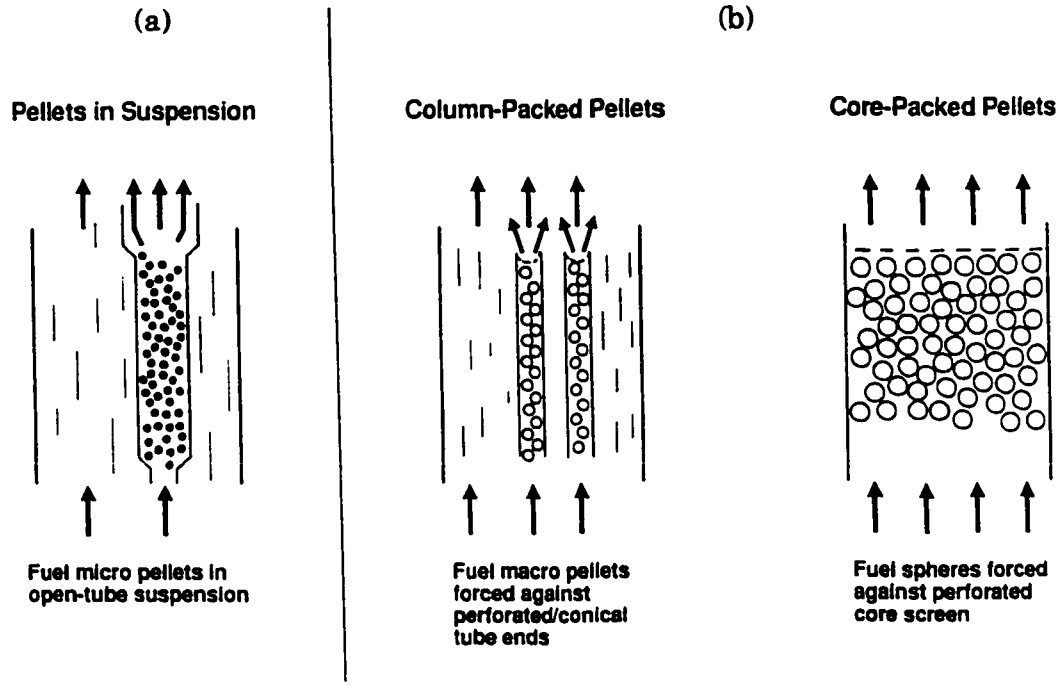

Figure 2.2: (a) Schematic of a suspension column for the PSR, and (b) possible variations which would still provide for inherent safety against LOCAs.

Fundamenski 1993). Packed-bed heat conduction in the catchment to assure fuel-melt avoidance appears tractable and choking, or clogging, of the narrower lower tube is eliminated by ensuring that its diameter is at least fifty times that of the pellets[5].

The process of pellet removal from the core in the event of a LOCA, and the geometry of the catchment device below the core, Figure 2.3, to assure subcriticality and perpetual removal of decay heat by packed bed conduction have all been addressed (Harms and Fundamenski 1993; Kornilovsky, Kingdon and Harms 1996; Kornilovsky and Harms 1996). Several options for the catchment geometry were initially considered, the current selection based mainly on the simplicity and utility of the conical annulus as there was little influence on other components of the reactor system. This design has shown that a geometric arrangement which provides for nuclear sub-criticality is consistent with one that assures the removal of all the radioactive decay heat from the fissile fuel to a large heat sink (i.e. a borated water sheath connected to an external reservoir). The bed size is determined by two main constraints: a sufficiently large volume to contain all the fuel particles from the reactor and a sufficiently thin annulus to ensure that packed bed heat conduction will prevent any of the fuel particles from melting. In addition, the descent of the particles from the reactor to the catchment area occurs sufficiently quickly to ensure that fuel does not melt while in transit to the annular packed bed.

This LOCA elimination by gravitational shutdown substitutes a core ejection process for mechanical or electrical sensor-driven systems and components -- essentially amounting to the transporting of a hot, non-stationary fuel pellet core into a perpetually cooled subcritical catchment, as opposed to the transport of an Emergency Core Coolant (ECC) into a hot stationary core, Figure 2.4 (Harms and

[5]This condition is easily satisfied, as will be shown in Chapter 3.

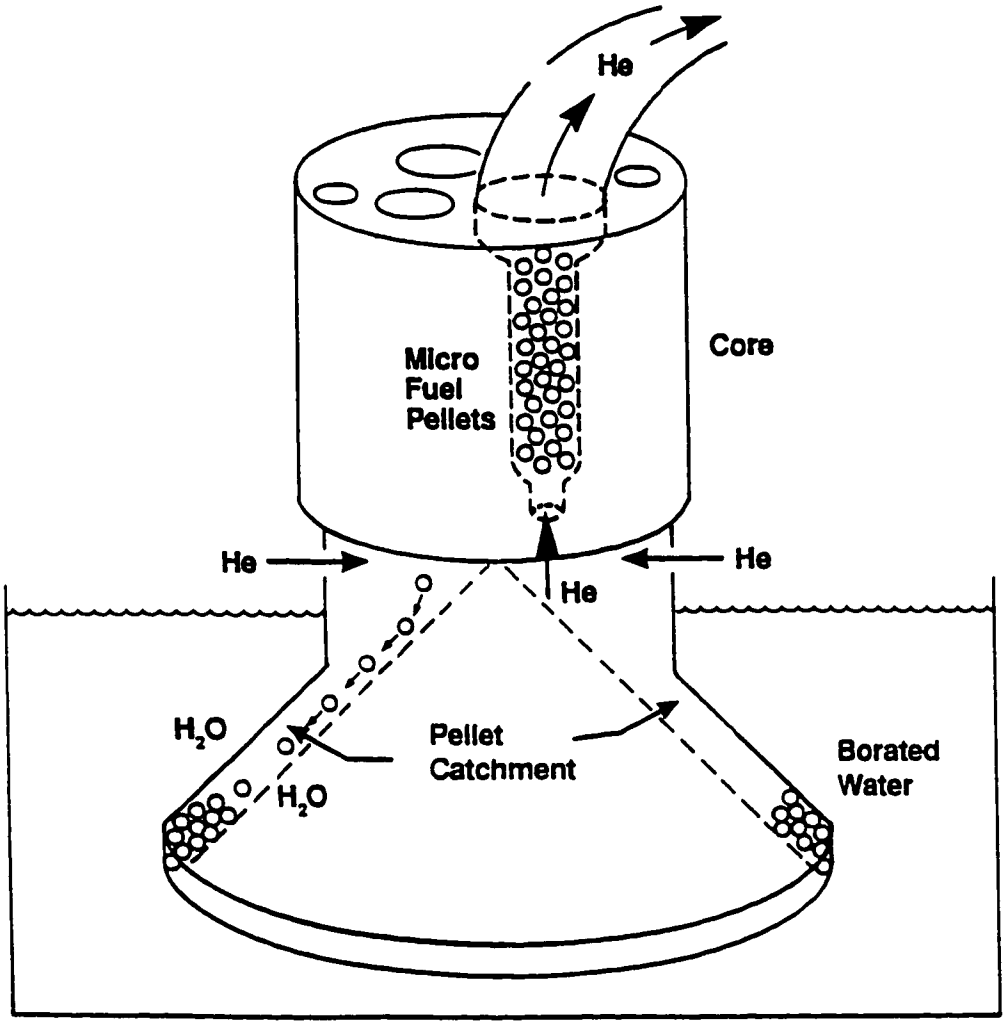

Figure 2.3: Conceptual layout of the PSR reactor core showing only one of several suspension columns and the catchment configuration into which the fuel pellets descend in the event of a reduction in primary coolant flow.

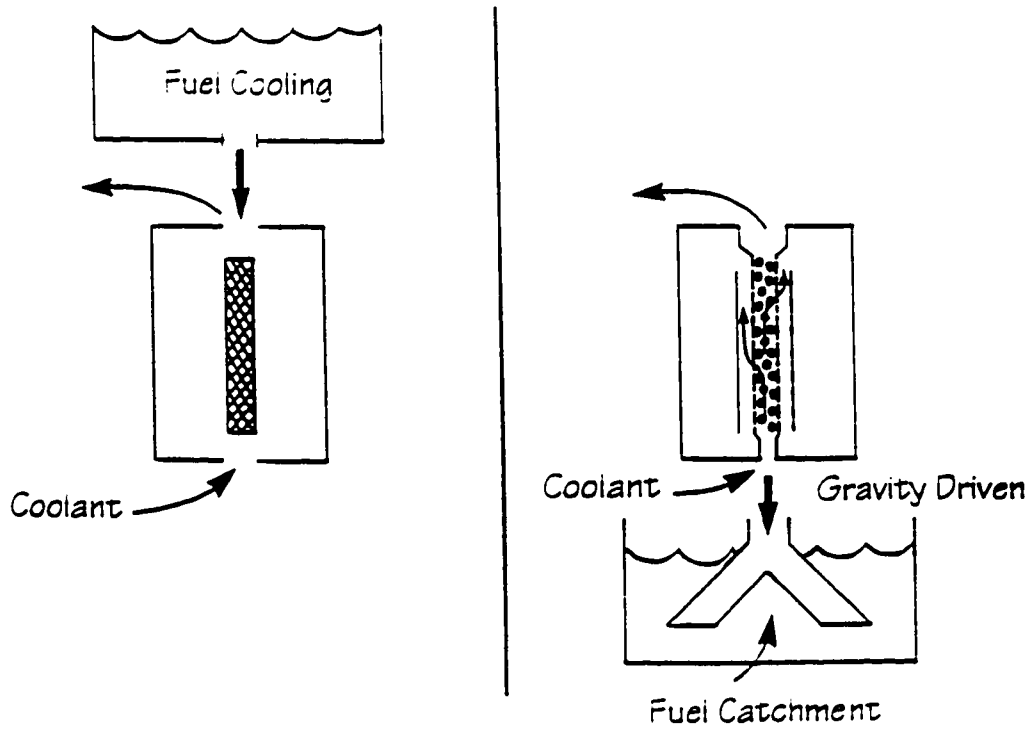

Figure 2.4: Schematic depiction illustrating two safety design principles: transport of an Emergency Core Coolant into a hot core versus transporting hot fuel pellets into a perpetually cooled catchment.

Kingdon 1994). The latter is used to avoid LOCA consequences in conventional fission reactors but is not always available during low power, refuelling or other operating conditions (Kugeler and Phlippen 1996). This is not the case in the PSR. In addition to always being available, there is no need for testing, inspection or maintenance of the LOCA-avoidance system, nor can it be biased by human action.

The provision for shutdown and total decay heat dissipation in the event of -- and as a consequence of -- a loss-of-coolant accident provides for inherent, passive and self-acting safety characteristics against LOCAs through the action of gravity. Since the failure of the cooling system results in the transformation to an assuredly safe configuration, the PSR is said to be fail-safe against loss-of-coolant accidents, and any dangerous consequences which may directly arise therefrom. Some other reactors, be they those operating today or advanced rigid-fuel reactors under design, claim to possess passive or inherent safety characteristics like those described above for the PSR by relying upon an ECC injection system. However, this action usually requires the opening of at least one valve or the breech of a pressure boundary, such as a rupture disc, to be invoked, and thus their passive characteristics are true only to a certain extent.

Further, following such ECC action there is usually a significant, expensive clean-up of the coolant system required, whereas in the PSR's core ejection scenario reactor restart can occur effectively immediately afterwards. Any such gravity-induced shutdown, be it due to unforseen circumstances or deliberate operator action, is followed by the collection of the fuel pellets by remote robotics from the catchment, the re-establishment of coolant flow and injection of the fuel pellets back into the columns from either the top or sides in order to resume reactor operation. Reactivity can be held down by fully inserting control rods until the entire fuel loading is re-established, at which time the rods would be withdrawn to achieve the desired power level.

The fuel pellet extraction provision can also be extended to normal operation to accomplish on-line refuelling and fission product management for a reduced radioactive inventory in the core. With low excess reactivity in the core, potential transients are limited and there is a reduced need for soluble, burnable neutron poisons in the moderator or coolant, and thus also any associated chemistry control systems. Fuel pellets could be withdrawn and injected into the pressurized columns through tubes of lower and higher pressure, respectively, which would drive the small fuel elements in the desired direction. All of the extracted pellets would be sent to a non-destructive quality assurance test station to determine the extent of fissile fuel burnup, the amount of fission product accumulation present, and for tests of material integrity, Figure 2.5. Pellets deemed capable of returning to the reactor -- those which had undergone relatively little fuel burnup and were still structurally sound -- could be put aside for recirculation to the core, while all others would be reprocessed on-site, removing only selected neutron absorbing fission products.

The method of electro-refining mass separation (Laidler et. al. 1997; Koyama et. al. 1997) is ideally suited for the removal of such species since it is less expensive than alternative means which employ isotope separation and yields no weapons-grade fissile material. While alleviating nuclear proliferation concerns, such a system would also significantly reduce the volume, activity, and lifetime of high-level waste as only certain fission products -- as opposed to all the components of the spent fuel -- would need to be stored and managed, allowing this task to be potentially accomplished on-site. All remaining fission products, the actinides and left-over fuel from the pellets would be returned to the core in newly manufactured fuel elements, "topped up" with additional fissile fuel[6]. This pellet manufacture could also occur on-site, potentially

[6]This fuel management system is discussed in Chapter 5.

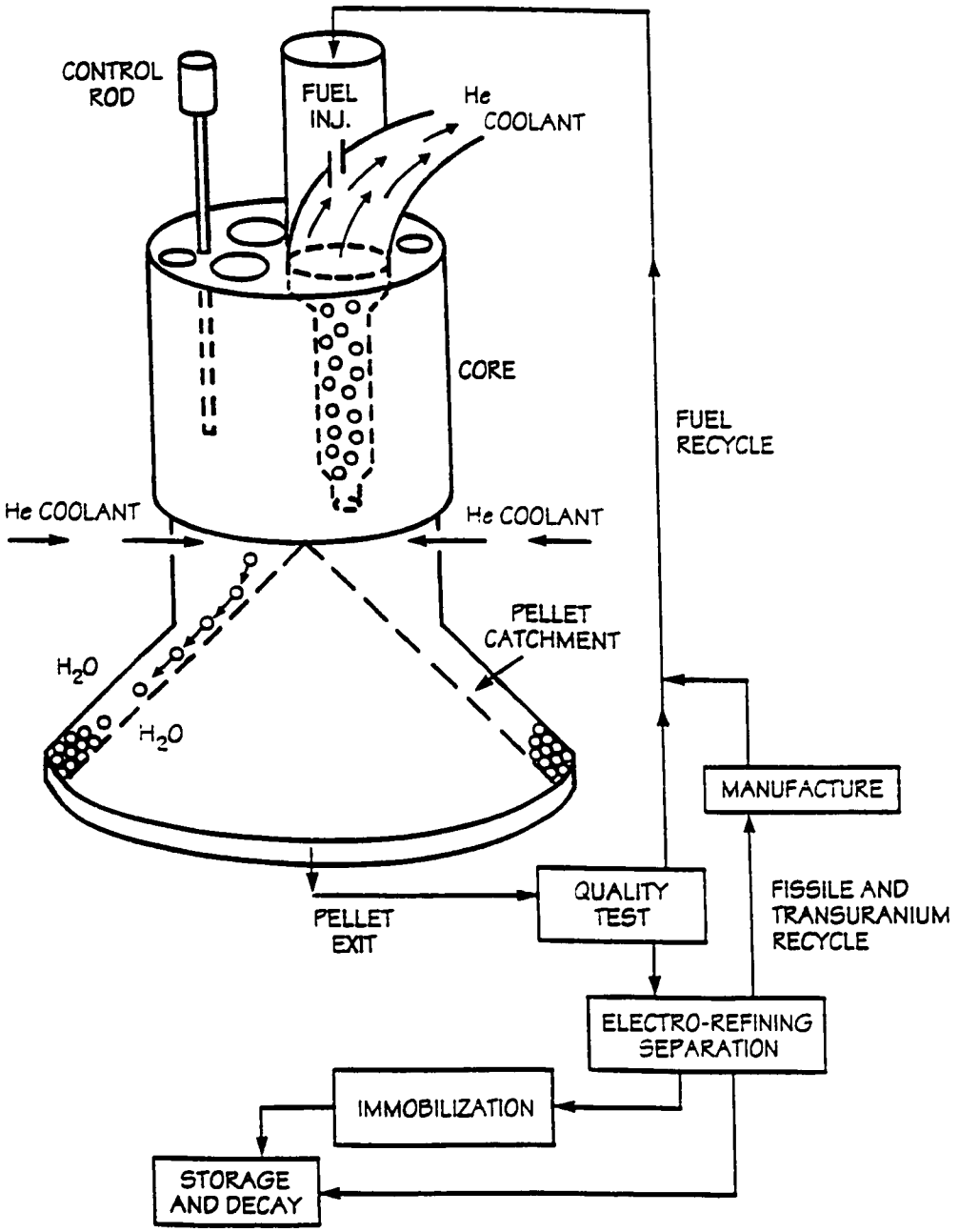

Figure 2.5: PSR conceptual layout including fuel inspection, electro-refining separation to remove neutron-absorbing fission products for on-site storage and decay, and fuel manufacture, including actinide recycling.

closing the nuclear fuel cycle for the PSR (Harms 1996; Khotylev, Kingdon, Harms and Hoogenboom 1997a, 1997b; Khotylev, Hoogenboom, Kingdon and Harms 1997).

Because helium gas is used for the reactor's coolant, the possibility of direct energy conversion also exists. In fact, this was in part the motivation for such a coolant. A sufficiently clean He gas stream could be used to turn a highly efficient (≈47-50%) gas turbine, as opposed to transferring the heat from the high temperature He to a secondary water system that would turn a conventional turbine (≈30-35% efficiency) -- as is the case for nearly all fission power reactors operating today.

Several reactor physics and thermodynamic characteristics of this reactor core concept have been investigated -- much of which will be the topic of subsequent chapters -- and are found to lie in domains very similar to conventional fission reactors. Operational considerations such as fuel pellet suspension stability and homogeneity have begun to be addressed, but require more work before being resolved. The technological requirements of such a system are generally in existence (manufacturing capabilities, methodologies, etc.) and of most significance is the reliance on no human action or electrically-driven sensors or valves to render the reactor transparently fail-safe against LOCA-induced catastrophic fuel-melt events. In addition, a modification to the fuel pellet structure and composition might also provide for the avoidance of reactivity excursions in the reactor solely through thermodynamic and drag force effects.

Recognition of the inherent LOCA mitigation characteristics described above suggests that the possibility of reactivity excursion accident avoidance without the need for active sensors or monitors also be considered. The spherical micro-pellets are envisaged to consist of a central core of fissile fuel encased by multiple shells to accomplish a variety of functions. Several layers immediately surrounding the fuel are incorporated to provide fission product retention (both gas and solid) within the pellet.

The outermost shell of the pellets would be a hard, durable material to withstand the physical collisional demands within the column.

Of most significance here, however, is a layer between the fuel core and the outer protective layer that consists of a material which sublimates from a solid to a gas when its temperature rises significantly above normal operating conditions, yet is small enough to have a negligible effect on suspension requirements and particle distribution homogeneity. This ablative layer could potentially initiate a mechanism to remove the fuel from the core in the event of a reactivity excursion, and thus eliminate any dangerous consequences thereof, through the following sequence: a reactivity increase in the reactor would cause an increase in the neutron population, subsequently increasing the power production within the fuel core of the pellets. If power or temperature reactivity feedback effects within the pellet -- or reactor as a whole -- do not result in a net reduction in reactivity, the increased power production would continue to raise the fuel temperature and then that of the ablator. Once the sublimation temperature of the ablative material was reached, the resultant change of phase would generate substantial pressure to break apart the outer protective shell of the pellet and thus change the geometric properties of the suspended material. If these changes in the drag force were sufficient, the suspended pellets would elutriate[7] out the top of the column -- where they would be collected -- for those particles whose terminal velocity is reduced below that of the velocity of the coolant. Alternatively, those fragments whose minimum fluidization velocity is increased above the suspension velocity would descend out the bottom (Davidson, Clift and Harrison 1985). This fuel removal would reduce core reactivity and potentially avert an excursion accident, but is obviously only applicable to the suspension column designs (Section

[7]Elutriation is discussed in Chapter 4.

2.2, Figure 2.2) which have no physical barriers at either the top or bottom.

For this accident avoidance mechanism to be successful -- rendering the PSR immune to a second reactor accident scenario -- comparison of the time scales of several processes is required. The generation and conduction of heat in the pellet, the ablation process, and the elutriation or gravitational fall of the pellet fragments out of the core must occur sufficiently quickly to remove enough fuel to reduce the reactivity to a stable level (Kingdon, Kornilovsky and Harms 1996).

The PSR is thus conceived of to use naturally assured processes including gravity, convective circulation, thermodynamics and elutriation to provide severe accident avoidance. These features are intended not just to mitigate the consequences of abnormal events, but to avoid them altogether. In addition, none of the natural processes may be "switched off" by human intervention. It is important to re-iterate, however, that no reactor is completely inherently-safe, but rather is only so with respect to specific failures or scenarios. The purpose of the PSR is to achieve such safety against loss-of-coolant accidents and to affect reactivity excursions as much as possible, while providing an option for closing the nuclear fuel cycle on-site. The terminology used throughout this work, in reference to safety characteristics, is that recommended by the International Atomic Energy Agency (IAEA 1991).

2.4 Inherent Accident Avoidance

The PSR design possesses inherent avoidance characteristics against many reactor accident scenarios -- often termed Design Basis Accidents (DBA) -- considered today in plant safety, licensing, and regulatory activities. The most transparent aspect is that of reactor shutdown and subsequent cooling when the fuel descends out the bottom of the core and into the pellet catchment below. This occurs for any scenario

in which there is a deviation from the normal upward coolant flow, such as direct pump failure, loss-of-flow through the core due to the failure of any pipe in the coolant system or a blockage in the coolant return loop between the core outlet and inlet, system depressurization or loss of inventory control, the loss of power to the pumping system, and others. Since the catchment is designed to provide subcriticality and perpetual cooling for any atmosphere, the inflow of a gas other than helium is accounted for as well. For cases where the flow is merely reduced rather than lost all together, some of the fuel pellets would still descend out the bottom of the reactor core, reducing the power output of that channel in the least, if not rendering the system sub-critical. In the unlikely event that this low flow rate were insufficient to cool the remaining pellets, even at the reduced power, shutdown and cooling could be achieved quickly and easily by shutting down the pumps altogether.

In an event of increased fuel temperature in the pellets, be there normal coolant flow or even for the case of reduced flow mentioned above, several mechanisms would begin to act to return conditions to normal. Negative temperature co-efficients of reactivity -- mainly for the fuel, coolant, and moderator -- would cause a decrease in the fission rate reducing the power and subsequently the fuel temperature. Alternatively, the ablative layer in the fuel pellets described in the previous section could cause the particles to fragment and elutriation would potentially remove some fuel from the core. These mechanisms could eliminate the consequences of loss-of-reactivity control accidents, unforseen reactivity insertions and subsequent excursions, loss-of-heat sink scenarios such as feedwater line failures, and others. In addition, due to the large volume of moderator between the suspension columns, there is the potential for this medium to act as a significant heat sink in an accident scenario. Of course, for any accident, coolant pump shutdown would remove the fuel from the core, halt the fission reaction and provide sufficient decay heat removal autonomously.

The elimination of loss-of-coolant accidents and reduction of reactivity excursion-type effects through passive, inherent means are to be provided by this concept. However, other deviations from normal operation are also conveniently addressed by the PSR and its coated-particle fuel form. Mechanical damage to the fuel that could potentially occur in refuelling and handling operations is minimized through the use of the durable micro-spheres. The likelihood of damaging many of these fuel elements in any one event is minimal due to their ability to move about one another, and any fragmenting that does occur could be dealt with by the quality assurance provisions already present for normal operation. The blockage of a fuel channel by a foreign object could potentially cause many fuel pellets to be trapped together, however negative reactivity feedback coefficients and pump shutdown are means by which reactor shutdown might be used to avoid any damage.

For even less likely events such as earthquakes, the pellet fuel would maintain its integrity in all but the most extreme conditions -- far more so than conventional rigid fuel which has no means of moving about within the core when such drastic vibrations occur. Since the PSR has no need for special safety systems such as ECC injection, the failure or reliability of such systems is of no significance to the shutdown or cooling capabilities of the reactor. This simplified means of providing safety is beneficial when considering the view that system accidents are in some ways normal, or expected in complex devices with strong coupling between components (Perrow 1984). By designing a simpler system with primary emphasis on safety reduces such complexity, improves the overall safety of the plant and likely reduces costs, making the reactor more attractive to utilities.

2.5 Material Properties

Various materials have been incorporated into the conceptual designs of the suspended pellet-type fission reactors outlined in Sections 2.2 and 2.3 above. The suspending fluids, when moving at the appropriate velocity, are to support the weight of the particles in each column. To date, the proposed fluids include pressurized helium (He), carbon dioxide (CO_2), water (H_2O), heavy water (D_2O), or liquid metals such as lead (Pb) or sodium (Na). In the determination of the required suspension velocities, three fluids -- which would also act as coolants but not necessarily moderators -- are analysed. The primary one is helium gas -- that which is a part of the PSR concept, chosen primarily as it is inert and has the potential to be used in a direct energy conversion system. However, light water and liquid lead are also analysed to allow for comparison with the other conceptual designs discussed in Section 2.2.

Table 2.2 contains expressions and references for the properties of these fluids needed in the calculation of suspension velocities (Chapter 3). The formulae for the density and viscosity of helium agree well with tabulated values in the literature (Tsederberg, Popov and Morozova 1971), a pressure of 5 MPa and a temperature of 800 K are generally assumed in subsequent calculations unless otherwise noted. These are typical coolant conditions in the PSR, partially determined from analysing the suspension requirements (Harms and Kingdon 1993), and are similar to those in present-day HTGRs (Duderstadt and Hamilton 1976). At such pressures and temperatures helium gas flow is essentially incompressible -- ie. its density is unchanged due to the flow itself -- since the speed of sound therein, $a_{He} > 1000$ m/s, is much greater than the velocities required for pellet suspension (Kingdon 1994). For light water as the suspending fluid, a pressure of 15 MPa and a temperature of 300°C

Table 2.2: Fluid and solid properties necessary for the calculation of the suspension velocities in Chapter 3. The pressure p is in MPa, and T is in Kelvin.

	density, ρ ($kg\ m^{-3}$)	viscosity, μ ($kg\ m^{-1}\ s^{-1}$)
helium (He)	$480.91 \cdot p/T$ [a]	$4.646 \times 10^{-7} \cdot T^{0.66}$ [a]
water (H_2O)	p and T dependent[b]	p and T dependent[b]
liquid lead (Pb)	10500	T dependent[c]
uranium carbide (UC)	13630	—
uranium dioxide (UO_2)	10970	—

[a](Dalle Donne and Sordon 1990).

[b]tabulated in Sengers and Watson (1986).

[c]tabulated in Rothwell (1962).

---

are assumed -- similar to today's pressurized water reactors (PWRs), while for liquid lead the conditions used in the concept of Taube et. al. (1986) are utilized (T = 500°C).

For the fluid velocity calculations in Chapter 3, the particles are considered to be made completely of uranium carbide (UC) or uranium dioxide (UO_2). Thus, any protective coatings around the fissile material are assumed to be sufficiently thin so that the coating density may be regarded as the same as the fissile material's in the calculation of the pellet mass. Since the dominant dependence of suspending velocity is pellet size, and since the protective layers are relatively very thin, this approximation introduces negligible error. From a manufacturing perspective, a sphericity[8] -- the measure of a pellets' nearness to ideal spherical shape -- of 0.95 is easily attained with good consistency (Baetson 1993) for UC pellets, however UO_2

---

[8]Sphericity is more formally defined in Chapter 3.

pellets are also compatible with the PSR design. Thus, significant variations in pellet shape are also of little concern.

Two materials have been considered for the vessels containing the fissile particles and helium gas. The first is a zirconium (Zr) alloy such as that used in CANDU reactor pressure tubes and other reactors' components, the other being carbon-based materials such as carbon composites (Figuerido et. al. 1990). In both cases, the inlet temperature of helium to the core region is approximately 250°C, similar to that of HTGR coolant cycles. However, as the Zr alloy may experience corrosion or other structural degradation at the high outlet temperatures typical of HTGRs, its use requires the gas exiting the core be limited to ≤400°C. The moderator of the PSR in such a case would be either H_2O or D_2O, but these are less desirable than graphite which has a much larger thermal inertia and thus resistance to temperature excursions.

Conversely, the newer carbon composite materials are consistent with a graphite moderator and capable of withstanding the higher outlet temperatures of gas-cooled reactor cycles. Thus, the helium temperature may be raised to at least 900°C for these materials. Regardless of the temperature (250-900°C), the superficial gas velocity required to support the pellets varies by only a few cm/s. This is of no consequence when compared to operating velocities on the order of m/s, as determined in Chapter 3.

Since the system considered here uses helium gas to suspend the particles and most likely carbon-based materials for the suspension columns, ablative materials for the fuel pellets that sublime near 1000°C were initially sought, as typical operating conditions in HTGRs could extend to ≈900°C. While at least half a dozen materials were identified, only a few were of a reasonably neutron-transparent composition -- crucial for use in a fission reactor. These included zirconium tetrafluoride (ZrF_4),

zirconium trifluoride (ZrF_3) and aluminum trifluoride (AlF_3), from which the first was selected for the initial calculations involving the ablator layer (Chapter 4) due to its sublimation temperature of ≈ 910°C.

A simple three layer pellet -- fuel core, ablative layer, and collision-resistant outer shell -- is used to model the pellets' thermal characteristics in Chapter 4. A fuel core of UC and outer shell of silicon carbide (SiC) are selected as representative materials for such components, some well established properties of which are summarized in Table 2.3. However, the ablative material used in these calculations suffered from the same lack of fundamental property data that did all the candidate ablative materials (Poulain 1996). In fact, the thermal conductivity of ZrF_4 -- a crucial parameter for these calculations -- is nearly non-existent in the literature. A few studies have been conducted at relatively low temperatures for this material, but there are none in the temperature range of interest. As such, the results of the temperature calculations are limited due to the poor material data available at this time.

2.6 Alternative Means of Pellet Suspension

The upper and lower boundaries formed by the expansion and contraction in the suspension column of the PSR are only one possible method of suspending micro-fuel particles in a fission reactor core while still retaining the same measure of inherent safety against LOCAs. One minor alteration was illustrated in Figure 2.4 -- the installation of a coaxial tube arrangement with the inner tube sufficiently porous for gas coolant transmission while restraining fuel pellet motion (Harms and Kingdon 1994), providing a linkage to previous particle bed reactors (Powell, Takahashi and Horn 1986). The minute perforations in the inner column provide an additional path for the coolant to flow upward through the core. Other variations include those of the

Table 2.3: Material properties for the components of the micro-fuel pellets modelled in Chapter 4.

	uranium carbide (UC)	zirconium tetra-fluoride (ZrF_4)	silicon carbide (SiC)
density, ρ (kg m^{-3})	13630	4430[a]	3220[a]
thermal conductivity, k (W m^{-1} K^{-1})	≈ 23[b] (600 - 2000 K)	~ 0.75[c]	≈ 50[d] (800 - 900 K)
specific heat capacity, C_p (J kg^{-1} K^{-1})	≈ 285[e] (@ ~ 1300 K)	≈ 620[f]	T dependent[g]
melting (sublimation) temperature T_{melt} (°C)	≈ 2500[a]	(sublimation) ≈ 910[h]	≈ 2750[a]

[a](Lide 1995).

[b](Kosolapova 1971).

[c](Poulain 1996).

[d](Samsonov 1974).

[e](Storms 1967).

[f](Chase et. al. 1985).

[g]C_p (J kg^{-1} K^{-1}) ≈ 104.5[13.25 - 2035 T^{-1} + 2.88×10^7 T^{-2} exp(-5680/T)], T in K.

[h](Barin, Knacke and Kubaschewski 1977).

---

concepts of Sefidvash (1996), Taube et al. (1986), and the remaining concepts described in Section 2.2, including a perforated upper boundary which allows for the passage of the coolant but not the fuel particles, Figure 2.2(b), and a lower trap door sustained by the coolant flow to act as the lower core boundary, Figure 2.6(a). Additional concepts include a suspended column supporting a fixed particle bed (Baetson 1993), and multiple vertically linked fluidized beds (Kornilovsky 1996), Figure 2.6(b) and 2.6(c), most of which were conceived of to improve the stability of the fuel particle distribution within the reactor core over that of a pellet suspension, as the latter may

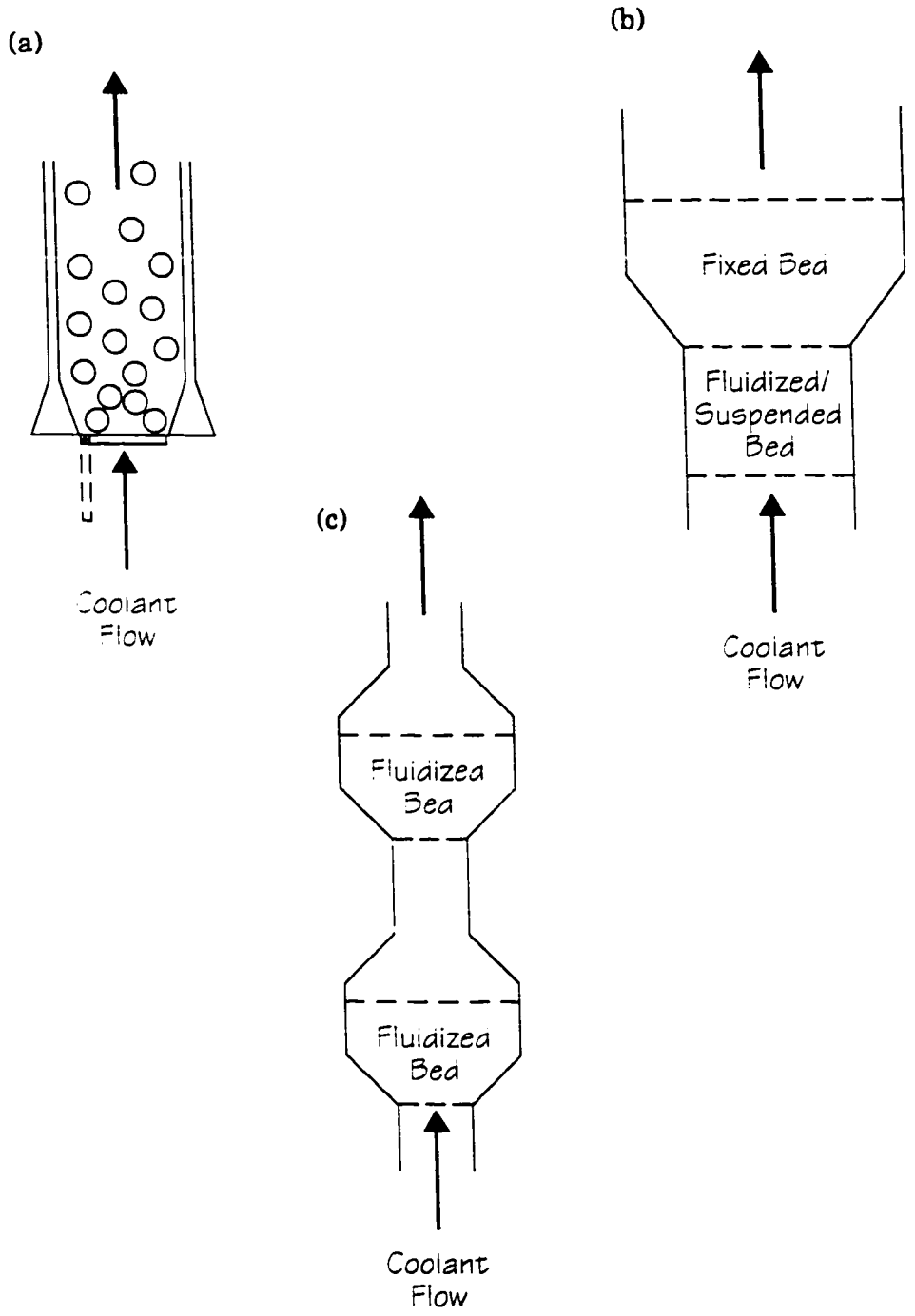

Figure 2.6: Additional methods of pellet suspension which still retain the mechanism of fuel ejection from the core for LOCA avoidance.

be subject to large density fluctuations.

2.7 Advantages of Pellet Suspension

In addition to the passive safety characteristics achievable in the PSR, there are many other advantages to using a suspended fuel pellet arrangement for a fission reactor. Because of the immense surface area per unit volume characteristic of pellet fuel, much higher heat transfer rates can be realized, lessening the thermal burden on materials used in the fuel elements and thus allowing for higher coolant temperatures. This subsequently increases the efficiency of conversion from thermal to electrical energy. The extensive mixing and agitation properties of suspended fuel arrangements also provide more uniform fuel temperatures throughout the fission core and result in more even burnup of the fuel compared to that of rigid-fuel reactors.

The well developed coating technologies provide the fissile fuel kernel with thin, concentric, protective shells of various materials, and thus allow for even greater temperature and burnup flexibility; examples of such particles are the bi-isotropic (BISO) and tri-isotropic (TRISO) types manufactured by, among others, General Atomics and discussed in more detail in Chapter 4. In addition, by manufacturing pellets with different fissile isotopes, several distinct fuels can be used in a single reactor at the same time, each in their own homogeneous molecular form (i.e. plutonium dioxide, PuO_2, thorium dioxide, ThO_2 , etc.) rather than as mixed-oxide (MOX) fuels. The latter are more difficult to manufacture, but as of yet are one of the few methods for burning additional fissile fuels -- over and above uranium -- such as the accumulated stockpile of weapons' plutonium in conventional fissile fuel-rod assemblies.

More generally, reactors being designed today benefit from the vast amount of

knowledge obtained since the conception of the current generation approximately half a century ago. The first generation of nuclear power plants were forced to compete with "cheap coal" and thus had to push the limits of pressure and power density for improved economies of scale. Such a restriction is not as tight now as it was then owing to the increased overall cost, including the environmental cost, of fossil fuel-based means of electricity generation. The PSR has the potential of incorporating all of these advantages into a "next generation" fission reactor design.

The following three chapters discuss, in turn, the aspects of the PSR which address loss-of-coolant accidents, reactivity excursion accidents, and closure of the nuclear fuel cycle, respectively. Each begins with a description of the technology to be applied to that area and how it is incorporated into the PSR to alleviate the particular concern relating to nuclear power. Analyses to determine the utility of each approach are then outlined and summarized. Finally, the implications of such analyses on the ability of the PSR to accomplish its goals are discussed, and possible improvements or alternatives presented.

Chapter 3

Pellet Suspension and Power Ratio

The most distinct feature of the PSR is the suspension of fuel particles in columns of upward flowing helium gas. It is this characteristic which provides for transparent loss-of-coolant accident avoidance through the natural action of gravity if the helium flow is disturbed. This straight-forward means of LOCA avoidance is always available and is not hampered by the reliability of -- or complex interactions between -- active monitoring components and safety systems.

The progression from densely packed particle beds to what are know as fluidized beds -- used in a variety of chemical engineering and other applications -- and finally to pellet suspensions is described in this chapter. From the velocities which are determined to be necessary to provide a pellet suspension, several conclusions regarding the PSR concept are drawn.

3.1 Packed Beds

To determine the upward fluid velocity necessary to establish and sustain the fuel pellets between the lower constriction and upper expansion in a column of the PSR, a well-founded development from work involving fluid flow through packed beds is a beneficial starting point. The following derivation is considered to be sufficient to provide context and justification for the lower velocity bound selected in a

subsequent section.

A packed bed is a static bed of solid particles through which a fluid is made to pass, Figure 3.1. Theory and experimentation have both been used to establish the pressure drop as the fluid passes through the bed of particles, most often in a cylindrical column. A critical review of such analyses by Ergun summarizes and synthesizes the results of other important contributors (see references in Ergun 1952). It is well established that the four main factors affecting energy loss -- or the more observable associated pressure drop -- through a packed bed are: (i) fluid velocity, (ii) fluid density and viscosity, (iii) the degree of particle packing in the bed, and (iv) particle size, shape and surface nature. Henceforth, all fluids will be assumed to be flowing upward in the vertical direction, meaning only the magnitude of the rate of flow -- i.e. the speed -- be specified. However, in the relevant literature, the term velocity is used to refer to this flow rate magnitude, with the direction of motion understood. A similar practice will be used here to retain consistency with the nomenclature common to this field, and should not cause undue confusion.

(i) Fluid velocity: For low flow rates, the pressure drop in a packed bed is observed to be proportional to the superficial fluid velocity, U, while at high flow rates this pressure decrease varies with U^2. Reynolds was the first to propose that the pressure drop, Δp, in a tube containing no particles over a length L could be expressed as the sum of two terms (Reynolds 1900):

$$\frac{\Delta p}{L} = C_1 U + C_2 \rho_f U^2 , \qquad (3.1)$$

where ρ_f is the mass density of the fluid, and C_1 and C_2 are parameters for a particular system. Experimental results from Ergun and others determined that Eq. (3.1) was also sufficient to express the pressure drop through a packed bed of particles

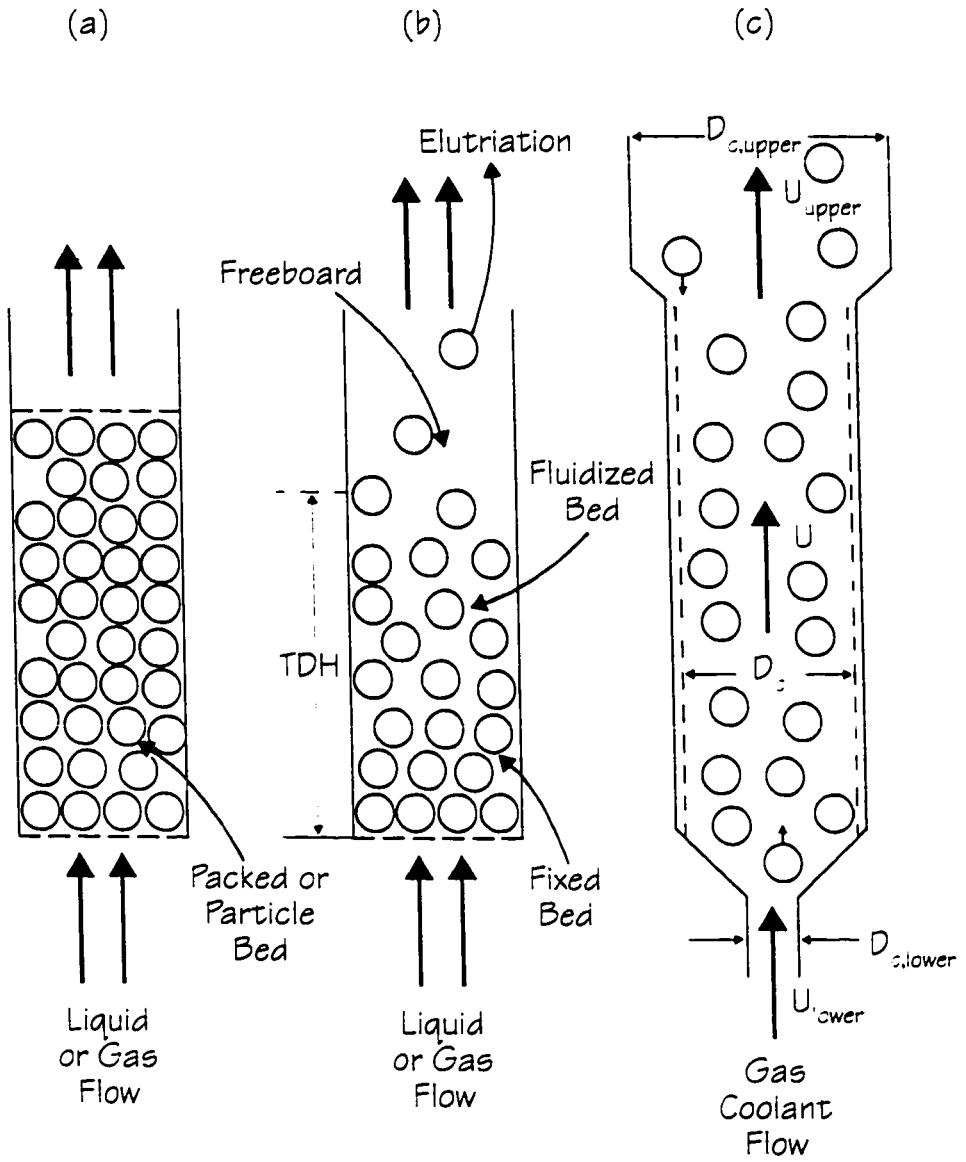

Figure 3.1: (a) Schematic depiction of a packed or particle bed, (b) a conventional fluidized bed, and (c) a suspension column for the PSR. The size of the particles has been enlarged for illustration purposes.

as a function of fluid velocity.

(ii) Fluid density and viscosity: In the limit as U→0, the ratio of pressure drop to velocity (Δp/U) tends to a constant, namely $C_1 \cdot L$ for Eq. (3.1). This is the condition for viscous fluid flow, and thus C_1 must include the fluid viscosity μ_f. The first term in Eq. (3.1) thus accounts for the viscous energy losses and the second for the kinetic energy losses (Ergun 1952). The latter are evident in the case of high fluid velocities where the flow becomes turbulent and kinetic energy losses dominate. These two effects are approximately equal in magnitude for Reynolds numbers[1] of 60 (Ergun and Orning 1949). Since the effect of density is already included in the kinetic energy losses, Eq. (3.1) can be re-written as

$$\frac{\Delta p}{L} = C_3 \mu_f U + C_2 \rho_f U^2 , \qquad (3.2)$$

where $C_3 = C_1/\mu_f$. Note Δp/L is really $\Delta(p/L + \rho_f \cdot g)$, where g is the acceleration due to gravity, but the latter term is negligible in comparison to the former for fixed beds. Corrections which are introduced below for determining U in fluidized beds indicate that this term is not always negligible, even for systems using a gas as the fluidizing medium.

(iii) Degree of particle packing in the bed: The effect of void fraction, ϵ -- the fraction of the system's volume not occupied by particles -- on the pressure drop through packed beds was the subject of much debate for some time. Once it was established that there were two contributions to the energy losses in the bed -- viscous and kinetic effects -- it was then determined that each possessed a different dependence on the bed

[1]The Reynolds number for fluid flow is defined in Section 3.2.

void fraction. The void fraction effect in the viscous term was found by Kozeny (outlined in Ergun 1952), who assumed that the bed was equivalent to a set of similar parallel channels. Therein it was established that the dependence of pressure drop on void fraction was $(1-\epsilon)^2/\epsilon^3$, which was later verified experimentally by numerous researchers (Ergun 1952 references).

The effect of void fraction in the kinetic term was determined by Burke and Plummer (1928), whose work relied on a theory that the total resistance to fluid flow by the bed could be expressed as the sum of the resistances due to each particle. They found the dependence of pressure drop on void fraction to be $(1-\epsilon)/\epsilon^3$, also later confirmed experimentally. Introducing these dependencies into Eq. (3.2) yields

$$\frac{\Delta p}{L} = C_4 \mu_f \frac{(1-\epsilon)^2}{\epsilon^3} U + C_5 \rho_f \frac{(1-\epsilon)}{\epsilon^3} U^2 , \qquad (3.3)$$

where C_4 and C_5 again are parameters of a particular system under consideration. Note the importance of accurate measurements or calculations of the void fraction as the pressure drop through the bed is very sensitive to ϵ.

(iv) Particle size, shape and surface nature: The effect of a particle's surface nature on Δp can become very complex for irregularly shaped particles. However, since the problem considered here involves only solid, non-porous spheres (or pellets which are very nearly spherical), many of these complexities can be ignored. Particle size and shape are combined with the use of an effective diameter d, which is the diameter of a sphere with a volume equal to that of a given particle. This allows all particles to be represented by a characteristic length d, which for perfect spheres is exactly equal to their diameter.

Ergun and Orning (1949) found that the pressure drop in a packed bed varied

as $1/d^2$ in the viscous term, and as 1/d in the kinetic term. Introducing these into Eq. (3.3) gives

$$\frac{\Delta p}{L} = C_6 \frac{(1-\epsilon)^2}{\epsilon^3} \frac{\mu_f U}{d^2} + C_7 \frac{(1-\epsilon)}{\epsilon^3} \frac{\rho_f U^2}{d}, \qquad (3.4)$$

where C_6 and C_7 are constants. Using the data from at least 640 experiments, Ergun (1952) determined that $C_6 = 150$ and $C_7 = 1.75$ by least squares analysis. Thus, the pressure drop through a packed bed of particles can be represented by what is now known as the Ergun Equation:

$$\frac{\Delta p}{L} = 150 \frac{(1-\epsilon)^2}{\epsilon^3} \frac{\mu_f U}{d^2} + 1.75 \frac{(1-\epsilon)}{\epsilon^3} \frac{\rho_f U^2}{d}. \qquad (3.5)$$

3.2 Minimum Fluidization Velocity

If the behaviour of a packed bed is examined as the fluid flow rate passing up through the bed is increased, a typical progression is observed, Figure 3.2. Through the fixed bed, the pressure drop rises with increasing fluid velocity until such time that this pressure drop balances the weight of all the particles in the bed -- where the maximum packed voidage is obtained. Further increases in the fluid velocity cause the bed to expand (ϵ increases) while the pressure drop remains essentially constant. This expanded bed is initiated at what is called the minimum fluidization velocity, U_{mf}.

When the fluid velocity has increased to the point that the weight of the bed -- less its buoyancy in the fluid -- is balanced by the pressure drop through the expanded bed, this pressure drop must be given by

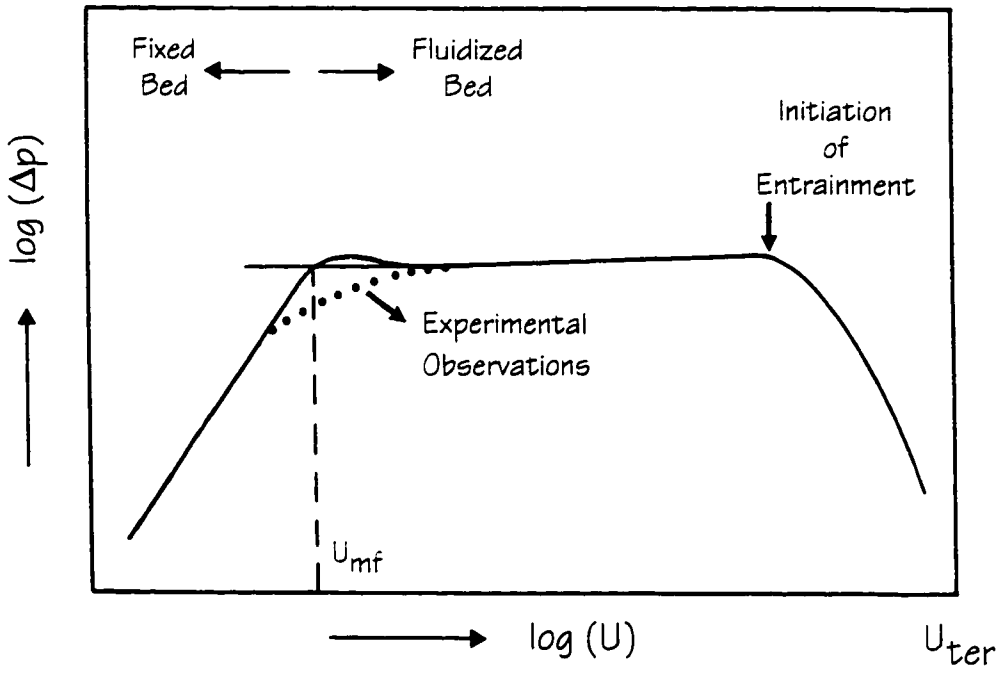

Figure 3.2: Pressure drop, Δp, as a function of fluid velocity, U, through a fixed or fluidized bed showing the minimum fluidization velocity, U_{mf} (theoretical and experimental determinations) and the onset of entrainment near the terminal velocity, U_{ter} (Davidson, Clift and Harrison 1985).

$$\frac{\Delta p}{L} = (1-\epsilon_{mf})(\rho_s-\rho_f)g\ , \qquad (3.6)$$

where ρ_s is the mass density of the particles. Eq. (3.5) can still be assumed valid in the expanded bed if one replaces ϵ with ϵ_{mf}, the porosity or voidage at the minimum fluidization velocity. Thus, equating Eqs. (3.5) and (3.6) and multiplying through by $d^3\cdot\rho_f/[\mu_f^2(1-\epsilon_{mf})]$ gives

$$\frac{1.75}{\epsilon_{mf}^3}\left(\frac{\rho_f U_{mf}\, d}{\mu_f}\right)^2 + \frac{150(1-\epsilon_{mf})}{\epsilon_{mf}^3}\left(\frac{\rho_f U_{mf}\, d}{\mu_f}\right) = \frac{d^3\rho_f(\rho_s-\rho_f)g}{\mu_f^2}\ , \qquad (3.7)$$

where $(\rho_f\cdot U_{mf}\cdot d\ /\mu_f) = Re_{mf}$, the Reynolds number of fluid flow past particles with an effective diameter d at the minimum fluidization velocity. Eq. (3.7) is a quadratic equation in U_{mf}, more apparent in the form

$$U_{mf}^2 + \frac{150}{1.75}\frac{\mu_f(1-\epsilon_{mf})}{\rho_f\, d}U_{mf} - \frac{\epsilon_{mf}^3\, d(\rho_s-\rho_f)g}{1.75\rho_f} = 0\ . \qquad (3.8)$$

Approximate solutions of Eqs. (3.7) or (3.8) can be obtained for low and high Reynolds numbers (Kunii and Levenspiel 1969), corresponding to mainly viscous or kinetic losses through the bed, respectively:

$$U_{mf} = \frac{\epsilon_{mf}^3\, d^2(\rho_s-\rho_f)g}{150\mu_f(1-\epsilon_{mf})}\ , \qquad Re_{mf} < 20\ , \qquad (3.9)$$

and

$$U_{mf} = \sqrt{\frac{\epsilon_{mf}^3\, d(\rho_s-\rho_f)g}{1.75\rho_f}}\ , \qquad Re_{mf} > 1000\ . \qquad (3.10)$$

These expressions for U_{mf} are, of course, limited since they come from an

extension of packed bed results. Over the last forty years there have been numerous examinations of the problem of estimating the minimum fluidization velocity, most being empirical correlations for more and more experimental data. Since, in practice, the transition from an increasing pressure drop to a constant pressure drop is a continuous process (shown by the dotted curve in Figure 3.2), U_{mf} is estimated by extending the two asymptotes of a pressure-velocity plot and taking their intersection. Different results have been obtained depending upon whether liquids or gases are used as the suspending medium. Davidson, Clift, and Harrison (1985) summarize many of these results. They include at least fourteen correlations for liquid-solid systems and at least eighteen for gas-solid systems. The theoretical determination of U_{mf} from the Ergun Equation is now recognized as insufficient in comparison to these more recent empirical correlations, but has been included here for historical context and comparison.

Davidson et. al. also establish which of the correlations were the most accurate at the time of their publication. Not surprisingly, the more recent equations for U_{mf} were the best, having incorporated more data than earlier versions. For liquid-solid systems, the empirical fit of Wen and Yu (in Davidson et. al. 1985):

$$Re_{mf} = \sqrt{(33.7)^2 + 0.0408\,Ga\,Mv} - 33.7\ , \qquad \textbf{(3.11)}$$

is used here for $Re_{mf} \leq 100$, where $Ga = d^3 \cdot \rho_f^2 \cdot g/\mu_f^2$ is the Galileo number, and Mv is the density ratio $(\rho_s - \rho_f)/\rho_f$, yielding

$$U_{mf} = \frac{\mu_f}{\rho_f \phi_s d_p}\left(\sqrt{(33.7)^2 + \frac{0.0408 g \rho_f (\rho_s - \rho_f) \phi_s^3 d_p^3}{\mu_f^2}} - 33.7\right) . \qquad \textbf{(3.12)}$$

For $100 \leq Re_{mf} \leq 1000$, the correlation of Riba et. al.:

$$Re_{mf} = 1.54\times 10^{-2} Ga^{0.66} Mv^{0.70} , \qquad (3.13)$$

or

$$U_{mf} = \frac{0.0154 g^{0.66} (\rho_s - \rho_f)^{0.70} \phi_s^{0.98} d_p^{0.98}}{\mu_f^{0.32} \rho_f^{0.38}} , \qquad (3.14)$$

is used. The Reynolds number of the system at the minimum fluidization velocity is now $Re_{mf} = \rho_f \cdot U_{mf} \cdot \phi_s \cdot d_p / \mu_f$. The shape of the pellets, previously incorporated into an average outer diameter d, is now accounted for with the pellet sphericity ϕ_s, which is given by

$$\phi_s = \frac{\textit{surface area of a sphere with the particle's volume}}{\textit{surface area of the particle}} . \qquad (3.15)$$

Thus, d has been replaced by $\phi_s \cdot d_p$ in the preceding equations, with d_p the mean diameter of the pellets.

For minimum fluidization velocities in gas-solid systems the correlation of Thonglimp in its second form is used:

$$Re_{mf} = \sqrt{(31.6)^2 + 0.0425 Ga\, Mv} - 31.6 , \qquad (3.16)$$

which can be expanded to

$$U_{mf} = \frac{\mu_f}{\rho_f \phi_s d_p} \left(\sqrt{(31.6)^2 + \frac{0.0425 g \rho_f (\rho_s - \rho_f) \phi_s^3 d_p^3}{\mu_f^2}} - 31.6 \right) . \qquad (3.17)$$

Note the similarities and differences between the several equations for the minimum fluidization velocity, U_{mf}, and recall that there are at least thirty others in the literature between the proposal of Eq. (3.7) and Eqs. (3.11), (3.13) and (3.16). The void fraction, ϵ, is not explicitly included in the latter three as it has also been correlated

as a function of U_{mf} and d_p, and thus its effect is implicit in the correlations.

3.3 Types of Fluidization

Fluidized beds are used in a wide variety of applications, including chemical processing and even some electrical power generation. The particles, which are not necessarily all of the same size, are generally fluidized by a liquid or gas -- a state that may be considered the reverse of sedimentation. The phases of the system are efficiently and extensively mixed in fluidization, resulting in excellent heat and mass transfer characteristics. Depending upon how much the superficial suspending velocity exceeds the minimum fluidization velocity, a variety of different flow regimes can result, Figure 3.3. In the most common -- and often the most interesting -- cases, known as the so-called bubbling, slugging and turbulent regimes, parameters such as particle velocity, gas pressure and void fraction tend to fluctuate in time. In addition, the presence of extensive voids or "bubbles" are often observed in these systems.

However, once the minimum fluidization velocity has been surpassed in a fluidized bed, liquid-solid and gas-solid systems behave in significantly different manners. For liquid-solid systems, further increases in U generally give a smooth progression of bed expansion where the distribution of solids in the fluidized bed is fairly uniform throughout. This is known as particulate fluidization, and is usually only encountered for $\rho_f \sim \rho_s$ (Figure 3.3). For gas-solid systems at low to medium pressure or for liquid-solid systems where $\rho_f << \rho_s$, "bubbles" and particle "slugs" tend to form and the resulting particle distribution in the bed is non-uniform. This is called aggregative fluidization.

For gas-solid systems at high pressure, both types of fluidization are possible. To classify which is occurring in a particular case, early experimental work by Wilhelm

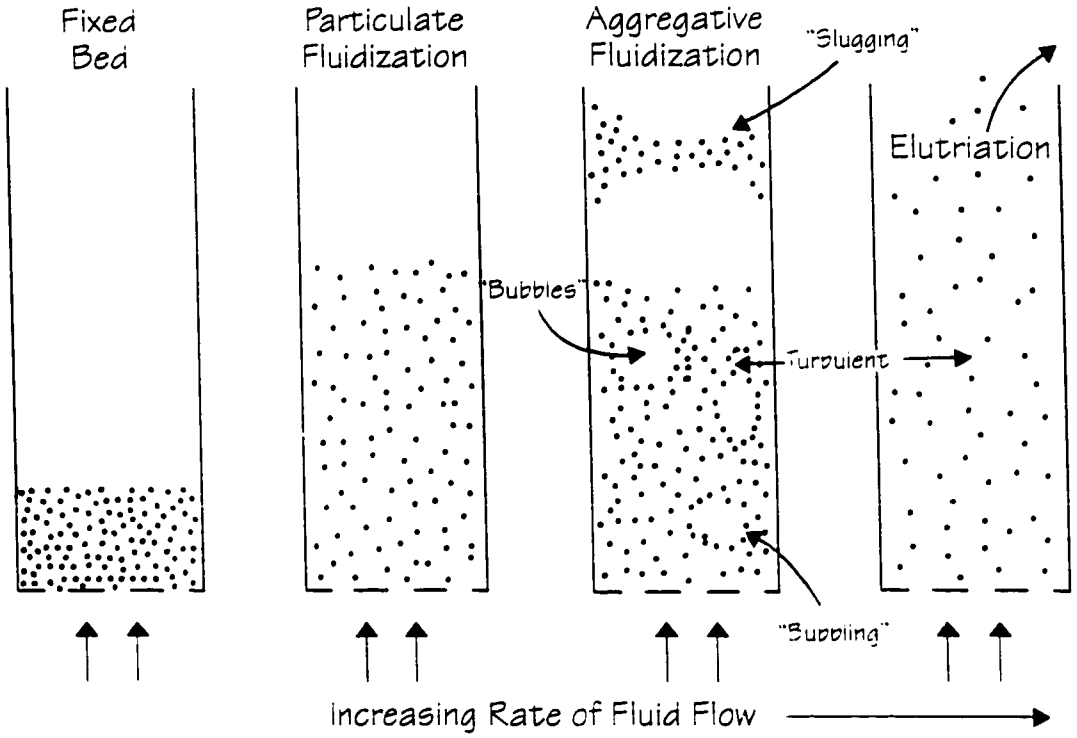

Figure 3.3: Schematic depiction of fixed, particulately and aggregatively fluidized beds, and the onset of elutriation (Kunii and Levenspiel 1969).

and Kwauk (1948) suggested that for Froude number $Fr_{mf} = U^2_{mf}/(d_p \cdot \phi_s \cdot g)$ = (inertial force)/(gravitational force) > 0.13, the bed was aggregative, and for $Fr_{mf} < 0.13$, the bed was particulate. A subsequent analysis by Romero and Johnson (outlined in Kunii and Levenspiel 1969) determined the boundary between the two regimes was more accurately expressed in terms of a product of four factors:

$$(Fr_{mf})(Re_{mf})(Mv)\left(\frac{L_{mf}}{D_e}\right) = C \,, \qquad (3.18)$$

where L_{mf} is the height of the bed at minimum fluidization, and D_t is the diameter of the column. For C < 100 the fluidization is smooth or particulate, and for C > 100 the bed is aggregatively fluidized, or bubbling. Tall, narrow tubes are the most susceptible to bubbling and slugging, and increased wall effects are present in smaller diameter columns.

In most applications to date, a large bed of small particles (diameters from micrometres to centimetres) is just slightly fluidized by the passage of a fluid up through the static bed (Figure 3.1). The gas or liquid flow rates are mainly dependent upon the particles' size and degree of fluidization desired, ranging from a few centimetres per second to metres per second. For the PSR, the hydrodynamic suspension of fuel particles in an upward flowing coolant against the force of gravity requires that the mean fluid velocity be greater than the minimum fluidization velocity. This velocity is, however, generally too small to provide a suspension of many particles -- as would be desired for most suspended pellet-type reactor cores -- but here will be used as a lower velocity bound for the mean fluid velocity which does provide such a suspension.

It should also be noted that for the PSR, helium pressure has a significant influence on the suspending velocity of the fuel pellets due to its effect on the helium

density in Eq. (3.17), and thus on the evenness of the particle distribution within the core. As uniformity tends to decrease with an increase in the superficial velocity of the suspending gas for aggregative fluidization, and since the required suspending velocity decreases at higher pressure, it is advantageous to operate the PSR gas system at an elevated pressure for suspension uniformity, as well as other considerations. Thus, a value of 5 MPa for the helium was deemed appropriate. This provides a significant decrease in the minimum fluidization velocity -- and, as will be shown in the next section, the terminal velocity as well -- over conditions of atmospheric pressure, and is also typical of the operating conditions in conventional high temperature gas reactors (HTGRs).

3.4 Terminal Velocity

An upper bound on the fluid flow rate required to provide a pellet suspension can be established with a particle's terminal velocity. The following is merely a brief outline of this concept, and that of the drag force on spheres. A complete description is not presented; only those aspects which directly correspond to the problem here are included. For a more comprehensive analysis of these topics, an investigation of the references cited is suggested.

If the velocity of a fluid through a fluidized bed is increased to the point that it reaches the terminal velocity, U_{ter}, of the particles, elutriation[2] -- the transport of particles out the top of the bed -- will occur (Figure 3.3). At the point that such particle entrainment begins, the pressure drop through the system begins to decrease, and will continue to do so until all the particles have been removed (Figure 3.2).

To determine U_{ter} for particles of interest here, complications of major non-

[2]Elutriation, or entrainment, is discussed in Chapter 4.

sphericity are again ignored. The terminal velocity is such that the upward drag force from the fluid on an individual particle plus the particle's buoyancy in the fluid is equal to the downward gravitational force acting on that particle, i.e.:

$$F_D + \frac{\pi d^3}{6}\rho_f g = \frac{\pi d^3}{6}\rho_s g \,, \tag{3.19}$$

where F_D is the drag force on the particle. This drag is commonly expressed as $F_D = C_D \cdot (\rho_f \cdot U^2_{ter}/2) \cdot A$, where C_D is the drag co-efficient and A is the cross-sectional area of the particle ($\pi \cdot d_p^2/4$ for a sphere) in the flow. Thus, Eq. (3.19) becomes

$$U_{ter} = \sqrt{\frac{4g\phi_s d_p(\rho_s - \rho_f)}{3C_D\rho_f}} \,. \tag{3.20}$$

Again the sphericity has been introduced -- as was done for the case of the minimum fluidization velocity -- to account for minor deviations of the particles from spherical. The drag co-efficient for smooth spheres has been determined through numerous experiments and is a function of the Reynolds number (Re) of the flow, Figure 3.4 (Clift, Grace and Weber 1978). The significant decrease in C_D at $Re \sim 4 \times 10^5$ is due to a flow transition in which the wake size behind the sphere decreases and the drag is reduced.

Clift et. al. summarize twelve empirical relationships for C_D for various ranges of Re that have been suggested in the literature. In addition, they provide recommended relationships for the drag curve based on recent data. A useful correlation for $Re < 1600$ is that of Kurten et. al. (in Clift et. al. 1978):

$$C_D = 0.28 + \frac{6}{Re^{1/2}} + \frac{24}{Re} \,. \tag{3.21}$$

This, of course, makes Eq. (3.20) transcendental. They also suggest the simple approximation of $C_D \approx 0.445$ for $750 < Re < 3.5 \times 10^5$, which is evident in Figure 3.4.

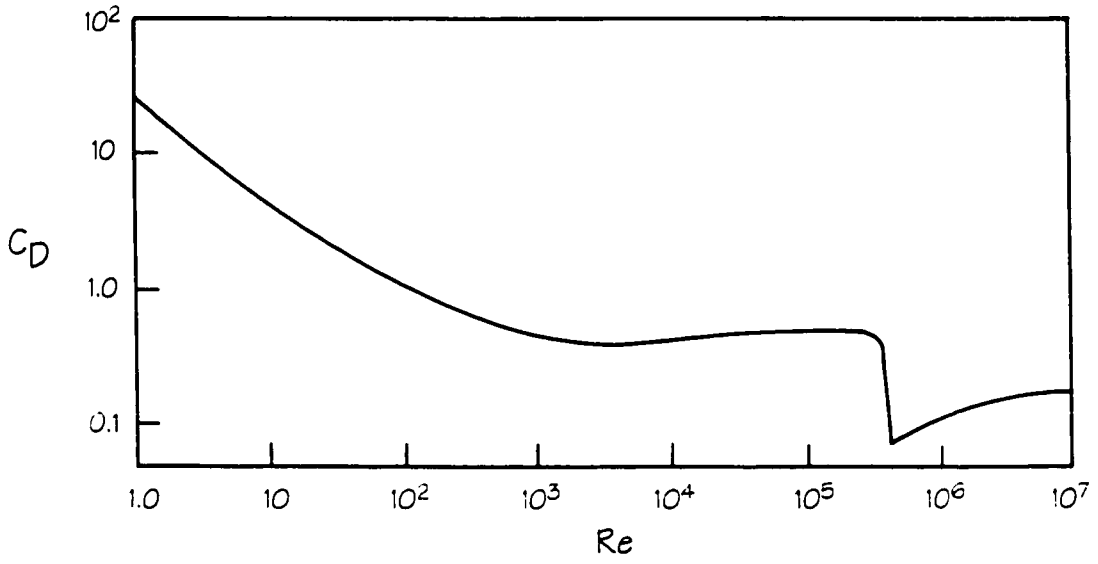

Figure 3.4: The drag co-efficient, C_D, for spheres as a function of Reynolds number, Re (Clift, Grace and Weber 1978).

Typically, the terminal velocity is about 10^2 times that of the minimum fluidization velocity at low Re, while at high Re the ratio is of the order of 10.

Using the terminal velocity as an upper bound thus provides for a range of fluid velocities which provide the necessary pellet suspension for the group of fission core concepts considered in this work. No further attempt is made to narrow this range of mean fluid velocity as, depending on the design in question, great variety may exist in the suspension requirements of the fluid.

3.5 Suspension Velocities

For the system depicted in Figure 3.1(c), a different fluid velocity will exist at several locations in the column. However, to suspend the particles between the constriction and expansion bounds, the requisite conditions on the fluid velocity are as follows:

1. $U_{lower} > U_{ter}$ in the lower column -- below the constriction -- so that any intact particles dropping out of the main column will be transported back into it by the fluid.
2. $U \geq U_{mf}$ just above the constriction to establish a state of fluidization -- as uniform as possible -- in the main column.
3. $U < U_{ter}$ just below the expansion at the top of the main column. The pressure drop and a temperature increase through the column will effectively cause the fluid velocity to increase, and this condition is necessary to ensure that an excessive number of particles will not be transported out of the column during normal operation.
4. $U_{upper} < U_{mf}$ in the upper column -- above the expansion -- so that any intact

particles entrained from the main column will fall back into it.

The minimum fluidization and terminal velocities can be determined for the three suspending fluids considered here – Section 2.5 – with the dominant dependence in each case on pellet diameter given that reasonable assumptions for the other parameters are made for a fission system. Fluid temperature, fissile particle mass density and pellet shape can be shown to have only minor effects on these velocities. Figures 3.5 and 3.6 display the regions of plausible suspension for uranium carbide and uranium dioxide fuel pellets, respectively, as a function of pellet diameter for He, H_2O, and liquid Pb as suspending fluids. There exists, evidently, little difference between these two fuels except for the case of liquid Pb. This is because both U_{mf} and U_{ter} are a function of the difference between the mass densities of the solid and fluid media (Eqs. (3.12), (3.14), (3.17) and (3.20)). The only case in which this difference is significantly altered by switching from UC to UO_2 pellets is that for liquid Pb as the coolant, since its density is of the same order as the fissile fuels'.

The boundaries of the regions in Figures 3.5 and 3.6 are determined by the minimum fluidization velocity, the terminal velocity, and pellet diameters that are deemed practical and reasonable for the suspending fluid of interest. Smaller pellets may become too difficult to manufacture and manage, or require suspension velocities that are very small when considering that the suspension regime is also part of a coolant system. Larger diameter pellets require much greater velocities for suspension and this can significantly reduce the power ratio (output to input) attainable by a system[3].

For gas-cooled systems (Watanabe and Appelbaum 1991, Harms and Kingdon

[3]This power ratio is discussed in Section 3.9.

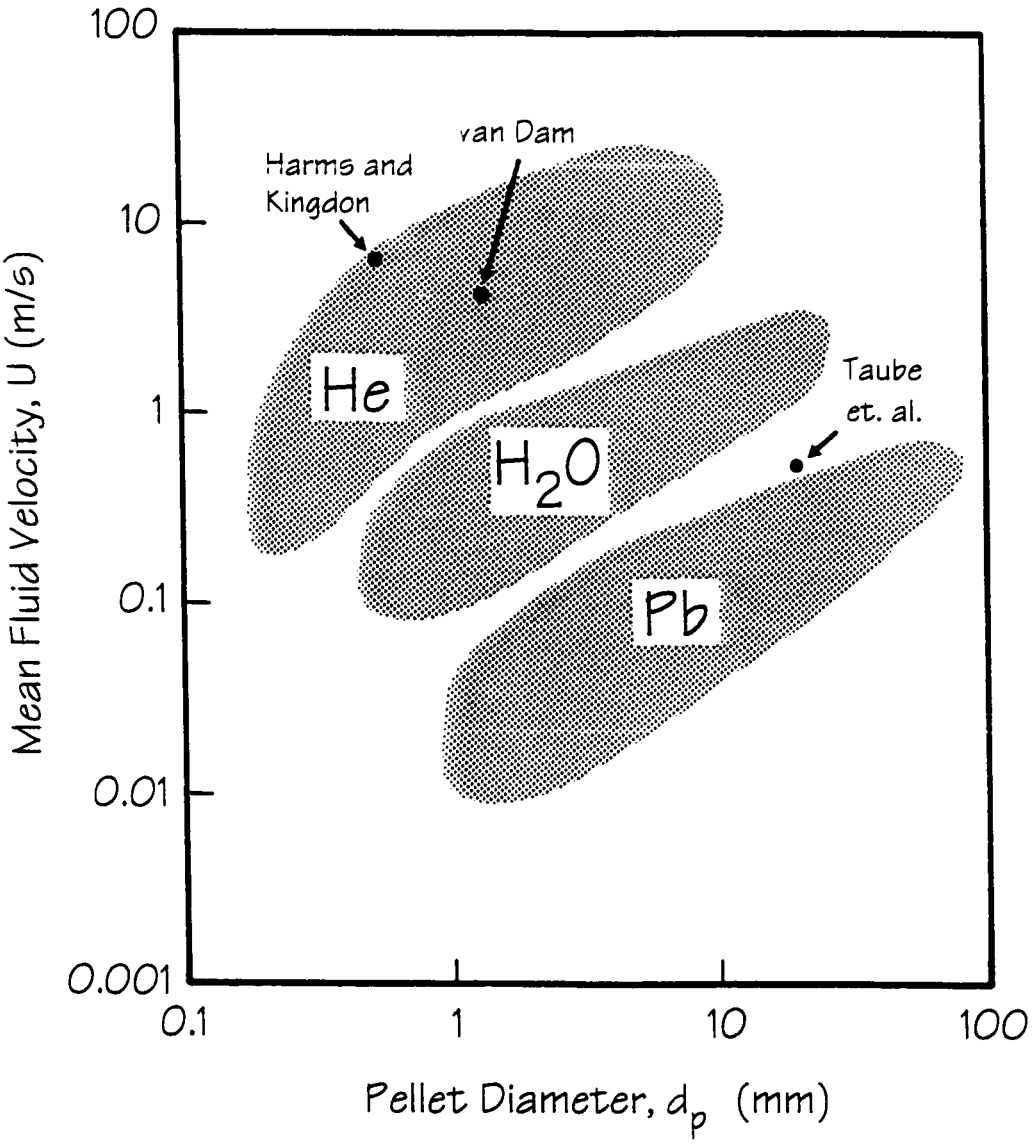

Figure 3.5: Mean fluid velocities that provide for UC fuel suspension as a function of pellet diameter for suspending media helium gas, light water, and liquid lead. Velocities used in previous concepts are also indicated.

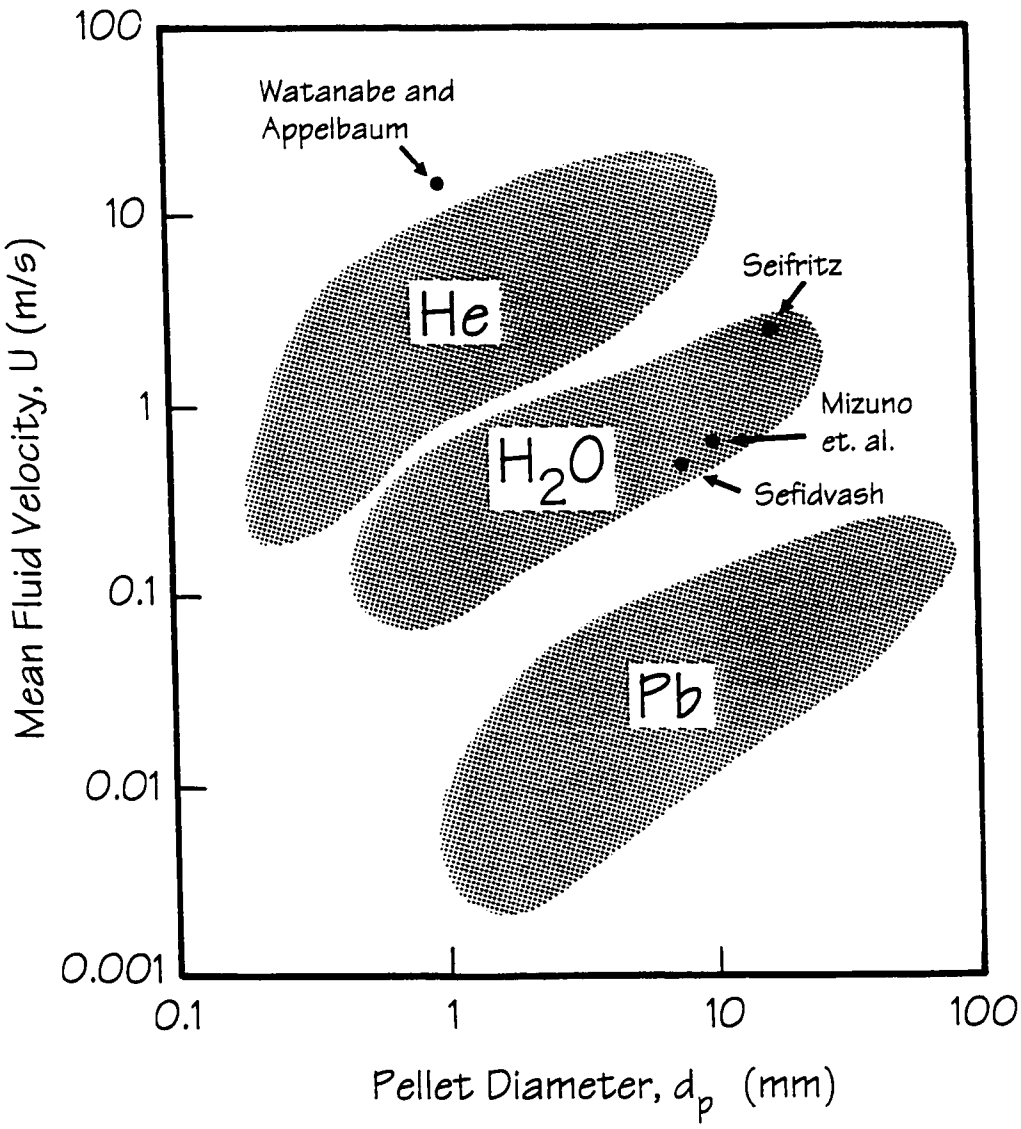

Figure 3.6: Mean fluid velocities that provide for UO_2 fuel suspension as a function of pellet diameter for suspending media helium gas, light water, and liquid lead. Velocities used in previous concepts are also indicated.

1993, van Dam 1996) in which heat generation occurs in parallel channels or columns of gas, the possibility of viscosity-induced flow instabilities leading to reduced coolant flow in the hotter channels exists (Ludewig et. al. 1996). However, analyses have shown that such an instability only occurs for a coolant temperature ratio of $(T_{out} - T_{in}) / T_{in} \geq 2.6$. While this criteria can be exceeded in the case of very high temperature coolants such as hydrogen for nuclear space propulsion systems as in the Nuclear Engine for Rocket Vehicle Application, or NERVA program (Ludewig et. al. 1996, Holman and Pierce 1986), suspended pellet-type reactors for terrestrial power generation are well below this limit and thus there is no possibility of such a viscosity-induced instability. Other effects such as turbulent flow in columns fed by a single pump may, however, need to be considered.

In a preliminary analysis of the PSR, an average pellet diameter of 0.5 mm and a corresponding helium velocity of ~ 5 m/s were selected, based on suspension uniformity considerations alone (Harms and Kingdon 1993). This, along with the operating points proposed in the conceptual designs discussed in Section 2.2 are depicted in Figures 3.5 and 3.6. For the case of Taube et. al. (1986), the operating velocity is slightly greater than the upper boundary that was established here. This, however, is consistent with the feature that the Swiss design does not use pellets in suspension, but instead packs the fuel pellets against an upper sieve in the columns thus requiring a velocity greater than U_{ter}. The only other significant contrast is for the work of Watanabe and Appelbaum (1991), whose operating velocity is again too high compared to these calculations. However, the system pressure given in their work is 1.8 MPa, which differs significantly from the 5 MPa taken for the helium case here. Since the lower pressure of such a system would require a higher fluid velocity due to ρ_f in Eqs. (3.17) and (3.20), this apparent discrepancy can be accounted for. In addition, Watanabe and Appelbaum also proposed the use of magnetic stabilization of

the pellets in the column, which would further allow for a greater fluid velocity and still provide the desired pellet suspension.

3.6 Particle Distributions

The effect of the mean pellet diameter, d_p, and the superficial gas velocity, U, on the distribution of pellets in the core is of considerable importance to ensure reasonably uniform fluidization characteristics. The effect of each quantity on the distribution is here assumed to be essentially independent of the other, allowing the technology of conventional fluidized beds to be extrapolated to the operating regimes determined in the previous section. However, the effects of these two parameters on suspension uniformity are undoubtedly linked and further analysis must include the extension of traditional concepts of fluidization to the PSR application.

To characterize the type of fluidization in the PSR, the two approaches discussed in Section 3.3 are employed. For a particle diameter of ~ 1 mm, $Fr_{mf} \approx 80 >> 0.13$, and $C \approx 10^8 \cdot L_{mf} >> 100$ for any reasonable height of the suspension. Thus, such a system would definitely be aggregatively fluidized -- as alluded to previously -- and subject to bubbling and extensive mixing. However, due to the very high porosity (90%), only a minimal amount of slugging would be expected.

During a previous development of this reactor concept, rough upper bounds of $d_p \sim 1$ mm and U ~ 10 m/s were established (Harms 1993). Both were primarily to ensure a sufficiently uniform pellet distribution in the core for reaction control and sustainment to be feasible. For particles larger than 1 mm, non-uniformities are fairly common in fluidized beds, and they obviously require large gas velocities (tens of metres per second) to be suspended (Figures 3.5 and 3.6). Suspending velocities of more than 10 m/s result in significant turbulence and the particle distributions become

very susceptible to localized density fluctuations -- often due to the passage of large bubbles through the particles. Such disturbances could cause uneven fission reaction conditions within the core and subsequent control problems. The alternate method of maintaining uniform particle distributions in the core using ferromagnetic pellets and magnetic fields proposed by Watanabe and Appelbaum (1991) is not incorporated into this study of the PSR.

The parameter and design restrictions associated with the dynamic stability of the fuel system have yet to be considered in complete detail. Recent analyses for the parameter ranges of interest suggest that there are, however, no fundamental deficiencies in the concept (van Dam 1996b; Borges and Vilhena 1995; Eskandari and Ghasemi-zad 1995; Ahlf, Conrad, Cundy and Scheurer 1990). Pellet dynamics issues within the suspension regime that have been modelled include the relaxation to a stable equilibrium and pellet removal by gravity, both sufficiently rapid -- on the order of a second -- and not hampered by collisional processes to indicate that spatial density variations and pellet trajectories will not cause unacceptably high reactivity changes over significant spatial dimensions (Kornilovsky, Kingdon and Harms 1996). Through the use of appropriate geometry choices, such as variable pellet sizes and slightly conically-shaped columns, many of the effects can be further reduced (Kornilovsky and Harms 1996; Sefidvash 1996). Even the effectiveness of delayed neutrons as the primary means of retaining reactor control, despite not always being produced at the same spatial location as the corresponding prompt neutrons due to the mobility of the pellets in the suspension, has been addressed and no fundamental problems identified (van Dam 1996a).

Fuel pellet integrity has also been investigated, more details of which are presented in Chapter 4. Here it is relevant to note that the manufacturing process used to make uranium carbide pellets results in particles very resistant to damage

from events such as collisions with other particles or vessel walls. Thus, deterioration of the pellets within the reactor should not be of primary concern. However, an estimate of the maximum speed of a pellet in the PSR may be necessary to design fuel particles or vessels capable of withstanding greater impacts. Individual particle velocity fluctuations within the freeboard of a fluidized bed have been estimated analytically (Pemberton and Davidson 1986) and agree with a more heuristic argument: since the particles are orders of magnitude too massive to have significant energies due to the bed temperature alone, the maximum velocity any individual particle can achieve must not be significantly greater than the superficial gas velocity. Thus, for the PSR parameters determined above the maximum velocity of a pellet impacting a vessel wall is of the order of 10 m/s, and the maximum relative velocity between two colliding particles is ≈20 m/s. These speeds are maximums -- the likelihood of such collisions occurring is very rare. Regardless, pellets and columns should be able to withstand such impacts in order to reduce the need for quality control and the added complications of particle elutriation. In actual experiments with a liquid fluidizing medium, the measured pellet velocities were drastically less than the suspending medium's mean velocity, and damage to the particles was very minor (Watanabe and Appelbaum 1991).

If for some reason the fuel pellets do become damaged such that their size, shape, or composition is altered, their corresponding terminal velocities will also change. For a change in composition or degradation of sphericity (shape), the change in terminal velocity is fairly small and has a negligible effect on the suspension in comparison to the extensive mixing occurring in the fluidized regime. If, however, the particles are damaged such that their size is significantly reduced, such as breaking into several pieces, their terminal velocities could decrease dramatically, resulting in a fraction of them being carried out of the core by the flowing helium gas (Figures 3.1

and 3.3). For fragments which are sufficiently small, the superficial gas velocity in the column above the core will also exceed the terminal velocity and the majority will be carried out of the upper channel and would have to be filtered out of the gas stream before the helium enters any heat transfer section of the power plant, particularly if direct conversion in a gas turbine is utilized. Such filtration is important so as to avoid damage to devices such as heat exchangers or turbines, depending on the design of the remainder of the power production facility.

3.7 Suspension Column Geometric Considerations

Having established the fluid conditions in the core of a suspended pellet-type reactor, the size and shape of the columns can be further considered to optimize the fluidized state. While the contraction and expansion in the columns of the PSR are to retain the particles within the core regime, the optimal height of this core can be estimated from the fluidization conditions therein. Traditional fluidized beds are characterized by a transport disengagement height (TDH), the vertical distance above the base of the bed beyond which elutriation losses become approximately constant. While such losses would evidently be different in a PSR than conventional beds, the TDH is an approximate parameter with which to match the core height as it is an estimate of the amount a fixed bed naturally expands based on superficial gas velocity and tube diameter. Matching the core height to the TDH could minimize a build-up or depletion of pellets near the top of the core which in turn aids in maintaining the evenness of the particle distribution.

The most extensive correlations for TDH are given by Zenz, where the transport disengagement height is given as a function of superficial gas velocity and tube diameter (Zenz 1977, 1983; Zenz and Weil 1958). The vertical fuel channels in

the PSR conceptual design have an inner diameter of 20 cm, the gas velocity required to suspend ≈ 1 mm diameter uranium carbide particles ≈ 5 m/s. Unfortunately, Zenz's correlation -- nor any other (Pemberton and Davidson 1986; Kunii and Levenspiel 1969) -- does not encompass superficial gas velocities this great. Extrapolation of the curves does however, give an estimate of ≈ 5 m for the TDH in the case of these conditions, but this is obviously just an approximation.

The temperature of the helium gas has a minimal effect on the gas velocity required to support the micro-pellets of fissile fuel, when considering Eqs. (3.17) and (3.20) at plausible He temperatures. Thus, the primary restriction on the helium temperature is that it be low enough not to cause damage to the structural material used to contain the flowing gas. The PSR is most likely to use graphite for its vertical columns, and a large helium temperature rise of up to ≈250-900°C is envisioned. Such a large ΔT normally results in significant structural end-to-end stresses, but these may be dealt with in the same manner as is done for graphite channels in typical HTGRs (Cameron 1982). The good mechanical properties of graphite, even at high temperatures, combined with careful manufacturing to provide a highly isotropic medium combats irradiation deformations and provides a structurally sound column capable of withstanding the high thermal demands placed upon it.

Also of concern is the shape of the fuel channels. As the helium gas passes up through the fissioning pellets it will be heated and thus may need to expand in order not to exceed the terminal velocity of the pellets. Pressure changes will generally be minimal compared to this nuclear heating due to the large increase in gas temperature envisaged. The fuel channel diameter must increase accordingly -- in addition to the constriction and expansion bounds which define the reactor core -- in order that as uniform a distribution as possible be maintained throughout the region. Depending on the outlet temperature of helium from the core, this tube expansion varies

significantly, and will not be considered explicitly here so that the analyses below give the most demanding constraints on the tube's upper expansion and lower constriction.

The constriction and expansion diameter changes can be established by noting that the fluid flow in the main column is turbulent ($Re_D \sim 2.75 \times 10^4$) and thus the velocity profile can be assumed to obey the 1/7 power law (Whitacker 1984). Further, as mentioned previously, the fluid flow is incompressible and thus there are no density changes because of the rate of flow itself (Kingdon 1994). From these considerations and the continuity principle it can be shown that the product of velocity and tube cross-sectional area will be constant. Thus,

$$U_x D_{c,x}^2 = U_{in} D_{c,in}^2 , \tag{3.22}$$

where U_{in} ($\geq U_{mf}$ -- as per the constraints of Section 3.5) and $D_{c,in}$ are the average fluid velocity and tube diameter at the bottom -- or inlet -- of the main column, respectively.

There are two considerations used to determine the diameter of the lower tube. First, the gas velocity therein must be greater than the particles' terminal velocity. Using Eq. (3.22) with $U_x = U_{ter}$ and $U_{in} = U_{mf}$ gives a required lower tube diameter of less than 6 cm for $d_p = 1$ mm and $D_{c,in} = 20$ cm. The second constraint is a nuclear design consideration to avoid choking of the pellets in the lower tube during a shutdown scenario, specifically that the lower tube diameter be at least ten -- preferably up to one hundred -- times greater than d_p. Studies involving granular motion have shown this to be a sufficient condition to avoid choking of the pellets, and is satisfied here as in the case above, the tube is at least sixty times larger than the pellet diameter.

The temperature increase up the column of helium is assumed to be from 250°C to 900°C. From ideal gas and incompressibility considerations in a simple

cylindrical column, it can be shown that

$$\frac{U_{out}}{U_{in}} = \left(\frac{p_{in}}{p_{out}}\right)\left(\frac{T_{out}}{T_{in}}\right), \tag{3.23}$$

which gives the gas velocity at the top of the core region -- or outlet -- to be U_{out} = 5.14 m/s for d_p= 1 mm.

The U_{out} values can then be compared to the terminal velocities of the particles for the reduced pressure and increased temperature at the top of the main column. In this case, U_{ter} = 13.6 m/s for d_p = 1 mm. The general results show that for d_p > 1.6 mm, $U_{out} > U_{ter}$, and thus the desired operating conditions are not satisfied. This further restricts the maximum particle diameter which can be used and that will obey the system's suspension constraints.

Finally, the upper tube diameter $D_{c,upper}$ can be estimated using Eq. (3.22) with $U_x \leq U_{mf}$, for U_{mf} calculated at the pressure and temperature above the upper boundary. For d_p = 1 mm, $D_{c,upper} \geq$ 46 cm. This is quite large simply from the point of view of geometry, but has been inflated by taking the gas to be at its terminal velocity at the top of the core and by disregarding a possible conical expansion of the column through the core which would reduce this upper column diameter.

3.8 Column Power Capacity

Having determined the fluid velocities necessary for the establishment of a pellet suspension, a preliminary assessment of how these velocities would fit into a fission reactor core system can be made. To estimate the possible power extraction from an individual suspension column -- noting that the flow of all three of the fluids considered is incompressible -- the relation

$$P_{th} = \dot{m}\Delta TC_p = \rho_f \pi R^2 U \Delta TC_p \,, \tag{3.24}$$

where $\dot{m}$ is the mass flow rate, ΔT is the temperature difference of the coolant between the inlet and outlet of the core, C_p is the fluid's heat capacity at constant pressure and R is the column radius, is utilized.

Assuming the temperature and pressure values used in the suspension velocity calculations for the three fluids investigated, a column diameter of 20 cm and a temperature increase of 450 K, 50 K, and 200 K for the helium, water, and liquid lead cases respectively, the thermal power output from a single suspension column is of the order of 1 - 10 MW_{th} when the fluids are moving at rates suitable for maintaining the pellet suspension, Table 3.1. These temperature increases, and the resulting power outputs, are similar to those of today's reactors, especially if one considers perhaps a hundred such columns making up a reactor core.

With several quantities pertaining to the PSR now established, a comparison of these characteristics can be made with the suspended pellet-type reactors discussed in Section 2.2 and with present-day fission reactors. In fact, one finds many similarities -- especially between reactors with similar coolant and moderator systems such as the PSR and HTGR, Table 3.2. The reactor power density, fissile fuel mass, coolant temperatures, and coolant flow rates of the new designs -- particularly those of the PSR -- are generally within the range of technological experience gained with the present generation of fission reactors. Such similarities provide valuable calculational and operational experience which may be drawn upon in the design of new fission reactor core concepts.

Table 3.1: Power output from a single vertical column for typical suspension velocities.

Power Output (MW_{th})	Required Helium Velocity (m/s)	Required Water Velocity (m/s)	Required Liquid Lead Velocity (cm/s)
0.1	0.45		0.96
1.0	4.5	0.12	9.6
10	45	1.2	96
50		5.8	

3.9 Pellet Power Ratio

While the coolant types, flow rates, and thermalhydraulic parameters in general, indicate that the power necessary to provide the upward coolant flow for suspended pellet-type reactors should be a small fraction of the system's total output, a more detailed calculation of such is considered here. To do so, a determination of the ratio of electrical power derivable from the fission process to the power required to sustain the pellet suspension is formulated.

3.9.1 Geometric Model

For the power ratio calculations, a general suspended pellet-type fission core with the geometry depicted in Figure 3.7 is employed. Note again that the suspending medium acts as the coolant but not the neutron moderator, except perhaps in the case of water suspension and cooling. Pellets of mean outer diameter d_p -- including any protective coatings -- are suspended in the fluid; the fissile material in the pellets extends to a diameter $d_{p,1}$ and has a total molecular weight A_{total} . The possibility of a central core of diameter $d_{p,0}$ in the pellets that contains non-fissile material, such as the ferro-magnetic material described in Watanabe and Appelbaum (1991) -- or even

Table 3.2: Comparison of several characteristic parameters for conventional (Duderstadt and Hamilton 1976) and suspended pellet-type reactors.

	thermal power (MW_{th})	mass of U (tonne)	specific[a] power (kW/kg U)	coolant outlet temp. T_{out} (K)	coolant temp. rise ΔT (K)	coolant flow rate (10^6 kg/hr)
PWR	3600	94.9[b]	37.9	606	33	68
BWR[c]	3579	138[b]	25.9	559	17	47
PHWR[c]	1612	80[b]	20.2	566	44	32.9
HTGR	3000	39[d]	76.9	1028	418	5
GCFR[c]	2530	28[e]	90.4	915	310	10
LMFR[c]	2410	19[e]	126.8	825	172	50
Sefidvash (1996)	5[f]	0.2[f]	25.1	698	135	0.063[f]
Taube[g] (1986)	360	33.1	10.9	873	200	41
Mizuno[g] (1990)	9[f]	0.19[f]	47.7	559	16	0.13[f]
Watanabe[g] (1991)	300	3.35	89.6	1000	400	0.23
Seifritz (1992)	10[f]	1.22[f]	8.2			0.047[f]
van Dam[g] (1996)	40	~ 8.4	~ 4.7	1023	500	0.057
PSR[h]	~ 293	~ 32.8	~ 8.9	~973	~450	~ 0.386

[a]per unit mass of uranium. [b]UO_2.

[c]see the List of Symbols for explanations of reactor acronyms.

[d]UC / ThO_2. [e]UO_2 / PuO_2.

[f]for one module or column only.

[g]only one name of each research group is used to identify the different reactor concepts (the complete list is included in the corresponding reference).

[h]for one possible configuration of the PSR concept.

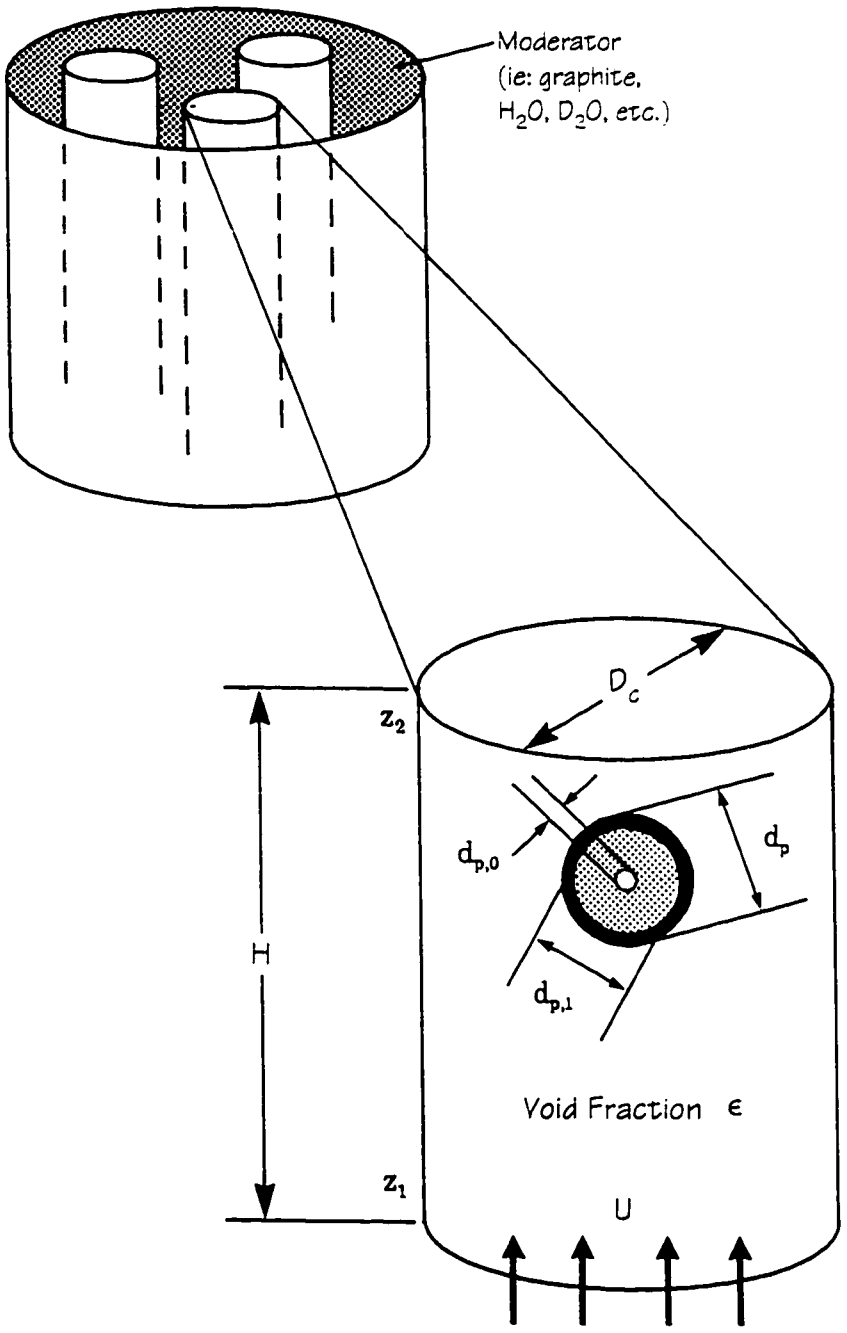

Figure 3.7: Schematic depiction of the general column and pellet geometry used for the power ratio calculations.

void -- is also allowed for. The volume of one pellet is V_p and the volume of fissile material compound in one pellet is $V_{f,p}$. One entire column has a volume V_c , and the number of pellets per column is N_p. Values for these and other parameters used in the calculations below are given in Table 3.3. Note, however, that with the exception of the PSR, the geometry of Figure 3.7, the values in Table 3.3, and other subsequent impositions differ from the concepts of the various suspended pellet-type reactors previously described (Section 2.2), and so comparison of those designs with the results established below must be done carefully and with the appropriate qualifications.

3.9.2 Individual Particle Formulation

An initial model to determine a fundamental estimate of the power ratio, independent of a specific reactor design, considers a system containing only one suspended particle. The corresponding input power is that required to establish a sufficient mean fluid velocity for the average volume of coolant associated with each individual fuel pellet. Maintaining the suspending fluid temperature at an elevated level relative to the ambient, such as lead in a liquid state, is not accounted for in this determination of the system power ratio. The kinetic energy due to the velocity of the coolant -- which comes from the pumping system -- is judged to be the dominant input power requirement, and so only it is considered.

The input power, P_{in}, for this analysis is thus

$$P_{in} = \frac{1}{\eta_{in}} P_{pump} = \frac{1}{\eta_{in}} \frac{d}{dt}(E_{pump}) = \frac{1}{\eta_{in}} \frac{d}{dt}\left(\tfrac{1}{2} m_c U^2\right), \qquad (3.25)$$

where P_{pump} is the power supplied to the appropriate volume of coolant by the pumping system, E_{pump} is the corresponding energy in unit time, and m_c is the mass of the average volume of coolant associated with a single fuel pellet. The efficiency with

Table 3.3: General column and pellet geometry parameters used in the power ratio calculations.

parameter	numerical value
column height, H	5 m
column diameter, D_c	0.2 m
void fraction, ϵ	0.9
twice the pellet coating thickness, $d_p - d_{p,i}$	0.2 mm
non-fissile central diameter, $d_{p,0}$	0

---

which electrical power is converted into pumping power, η_{in}, is a combination of the efficiencies of converting electrical power to mechanical power and mechanical power to pumping power. With the appropriate choice of motor and pump, this overall input efficiency -- sometimes called the "wire-to-water" efficiency when water is the fluid of interest -- can be conservatively estimated to be ≈ 0.75 (Karassik 1986; Warring 1984a, 1984b). Both η_{in} and η_{out} -- the latter of which is introduced below -- do not consider the effects of an entire fission power plant as no account has been made of other energy requirements such as those of fuelling mechanisms, quality control systems, or other components which may add to the power input requirements. The calculations here are solely to compare the electrical power derived from the fission system to that required to suspend the fissile fuel -- the single dominant feature that distinguishes these new reactor cores from existing rigid-fuel reactors.

Since the mean coolant velocity is intended to remain virtually constant throughout the column, only the mass of helium considered changes with time -- effectively a mass flow rate. Equation (3.25) can thus be reduced to

$$P_{in} = \frac{U^2}{2\eta_{in}}\frac{dm_c}{dt} = \frac{U^2}{2\eta_{in}}\left(\frac{\rho_f \pi D_c^2 U}{4N_p}\right) = \frac{\pi \rho_f \phi_s^3 d_p^3 U^3}{12\eta_{in}(1-\epsilon)H}, \qquad (3.26)$$

where $N_p = (1-\epsilon)V_c/V_p = 3(1-\epsilon)D_c^2 H/(2\phi_s^3 d_p^3)$, and H is the height of the suspension column.

The output power, P_{out}, from an individual fuel pellet is calculated from the expression for the local fission reaction rate integrated over all neutron energies, E_n, and the fuel volume of the pellet, $V_{f,p}$:

$$\begin{aligned} P_{out} &= \eta_{out} P_{fi} = \eta_{out} \int_{V_{f,p}} \int_{E_n} \sigma'_{fi}(E_n) v'_n(E_n) N_n(E_n, V_{f,p}) N_{f,p}(V_{f,p}) Q^*_{fi} dE_n dV_{f,p} \\ &= \eta_{out} \sigma_{fi} v_n N_n N_{f,p} Q^*_{fi} V_{f,p}, \end{aligned} \qquad (3.27)$$

where P_{fi} is the fission power from one fuel pellet, and η_{out} is the overall efficiency at which fission power is converted into electrical power (≈ 0.3) (Duderstadt and Hamilton 1976). The suitably averaged microscopic fission cross-section of the fissile isotope is σ_{fi}, and v_n is the average neutron speed. The average number density of neutrons and the atom density of the fissile isotope in a pellet are N_n and $N_{f,p}$ respectively, and Q^*_{fi} is the average recoverable fission energy from each fission event. Converting some of these quantities into more convenient units and expressing the fissile isotope number density in terms of the fissile fuel mass density yields

$$P_{out} = \frac{1.6\times10^{-15}\pi\eta_{out}\sigma_{fi}\phi_n\rho_s\xi Q^*_{fi}(d_{p,1}-d_{p,0})^3}{A_{total}}, \qquad (3.28)$$

where ϕ_n is the thermal neutron flux in the vicinity of the pellet; σ_{fi} is now in units of barns, and Q^*_{fi} in MeV -- taken here to be $Q^*_{fi} = 175$ MeV.

The quantities σ_{fi} and ξ vary depending upon the moderating medium and the coolant type used. For water-cooled and moderated systems, an average neutron

fission cross-section of 575 barns and an enrichment of 2% are typical (Duderstadt and Hamilton 1976). For graphite moderated systems the neutron spectrum is slightly harder, and thus σ_f is somewhat smaller. However, helium cooled and graphite moderated systems generally also utilize more highly enriched fuel. International safeguards allow up to 20% uranium enrichment which, as an extreme, would compensate for an average neutron energy shift to the order of 10's of eV -- a value well into epithermal neutron energies and far surpassing the well moderated characteristics of the suspended pellet-type reactors considered here. Thus the product $\sigma_f \cdot \xi$ is taken to be (575 b)(0.02), recognizing that for slightly less thermalised reactors (i.e. graphite moderated) an increase in fuel enrichment would sufficiently compensate for the reduced fission cross-section.

The ratio of P_{out} to $P_{in} \cdot \phi_n$ is shown as a function of pellet diameter in Figure 3.8 and 3.9 for UC and UO_2 fuel, respectively. The flux-normalized power ratio is depicted because otherwise a specific output power would be specified by Eq. (3.28). The ratio of P_{out} to $P_{in} \cdot \phi_n$ also allows for the insertion of the appropriate neutron flux for any particular reactor type or design. Typical average neutron fluxes in fission power reactors today are 10^{18} - 10^{19} $m^{-2} \cdot s^{-1}$, however, the more general formulation is retained to roughly compare the results for different suspending fluids.

Note that there is little difference between the two fuels except for the case of liquid lead, which results from the change in suspending velocities for that fluid discussed in Section 3.5. The minimum bounds in Figures 3.8 and 3.9 correspond to systems operating at U_{ter}, the upper bounds for those at U_{mf} . The power ratio's dependence on the size of the suspended pellets enters not only through the d_{px} factors in Eqs. (3.26) and (3.28), but also through the dependence of the fluid velocity on pellet diameter -- U_{mf} and U_{ter} -- Eqs. (3.11) to (3.17) and Eqs. (3.19) to (3.21). Each fluid encompasses different areas of the figures due dominantly to these size and velocity

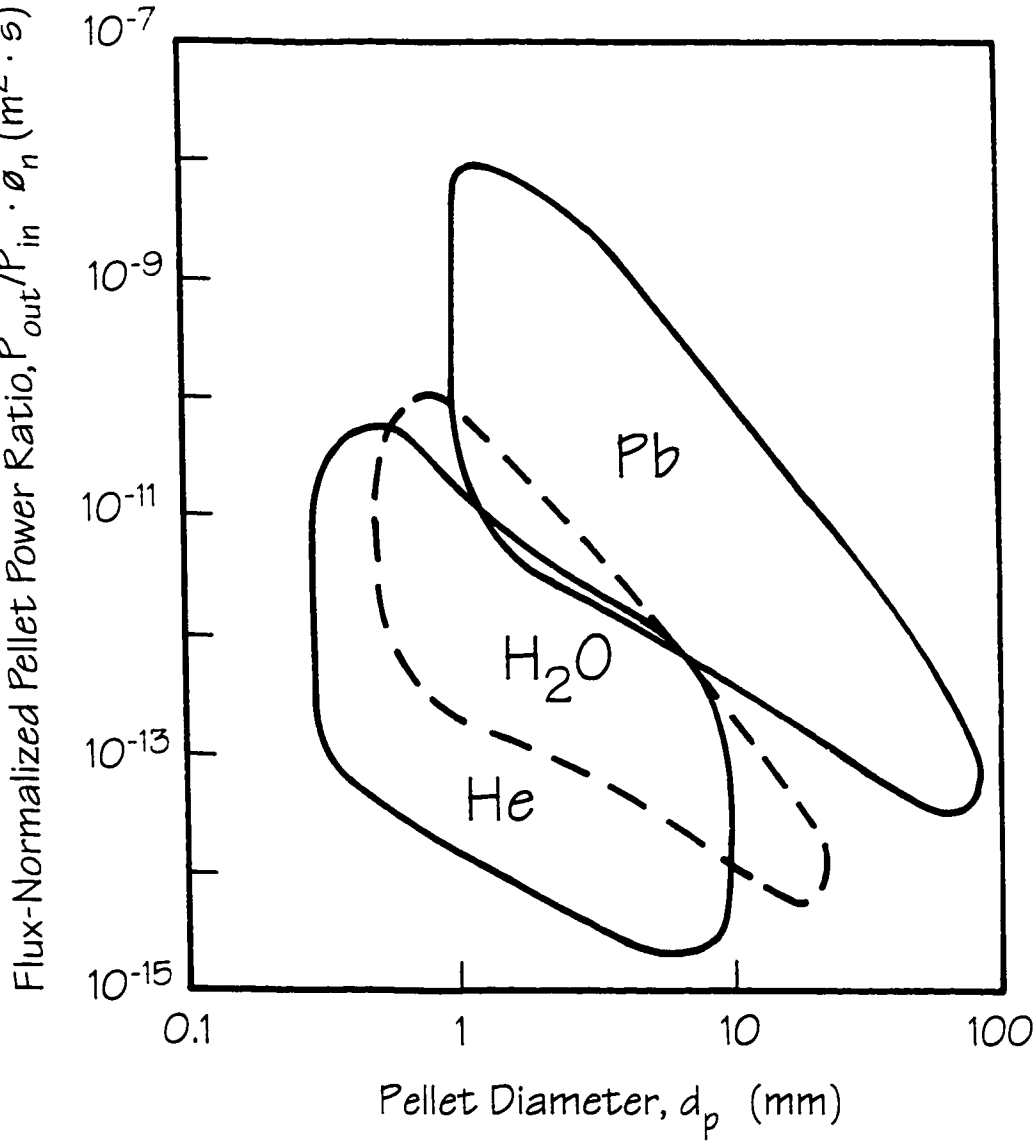

Figure 3.8: The flux-normalized power ratio, $P_{out}/(P_{in} \cdot \phi_n)$, as a function of pellet diameter for the three suspending fluids of interest and UC fuel, as determined from the initial analysis.

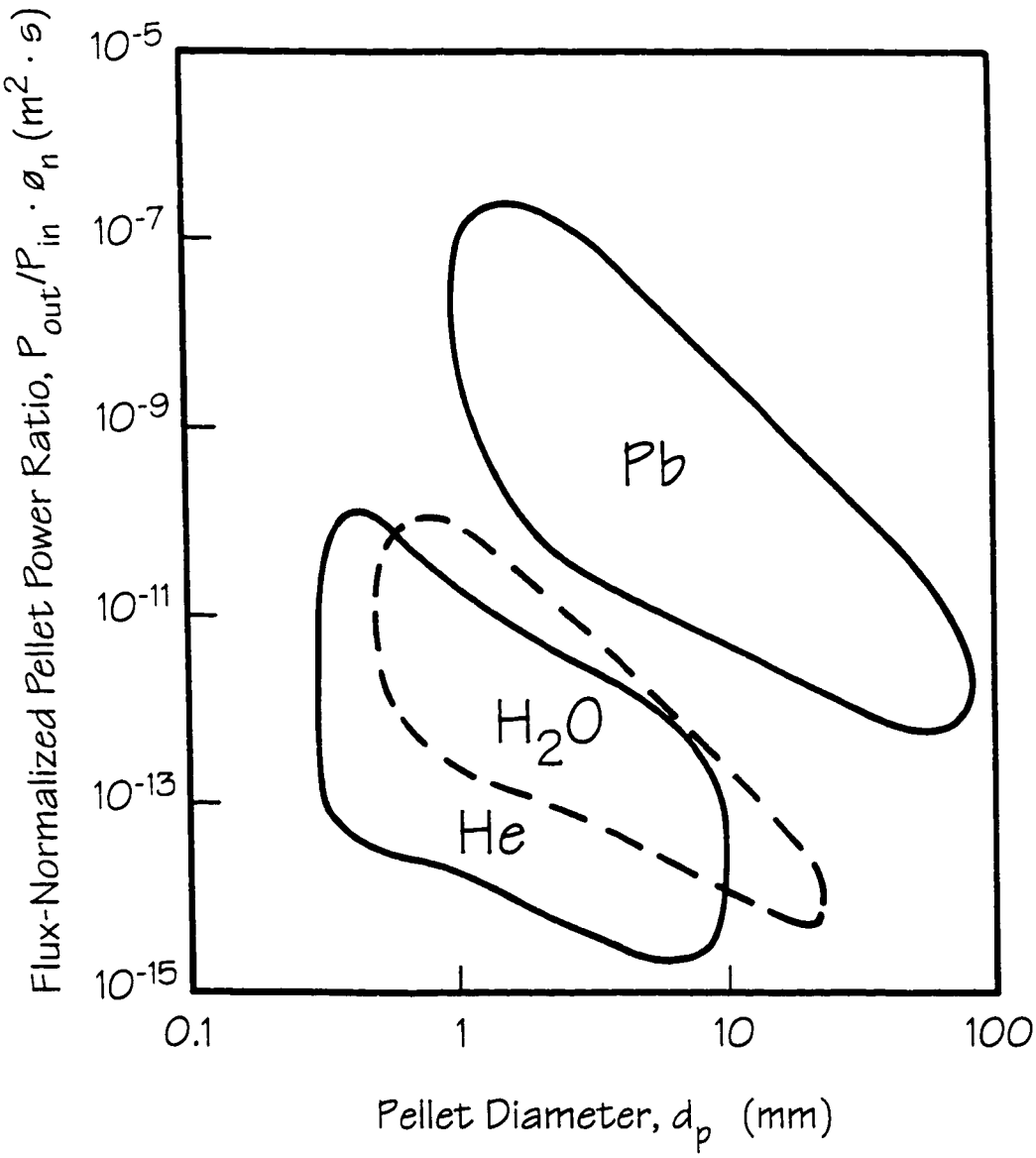

Figure 3.9: The flux-normalized power ratio, $P_{out}/(P_{in} \cdot \phi_n)$, as a function of pellet diameter for the three suspending fluids of interest and UO_2 fuel, as determined from the initial analysis.

dependencies, the ρ_r factor in Eq. (3.26), and the bounds of practical pellet size that have been imposed for each fluid. For all cases the power multiplication exceeds 10^3 - 10^4 for typical values of the neutron flux. This preliminary analysis thus indicates that all such systems appear capable of providing a sufficient power ratio to be useful as a fission power reactor when operated in the appropriate regime.

3.9.3 Entire Column Formulation

In an attempt to obtain a more comprehensive estimate of the power ratio, a similar but more rigorous analysis is carried out from the point of view of one entire column in which the fuel pellets are suspended. Again, the pumping of the fluid is assumed to be the major power input requirement and thus no heating of the suspending fluid or other auxiliary power demands are considered. To estimate the pumping power in this case, a formulation from pump-engineering is used. The power required for a general pumping system can be formulated (Karassik 1986; Warring 1984a, 1984b) as

$$P_{pump} = \begin{pmatrix} \textit{volume flow} \\ \textit{rate of fluid} \end{pmatrix} \begin{pmatrix} \textit{specific weight} \\ \textit{of fluid} \end{pmatrix} \begin{pmatrix} \textit{head loss through} \\ \textit{the system} \end{pmatrix} . \qquad \textbf{(3.29)}$$

The head loss, ΔH_L, or net work done on a unit weight of fluid, for an average fluid velocity which is approximately constant through the column is given by

$$\Delta H_L = \frac{1}{\rho_f g}(p_2 - p_1) + (z_2 - z_1) = f_p \frac{HU^2}{2gD_c} + H , \qquad \textbf{(3.30)}$$

where p_1 and p_2 are the fluid pressure at the entrance and exit from the core column respectively, and z_1 and z_2 the corresponding elevations of these points (Figure 3.7).

The input power follows therefore as

$$P_{in} = \frac{1}{\eta_{in}} P_{pump} = \frac{1}{\eta_{in}} \left(\frac{\pi}{4} D_c^2 U \right) (\rho_f g) H \left(\frac{f_p U^2}{2 g D_c} + 1 \right) , \qquad (3.31)$$

where f_p is the pipe friction factor for the case of developing turbulent flow in smooth pipes (Benedict 1980), approximated by

$$f_p = \frac{0.296}{\left(Re_D \left(\frac{H}{D_C} \right) \right)^{0.2}} = \frac{0.296}{\left(\frac{\rho_f U H}{\mu_f} \right)^{0.2}} . \qquad (3.32)$$

The Reynolds number based on the column diameter D_c is $Re_D = \rho_f \cdot U \cdot D_c / \mu_f$.

The corresponding output power for an entire column is the number of pellets present in one column multiplied by the output power from an individual pellet, Eq. (3.28). This output power[4] is thus

$$P_{out} = \frac{2.4 \times 10^{-15} \pi \eta_{out} (1 - \epsilon) \sigma_{fi} \phi_n \rho_s \xi Q_{fi}^* (d_{p,1} - d_{p,0})^3 D_c^2 H}{A_{total} \phi_s^3 d_p^3} . \qquad (3.33)$$

As in the first analysis, pellet diameter is the crucial parameter. The ratio of P_{out} to $P_{in} \cdot \phi_n$ is shown as a function of pellet diameter in Figures 3.10 and 3.11 for UC and UO_2 fuel, respectively. Again there is little difference between the fuels except for the case of liquid lead as the suspending fluid. The bounds in Figures 3.10 and 3.11

---

[4]Note that the output power from an entire column could be calculated with Eq. (3.24), eliminating the need for nuclear properties such as σ_{fi}, ξ and others. However, the seemingly more complex formulation of Eq. (3.33) was used because the output power from an individual pellet, Eq. (3.28), had already been evaluated and to extend this to an entire column by multiplying by the number of pellets per column, N_p, is even more straightforward than Eq. (3.24). Both methods do, in fact, yield the same result for the entire column formulation of the pellet power ratio.

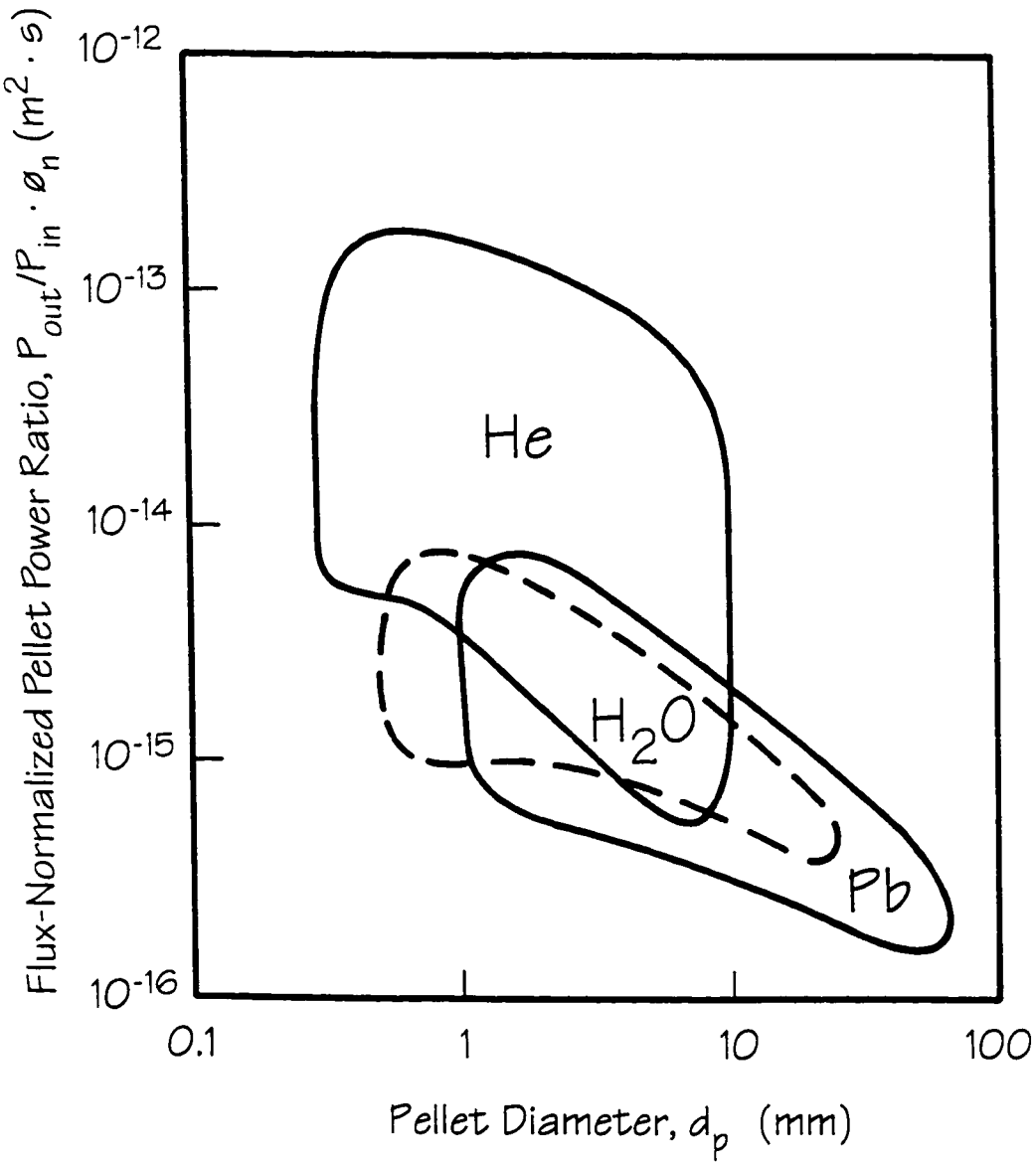

Figure 3.10: The flux-normalized power ratio, $P_{out} / (P_{in} \cdot \phi_n)$, as a function of pellet diameter for the three suspending fluids of interest and UC fuel, as determined by the entire column formulation.

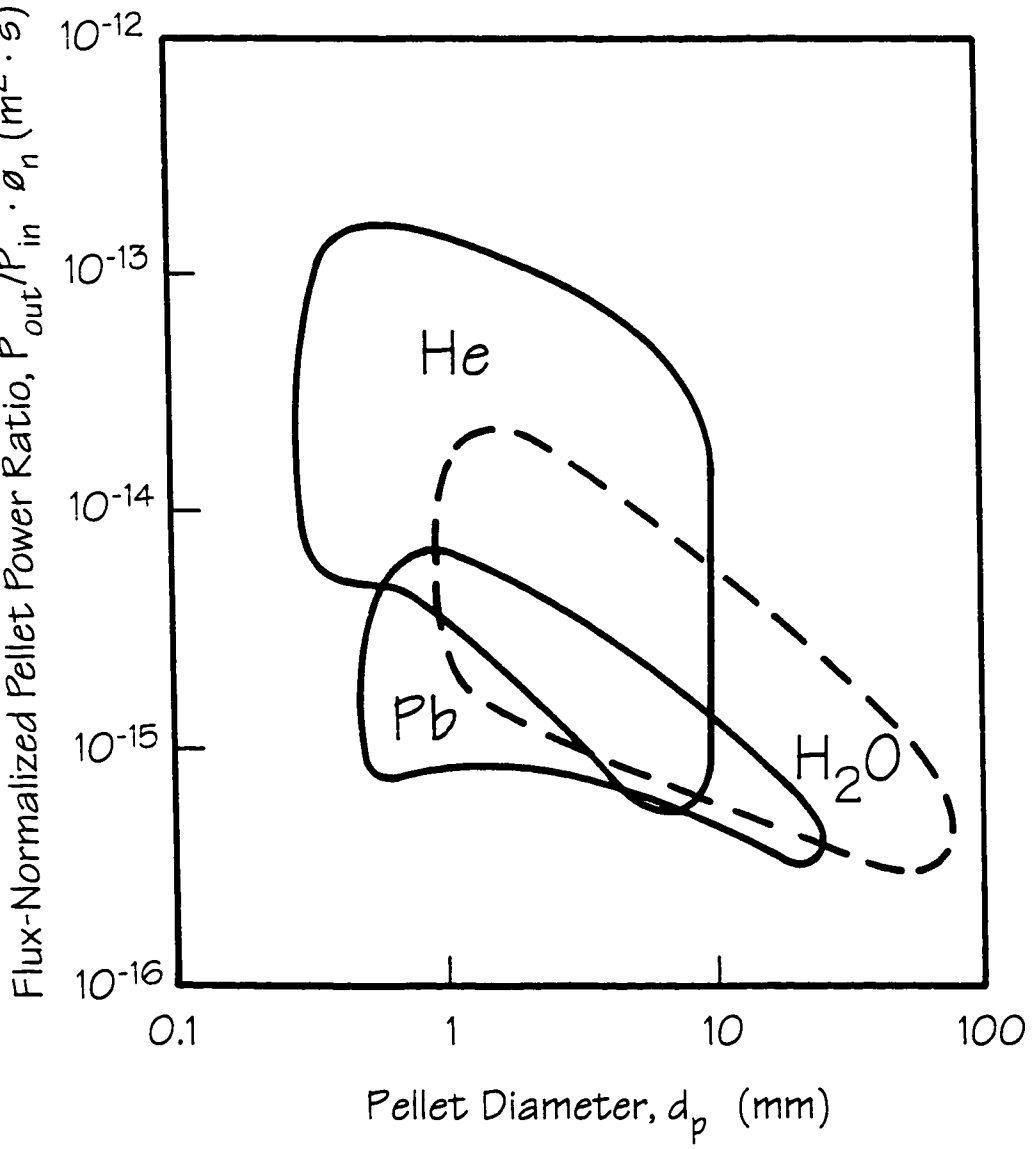

Figure 3.11: The flux-normalized power ratio, $P_{out}/(P_{in}\phi_n)$, as a function of pellet diameter for the three suspending fluids of interest and UO_2 fuel, as determined by the entire column formulation.

are determined in the same manner as those in Figures 3.8 and 3.9 and the dependence of these power ratios is again mainly determined by the size of the suspended pellets, by the dependence of the suspending fluid velocity on pellet diameter, and by the fluid density. This more rigorous analysis leads to slightly reduced power ratio values. However, in all cases P_{out}/P_{in} still exceeds 10^2 - 10^3 for the typical neutron fluxes and reasonable pellet sizes discussed above, and thus all such systems still appear capable of providing the necessary power ratio for use as a fission power reactor.

The two analyses discussed here have revealed that a sufficient power ratio is attainable from suspended pellet-type fission reactors for conceivable power production. However, these suitable power ratios are only true for the pellet diameter ranges displayed in Figures 3.8 to 3.11. For a system using a given coolant outside the ranges depicted therein, the ratio of P_{out} to P_{in} may be significantly less than what is required for a power production facility. In addition, the pumping power for the suspending medium is assumed to be the dominant power demand in such a system, and no account has been made of additional operational requirements which will add to the input power and detract from the P_{out} to P_{in} ratio.

For the entire column analysis, the maximum pellet sizes which still yield a minimum power multiplication of 10^2 for a system in which the average neutron flux is 10^{18} $m^{-2} \cdot s^{-1}$ are, for helium gas ≈10 mm, and for both light water and liquid lead ≈100 mm. For the conditions assumed here, larger pellet sizes, which require larger fluid velocities to be suspended, no longer possess this ratio of P_{out} to P_{in}.

Although these calculations were applied to systems involving pellets in suspension, the same analysis is equally applicable to several variations on this design. For example, if the fuel pellets were densely packed against an upper boundary, such as in Taube et. al. (1986), which allowed the transmission of the coolant but not the

pellets themselves (obviously requiring a coolant velocity ≥ U_{tr}), these analyses could be modified to evaluate the power gain from such a concept by simply using the operating velocity of the design. In addition, extensive work has been done using packed beds as reactor cores (Ludewig et. al. 1996; Holman and Pierce 1996), a concept which is also easily evaluated in terms of its pellet power ratio from the above analyses.

This chapter has discussed several pellet suspension aspects of the PSR. Such considerations are essential to allow for inherent LOCA avoidance characteristics through natural effects alone, i.e. gravity drop of the fuel out of the reactor core in the event of coolant flow disruption followed by packed bed heat conduction and convective circulation to dissipate the decay heat. The simplicity and passive nature of this LOCA avoidance system leave the reactor core in a safe and stable state following any deviation from normal cooling conditions, rendering the PSR fail-safe with respect to loss-of-coolant accidents. In addition, the possibility of re-starting the reactor soon after any such incident exists as the configuration avoids the consequences of LOCAs, rather than just mitigating them. This provides for an improved economic performance of the system.

The following chapter considers the possible action of ablative fuel pellets as a mechanism for limiting reactivity excursion effects.

Chapter 4

Fuel Pellets and Ablation

A fundamental aspect of the PSR concept is the use of fissile fuel in the form of small, spherical pellets. This chapter begins by introducing some well developed examples of such pellets, and recalls several advantages and disadvantages that particle-fuel possesses relative to conventional fuel rods.

Having considered the inherent LOCA avoidance characteristics of the PSR suggests the possibility that reactivity excursion accident avoidance might also be attained -- or the effects reduced -- again without the need for active sensors or monitors. To provide such, the pellet fuel is envisaged to be removed from the fission reactor core in the event of an increase above normal operating temperatures through passive, natural mechanisms combining aspects of thermodynamics and thermalhydraulics. The use of these natural processes simplifies the reactor system, and its ability to affect reactivity excursions is here assessed.

4.1 Pellet Fuel

Micro-fuel pellets consisting of fissile cores of UC, uranium dicarbide (UC_2), UO_2 and others, surrounded by layers of pyrolytic carbide (PyC) -- a very hard, durable form of carbon (C) or graphite -- niobium carbide (NbC), silicon carbide (SiC), zirconium carbide (ZrC) or other impact and wear-resistant materials are routinely

manufactured and in use today (Ahlf, Conrad, Cundy and Scheurer 1990; Dobranich and El Genk 1991; Ludewig et. al. 1996). The number of collisions that such particles need to endure -- with each other and with column walls -- in a suspended pellet-type arrangement has been estimated by Matsumoto, Ohnishi and Maeda (1978) and indicates that great impact durability needs to, and does, exist. Enrichment of the fissile fuel can easily be done with conventional technology, and has been realized in many previously manufactured pellets. In addition, the advantages of pellet fuel discussed in Section 2.7 should be recalled.

The primary disadvantage of fuel pellets -- of the sizes considered here -- is the enormous number of particles required for a fission reactor. Management of the order of 10^7 particles per column poses a major challenge -- albeit not a problem with the particles themselves -- that must yet be appropriately resolved for the PSR to become a plausible fission reactor system.

4.2 TRISO Micro-Fuel Particles

The spherical micro-pellets envisaged for the PSR, whose outer diameter is ~1 mm, consist of a central core of fissile fuel encased by multiple shells which accomplish a variety of functions. Several layers immediately surrounding the fuel are incorporated to provide both solid and gaseous fission product retention within the pellet, while the outermost shell of the pellets consists of a hard, durable material which can withstand the physical collisional demands within the column. In connection with the development of high temperature gas reactors (HTGRs), the design and manufacture of fissile micro-fuel particles has become very extensive (Powell, Takahashi and Horn 1986). During their design and testing, several progressions have been made in the complexity of the particles, but the essentials remain intact, Figure

4.1. The acronyms BISO (bi-isotropic) and TRISO (tri-isotropic) have been coined to describe two versions of the pellets.

For all pellet types, a central fuel kernel of U, Pu, or Th carbide or oxide is surrounded by one or more thin layers to form the fuel micro-sphere. The coatings are made of a variety of materials: PyC and SiC mainly for retention of fission products and structural integrity (Vrillon, Carre and Proust 1988), or ZrC and NbC coatings for very high temperature applications such as nuclear rocket propulsion systems. In the latter case, the ZrC or NbC coatings are to prevent chemical reactions between the hydrogen coolant and the graphite, however such provisions are not necessary with a helium coolant at significantly lower temperatures (Bleeker, Moody and Kesaree 1993; Caveny 1984; Lundberg and Hobbins 1992). Thus, the SiC and/or PyC coatings are most relevant for use in the PSR where the inert He will not react with a carbide coating on a standard TRISO pellet.

For the carbide-coated pellets, testing and experimentation has shown them to possess great durability and compatibility with the structural materials of the suspension columns (Ludewig et. al. 1996). These pellets have been made as small as 250 μm in diameter with good precision, and with coatings as thin as 10 - 20 μm (Powell, Takahashi and Horn 1986; Malloy and Rochow 1993; Aithal, Aldemir and Vafai 1994; Caveny 1984). Uranium enrichments of up to 20% are routinely used, although very high values of ξ up to 96% have also been reported.

The main purpose of the multi-layered coatings is to contain the radioactive -- and thus hazardous -- fission products within the fuel elements, i.e. the pellets themselves. The inner fuel kernel provides not only the fission energy but also retains most of the solid, short-lived fission products so as to render their release of no concern provided that the fuel compound remains intact. The porous PyC, or "buffer" layer as it is known, adjacent to the central fuel kernel is to compensate for the fission-induced

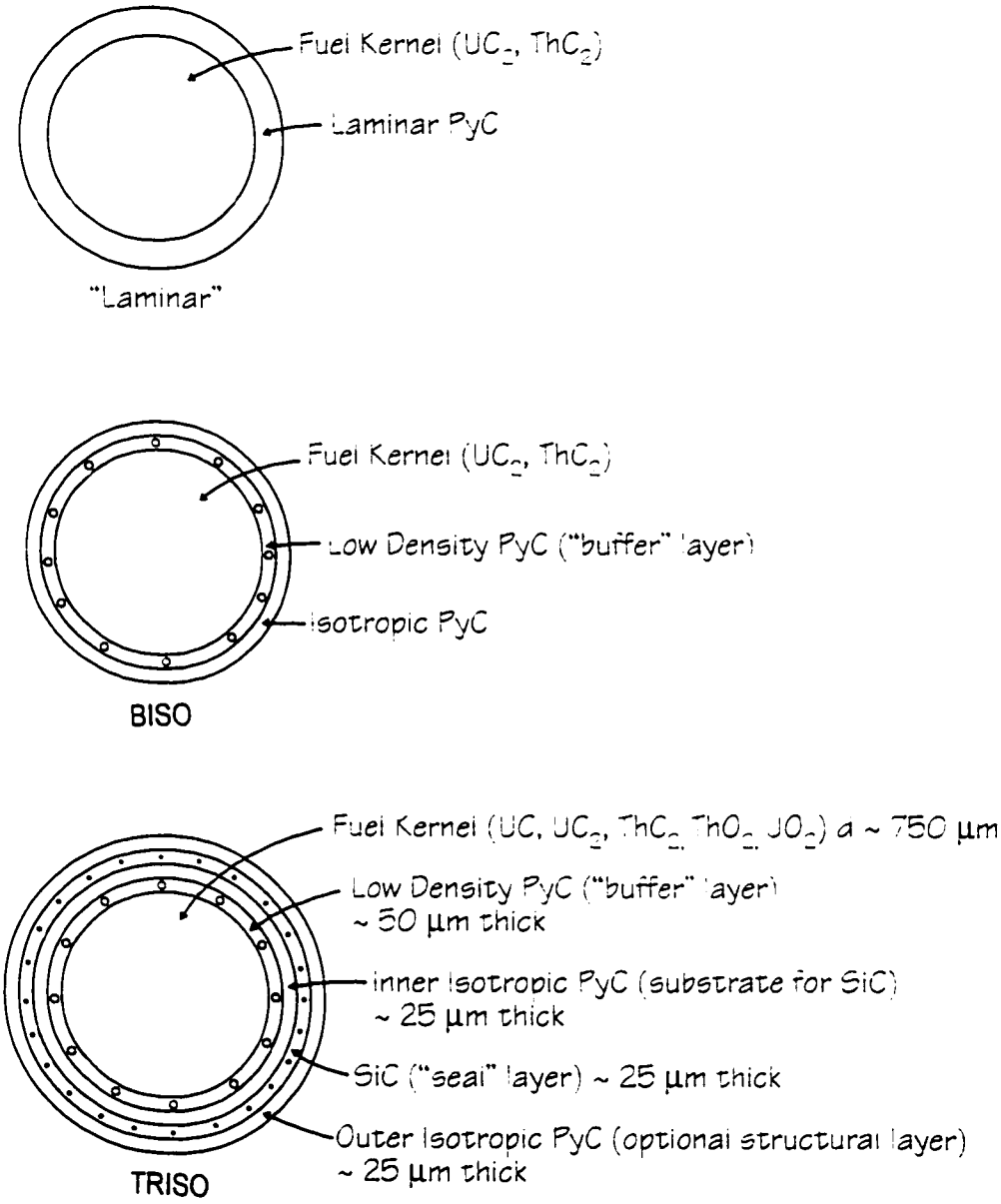

Figure 4.1: Schematic depiction of the layered structures of BISO and TRISO fuel micro-particles -- including sample dimensions for the TRISO case -- and one of their simple predecessors.

swelling of the fissile fuel, as well as to provide volume for the gaseous fission products produced (Figure 4.1). Due to its low density, this is the only layer whose thickness cannot be controlled to great precision during manufacturing; the thickness typically varying by up to 15% between pellets. This buffer layer allows for much higher fissile fuel burnup than that of conventional fuel assemblies which are often limited by fuel swelling and the subsequent structural degradation. The next PyC layer -- isotropic and of normal density -- provides a substrate for the subsequent SiC layer during manufacturing. This SiC layer provides an excellent barrier to iodine, noble gas and metallic fission product release from the pellet because of a lower diffusion coefficient than that for PyC (Sawa, Minato, Tobita and Fukuda 1997). An outer coating of either silicon (Si), or more often PyC, adds a final barrier to fission product release from the fuel elements, as well as a structural coating to the pellet. With this layered composition, TRISO particles have been shown to retain > 99.9% of all fission products within the pellets themselves, even at high burnup (Powell, Takahashi and Horn 1986; Aithal, Aldemir and Vafai 1994; Ahlf, Conrad, Cundy and Scheurer 1990) and high temperature conditions (Hejzlar, Todreas and Driscoll 1996; Kugelar and Phlippen 1996). In addition, due to the mobility of the pellets about one another in a suspended arrangement, the integrity of the fuel matrix would be maintained, even in catastrophic events such as earthquakes, more so than for fuel elements which are rigidly constrained within the reactor core structure.

These pellets have been tested at power densities in the 1000's of MW/m^3 range (Dobranich and El Genk 1991; Ludewig et. al. 1996; Bleeker, Moody and Kesaree 1993), which greatly exceeds the requirements of any of the suspended pellet-type reactors discussed in Section 2.2 and 2.3, and surpasses the capabilities of conventional fuel rods in present-day reactors. In addition, temperatures in the fissile fuel kernel of up to ≈1900 K (Ahlf et. al. 1990) have been achieved with no damage or release of

fission products, primarily due to the thin coatings. Stresses induced in the pellets -- mainly between layers -- due to fission gas pressure, CO_2 gas pressure resulting from the fissile burn of UO_2 kernels and radiation-induced shrinkage of PyC from fast neutrons has been determined to be the primary means of pellet failure (Sawa, Shiozawa, Minato and Fukuda 1996). However, analyses indicate essentially no failures will occur, even at very high temperatures, provided the buffer layer thickness is > 30 μm.

Temperature differences between the fuel and coolant are often less than 10 K, mainly because the layers about the central fuel core are so thin, and also because they are quite similar to one another -- and the fuel matrix itself -- in terms of thermal conductivity (Caveny 1984). This allows for rapid temperature transients in the core to be permitted without inducing significant thermal stresses in the pellets. Full power may be attained in seconds or minutes as opposed to many minutes or hours, the latter time scales being more typical of reactors using conventional forms of reactor fuel. The carbide coatings also provide excellent chemical stability in the He coolant, even at high temperatures.

TRISO particles have been used in thermal neutron fluxes of up to 2×10^{20} m^{-2} s^{-1}, and the on-line removal and addition of particles from the reactor for refuelling has also been considered.

4.3 Proposed Fuel Removal Mechanism

In the analyses below, several of the TRISO pellet coatings are disregarded and the centre of each pellet is considered to contain just the fissile material for simplicity in this initial study, Figure 4.2. The outermost shell of the pellets still consists of a hard, durable material such as SiC which can withstand the physical collisional

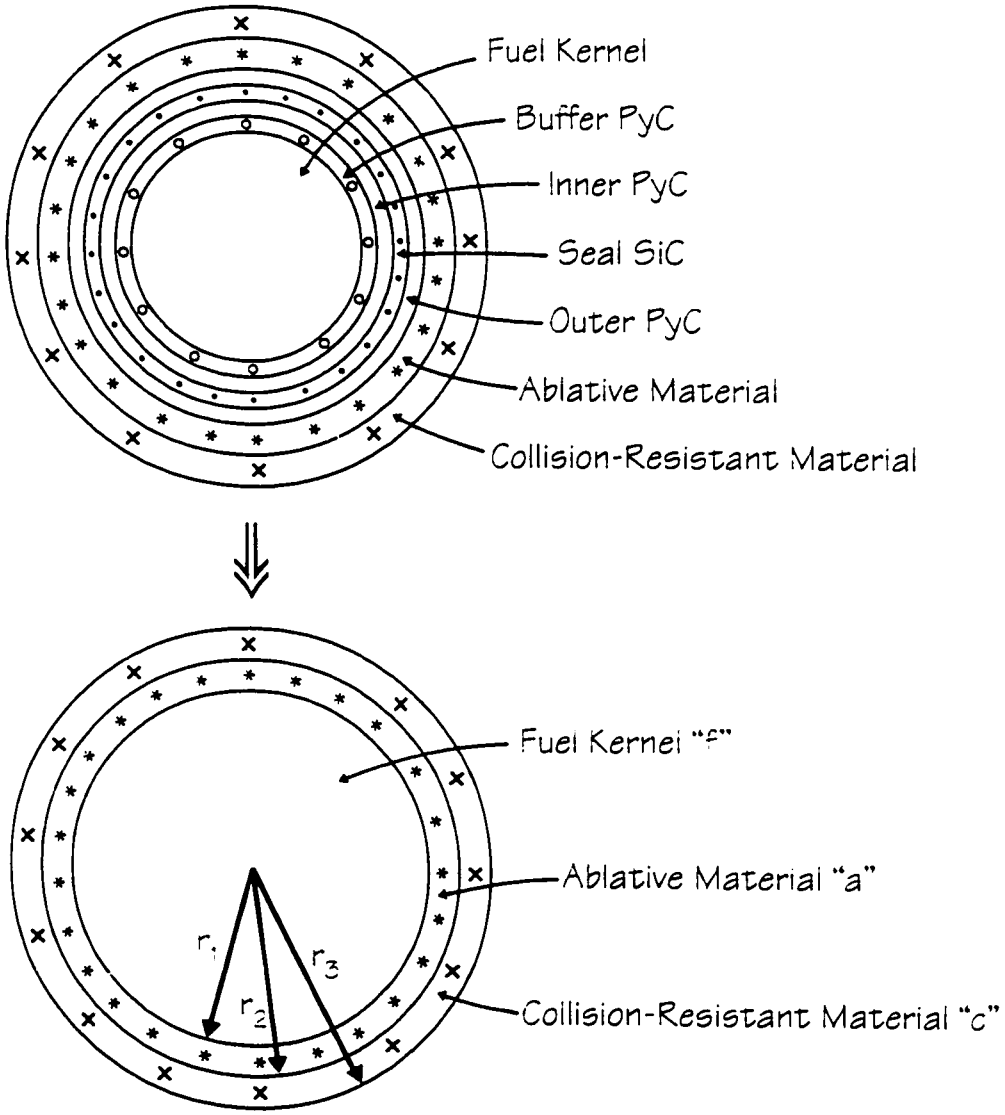

Figure 4.2: Simplification of the multi-layered fuel particles for modelling purposes.

demands in the suspension columns of the reactor core.

Of most significance here, however, is an additional layer between the fuel core and the outer protective layer that consists of a material which sublimates from a solid to a gas when its temperature rises significantly above normal operating conditions, Figures 4.2 and 4.3. Recall that the PSR operates with He temperatures similar to HTGRs and thus "ablative" materials were selected based on coolant temperatures reaching up to ≈900°C. The deviations from normal operation could be natural, accidental -- such as the failure of the control rod system, or due to a malicious operator who purposely mis-uses control and/or fuelling systems. This so-called ablative layer initiates a mechanism to potentially remove the fuel from the core in the event of a reactivity excursion -- and to thus avoid many consequences thereof -- through the following sequence: A reactivity increase in the reactor causes an increase in the neutron population, subsequently increasing the power production within the central fuel kernel of the pellets. If power or temperature reactivity feedback effects characteristic of the reactor do not result in a net reduction in reactivity, the increased power production would continue to raise the fuel temperature and that of the ablator. Once the sublimation temperature of the ablative material is surpassed, the ensuing change of phase could generate substantial pressure to break apart the outer protective shell of the pellet and thus significantly change the geometric properties of the suspended material (Figure 4.3). The changes in the drag force would cause some fragments to elutriate[1] out the top of the column -- those whose terminal velocity was reduced below that of the velocity of the coolant. Alternatively, those pellets whose minimum fluidization velocity is increased above the suspension velocity would descend out the bottom. This fuel removal could reduce core reactivity until such time

[1]Elutriation will be discussed in Section 4.8.

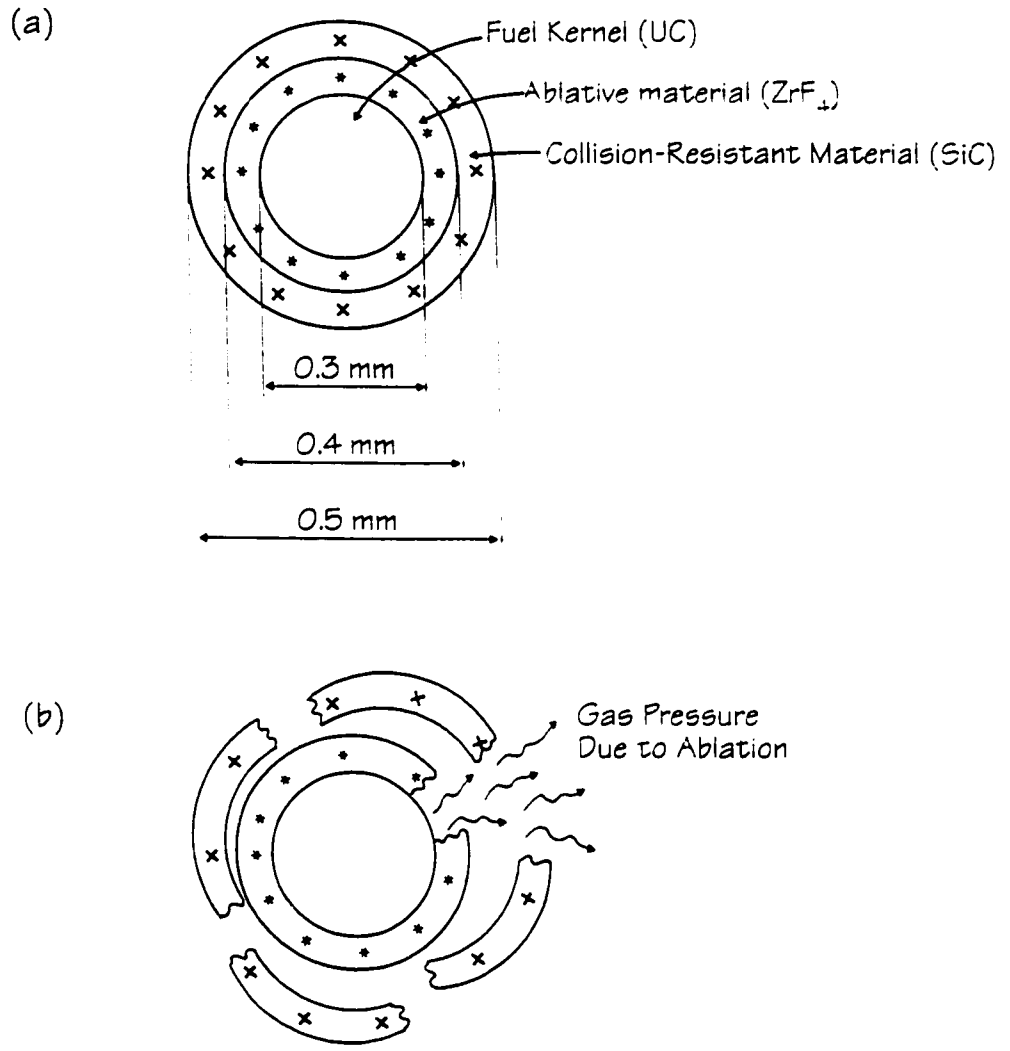

Figure 4.3: Schematic depiction of a three-layer ablative pellet: (a) micro-fuel pellet with ablative layer; and (b) reactivity excursion scenario where ablative layer sublimates and breaks up the particle into smaller fragments.

that the temperature of the fuel had returned to normal, thus potentially limiting or curbing the excursion accident.

As was alluded to in the previous section -- and will be shown later in this chapter -- the ablator's temperature follows that of the fuel very closely and thus the sensitivity of the ablator to temperature changes in the fuel is generally quite good. To break apart the outer protective layer of the pellet, however, a significant build-up of pressure is likely required, and thus a good portion of the ablative material must exceed its sublimation temperature before this reactivity excursion avoidance mechanism is invoked. While any revolutionary fission reactor core such as the PSR would, essentially by definition, possess negative power and temperature reactivity co-efficients, these are based on the core as a whole -- including effects from the moderator and coolant as well as the fuel. The ablative process discussed here is envisaged to provide an additional mitigation mechanism to potentially enhance the level of safety in the PSR against fuel temperature increases over and above that of reactivity co-efficients. One design variation that has also been proposed is that of tiny kernels of fuel -- even smaller than the central fuel kernel in the layered-pellet case considered here -- embedded in an ablative host medium surrounded by the collision-resistant layer, Figure 4.4. While this appears more favourable in terms of accomplishing the ablation process based on the fuel and ablator temperature distributions (Kornilovsky 1996), the analyses here are restricted to the layered geometry.

4.4 Additional Reactivity Excursion Avoidance Schemes

Prior to a preliminary examination of this ablative pellet strategy, a comparison to other approaches suggested for use in nuclear reactors which are similar

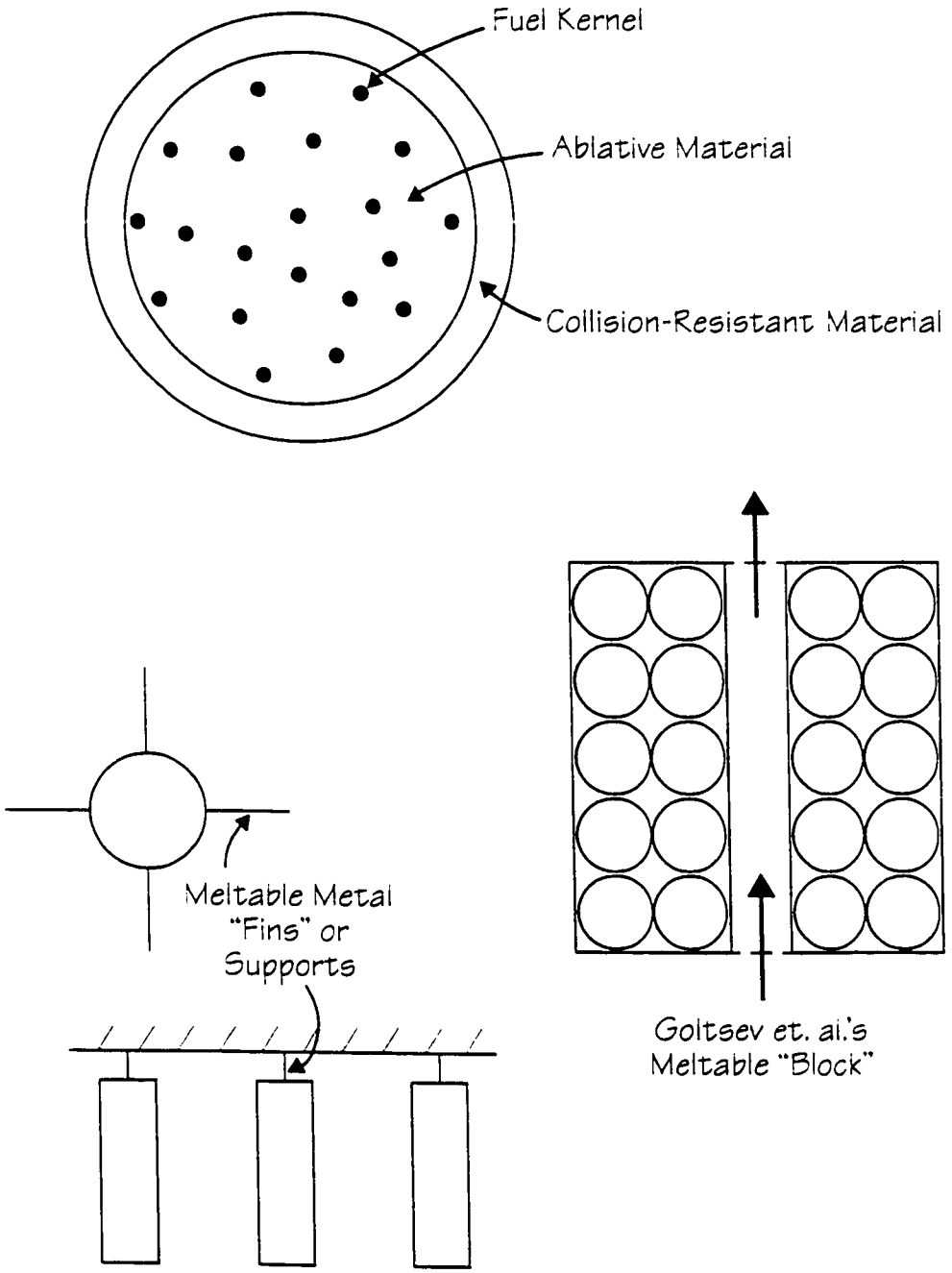

Figure 4.4: Additional reactivity excursion avoidance mechanisms that have been suggested.

to the PSR is made. One such proposal suggests mixing elements such as tantalum (Ta), which have a much greater neutron absorption cross-section at elevated temperatures versus normal operating conditions, into the fuel elements (Sefidvash 1996). Thus, in the event of a fuel temperature increase, this larger neutron absorption would reduce reactivity to the point that temperature and other reactor parameters would return to normal. Such a design effectively renders the fuel temperature coefficient of reactivity more negative than it would be without the addition of Ta.

Much more akin to the concept proposed here is the use of neutronically transparent metals -- possessing appropriate melting points -- which are used to aid in the suspension of the fuel, but would no longer do so if the temperatures were to increase beyond the metals' melting points. In such cases, the fuel would then be removed from the core by gravity, as occurs in the case of a LOCA in the PSR, to reduce reactivity and subsequently return operating parameters to normal (Figure 4.4). The metal could potentially be used as supports for fuel elements "hung" in the core, or perhaps as "fins" or other drag-increasing modifications to spherical fuel pellets in order to accomplish these suspension enhancements (Kornilovsky 1996).

Another proposal is the use of metal blocks or "boxes" that contain the spherical fuel elements. The melting of these boxes would result in the removal of the fissile fuel from the reactor core by gravity (Goltsev et. al. 1994). Of course, all such reactivity mitigating schemes are merely an additional provision to negative temperature and power reactivity co-efficients which, from a more fundamental standpoint, are crucial to the avoidance of reactivity excursion events.

4.5 Steady State Thermal Conditions

Exhaustive studies to determine the maximum reactivity insertion that can be affected or potentially be curbed by the ablative-pellet action are yet to be undertaken. Here, an investigation of the heat transfer and temperature characteristics in the pellets and the elutriation time scales are addressed for a simplified scenario to give a preliminary assessment of the proposed ablative pellet strategy.

To model the heat transfer and temperature development in the fuel pellets during a reactivity excursion, use is made of the spherical symmetry of the pellets. Thus, the general heat conduction equation in spherical polar co-ordinates has only a radial component to consider, specifically:

$$\rho C_p \frac{\partial T(r,t)}{\partial t} = \frac{1}{r^2}\frac{\partial}{\partial r}\left(r^2\, k(r) \frac{\partial T(r,t)}{\partial r} \right) + w(r,t) \,, \qquad (4.1)$$

where ρ is the mass density of the pellet material, C_p its specific heat capacity, T(r,t) is the temperature at a radial distance r from the pellet's centre at time t, k(r) is the thermal conductivity of the material at radius r, and w(r,t) is the fission power density in the fissile fuel at radius r and time t.

Since each pellet -- and also the thickness of each of the coatings -- is small, and since the variation of thermal conductivity with temperature for the materials of interest is generally fairly weak, the thermal conductivity of each layer was taken to be a constant, k_i, over the relevant temperature range (Table 2.3). Similarly, the fission power density in the fissile fuel was also taken to be spatially uniform, i.e. w(t), throughout the central fuel kernel as any neutron flux variation over such a small dimension would be minimal, the same being true of self-shielding effects. Self-shielding would, however, generally reduce the actual fission power output compared

to that modelled here, and so these analyses err on the conservative side with this assumption. Eq. (4.1) can thus be reduced to

$$\rho C_p \frac{\partial T(r,t)}{\partial t} = \frac{k}{r^2}\frac{\partial}{\partial r}\left(r^2 \frac{\partial T(r,t)}{\partial r} \right) + w(t) . \qquad (4.2)$$

At steady state, Eq. (4.2) can be further reduced to

$$\frac{1}{r^2}\frac{d}{dr}\left(r^2 \frac{dT(r)}{dr} \right) + \frac{w}{k} = 0 , \qquad (4.3)$$

where T(r) is now the pellet temperature at a radial distance r from the pellet's centre and w is the steady state fission power density. The determination of the temperature profiles in a three layer pellet requires the solution of Eq. (4.3) in each layer, subject to the following boundary conditions:

pellet symmetry: $\partial T(r)/\partial r = 0$ at $r = 0$; **(4.4a)**

temperature continuity between layers: $T_i(r = r_i) = T_{i+1}(r = r_i)$,

for $i = 1, 2$; **(4.4b)**

heat flux continuity between layers:

$-k_i \cdot \partial T_i(r = r_i)/\partial r = -k_{i+1} \cdot \partial T_{i+1}(r = r_i)/\partial r$, for $i = 1, 2$; **(4.4c)**

and forced convective heat transfer: $-k_3 \cdot \partial T_3(r_3)/\partial r = h(T_3(r = r_3) - T_\infty)$. **(4.4d)**

The fuel kernel extends to a radius r_1, the ablative material to radius r_2, and the outer pellet radius is r_3 (Figure 4.2). The thermal conductivity of the fuel, ablator, and collision-resistant layers are $k_1 = k_f$, $k_2 = k_a$ and $k_3 = k_c$ respectively, and the heat transfer coefficient from the pellet surface to the ambient fluid (helium gas) -- which is at a temperature T_∞ beyond the thermal boundary layer -- is h. The solution

of Eq. (4.3) subject to the constraints of Eqs. (4.4a) to (4.4d) yields the well established temperature profiles for the three regions of the pellet (subscript 1 or f - central fuel kernel, subscript 2 or a - ablator layer, and subscript 3 or c - collision-resistant layer):

$$
\begin{aligned}
T_f(r) - T_\infty &= \frac{-wr^2}{6k_f} + \frac{wr_1^3}{3}\left(\frac{1}{hr_3^2} - \frac{1}{k_c r_3} + \frac{1}{k_c r_2} - \frac{1}{k_a r_2} + \frac{1}{k_a r_1} + \frac{1}{2k_f r_1}\right), && r \le r_1, \\
T_a(r) - T_\infty &= \frac{wr_1^3}{3k_a r} + \frac{wr_1^3}{3}\left(\frac{1}{hr_3^2} - \frac{1}{k_c r_3} + \frac{1}{k_c r_2} - \frac{1}{k_a r_2}\right), && r_1 \le r \le r_2, \\
T_c(r) - T_\infty &= \frac{wr_1^3}{3k_c r} + \frac{wr_1^3}{3}\left(\frac{1}{hr_3^2} - \frac{1}{k_c r_3}\right), && r_2 \le r \le r_3.
\end{aligned}
\tag{4.5}
$$

The surface temperature of a pellet is thus $T_s = T_c(r_3) = wr_1^3/(3hr_3^2) + T_\infty$.

The heat transfer coefficient for a single sphere in an infinite moving fluid has been correlated as

$$Nu = 2 + (0.4Re^{1/2} + 0.006Re^{2/3})Pr^{2/5}\ ,\ 3.5<Re<80000\ ,\ 0.7<Pr<380\ , \tag{4.6}$$

where Nu, Re, and Pr are the dimensionless Nusselt, Reynolds, and Prandtl numbers, respectively (Bayazitoğlu and Özişik 1988). For the case of helium gas as the fluid moving around the exterior of pellets of outer radius r_3, this can be expanded to

$$h = \frac{k_{He}}{2r_3}\left[2 + \left(0.4\left(\frac{\rho_{He}U_{He}2r_3}{\mu_{He}}\right)^{1/2} + 0.06\left(\frac{\rho_{He}U_{He}2r_3}{\mu_{He}}\right)^{2/3}\right)Pr_{He}^{2/5}\right], \tag{4.7}$$

where k_{He}, ρ_{He}, U_{He}, μ_{He} and Pr_{He} are the thermal conductivity, mass density, speed, viscosity and Prandtl number of helium, respectively.

While such a heat transfer coefficient is applicable to isolated spheres in a moving fluid, it is not the most appropriate one for the suspension conditions in the PSR. Instead, the correlation deemed most relevant to these analyses is that for

fluidized bed heat transfer between the particles and the fluid. Such a heat transfer coefficient is used to account for the similarities between the suspension column and fluidized beds: collisions between particles, the large surface area-to-volume ratio for the source of heat in the column, and others. There are over a hundred correlations for particle-to-gas heat transfer coefficients in fluidized beds in the literature (Leva 1959; Zabrodski 1966; Kunii and Levenspiel 1969; Boothroyd 1971; Gupta, Chaube and Upadhyay 1974; Balakrishnan and Pei 1975; Botterill 1975; Pandey, Upadhyay, Gupta and Mishra 1978; Cheremisinoff and Cheremisinoff 1984; Bisio and Kabel 1985; Davidson, Clift and Harrison 1985; Geldart 1986; Pell 1990). However, at low Reynolds numbers many of these vary by as much as an order of magnitude or yield a Nusselt number less than the theoretical minimum for a single sphere in an infinite stationary fluid. The resolution of this problem is outlined in Davidson et. al. (1985) and thus use is made of the correlation that they recommend, specifically

$$Nu = \frac{2hr_3}{k_{He}} = 2 + 1.1Re^{3/5}Pr^{1/3}, \quad Re > 15 . \tag{4.8}$$

It should be noted, however, that this formulation ignores heat transferred to the column walls and that by radiation, accounting only for thermal energy transferred from the hot pellets to the cooling gas. This simplification is valid at normal operating temperatures, but not during a reactivity excursion or near sublimation temperatures. Such a correlation is chosen, in part, to give the most demanding conditions required of the fluid to cool the pellets, as radiation removes additional heat from the particles. Since such additional heat removal would slow the temperature increase in the ablative layer and thus delay ablation, this assumption would only affect the results of this assessment if the overall reactivity excursion avoidance mechansim appeared sufficiently rapid to be successful (which is not the case, as is shown below). Thus, Eq.

(4.8) is deemed the appropriate heat transfer co-efficient correlation for this system, and when expanded for the case of He gas as the cooling fluid yields

$$h = \frac{k_{He}}{2r_s}\left[2 + 1.1\left(\frac{\rho_{He}U_{He}2r_s}{\mu_{He}}\right)^{3/5} Pr_{He}^{1/3}\right], \qquad (4.9)$$

which is used in Eq. (4.5). For all calculations here, the temperature dependencies of the helium gas properties -- k, ρ, μ, Pr, and C_p below -- are accounted for throughout (Dalle Donne and Sordon 1990).

Figure 4.5 depicts the heat transfer correlation for that of a single sphere and for spheres in a fluidized bed. Note that there is better heat transfer for the latter, as would be expected since it represents the more agitated system which is more efficient at the transfer of thermal energy.

Figure 4.6 shows typical steady state temperature profiles for the fuel pellets, Eq. (4.5). Note the small overall temperature drop from the interior of the pellets to their surface, and the relatively large temperature gradient in the ablative layer. This will be shown to have greater significance in the transient analyses of Section 4.7.

4.6 Steady State Thermal Conditions for a Column

Since the diameter of the suspension columns for the PSR is much less than their height, and since radial variations in the pellet density or gas temperature would thus be limited to spatial extents of the order of D_c, an estimate of the helium temperature as a function of height in the suspension columns was performed using a radially lumped analysis, Figure 4.7. The energy balance for the suspending fluid at steady state equates the rate of energy extracted per unit volume from the pellets

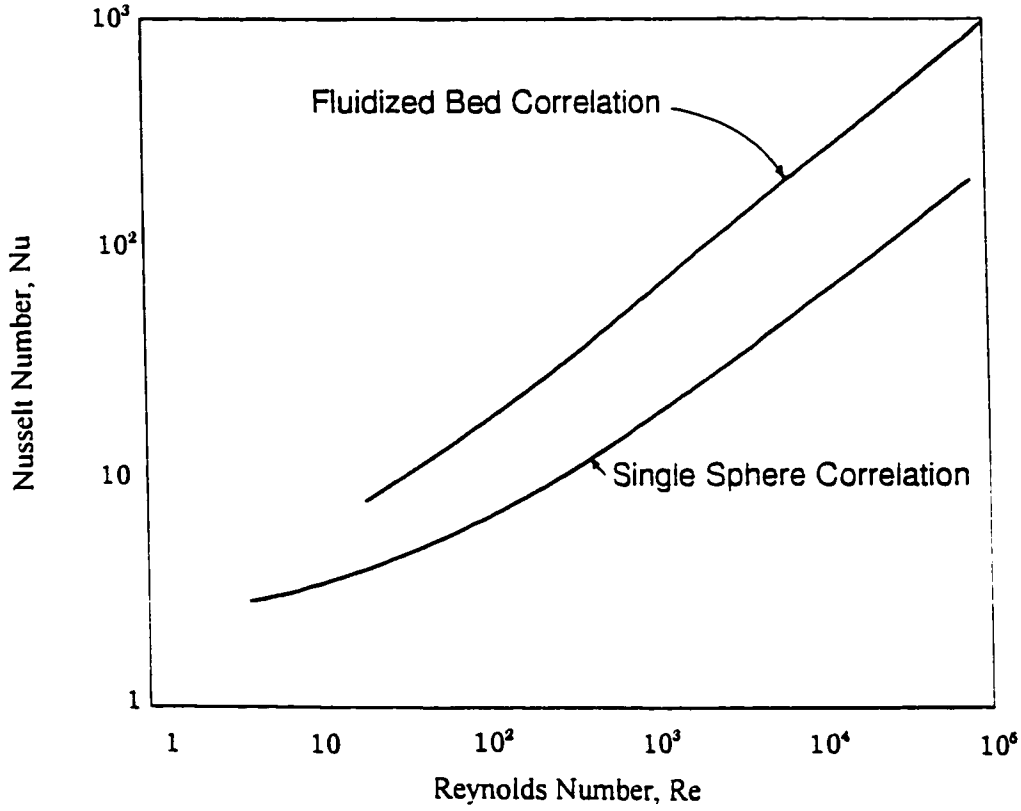

Figure 4.5: Comparison of the heat transfer coefficient for a single sphere in a moving, infinite fluid to the particle-to-gas correlation for a fluidized bed.

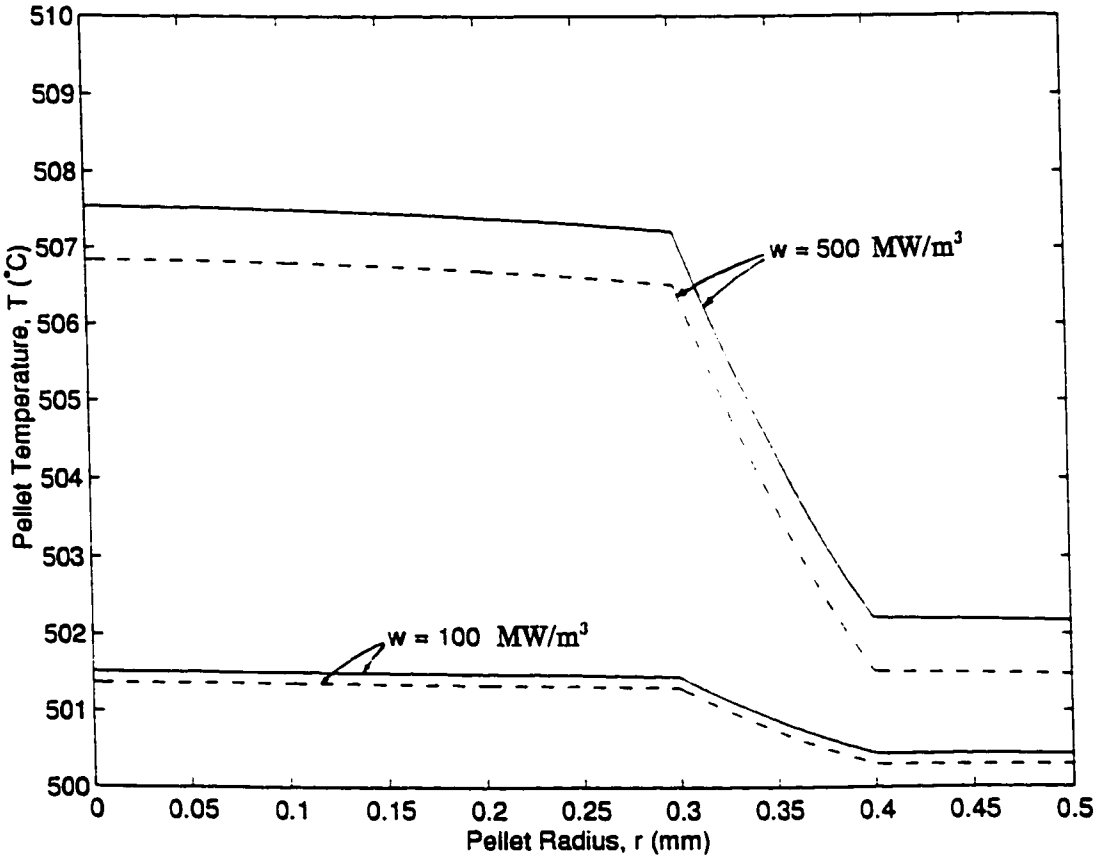

Figure 4.6: Steady state temperature profiles of a micro-fuel pellet (radius of fuel core = 0.3 mm, thickness of both ablative and collision-resistant layers = 0.1 mm). Power densities are measured with respect to the volume of the fuel kernel alone. Solid and dashed lines are for U_{He} = 3 m/s and 6 m/s, respectively, and a fluid temperature of T_{He} = 500°C is assumed.

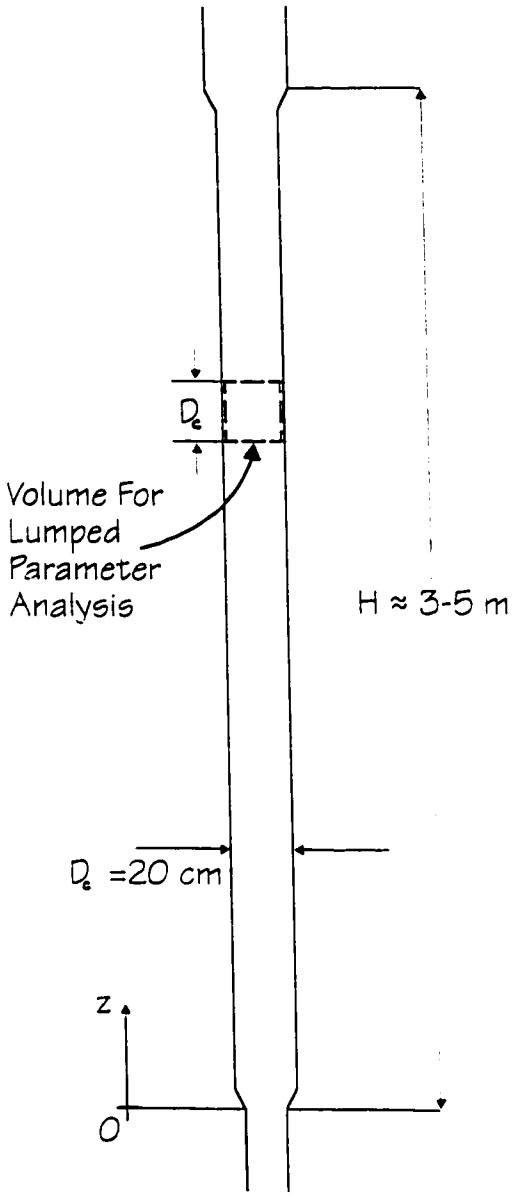

Figure 4.7: Schematic of the relative size of column diameter and height, and thus the motivation for the radially lumped axial heat transfer analysis.

to the rate of energy acquisition per unit volume by the fluid medium as it passes up through the column, or

$$h(T_c(r_3) - T_{He})\left(\frac{A_s}{V}\right) = \rho_{He} C_{p,He} U_{He} \frac{dT_{He}(z)}{dz} \quad . \tag{4.10}$$

The total surface area of the pellets per unit volume of the suspension column is (A_s/V), the heat capacity of helium is $C_{p,He}$, and z is the vertical axial dimension of the column with z = 0 taken at the bottom of the core (Figure 4.7). Cylindrical symmetry is assumed for the entire height of the column, the tube diameter D_c = 20 cm, and the column height H ≈ 3 m. Assuming an average void fraction ϵ for the suspension, the surface-to-volume ratio can be shown to be $3(1 - \epsilon)/r_3$, and thus Eq. (4.10) reduces to

$$\frac{dT_{He}(z)}{dz} = \left(\frac{3(1 - \epsilon)}{C_{p,He} U_{He} r_3}\right)\left(\frac{h}{\rho_{He}}\right)(T_c(r_3) - T_{He}) \quad . \tag{4.11}$$

Using Eq. (4.5) to substitute for $T_c(r_3)$, and noting that $T_{He} = T_\infty$ therein, reduces Eq. (4.11) to

$$\frac{dT_{He}(z)}{dz} = \frac{(1 - \epsilon) r_1^3 w(z)}{C_{p,He} U_{He} r_3^3 \rho_{He}} \quad . \tag{4.12}$$

The only significant dependence on He temperature on the right-hand-side of Eq. (4.12) is in ρ_{He}, and allowance has now been made for an axially-dependent fission power density, w(z).

Eq. (4.12) was solved for $T_{He}(z)$, given an entrance temperature $T_{He}(0)$, resulting in the temperature profiles of Figure 4.8. A constant power density (w(z) = W) and an axially sinusoidal power density ($w(z) = W \cdot \sin(z\pi/H)$) were both considered. Although neither is truly indicative of the axial power density distribution for the PSR, they do

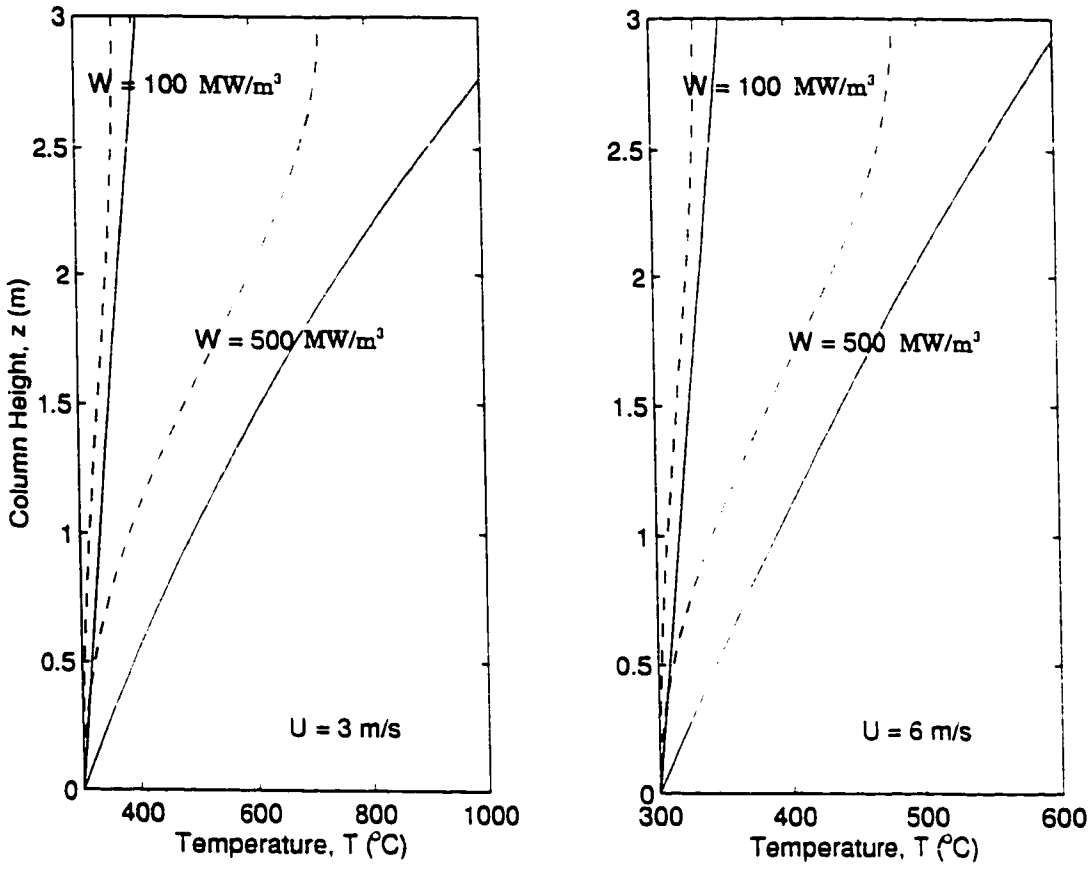

Figure 4.8: Axial helium temperature profiles for a suspension column. Solid lines are for w(z) = W, and dashed lines are for w(z) = W·sin(zπ/H) in Eq. (4.12). The pellets have a fuel core radius of 0.3 mm, and the thickness of both the ablative and collision-resistant layers is 0.1 mm. Power density magnitudes (W) are measured with respect to the volume of the fuel kernel alone.

represent two extreme cases, the actual profile lying somewhere between them. For either case, however, a fairly uniform helium temperature increase through the column exists, and for the higher power density case the temperature rise over the height of the core is very similar to that of HTGRs.

The lower power density of 100 MW/m^3, as measured with respect to the fuel volume alone, has been considered a minimum bound for the PSR and corresponds to a neutron flux of $\phi_n \sim 10^{17}\ m^{-2}\cdot s^{-1}$ (an order of magnitude smaller than those considered in Section 3.9). This indicates that a larger core (up to ≈5 m) is permissible, and that the helium temperature rise may not reach the ≈400 K previously considered unless a higher power density is allowed. A fair amount of flexibility thus exists in the selection of H -- when appropriately combined with W -- from a thermalhydraulic standpoint, an important characteristic since pellet distribution uniformity will likely be the dominant determinant of column height. While a lower ΔT_{He} would reduce the power output of each column, a total output power may still be achieved by simply designing a reactor with more columns, a fairly straight-forward task due to the modularity of each column. A lower ΔT_{He} would also reduce the mechanical strains induced on the columns which normally must be dealt with by using durable, high-quality graphite and occasionally segmented tubes with extensive support structures (Liem 1996; Ahlf, Conrad, Cundy and Scheurer 1990; Reutler and Lohnert 1983).

4.7 Transient Analyses

As a preliminary estimate of the thermal response in a pellet during a reactivity excursion, in particular the rate of temperature increase in the ablative material, the general transient heat conduction equation in the radial direction for spherical polar co-ordinates, Eq. (4.2), must be solved. The assumptions and boundary

conditions used in Sections 4.5 and 4.6 are again employed, while the initial condition is given by the steady state temperature profiles, Eq. (4.5). An exponential power density increase in time is considered:

$$w(t) = w(0)\exp(t/\tau) , \qquad (4.13)$$

where w(0) is the fission power density at the onset of the excursion and τ is a time characterizing the rate of the exponential excursion -- specifically the time for the power density to increase by a factor of $e = 2.718$ which is also known as the reactor period.

This model results in a most aggressive time behaviour for the reactivity excursion, more so than that which is most likely to occur in an actual reactor (Duderstadt and Hamilton 1976). An effective neutron lifetime -- a parameter which, in part, determines τ, Table 4.1 -- of 10^{-2} s is assumed, which is smaller than the value for an actual graphite or D_2O-moderated reactor. These assumptions result in a faster increase in power density than would actually occur, but are deemed sufficient for this analysis as they provide a relatively simple model which forms one limit of possible reactivity excursion behaviour.

Several values for the reactor period are considered, the corresponding neutron multiplication factors and reactivities given in Table 4.1. Note that only cases of $\rho < 0.007$ are considered, since the possibility that prompt criticality ($\rho \geq 0.007$) could even occur is inconsistent with the overall objective of the PSR, and the design must attempt to inherently exclude this possibility by other means. A much more comprehensive model for calculations would also be required in such cases.

The resulting temperature histories in various layers of a pellet for several parameter combinations are depicted in Figures 4.9 and 4.10. The thermal response of the pellets lags noticeably behind the reactivity changes, as expected. This thermal

Table 4.1: Reactor periods, corresponding neutron multiplication factors and reactivities, based on the simple exponential model, Eq. (4.13), for an effective neutron lifetime, $\ell = 10^{-2}$ s.

reactor period, τ (s)	2	3	4	7
neutron multiplication, $k = \ell/\tau + 1$ [a]	1.005	1.0033	1.0025	1.0014
reactivity, $\rho = (k - 1)/k$	0.005	0.0033	0.0025	0.0014

[a](Duderstadt and Hamilton 1976).

---

lag is a consequence of the composition of the pellet fuel and allows a period of time before the sublimation temperature of the ablator is reached, even in the fastest excursions modelled. In addition, the significance of the ablative material's thermal conductivity, although not crucial during normal operation (as seen from the small temperature variation in the pellet -- Figure 4.6), is brought to the fore in these transient analyses (Figure 4.10). Since the thermal conductivity of the ablator is more than an order of magnitude less than that of the adjacent two layers', it acts as a major barrier to heat removal from the pellet when the temperatures rise rapidly, and thus a large temperature gradient develops within the ablative layer as the excursion proceeds. Large temperature gradients in the ablator layer may result in thermal stresses that are inconsistent with the fuel pellets' ability to maintain a high degree of integrity (Dobranich and El-Genk 1991). Thus, when seeking a material for the ablative layer, one which is easily compatible with existing layered-pellet manufacturing technology, which sublimes from a solid to a gas at a temperature $\approx 10^3$ °C, and whose thermal conductivity is several times less -- but not orders of magnitude less -- than the fuel and collision-resistant materials' appears to be a desirable candidate. To date, ZrF_4 is the sole candidate investigated for such a role. However,

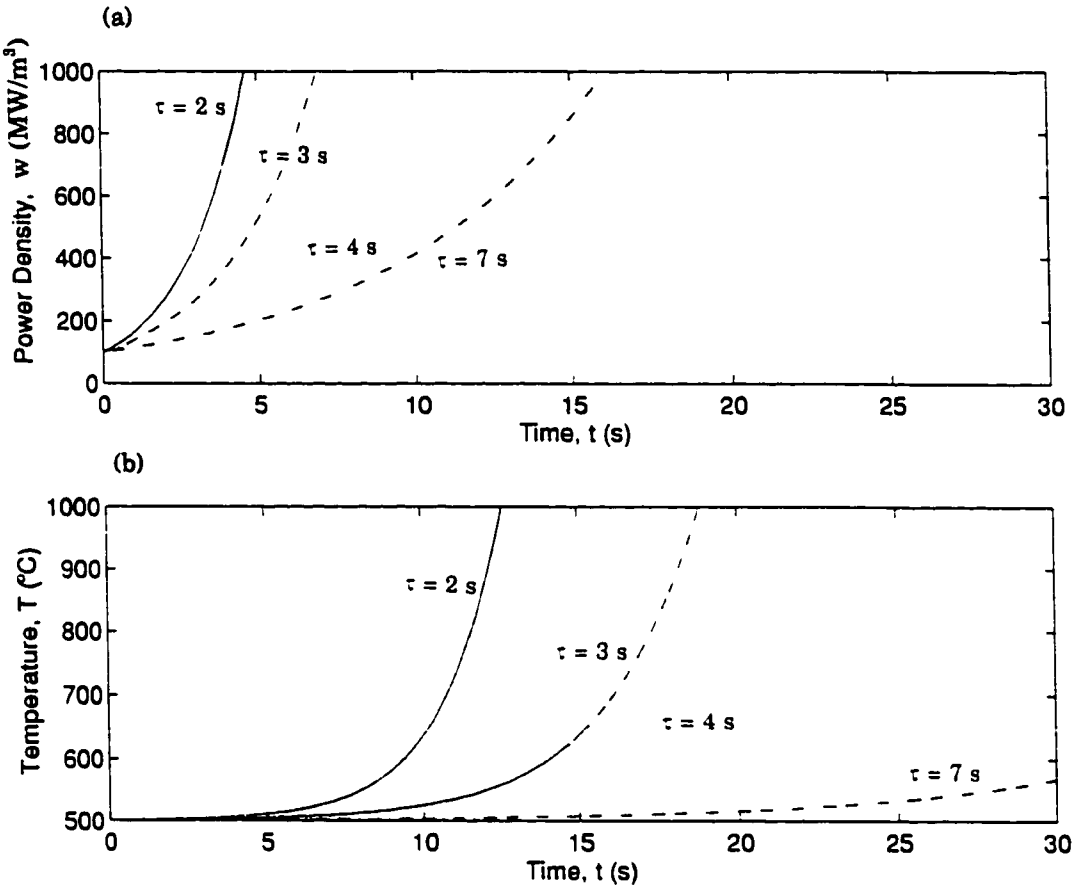

Figure 4.9: Power density and pellet temperature evolutions in time for reactivity excursion modelling: (a) fuel power densities given by Eq. (4.13) for $w(0) = 100$ MW/m^3 for four reactor periods; (b) temperature at the interface between the fuel core and the ablative layer. A suspending fluid temperature of $T_{He} = 500°C$ and a coolant velocity of $U_{He} = 5$ m/s are assumed.

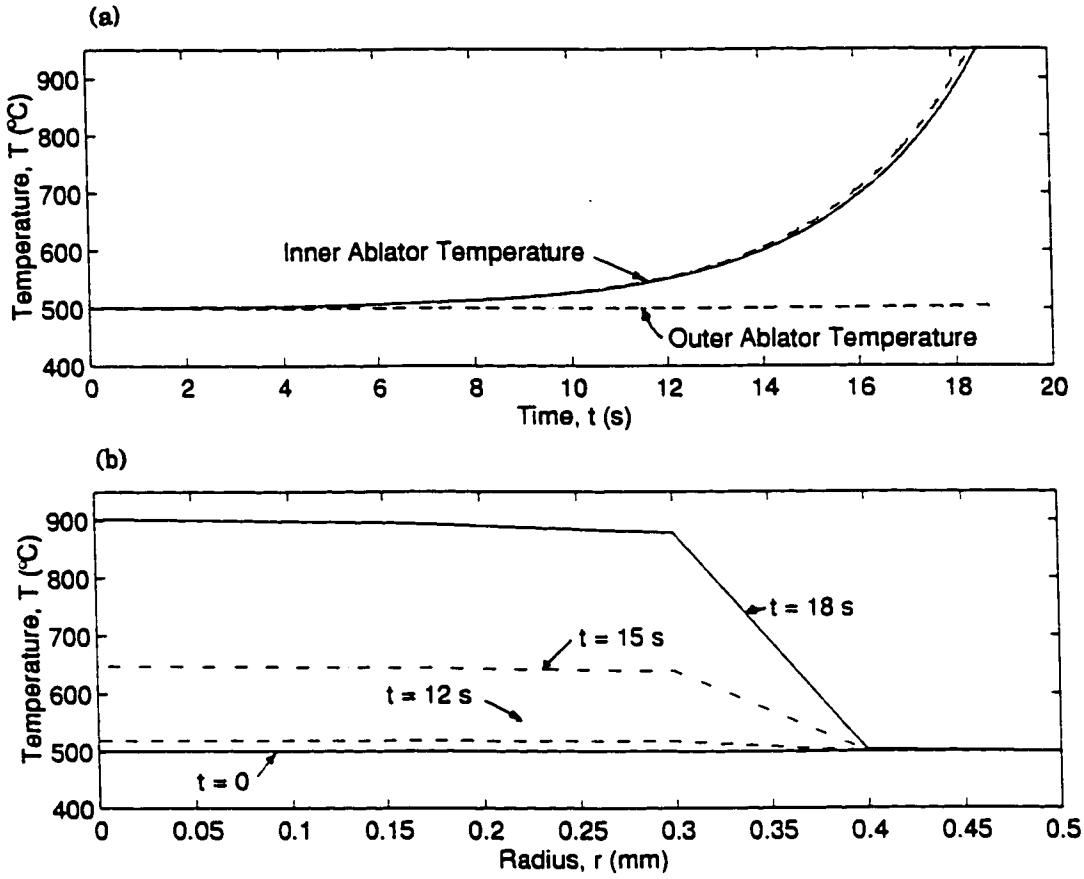

Figure 4.10: Pellet temperature evolutions in time and temperature profiles resulting from reactivity excursion modelling. The fuel power density is given by Eq. (4.13) for $w(0) = 100$ MW/m^3 and $\tau = 3$ s. (a) The temperatures in the ablator layer of a pellet, and (b) temperature profiles in a pellet. A suspending fluid temperature of $T_{He} = 500°C$ and a coolant velocity of $U_{He} = 5$ m/s are assumed. Apparent straight lines are due to a relatively course mesh of nodes in the numerical calculations.

being an amorphous compound it may be poorly suited for such from a manufacturing capability perspective. In addition, its low thermal conductivity and the lack of investigation thereof (Section 2.5) suggest that more suitable materials need to be found to improve this proposed ablative pellet concept.

The steep temperature gradient in the ablative layer is, however, advantageous from the perspective that the inner region of the ablator possesses nearly the same temperature as the fuel core at all times. Thus, if the fuel temperature begins to rise, the temperature of the inner part of the ablative layer will follow suit. For particle break-up to occur, however, a significant amount of the ablative layer will likely need to undergo sublimation, which will require an even greater length of time due to the temperature gradient in the ablative layer. Further, such a significant thermal barrier is not desirable if it is too large since, during a fast reactivity excursion and temperature transient insufficient heat may be removed from the pellet in an adequate period of time to prevent possible fuel kernel failure or melt.

The delay incurred as energy is absorbed by the ablative layer while undergoing the phase change from solid to gas has also been neglected in these analyses. However, such a simplifying assumption, along with all the others used here -- including ignoring self-shielding effects, assuming a short effective neutron lifetime, and using a strictly exponential model for the power density excursion -- tend to increase the rate at which ablation would act in the event of a temperature increase so as to avoid the consequences of a reactivity excursion (Duderstadt and Hamilton 1976). Despite this, the thermal response of the pellets is still quite sluggish -- on the order of 10's of seconds for reactivity insertions of a reasonable magnitude. While the initial power density, $w(0) = 100$ MW/m^3 is perhaps a bit low, this has little impact on the time response of the temperatures due to the overriding influence of the exponential function in the excursion model.

The actual thermal response in the pellets would be even slower than calculated here, as the model has incorporated assumptions which result in excessively fast temperature transients. In addition, the thermal response is slower than those which result from reactivity feedback effects, most notably that from the fuel temperature, which is most often -- and for the PSR would necessarily be -- negative. Effects such as Doppler Broadening of absorption cross-section resonances, which occur with increased fuel temperatures, reduce the fission rate more quickly and act faster than the proposed ablative action. Thus, it appears as though such ablative pellets could, at best, only be considered as an additional provision against reactivity excursions. Claims of inherent avoidance of such events in the PSR would have to be based primarily on the neutronics and reactivity feedback effects rather than the ablative pellet action proposed here, unless modifications to the present configuration are subsequently introduced.

4.8 Removal of Pellet Fragments

The separation and removal of different sized particles from fluidized beds is described by a variety of terms. Davidson et. al. (1985) use entrainment to describe the movement of particles from the bed to the freeboard (Figure 3.1(b)), and elutriation to describe the separation of particles by size in the freeboard. Both terms, however, have also been used to describe the removal of solids from the column altogether (Pemberton and Davidson 1986), for which Davidson et. al. use carry-over. For simplicity, in this work all three will be used to describe the removal of particles out the top of the suspension column.

In the ablative pellet scheme described in Section 4.3 it was mentioned that some pellet fragments may descend out the bottom of the columns, in addition to those

being entrained out the top. Only those fragments whose minimum fluidization velocity is increased above that of the operating velocity would leave through the bottom, and to do so would require a significant increase in density and sphericity to counteract the reduction in size which dramatically reduces the fragments' U_{mf}. One possible example is if only the fuel core of the pellet remains, as it is highly symmetric and of higher density than that of the particle layers prior to the ablative break-up. However, as such fragments -- which would be predominantly at the top of the column where the temperature is highest and ablation would occur first -- descend through the suspension they will undergo collisions with other particles and thus take a significant length of time to exit the column.

It is therefore expected that the amount of core material leaving through the bottom would be quite small. However, to assess this quantitatively, detailed U_{mf} and U_{ter} calculations were done for the three-layer pellets used in the heat transfer modelling of Sections 4.5 - 4.7 using an effective pellet density which incorporates the densities of all three layers via

$$\rho_{eff} = \frac{\sum_{i=1}^{3} \frac{4}{3}\pi\left(r_i^3 - r_{i-1}^3\right)\rho_i}{\sum_{i=1}^{3} \frac{4}{3}\pi\left(r_i^3 - r_{i-1}^3\right)}, \qquad (4.14)$$

where r_i is the outer radius and ρ_i is the mass density of the i-th layer, respectively. For the pellets depicted in Figure 4.2 and using the dimensions considered in Section 4.7, U_{mf} = 0.62 m/s and U_{ter} = 7.0 m/s. Corresponding values for the fuel core fragment alone -- with a sphericity of 1.0 -- are U_{mf} = 0.59 m/s and U_{ter} = 7.3 m/s.

The fact that the two bounding suspension velocities remain virtually unchanged is in part coincidence, as the density and sphericity increases nearly offset the size reduction exactly. However, this also reveals that for the pellet and coating

sizes considered here, effectively no pellets would descend out the bottom of the column -- as U_{mf} remains essentially unchanged. In addition, for cases where the ablative action leaves only the fuel core behind, very little fissile fuel would elutriate out the top of the column as U_{ter} also remains essentially the same. The majority of any small fragments of collision-resistant material and any loose ablator material would be entrained, but both are of little significance neutronically. Thus, the concept of elutriation reducing the amount of fissile fuel in the core in the event of a significant temperature excursion in the fuel pellets appears not to be possible, unless different pellet dimensions -- and possibly compositions -- are considered. Such changes would influence the suspension considerations of Chapter 3, and also the fuel management aspects to be discussed in Chapter 5. These findings of an inadequate amount of fuel removal are consistent, however, with previous work which showed that a significant change in pellet size is required for the hydrodynamic drag to change sufficiently so that the resulting fragments will leave the suspension region (Kingdon and Harms 1996, Davidson, Clift and Harrison 1985). Thus, the thickness of the ablative layer relative to the radius of the fuel core and the outer radius of the pellet will need to be greater than for the cases discussed here if fuel fragments are to be removed from the core at all. The break-up of the fuel core to achieve even smaller fragment dimensions, which would increase the amount of elutriation, is not desired as that would also mean the release of fission products from the fuel matrix.

Therefore, further calculations assume that the complete inner fuel core is the sole remaining fragment following ablation, and the time scale on which fuel is entrained from the core is determined for several pellet layer thicknesses. Effectively, the value of $d_{p,1}$ relative to d_p is the crucial parameter. An equal thickness for the ablator and collision-resistant layers, and an outer diameter of 1 mm are imposed. This maintains the fluidization characteristics for normal operation near those outlined

previously for the PSR, but perhaps changes the required number of pellets in each column -- from a neutronics perspective -- and thus the void fraction in each column. The neutronics can likely be compensated for more easily than the suspension aspects as the former are also dependent upon components such as control rods and lattice pitch which are external to the suspension column. Regardless of other implications, the following calculations are merely to identify parameter ranges where the elutriation mechanism may be effective at removing fuel from the core, and the time scale on which this takes place.

Any pellet fragments reduced in size following sublimation of the ablative material such that their terminal velocity is less than the superficial gas velocity in the core region will approximately obey the elutriation characterizations determined for fluidized beds, i.e.:

$$\begin{pmatrix} \textit{instantaneous} \\ \textit{removal rate} \\ \textit{of particles of} \\ \textit{diameter } d_i \end{pmatrix} = \begin{pmatrix} \textit{elutriation} \\ \textit{constant for} \\ \textit{particles of} \\ \textit{diameter } d_i \end{pmatrix} \cdot \begin{pmatrix} \textit{bed} \\ \textit{cross-} \\ \textit{sectional} \\ \textit{area} \end{pmatrix} \cdot \begin{pmatrix} \textit{mass fraction} \\ \textit{of particles} \\ \textit{of diameter} \\ d_i \textit{ at time } t \end{pmatrix}, \qquad \textbf{(4.15)}$$

$$R_i = \frac{d}{dt}(x_i m_b) = K_{i,\infty}^{*} A\, x_i ,$$

where R_i is in $kg \cdot s^{-1}$ for $K_{i,\infty}^{*}$ – the elutriation constant -- in $kg \cdot m^{-2} \cdot s^{-1}$ (Davidson, Clift and Harrison 1985). If the total mass of pellets in the bed m_b does not decrease by more than ≈15%, Eq. (4.15) can be straightforwardly solved for the fraction of particles of diameter d_i remaining in the bed,

$$x_{i,r} = x_{i,o} \exp\left(-\frac{K_{i,\infty}^{*} A t}{m_b} \right), \qquad \textbf{(4.16)}$$

or leaving the bed,

$$x_{i,l} = x_{i,o}\left[1 - exp\left(-\frac{K_{i,\infty}^{*} A t}{m_b}\right)\right], \qquad (4.17)$$

where $x_{i,o}$ is the fraction of such particles at a reference start time. Many empirical correlations for the elutriation constant have been proposed, most assuming that carryover occurs above the transport disengagement height (TDH) and that a uniform distribution of particles exists in the bed. While the latter is not true of the PSR, as the hottest pellets and thus the first to fragment would be near the top of the columns, these analyses use such a correlation to provide an estimate of the elutriation resulting from the pellet fragmentation proposed in the reactivity avoidance scheme. In addition, as is shown below, there is negligible elutriation of fuel from the core due to the geometry change of the current pellet design -- a result independent of the elutriation constant which determines primarily the rate of fragment removal from the fluidized bed. Most correlations also concede that they are only accurate to within a factor of ± 2-5 when $U > U_{ter}$. For $U \leq U_{ter}$, $K_{i,\infty}^{*} = 0$ by definition, although a small amount of elutriation may occur due to the collective action of the pellets in the column. This is generally minimal compared to the fuel removal envisaged for abating a reactivity excursion. Here, the correlation

$$\begin{aligned} K_{i,\infty}^{*} &= 0.011\rho_s\left(1 - \frac{U_{ter,i}}{U}\right)^2, \quad U_{ter,i} < U \\ &= 0, \qquad\qquad\qquad U_{ter,i} \geq U, \end{aligned} \qquad (4.18)$$

where $U_{ter,i}$ is the terminal velocity of particles of diameter d_i and U is the superficial gas velocity, is used (Colakyan and Levenspiel 1984).

Eq. (4.17) is thus solved for $(x_{i,l} / x_{i,o})$, with $K_{i,\infty}^{*}$ evaluated from Eq. (4.18) and $U_{ter,i}$ from Eqs. (3.20) and (3.21). Figure 4.11 depicts the fraction of fuel cores -- and thus also the fraction of fissile fuel -- leaving the column as a function of r_1 and time.

$$U = \frac{U_{mf} + U_{ter}}{2}$$

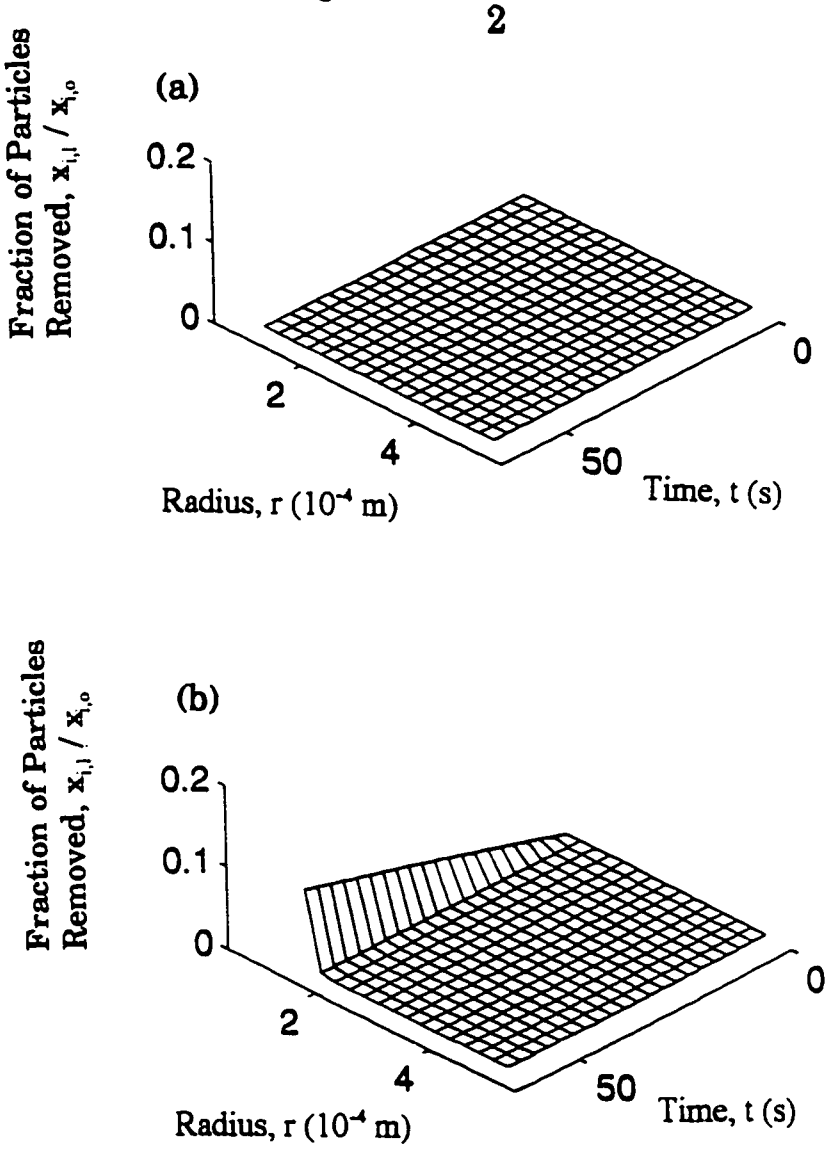

Figure 4.11: Elutriation of particles from a suspension column: (a) normal operating conditions consisting of $\phi_s = 0.95$, $T_{He} = 500°C$, p = 5 MPa and H = 5 m, changing to $\phi_s = 1.0$ and $T_{He} = 1000°C$ during the transient; (b) the same as case (a) except for H = 3 m and $\phi_s = 0.9$ during the transient;

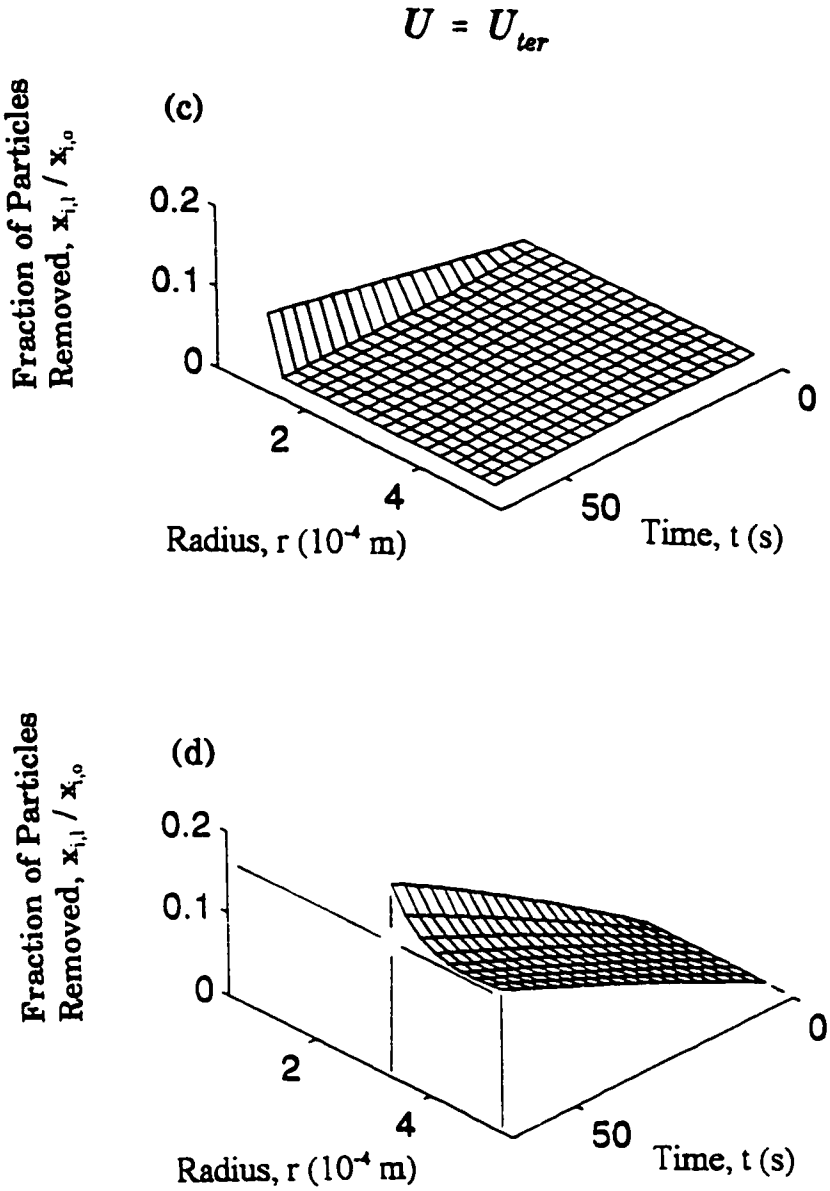

Figure 4.11: (continued) (c) the same as case (a) except for the higher operating velocity, U_{ter}; and (d) normal operating conditions as in case (a) except for T_{He} = 250°C and H = 3 m, changing to ϕ_s = 0.9, T_{He} = 1500°C and p = 25 MPa during the reactivity excursion.

Note that for a typical initial operating velocity of $U = (U_{mf} + U_{ter})/2$, Figure 4.11 (a) and (b), no fuel removal would even occur except for the case of $\phi_s = 1.0$ and $H = 3$, and even then only for $r_1 < 0.2$ mm. Such a pellet structure differs significantly from that envisaged to date, and re-itterates that the present ablative pellets will not accomplish the desired task. The assumption of equal thicknesses for the ablative and collision-resistant layers has essentially no effect on these results as the fuel core diameter relative to the initial particle diameter is the major influence on the elutriation calculations. If a scheme was found in which ablative action was able to achieve some measure of effectiveness against reactivity and temperature excursions, the thickness of the ablative layer would, however, need to be sufficiently large such that the pressure generated upon sublimation would break away enough of the collision-resistant material.

Other parameters which have minor effects upon the elutriation calculations include the temperatures and pressures assumed for the helium gas both before and during the transient. Alone, none has a significant impact on the size of particles removed from the column, although the rates of removal do vary. When combined with somewhat more sensitive parameters such as H, ϕ_s, and primarily U, however, a noticeable effect on the size of particles which can be removed is revealed. Figure 4.11(d) shows that for extreme values of all these parameters, particles whose inner fuel core is nearly as great as the 1 mm outer pellet diameter can still be removed by the elutriation mechanism. Such extreme conditions are unlikely, and combined with the uncertainty in the elutriation constant correlation, suggest that such apparent positive results should be qualified in some way. For the expected conditions, even operating initially with $U = U_{ter}$ -- a condition which makes the entrainment mechanism most successful following any change to the pellet structure -- yields only a small amount of elutriation, and only for irregular pellets with $r_1 < 0.2$ mm, Figure

4.11(c).

The time scale for a significant removal of fuel (~10's of seconds) is, much like the previous thermal analyses, an indication that the rate of fuel removal from a column by the ablative action of the pellets would be quite slow, especially considering the desire for a rapid reversal of any temperature or reactivity excursion and the rate at which temperature coefficients of reactivity act.

Thus, while layered pellet fuel is a well developed technology and is certainly advantageous for the PSR for LOCA avoidance, fission product retention, and normal thermal operation perspectives, the proposed ablative mechanism for reactivity excursion avoidance does not appear sufficient at this point in the development of the PSR reactor concept. The relatively slow thermal response in the fuel pellets -- even for excessively fast transients in the fission power density, the slow elutriation time scale for expected conditions -- assuming that sufficient sublimation of the ablative layer generates enough pressure to break apart the outer collision-resistant layer at all and leaves behind only the inner fuel sphere separate from the other fragments, and the need for a significant difference between the fuel core radius and outer pellet radius for a reasonable fraction of the fissile fuel to be removed from the suspension column -- even at conditions optimal for elutriation such as $U = U_{ter}$, all indicate that the ablative pellet strategy considered here will not alone be sufficient to achieve fail-safe characteristics against reactivity excursions. Substantially different fuel pellet dimensions, if still feasible for a suspended pellet-type reactor from suspension and fuel cycle considerations, combined with a primary reliance on negative temperature and power reactivity coefficients could potentially result in a passive mechanism which has inherent safety characteristics against reactivity excursions, but has not yet been achieved at this point in the development of the PSR. The ablative pellet approach to simpler, passive, more acceptable reactor safety -- with respect to reactivity excursions

-- thus appears little better than conventional provisions available at this time.

The following chapter discusses fuel management procedures to help alleviate concerns over the closure of the nuclear fuel cycle and the disposal of its wastes.

Chapter 5

Waste Management and Fuel Recycling

Fission reactors, be they for electricity generation, research, or radioisotope production, all produce nuclear waste -- primarily in the form of spent fuel elements. This spent fuel generally includes fissile nuclei that have not fissioned, fission products, actinides and various activation products. The waste is initially highly radioactive and must be stored, treated or disposed of with considerable care.

This chapter examines a spent fuel management scheme for the PSR (or potentially any other reactor type) which results in a significantly reduced inventory of waste material -- and reduced radioactivity as well -- compared with conventional systems, while also making more efficient use of fissile fuel reserves and providing resistance to the proliferation of nuclear materials. The spherical fuel pellets used in the PSR, while perhaps not ideally suited for the ablative pellet scheme discussed in Chapter 4 are, however, easily adaptable to the electro-refining fuel treatment process which is the central component of the waste management and fuel recycling strategy considered here.

5.1 Conventional Waste Management Strategies

To date there have been several approaches taken to manage spent nuclear fuel. The simplest is that of storing the used fuel assemblies in pools on-site at the

reactor facility. The water provides cooling and shielding for the radioactivity until such time -- typically ≈6 years -- that the need for both has diminished sufficiently and the fuel bundles may be transferred to dry storage containers. These concrete storage casks continue to provide cooling and shielding and may remain on-site or can be transported to a centralized facility.

A second approach is to reprocess the spent fuel, effectively to separate any remaining uranium (U) or plutonium (Pu) -- perhaps for use in MOX fuel -- from the rest of the waste. This is usually a complicated chemical process -- one example of which is the PUREX (Plutonium URanium EXtraction) process -- which results in large volumes of solid and liquid radioactive wastes which again must be stored in appropriately shielded and cooled containers to ensure that any emissions do not adversely affect the environment.

In these or any other spent fuel management scheme, several issues arise which are significant concerns of the nuclear industry and the public. One focus is the lack of a final disposal strategy for the wastes -- in effect, no closure of the nuclear fuel cycle, since none of the containers mentioned above are intended to be the final repository for the wastes. Instead, most are designed only for storage purposes until such time as a permanent disposal strategy is implemented. While several concepts -- including burial of engineered casks containing the spent fuel elements in deep, stable geological formations -- have been examined, no final resolution has yet been provided which is acceptable to all those concerned. Some estimates even project that there will be sufficient spent fuel accumulated by the time any geological disposal facility being considered in the United States is built that its capacity will be completely exhausted, leaving no space for subsequently generated spent fuel (Laidler et. al. 1997). The technical requirements demanded for acceptability of a waste disposal facility can be eased, however, by reducing the volume and activity of waste which requires storage

or disposal, and more so by reducing the length of time for which assured isolation is required (see also Blix 1997). Section 5.2 describes a waste management scheme for the PSR which includes these very features.

Additional concerns about nuclear waste include the possibility that fissile materials -- in particular Pu -- remaining in spent fuel assemblies may be collected and diverted to groups or states which desire them for the production of weapons. Safeguards against this currently include the option not to reprocess the spent fuel and thus not to isolate any fissile materials from the hazardous radioactive medium in which they are embedded, to re-use the Pu in new fuel elements so as to burn part of it up, appropriate security measures at fuel reprocessing and storage facilities, and organizations like the International Atomic Energy Agency (IAEA) which oversees the monitoring, inspection and accounting of nuclear materials around the world. Also of relevance is the fact that disposing of spent fuel without first extracting the fissile, fissionable, and fertile materials is, to some, throwing away a valuable resource which could be used for future energy production or other applications. While these two issues tend to conflict with one another, fuel recycling via electro-refining -- discussed below -- provides for more efficient resource utilization without the isolation of Pu or highly enriched uranium and thus ensures nuclear proliferation is made no more -- if not less -- possible than in conventional fuel management strategies.

5.2 Fuel Recycling with Electro-refining

An overview of the fuel management scheme proposed for the PSR is depicted schematically in Figure 2.5. Fuel pellets removed from the reactor during normal refuelling or following an abnormal event in which they are ejected from the core are examined in a quality test procedure. Those which have burned up beyond the extent

allowed, or any which are damaged structurally are removed from the fuel stream, the rest remaining available for continued use.

The removed pellets are directed to a pyroprocessing facility which removes selected neutron-absorbing fission products but retains the remainder of the fuel -- notably all of the fissile and transuranic materials -- for use in the manufacture of new fuel pellets, Figure 5.1 (Laidler et. al. 1997). Such a process can also be applied to other reactor types as most differences in fuel composition do not significantly affect the electro-refining operation -- the heart of the pyroprocessing technique (McPheeters, Pierce and Mulcahey 1997). A closer examination of such a scheme reveals how a reduced volume, activity and lifetime of the wastes requiring disposal is achieved, and how these features ease some of the problems involved with current spent fuel strategies.

The main long-term (≥500 - 1000 years) radiological hazards in spent nuclear fuel are the minor actinides[1] and other transuranic elements including Pu. Their long half-lives, and the substantial decay heat emitted by many of these species mean that any isolation barriers involved in a disposal concept are generally required to exhibit insolubility and immobility for ~10 000 - 100 000 years, or longer. If, however, these long-lived isotopes were re-inserted into the reactor core until they were destroyed -- fissioned or transmuted into more stable isotopes -- only the relatively short-lived (≈500 years) fission products would require disposal. This reduces the time scale for which the isolation barriers in a waste management facility would need to remain intact, easing the technical requirements on any type of storage or disposal concept.

Rather than using the expensive and somewhat cumbersome PUREX chemical process developed in the 1950's -- and still used for the bulk of fuel reprocessing

[1]Appendix A explains the element classification terminology used here.

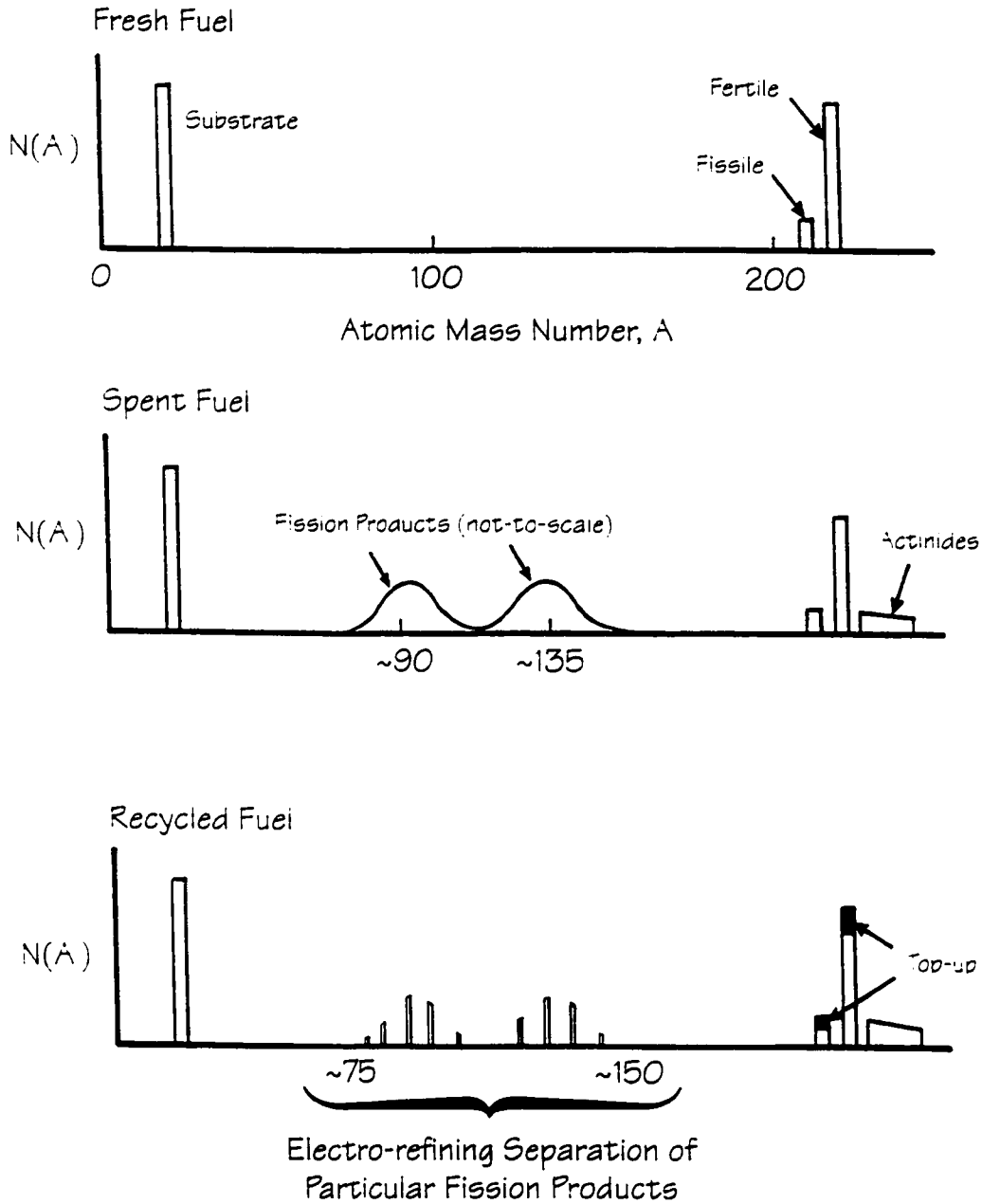

Figure 5.1: Schematic depiction of the composition of fresh fuel, that following burnup in a reactor, and what would exist after the electro-refining operation.

operations today -- electro-refining is here envisaged for separating unwanted fission products from the remainder of the spent fuel that will be recycled. In such a process, high temperature (≈500°C) molten-salt and molten-metal solvents are employed to remove over 99.9% of the U, Pu, and other transuranic elements from the spent fuel through electrolysis (Laidler et. al. 1997). Initially developed in the 1960's for the fuel cycle of fast breeder reactors which require -- essentially by definition -- Pu recycling, the electro-refining operation recovers actinide material of which roughly 30% is uranium that has not yet fissioned or been transmuted via neutron capture. Most importantly, all such elements are removed collectively as one medium, and thus there is no isolation of Pu or highly enriched uranium (HEU) with the attendant risks of their proliferation. This is the main reason that some nations have chosen to no longer use the PUREX procedure to reprocess reactor fuel from civilian reactors.

The electro-refining operation takes place in a well-shielded hot cell facility and begins by chopping up the spent fuel assemblies into small pieces (≈6 - 7 mm). These are placed in a steel basket that acts as the anode in an electrolytic cell, Figure 5.2. For the PSR, its small fuel elements would not likely require any such size reduction, easing the processing requirements for its fuel recycling system. However, the pellets may require some crushing to expose the fuel kernel to the electrolyte, while the carbon coatings would remain in the anode basket. Placing the anode and cathodes in a lithium chloride (LiCl) and potassium chloride (KCl) molten-salt (T_{melt} = 350°C) and cadmium (Cd) molten-metal (T_{melt} = 321°C) bath, a voltage (≈1 V) is applied to complete the circuit. A solid steel cathode collects essentially pure uranium, while U, neptunium (Np), Pu, Americium (Am), Curium (Cm) and certain rare-earth fission products -- which are later separated from the actinides (Sakamura et. al. 1998) -- are collected at a liquid cadmium cathode. The transport of elements through the molten-salt and molten-Cd mediums has elsewhere been successfully modelled with a

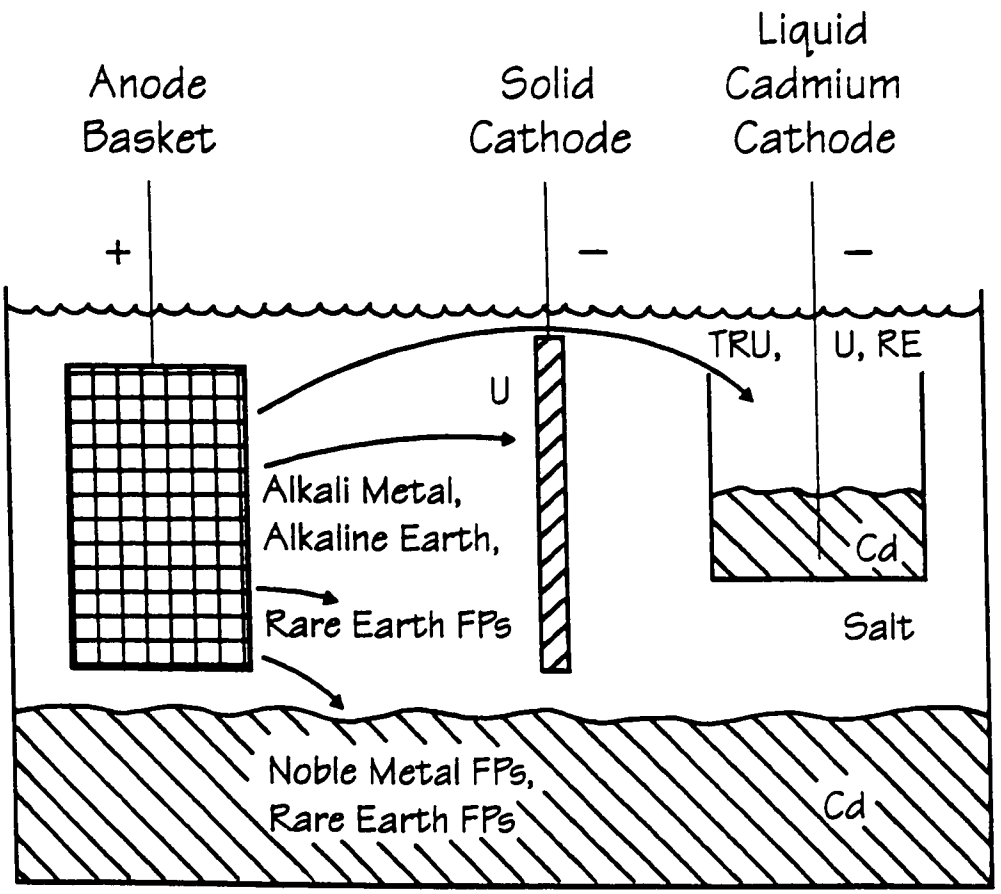

Figure 5.2: Schematic diagram of an electro-refining crucible and the pathways of various fission products (FPs, RE = rare earth) and transuranic (TRU) species (Laidler et. al. 1997).

standard diffusion formulation (Koyama et. al. 1993).

The majority of the fission products (i.e. alkali metals, alkali-earth metals and rare-earths) are left behind in the electrolyte salt, while structural materials and a few other fission products (i.e. noble metals) remain in the molten-Cd layer or in the anode basket itself (McFarlane and Lineberry 1997; Chow, Basco, Ackerman and Johnson 1993). Due to the high temperature of the electrolytic bath, several species in the spent fuel may be volatile and evaporate. However, all fission product gases like xenon (Xe) and krypton (Kr), and any other gases such as tritium are captured in the argon (Ar) over-gas during the electrolysis operation and subsequently are recovered and stored for decay. The alkali metal, alkali-earth, rare-earth and halide fission products are extracted from the electrolyte by ion exchange to form a mineral waste medium known as sodalite (Nishimura, Koyama, Iizuka and Tanaka 1998). Synthesized in a dry process that involves no gas formation, the sodalite waste medium has a very low leachability, comparable even to vitrified waste forms. Finally, the actinides remaining in the salt are extracted -- again at the cathodes -- and the clean salt is returned for the next electrolysis operation (Ackerman et. al. 1997).

Laboratory engineering-scale tests using a steel vessel 1 m in diameter and 1 m high at the Argonne West Laboratory in Idaho resulted in a 100% collection efficiency of all materials placed in the anode basket. This included ≈4 kg of Pu and other actinides at ≈3 g/A·hr, ≈1 kg of U and several hundred parts per million of rare-earth fission products -- all at the liquid cadmium cathode, and ≈15 kg of U (with essentially nothing else) at ≈415 g/A·hr at the solid steel cathode. Improvements in the geometry of the cathodes would improve the collection rates by an order of magnitude, and are needed for commercialization. However, this development is thought to be straightforward (Laidler et. al. 1997).

Generally, the various mediums extracted from the spent fuel are removed in

batches from the electrolytic bath when the decay heat in any section reaches the limits of the components therein. The cathode deposits are melted in a high temperature furnace to evaporate the cathode materials and any other impurities like the electrolyte salt, leaving behind metal ingots ready to be made into new fuel. All components of this fuel recycling, waste disposition, and fuel manufacture system have been built and tested -- some at full scale -- for a metal-fuelled reactor. The design for a complete operating facility requires only 280 m^2, one cell with an air atmosphere (60 m^2) and a second with an Ar atmosphere (220 m^2) (McFarlane and Lineberry 1997).

The entire electro-refining operation has also been tested at an engineering-scale in Japan (Koyama et. al. 1997). Following the dissolution of metal fuel elements the extraction of uranium on a solid cathode was achieved. The collection efficiency was found to be greatly improved by roughing the surface of this cathode, and by rotating both it and the anode in the salt electrolyte. As in the previous work, a liquid Cd cathode was then used to extract the remaining U, Pu, and other actinides as one medium, some enhancement of which was accomplished by slightly agitating or stirring the liquid Cd.

While the initial design and testing of this electro-refining process was for metallic uranium fuel, the same procedure has been investigated -- and shown to be applicable -- to other forms of reactor fuel as well, the sole notable exception being aluminum-based fuels. This is because the electro-chemistry of Al interferes with that of the actinides. This, however, would be of no consequence in the PSR as its fuel elements are carbide, or perhaps oxide, compounds with Si or carbide coatings. Generally, the only changes required for non-metallic fuels are in the preliminary steps which prepare the spent fuel elements for deposition in the anode basket. For example, in the processing of light water reactor (LWR) fuel, the zircalloy cladding is first removed followed by reduction of the oxide fuel to metallic form by a lithium

reactant. The remainder of the fission product extraction process is the same as previously described and the lithium reactant is recovered by electrolysis prior to the manufacture of new fuel elements (McPheeters, Pierce and Mulcahey 1997). It is assumed that similar spent fuel preparations could also be applied to make the operation applicable to the layered pellet fuel of the PSR.

This electro-refining procedure thus allows for better utilization of fissile, fissionable, and fertile resources by not disposing of any such species. Instead, all are recycled back into fuel elements and a larger fraction of these limited isotopes are utilized. More importantly, in doing so there is no isolation of Pu or the fissile isotopes of U, nor is there a build up of these or any other weapons-type materials in spent fuel assemblies at nuclear waste storage sites. Both factors are important in that they reduce the possibility of fissile materials being diverted to groups desiring them for non-peaceful purposes.

Following the electro-refining operation, the metal ingots of recyclable materials are used in the manufacture of new fuel assemblies, while the wastes are collected and stored on-site. Because the majority of the waste is material with a half-life of $\leq$100 years, at least two options subsequently exist. Disposal in an engineered facility is possible if desired, the demands on the engineered barriers to prevent radioactive release less stringent as the length of time necessary for their required integrity is significantly reduced from ~10 000 years to ≈500 - 1000 years.

Alternatively, since the volume and lifetime of waste is significantly reduced by only disposing of fission products and perhaps some structural materials, the option of permanent on-site storage can now be considered, Figure 5.3. The volume of spent fuel would not become prohibitively large over time (demonstrated in Section 5.5 below), and most importantly the lifetime of the radiological hazards would be sufficiently short for monitoring and management to be a viable option -- even if the

ONCE-THROUGH MANAGEMENT:

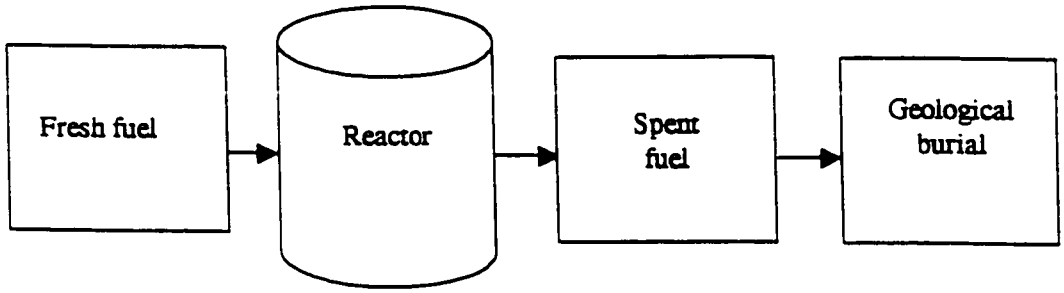

ON-SITE MANAGEMENT:

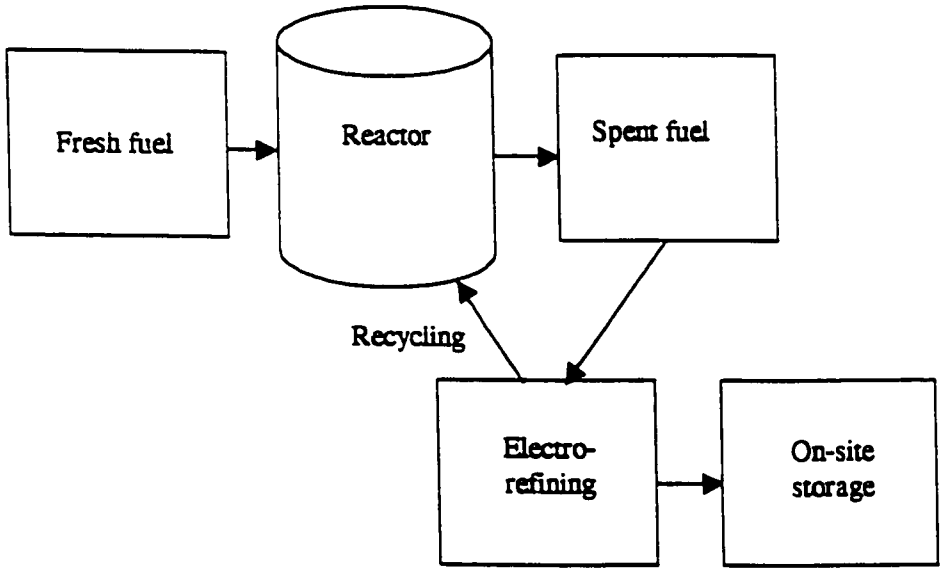

Figure 5.3: Conceptual comparison of conventional once-through fuel management to the proposed on-site strategy employing electro-refining and fuel recycling.

site were to store waste generated over several decades or centuries. In addition, by keeping the waste on-site, any dangers associated with its transportation to a central disposal facility are avoided.

5.3 Assessment of Reduced Waste Inventory

To evaluate the merits of this spent fuel management scheme employing electro-refining and fuel recycling, a comparison of the waste stream's radioactivity and volume -- as functions of time -- derived from such an operation is made to those of the conventional once-through fuel cycle (without reprocessing). Essentially the build-up of activity for the materials extracted during the electro-refining operation is calculated, subject to typical operational and fuel burnup scenarios. Removal of the fuel in batches following each burnup period was used for both the once-through and on-site calculations to avoid having any details of on-line refuelling unnecessarily complicate or obscure the results. Such calculations are intended to demonstrate a reduced volume and radioactivity of the wastes, and also the shortened time scale for which management is necessary.

The approach taken is to consider a typical volume from within the reactor core, initially with a fresh fuel loading. Following operation at a steady power density for a standard burn time, selected fission product elements are removed and replaced with new fuel. All remaining fission products and all the actinides created during the burnup period remain in the volume being analysed. The burnup cycle is then repeated and again removal of certain fission product elements and top-up with fresh fuel occurs (Figure 5.1). The procedure is repeated, and the accumulation of the activity of the waste removed between each cycle is calculated. Comparison of this activity accumulation with that of removing the entire unit volume following each cycle

provides a measure for the reduced amount of radioactivity generated using this fuel management strategy versus that of the once-through approach.

Burnup calculations are made with the Standardized Computer Analyses for Licensing Evaluation (SCALE) 4.3 code sequences, which are distributed by the Radiation Safety Information and Computational Centre (RSICC) and recognised by the Nuclear Regulatory Commission (NRC) of the United States as valid for reactor licensing requirements (RSICC Computer Code Collection: SCALE 4.3, 1995). An initial input file is created for the Safety Analysis Sequence (SAS2H) code which performs neutronics calculations and generates cross-section libraries considering ≈200 distinct species. These libraries are then used along with the initial material concentrations by the ORIGEN-S (Oak Ridge Isotope Generation-S) code to assess the burnup of ≈2000 isotopes over the duration of the burnup cycle, Figure 5.4 (Khotylev, Kingdon and Harms 1997). Typical input files for the SAS2H code for the first burnup period and a burnup stage hundreds of years into the assessment are given in Appendix B.

Neutronic modelling begins by considering a homogeneous distribution of pellet materials in a PSR suspension column. This simplification was considered sufficient as the subsequent burnup calculations are the most important aspect of assessing the merits of the on-site waste management approach. Thermalhydraulic aspects are taken into account by SAS2H, and only neutronically-significant nuclides are included in the input to the neutronics codes so as to minimize complications from the presence of a large number of neutronically-insignificant fission product isotopes.

The SCALE cross section library identified by "27BURNUPLIB" is used for neutronic calculations. This is a 27-group library composed of 14 fast groups and 13 thermal groups (below 3 eV). The group structure was chosen such that the neutronic calculations meet a criterion of $\Delta k_{eff} / k_{eff} < 0.3\%$ when compared with the 218-group

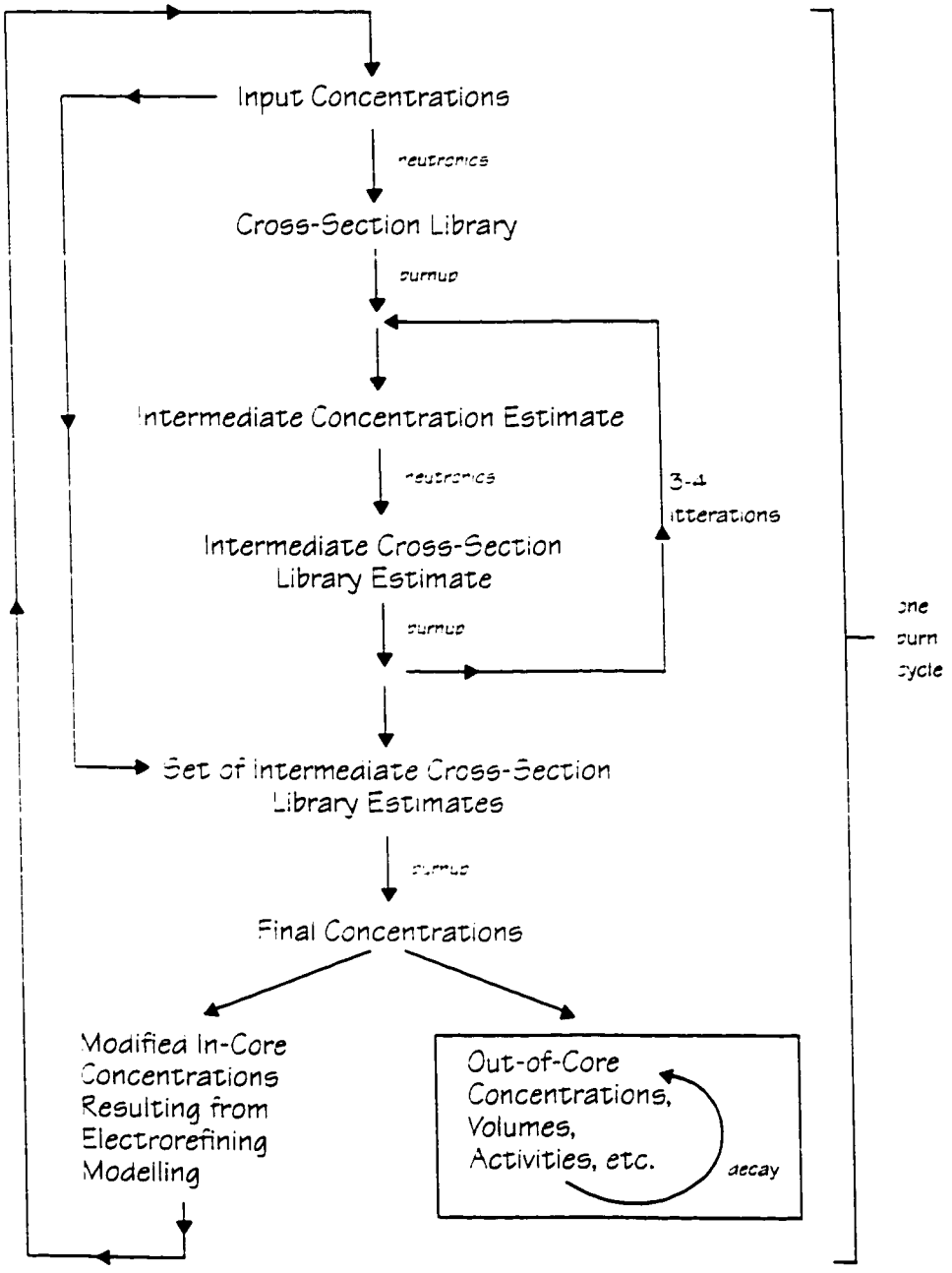

Figure 5.4: Simplified flow chart showing the sequence for burnup calculations with the SCALE 4.3 code package (RSICC Computer Code Collection: SCALE 4.3, 1995). Italics indicate the nature of the calculations performed during each step.

calculations performed by the XSDRNPM code. The 27-group library has been extensively validated against critical experiments. Areas of validation include highly enriched uranium-metal, compound and solution systems, moderated low-enriched uranium, heterogeneous and homogeneous systems, and plutonium metal and solution systems. As a result of validation it was detected that the library has a 1 to 2% positive bias for highly thermal ^{239}Pu systems and negative bias of 1 to 2% for light water reactor fuel lattices, depending on the degree of lattice moderation.

For these investigations there are a number of reasons why this library is preferred to others available. The first is that the validated areas of the library include the reactor configurations being modelled here. Significant neutron spectrum shifts, a build up of Pu, and a higher U enrichment all occur due to the on-site fuel management strategy and modelling of reactor operation over hundreds of years (as will be shown in Section 5.5 below). Also, this is a preferred library for depletion analysis because of the large number of nuclides that can be processed explicitly for use in the ORIGEN-S depletion analysis. For the depletion analysis, libraries containing three-group cross sections, radioactive decay data and fission products for about 750 light nuclides, more than 100 actinides and more than 1000 fission products were utilized (Kloosterman and Hoogenboom 1995).

Because of changes in the nuclide concentrations, and because of the resulting shift in the energy spectrum of the neutron flux, a number of cross-section sets have to be produced in order to calculate nuclide concentrations at the end of each burnup period. A standard approach in which SAS2H repeatedly passes through the neutronic-depletion procedure was used. For the depletion computations, every burn period was split into three parts and one new cross section set per part was determined. While SAS2H allows wide flexibility in setting the number of cross-section sets, the optimum number, which ensures high accuracy and requires low

computational time, was chosen from a comparison of calculated results given in Section S2.6 of the SCALE 4.3 documentation (RSICC Computer Code Collection: SCALE 4.3, 1995).

Once the time dependent cross section libraries for a burnup period have been calculated, criticality is determined and $k_{eff} > 1.01$ is required to exist for the entire duration of the burnup period. If it is determined that the reactor is not critical throughout, more fission products have to be discharged from the previous fuel composition, and calculations for the same campaign must be repeated using the new fuel composition. Once the required criticality is attained, the up-dated ORIGEN-S cross section libraries are generated and the inventory of discharged fission products is determined. The former are used in calculations of in-core depletion, the latter participate in out-of-core decay calculations.

A typical volume from within the reactor core is considered as a means to isolate the essential material compositions -- both in the core and in the waste stream. Spatially-dependent analyses that encompass an entire core become cumbersome and case specific, and could obscure the essential aspects of this study -- to assess the effectiveness of the on-site spent fuel strategy at reducing the activity and lifetime of the nuclear waste requiring disposal -- with unnecessary details.

Thus, as a typical volume or lattice cell, one PSR suspension column and its surrounding structure and moderator is chosen as representative of the reactor, Figure 5.5. Three distinct cases are treated. First, to verify previous calculations (Whitlock 1993), a heavy water moderator and purely UO_2 pellets are considered, Figure 5.5(i). The suspension column is akin to CANDU pressure tubes, i.e. a double-tube composed of a zirconium alloy. A second case, using more realistic materials for the PSR but retaining the geometric simplicity of the first, incorporates a graphite moderator and the three-layer pellets used in the heat transfer modelling (Figure 4.3). A third and

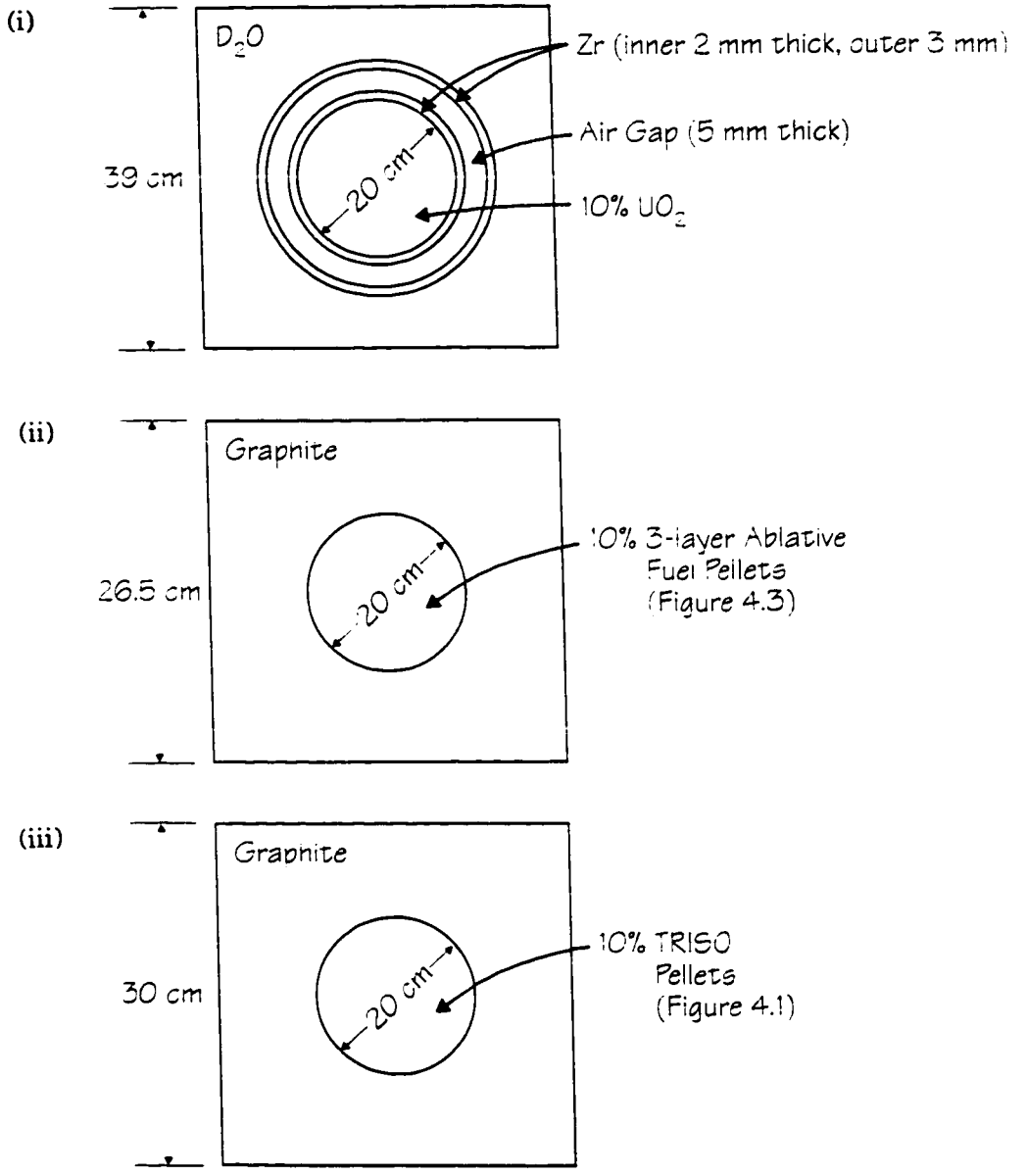

Figure 5.5: Lattice cells used to model the three PSR material compositions and geometric layouts considered in assessing the on-site electro-refining fuel management scheme.

final case investigated is one whose layout is consistent with the PSR, but for which operational parameters similar to those of an HTGR are selected, Table 5.1. The TRISO micro-fuel particles of Figure 4.1 are used, and no ablative material is incorporated to retain consistency with HTGR fuel. Table 5.1 also contains other parameters necessary for the input files of the reactor codes, including temperatures of the various components for each of the three cases considered. These three cases are selected to encompass the primary material and geometric combinations envisaged for the PSR at this stage of its development.

5.4 Recycling Constraints and Waste Removal Criteria

Following each burnup period the composition of the spent fuel is examined and a variety of fission product species are removed based on several criteria. Fuel cladding and any structural, cooling, moderating, or control media are not assessed in the burnup calculations as only the fuel wastes are the focus of this investigation. Also, any radioactivity in the latter materials is typically negligible compared to that of the fuel, fission products, and actinides produced.

All gaseous species -- be they fission products such as Kr, Xe, bromine (Br), cesium (Cs) or iodine (I), or any others such as helium (He) -- are removed, as they escape the fuel medium during the electro-refining operation, or occasionally during normal reactor operation. Recall that those released during electro-refining are collected in the Ar over-gas for storage and subsequent decay. Similarly, for the case of oxide fuel, a fraction of the oxygen is removed corresponding to the fraction of the uranium which undergoes either fission or capture. This assumes that oxygen is released from the fuel compound as a gas following either type of interaction (Tomlinson 1997).

Table 5.1: Selected parameters used in the SCALE 4.3 code package to assess the proposed on-site fuel management scheme for the three PSR configurations depicted in Figure 5.5.

	case (i)	case (ii)	case (iii)
column height (m)	5	5	3
initial fuel enrichment	natural	≈ 2 %	≈ 5 %
thermal power per column (MW_{th})	1.07	0.93	0.93
length of each burnup cycle (years)	≈ 4	≈ 2	≈ 6
maximum fuel temperature (K)	2000	1000	1000
suspension column material and temperature (K)	Zr 563	none	none
moderator temperature (K)	343	800	800

For each of the solid isotopes present in the spent fuel, a spectrum-averaged macroscopic absorption cross-section is calculated along with the radioactivity per unit volume of each species. Since all isotopes of an element are extracted together in the electro-refining operation, fission product elements are sequentially removed in ascending order of their radioactivity per unit volume until sufficient negative reactivity has been removed and sufficient volume is emptied so that replacement with the fuel compound will restore the reactivity of the unit volume to near that at the beginning of the burnup period. While individual fission product elements are removed one at a time in the modelling, it is found that nearly all need to be removed to allow for criticality throughout the subsequent burnup period. Only the most radioactive -- and thus least desirable for removal from the perspective of a reduced activity in the out-of-core waste stream -- are left in the fuel element with the actinides and the fissile fuel. The added uranium is permitted, if necessary, to be enriched to levels greater than that at the beginning of normal operation -- to a

maximum of 20% for the entire element -- in order to reduce the amount of volume which must be freed-up by fission product removal. The 20% uranium enrichment limit is that of the IAEA which is to prevent highly enriched uranium use -- a fuel which can also be used for non-peaceful applications.

A constant volume constraint may be quantified in a manner useful for data processing in the calculational assessment by noting that the initial volume can not be exceeded following each fuel management operation, i.e. fission product extraction and fresh fuel top-up. Simply requiring that the total number of atoms, or the atomic density, be returned to the initial value is not sufficient, since each fission event eventually replaces one uranium atom with two or more fission product atoms of significantly different mass and volume. Other transmutation reactions during reactor operation would further complicate this balance.

Thus, the requirement for the volume considered, V_o, is

$$\sum_i V_i(t>0) \le \sum_i V_i(t=0) = V_o \qquad \textbf{(5.1)}$$

where V_i is the volume of i-type material, i = {fissile, fertile, fission product, actinide, and others such as oxygen}. Obviously, no allowance is made for possible material expansion due to thermal or irradiation effects. This is for simplicity or alternatively, such allowance can be considered to already be a part of the initial volume element.

Since $\rho_i = m_i/V_i$, where ρ_i is the density of a purely i-type medium and m_i is the mass of i-type material in the volume of interest, respectively,

$$V_i = \frac{m_i}{\rho_i} = \frac{N_i^* \cdot m_{atom,i}}{\rho_i} = \frac{N_i \cdot V_o \cdot m_{atom,i}}{\rho_i}, \qquad \textbf{(5.2)}$$

where N_i^* and N_i are the total number of atoms and the atom density of the i-type species in the volume element, and $m_{atom,i}$ is the mass of one atom of i-type material.

Here use has been made of the definition $N_i = N_i^* / V_o$.

The constraint on the volume element considered, Eq. (5.1), is thus reduced to

$$\sum_i \frac{N_i \cdot V_o \cdot m_{atom,i}}{\rho_i} \leq V_o , \qquad (5.3)$$

or

$$\sum_i \frac{N_i \cdot m_{atom,i}}{\rho_i} = \sum_i \frac{N_i}{N_{i,max}} \leq 1 , \qquad (5.4)$$

where $N_{i,max}$ is the atom density of a purely i-type medium, corresponding to the density ρ_i. The constraint of Eq. (5.4) is satisfied for all operations where fission product elements are removed and replaced by fuel prior to the fuel volume being assessed in a subsequent burnup cycle.

Since the PSR may incorporate on-line refuelling, a burnup period commensurate with the time for the whole core to be refuelled -- i.e. ≈2-6 years (Table 5.1), depending upon the configuration considered -- is utilized.

5.5 Computational Results

Since the electro-refining fuel strategy considered here allows for the possibility of on-site waste storage, a "site" is envisaged where energy is produced for several decades, perhaps even centuries. While such a location may require several generations of nuclear reactors over the course of this extended lifetime, the nuclear fuel cycle would end with the relatively short-term storage of fission product wastes -- all within its borders. Thus, the calculational scheme described above to assess the effectiveness of the recycling fuel strategy proposed is extended to several hundred

years to compare the radioactivity and volume of out-of-core waste resulting from this scheme with those of the once-through approach (Figure 5.3). After ≈100 years, as is shown below, the on-site waste activity reaches its asymptotic value, while in the once-through approach waste activity continues to rise even after 400 years.

Due to the relatively short lifetime of the fission product wastes, the ratio of the activity of the materials extracted from the fuel following any one burnup cycle of this scheme to that of the once-through approach is indicative of the reduced activity ratio realized at asymptotic values. This is because the on-site strategy leaves only fission products as contributors to the waste activity, and thus each addition to the waste stream becomes a major component thereof. The majority of the previously extracted materials decay away relatively quickly.

A listing of all isotopes present in significant quantities ($>10^{-10}$ g) in the volume being modelled for case (ii) is given in Appendix C at selected times during the 400 year simulation. Isotopes are ordered by decreasing mass following the second burnup cycle (after 4 years) and are indicative of the results obtained for all three cases considered. The depletion and top-up of fuel species (^{235}U and ^{238}U) and the build up of all other transuranic species over time is evident in the tabulation of actinides. The listing of fission products provides examples of elements which are extracted after each burnup period, some burnup periods, or not at all, depending upon how the constraints of Section 5.4 are met at the particular time in the burnup history.

Figures 5.6(a), 5.7(a) and 5.8(a) depict the waste stream radioactivity per unit energy generated for both the once-through and on-site waste management strategies for the three PSR configurations considered. The asymptotic activity ratios are 18%, 25% and 5.3%, respectively. All three are indicative of the average fraction of the total activity extracted following each burn cycle, as intuitively predicted above.

The oxide fuel case obtains a greater reduction in activity than that of case (ii)

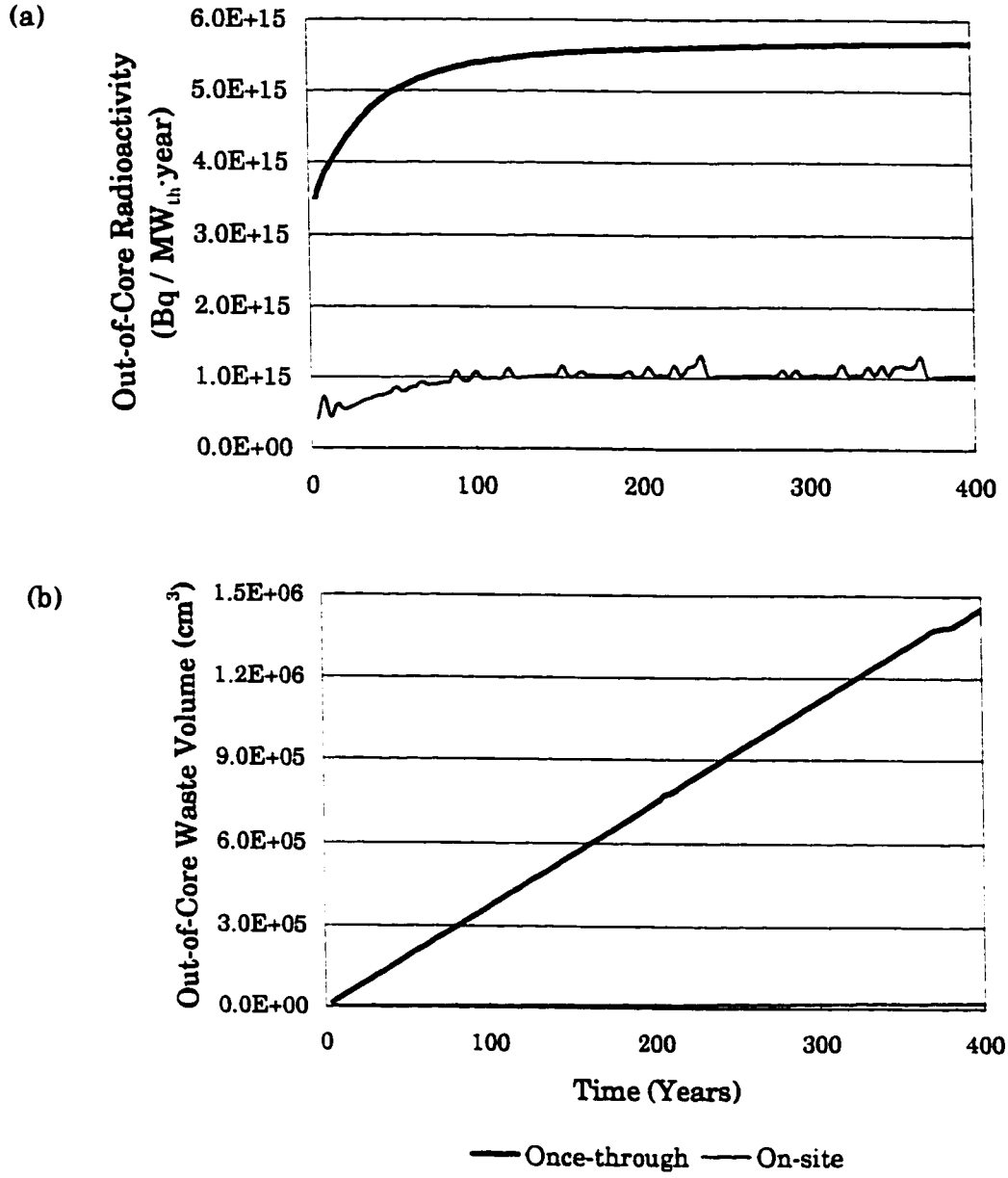

Figure 5.6: Waste stream (a) activity per unit energy generated, and (b) volume, for the on-site (lower curve in each plot) approach as compared to the once-through (upper curves) fuel management strategy for case (i).

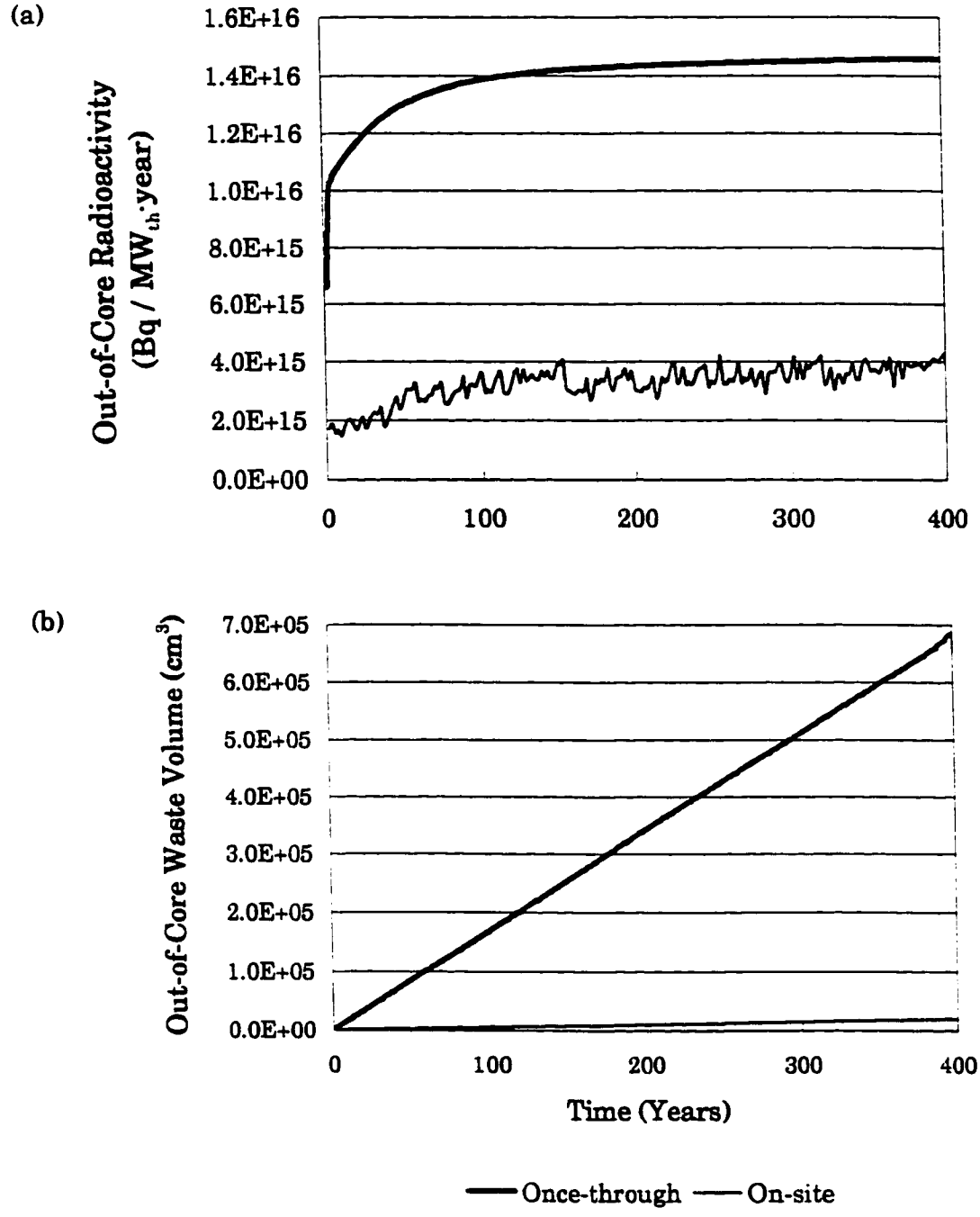

Figure 5.7: Waste stream (a) activity per unit energy generated, and (b) volume, for the on-site (lower curve in each plot) approach as compared to the once-through (upper curves) fuel management strategy for case (ii).

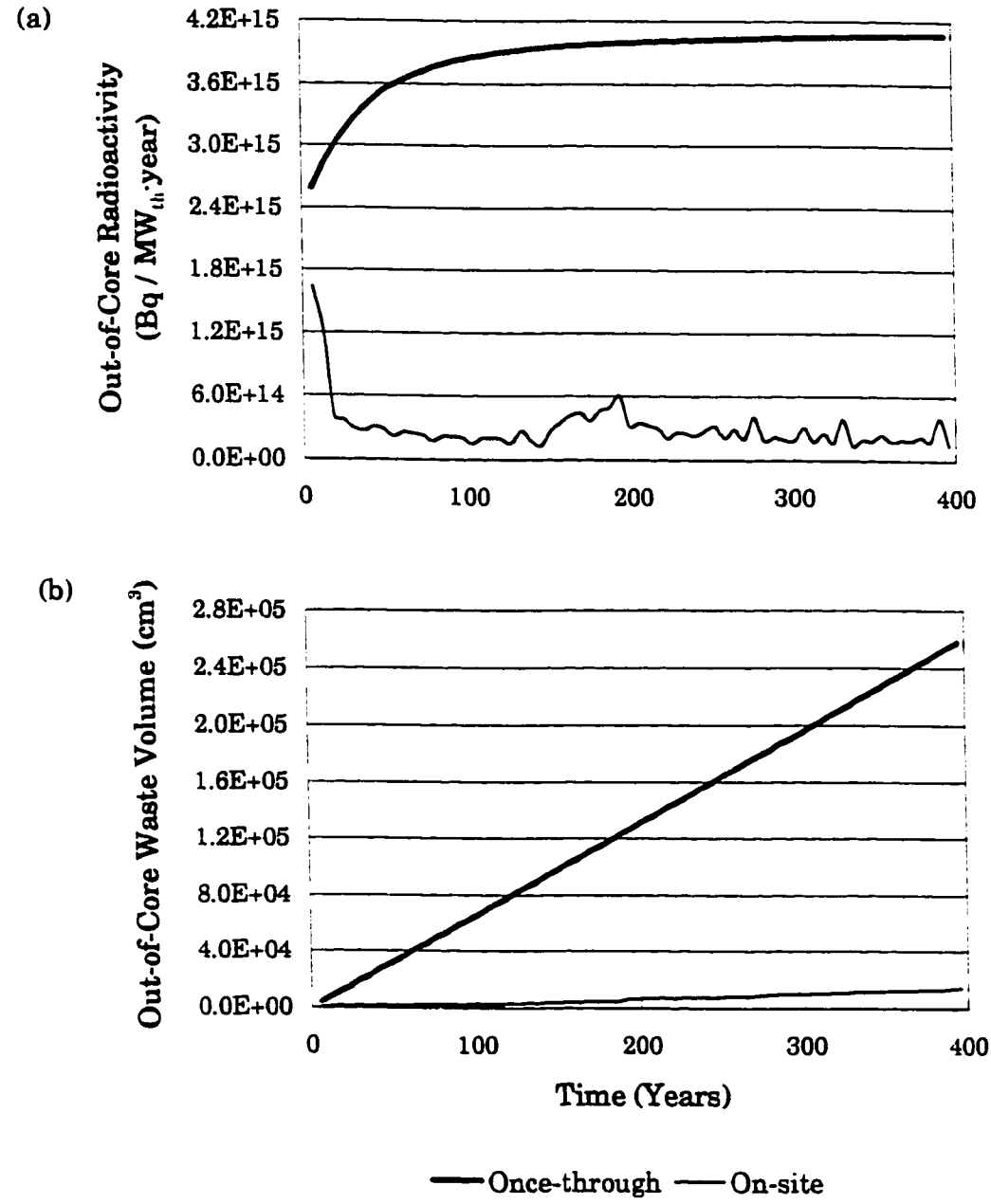

Figure 5.8: Waste stream (a) activity per unit energy generated, and (b) volume, for the on-site (lower curve in each plot) approach as compared to the once-through (upper curves) fuel management strategy for case (iii).

in part due to the release of O_2 from the fuel volume following uranium fission or transmutation (Section 5.4). For carbide fuels, no such volume reduction exists, necessitating more fission product removal to the out-of-core waste stream to allow fresh fuel top-up to provide the required reactivity credit. Despite this, the first two PSR scenarios investigated show at least a 4-5-fold reduction in waste activity over the once-through approach. Case (iii) is significantly better at reducing the out-of-core waste due primarily to its long burnup cycle duration (≈6 years, Table 5.1). This results in a larger volume of fission products which, when removed, provide sufficient volume for fuel top-up to restore the reactivity. The discharged waste materials have a lower radioactivity than those of the corresponding discharges from cases (i) or (ii).

The oscillatory character of some of the on-site curves is a consequence of the step-wise procedure for fission product discharge. Due to the nature of the electro-refining separation process, each chemical element can be either totally discharged from or kept within the fuel volume being modelled. This means that the total discharged activity may not be the same following each burnup cycle. The oscillations originate from the method by which the recycling algorithm minimises the waste disposal after every cycle. If, by increasing the fuel enrichment within the allowed range, the algorithm cannot provide criticality for the reactor with a certain small fraction of fission products discharged, this fraction is increased. This means that the activity discharged after the (N-1)-th campaign may be much higher or lower than that after the N-th campaign. The addition of fission products discharged after each campaign to the out-of-core waste stream causes a discontinuous jump of accumulated activity, the magnitude of which depends on the radioactivity and composition of each new portion. A smooth curve would correspond to the case when an equal activity is extracted following each campaign, but is not consistent with the nature of the fuel management procedures.

The differences between the activity reduction for the three cases considered are a consequence of the different geometries and material compositions -- for example, oxide versus carbide fuel compounds -- and the ability of the code sequences to capture the essential burnup aspects of each case to different degrees. Additional work has determined the corresponding waste activity, volume and lifetime reduction for PWR, BWR and CANDU reactor types, Table 5.2 (Khotylev, Kingdon and Harms 1997; Khotylev, Kingdon, Harms and Hoogenboom 1997a; Khotylev, Kingdon, Harms and Hoogenboom 1997b). Since the SCALE code package is intended primarily for use with PWR and BWR reactors, and since it is optimized for such from the perspective of group structure and other components, the results for these two reactor types are most reliable. However, the weak dependence between the several types investigated and the flexibility of the codes to incorporate other geometries and compositions -- while still maintaining burnup records for ≈2000 isotopes -- yield confidence that the calculations for CANDU, and most importantly here for the PSR, are reliable first-order estimates of the reduced waste inventory resulting from this on-site spent fuel management strategy (Khotylev, Kingdon and Harms 1997).

The volume of out-of-core waste accumulation for both the once-through and on-site strategies for each of the three PSR cases is depicted in Figures 5.6(b), 5.7(b) and 5.8(b). No asymptotic values are obtained, obviously, as the volume of waste material continues to rise over time. However, reductions by 98.7%, 97.1% and 94.7% for cases (i)-(iii), respectively, represent significant improvements over the once-through fuel management approach. Today's temporary on-site storage facilities, typically the size of a large swimming pool or two, are normally capable of storing at least 10 years of spent fuel, if not more. With the electro-refining operation, this would increase to ≥200-500 years, or more. On-site storage of all wastes from a power generation "site" could thus be housed in a warehouse-sized facility, while monitoring

Table 5.2: Out-of-core waste radioactivity and volume from the on-site approach as a fraction of that of the once-through fuel management strategy for the PSR and other reactor types (Khotylev, Kingdon and Harms 1997).

reactor type	asymptotic activity fraction	reduced volume fraction
PSR case (i)	0.18	0.013
case (ii)	0.25	0.029
case (iii)	0.053	0.053
PWR	0.20	0.02 - 0.04
BWR	0.13	0.02 - 0.04
CANDU	0.21	0.02 - 0.04

---

would only be required for ≈500-1000 years due to the shorter lifetime of the primarily fission product waste stream.

An important aspect of this on-site strategy is that a number of specific fission products are retained in the fuel elements during reactor operation. Following each burnup cycle the volume of fission products inside the fuel increases. This leads to two effects: neutron absorption increases and the volume available for new fuel is reduced. Both effects introduce negative reactivity. Fortunately, a competitive process -- a build up of new fissile nuclides including plutonium (Appendix C) -- also occurs, and this improves the reactivity balance. Nevertheless, the uranium enrichment needs to be increased after a certain number of cycles in order to maintain reactor criticality. Although it is difficult to make a theoretical assessment of the dependence of the final fuel enrichment with time, the general character of such can be observed from the calculational results. The final enrichment rises with the amount of radioactivity reduction. Additionally, changes in the plutonium content and its accumulation are

also observed. This is a result of the interaction of fuel compositions, operational histories and neutron energy spectrum shifts.

Calculations presented here report waste radioactivity per unit of thermal energy generated, i.e. in Bq/MW_{th}·year. However, this description makes no allowance for the nature of the activity and simply counts events. A somewhat more useful way to express the results would be to calculate the energy associated with each radioactive decay, which may be expressed as a fraction of the reactor thermal power. However, neither of these methods takes into account the biological effects of different isotopes. In order to do so the concept of biological hazard potential (Steiner and Fraas 1972) can be used. The biological hazard potential for an isotope is usually expressed as the amount of air or water required to dilute that isotope to maximum permissible concentrations. As all these methods are incorporated in the ORIGEN-S code, it is a straightforward task to employ any of them for comparing different strategies or designs. However, an attempt to use the biological hazard potential suffers from the obvious defect that it assumes all isotopes are to be diluted at one point in time. In an effort to account for different half-lives of the many isotopes taken into account, the presentation of results in Bq/MW_{th}·year provides a most simple and transparent figure of merit for comparison.

It is also significant to note that if one is concerned with the amount of waste activity reduction far into the future, which would be of importance to a strategy involving a deep geological repository, the initial waste activity reduction from any one cycle does not indicate the value of this approach. Instead, it is the ratio of waste radioactivities from any single cycle between the electro-refining strategy and the once-through approach many years -- perhaps even centuries -- after withdrawal from the reactor which discloses the former's effectiveness. The reduction of long-term radiological hazards and thus the lessening of the requirements on the barriers needed

to isolate the waste from the environment are greater in the long-term, Figure 5.9. The activity of just one "batch" of waste -- that which is generated in one burnup cycle -- reveals at least a 100-fold reduction of after ≈400 years, compared to the ≈2-fold activity reduction after ≈150 years.

5.6 Implications and Extensions

Modelling of this on-site fuel management scheme has indicated a reduced radioactivity, volume and lifetime of nuclear waste from such an approach. There are, however, additional provisions which could possibly be incorporated to further increase its merit. Reduction of the world's plutonium and HEU inventories could be aided by using their weapons stockpiles as the make-up material following each burnup cycle. This would reduce the need for uranium enrichment, perhaps reduce the amount of fission product waste required to be removed from the fuel elements so that make-up provides the necessary reactivity restoration, and would reduce these fissile inventories in the process. Spectrum shifts due to an increasing Pu content in the fuel should not be any more difficult to analyse, fundamentally, than those which result from the build up of actinides in the reactor and which are inherent in this fuel strategy.

In addition, the volume of out-of-core waste calculated here can be regarded as a maximum value. If separation of the stable isotopes -- formed following sufficient decay of waste fission products -- from the waste stream occurs, its volume is further reduced and the capacity for the on-site storage of nuclear waste is enhanced. Thus, the on-site electro-refining fuel management and recycling strategy discussed here could potentially become a vital component of the nuclear fuel cycle -- both for the PSR and other reactor types.

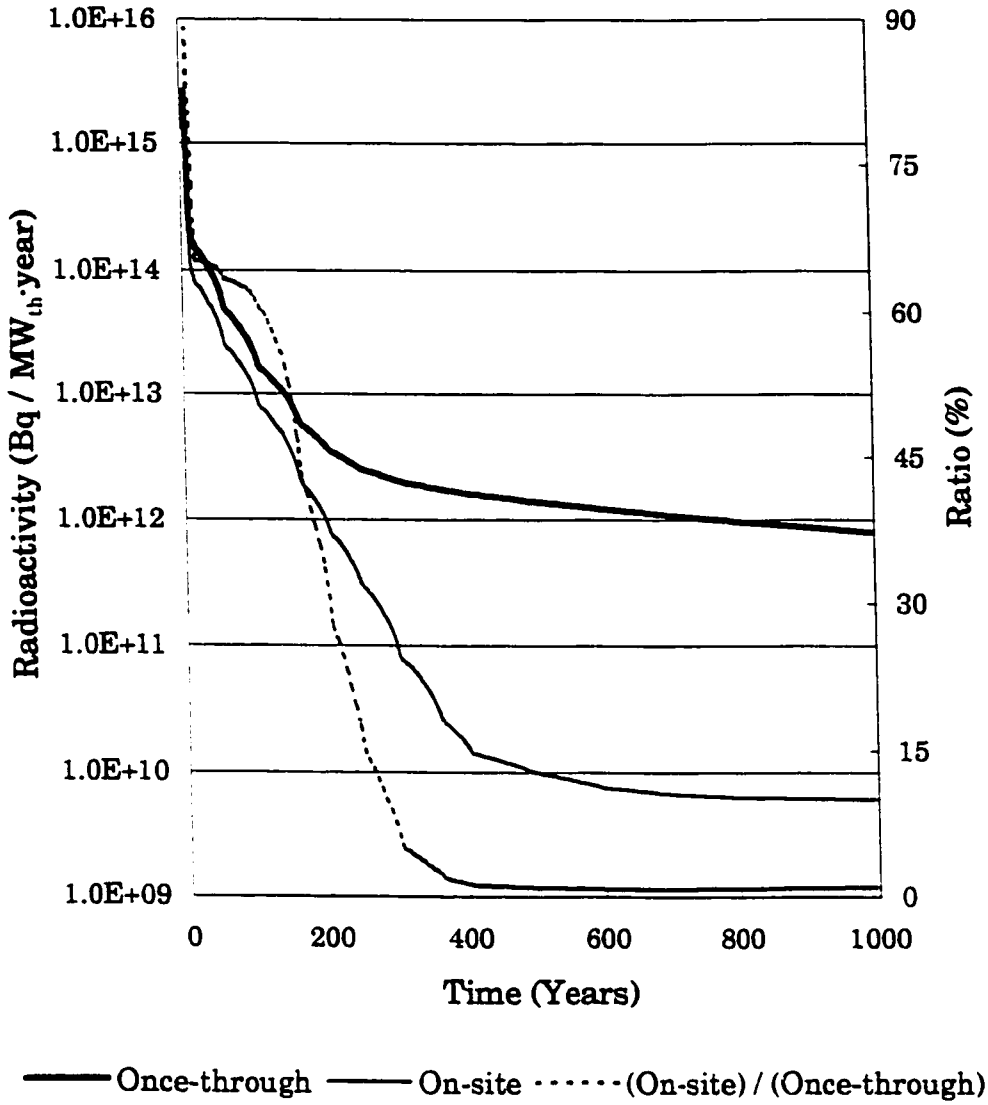

Figure 5.9: Activity per unit energy generated of the waste from one burnup cycle for PSR case (iii), showing the increased activity reduction in the distant future as compared to the first few hundred years.

Chapter 6

Summary and Conclusions

The present slowdown in the world-wide expansion of fission power generation has, in part, suggested that new reactor designs be considered which possess more intrinsic safety features and other advancements. Here, such a nuclear reactor core concept and fuel management strategy have been proposed. Analyses have been carried out to determine the potential of attaining the goals of inherent and passive safety against loss-of-coolant accidents, of limiting reactivity excursion tendencies, as well as closing the nuclear fuel cycle.

The Pellet Suspension Reactor (PSR) is a revolutionary concept that does not have a direct predecessor to which refinements and improvements were made in order to arrive at the new design. Instead, an extension which parallels that of work involving previous fission reactor concepts and the incorporation of much of the experience gained in the past decades of reactor design and operation are used in its development.

6.1 Summary of Core Concept

The PSR core concept is based on the hydrodynamic suspension of fuel particles by an upward flowing coolant. Specifically, pellets ≈1 mm in diameter are suspended in vertical columns by pressurized helium gas, the tubes separated by an appropriate

neutron moderating material. With a sufficient gas flow rate, these pellets containing fissile fuel form a critical arrangement between an upper and lower bound of the core -- defined by an expansion and contraction in the suspension columns, respectively (Figure 2.3). In the event that the coolant flow is interrupted, the fuel pellets are no longer suspended and thus descend under the force of gravity alone to a subcritical and perpetually cooled conical annulus below the core. This fail-safe design provides LOCA avoidance by relying on a natural and assured process, i.e. gravity, rather than electro-mechanical signals and devices which always have some finite, albeit usually small, probability of failure. In addition, the simplified means by which the safety measures are provided reduces both the cost and the complexity of the reactor, leading also to a more transparent system.

On-line refuelling capabilities are conceived of for the pellet fuel by extraction from and injection to the suspension columns from either the side or top. The particles themselves are to contain not only the fissile fuel, but also a layer of material which sublimates from a solid to a gas if its temperature rises significantly above normal operating conditions (Figure 4.3). If such a situation were to occur -- most likely due to a reactivity excursion -- this action will lead to the breakup of the pellets due to the pressure generated as the ablative layer undergoes sublimation. With the size and shape of the suspended fragments altered, the suspension conditions would no longer be met and the fuel will subsequently elutriate out the top of the reactor core or descend out the bottom where it again would be collected and safely stored until required. Sufficient fuel removal is intended to curb the reactivity excursion and thus also any dangerous consequences that may arise from such an event. These additional accident avoidance characteristics are also to be provided by using only naturally assured processes -- in this case thermodynamics -- rather than the signal-driven safety systems relied upon in present-day reactors.

The demands for permanent nuclear waste disposal are considerably reduced with an on-site fuel management strategy that uses selected fission product removal and actinide recycling to reduce the volume, activity, and lifetime of the waste. Following a typical burnup period, certain fission product elements are electrochemically removed from the fuel elements and replaced with fissile material so as to restore the reactivity level to that of fresh fuel and to minimize the out-of-core waste radioactivity. The removed fission products are stored on-site, while the rejuvenated fuel -- containing all the actinides generated during irradiation, the remaining fission products and make-up fissile material -- is recycled for continued use in the reactor core (Figure 5.3). Since the waste stream contains only relatively short-lived fission products -- compared to transuranic species which form the main long-term challenge for disposal concepts in conventional spent fuel management schemes -- its reduced volume, activity and lifetime allow for on-site waste storage to be a viable and sufficient option to close the nuclear fuel cycle. In addition, none of the fissile, fertile, or fissionable resources are disposed of, nor does the electro-refining separation operation isolate Pu or other weapons' grade materials. This provides improved resistance to the proliferation of nuclear materials over strategies which use conventional isotopic separation.

Various aspects of the PSR have been compared to several conventional reactor types (Table 3.2) and to other suspended pellet-type reactor concepts which have been proposed in recent years (Table 2.1). This has aided the selection of appropriate materials for reactor components and shown that the suspended-core arrangements are very similar to today's fission reactors with respect to many neutronic and thermalhydraulic characteristics including power density, coolant flow rates, temperatures and others. Such similarities are important since experience gained with the reactors which have been operating for the past four decades is thus transferrable

-- at least in part -- to the newer reactor core concepts and their development.

6.2 Analyses and Findings

Several contributions to knowledge have resulted from the work undertaken here. These may be grouped according to the three main focus areas (Chapters 3-5). Those concerning the suspension of pellets and the related fluidization characteristics include the following:

- the identification of the minimum fluidization velocity and terminal velocity as bounds for the fluid velocity which provide for pellet suspension in vertical columns, and the calculation of these ranges for three coolant media relevant to suspended pellet-type reactors;
- the design of the open-ended suspension columns and characterization of the fluidized state therein -- including aspects such as gas pressure, tube height, a conical expansion, constraints on the lower and upper contraction and expansion, and pellet injection and removal methods -- in order to assess the uniformity and stability of the pellet suspension;
- formulations for and calculation of the pellet power ratio to show the energetic viability of suspended pellet-type fission reactors;
- the comparison of a number of neutronic and thermalhydraulic characteristics of various suspended pellet-type reactors with those of present-day fission systems.

A number of significant contributions pertaining to fuel pellets and the envisaged ablative action have also been established:

- the incorporation of a temperature-sensitive layer of ablative material in the

fissile micro-particles for the purpose of initiating a fuel ejection mechanism in the event of a significant temperature rise in the fissile material over normal operating conditions;

- the identification of some desirable thermal, mechanical, and nuclear properties for preliminary ablative material candidates;
- the comparison of thermal and elutriation time scales resulting from power excursions in the ablative pellets with nuclear time scales, and the consideration of variations in pellet geometry on the effectiveness of the fuel-ejection process;
- the formulation and calculation of column temperature profiles and energy extraction capability of suspended pellet arrangements.

Finally, some alternative fuel recycling and waste management strategies of considerable promise have been considered, which include:

- the conceptualization of selected fission product removal from spent nuclear fuel and complete actinide recycling in order to reduce the radioactivity, volume and lifetime of waste requiring disposal and to render on-site storage a sufficient means of closing the fuel cycle;
- the formulation of constraints on the particular fission product removal such as complete gas extraction, minimal radioactive discharge to the waste stream, volume restrictions and the imposition of a maximum enrichment resulting from actinide recycling and fresh fuel top-up;
- the assessment of the on-site scheme by repeated burnup stages and recycling operations -- using simulations which account for the accumulation, burnup and decay of ≈2000 isotopes -- over several centuries to determine the reduced out-of-core waste radioactivity, volume and lifetime as compared to the

conventional once-through fuel management approach.

6.3 Conclusions

Many specific safety principles and advancements have been suggested for the next generation of fission reactor cores, some of which are outlined in Chapters 1 and 2. The Pellet Suspension Reactor (PSR) investigated here (Figure 2.5) is designed to possesses several of these improvements, including fail-safe characteristics with respect to loss-of-coolant accidents which are transparent even to the non-specialist. Also, the reduction of reactivity excursion effects and the closure of the nuclear fuel cycle on-site -- without the need for permanent waste disposal -- are desired. All such provisions are intended to assure that no significant radioactive release to the biosphere or reformation of a critical mass occurs.

Inherent loss-of-coolant accident (LOCA) avoidance is achieved by using the natural action of gravity to remove the fuel from the core to a perpetually cooled and sub-critical geometry in the event of a disruption from normal coolant flow conditions. In addition, this passive fail-safe action leaves the reactor in a state from which re-start can be accomplished almost immediately.

The ablative pellet provision is to limit reactivity excursion tendencies through thermodynamic effects alone in the present configuration. However, due in part to the amorphous nature of the ablative material chosen the current design may not be the optimal configuration for this task. Further analyses are required for the identification of better suited materials, the acquisition of improved material data, the investigation of more appropriate pellet structures that are still consistent with a pellet suspension, and a more comprehensive analysis of the proposed accident avoidance mechanism in order to further reduce adverse reactivity excursion effects.

The PSR's fuel management strategy examined here allows for fuel manufacturing, testing, re-cycling, and long-term waste storage all to be accomplished at the power production site since a significant reduction in the waste stream volume, radioactivity, and lifetime -- when compared to the present once-through fuel management approach -- is achieved. This also reduces the transportation requirements compared to those of reactor fuel fabrication techniques used today, and as with all aspects of the PSR, utilizes only existing or near-term technology.

The PSR concept thus possesses characteristics suitable for a second generation of fission reactors. From the work conducted to date, it appears that all aspects of the design warrant more detailed analyses and further development.

Appendix A

Terminology

Several terms referring to groups of elements in the Periodic Table which are used in the description of the on-site spent fuel management strategy and electro-refining procedures presented in Chapter 5 are defined in Figure A.1.

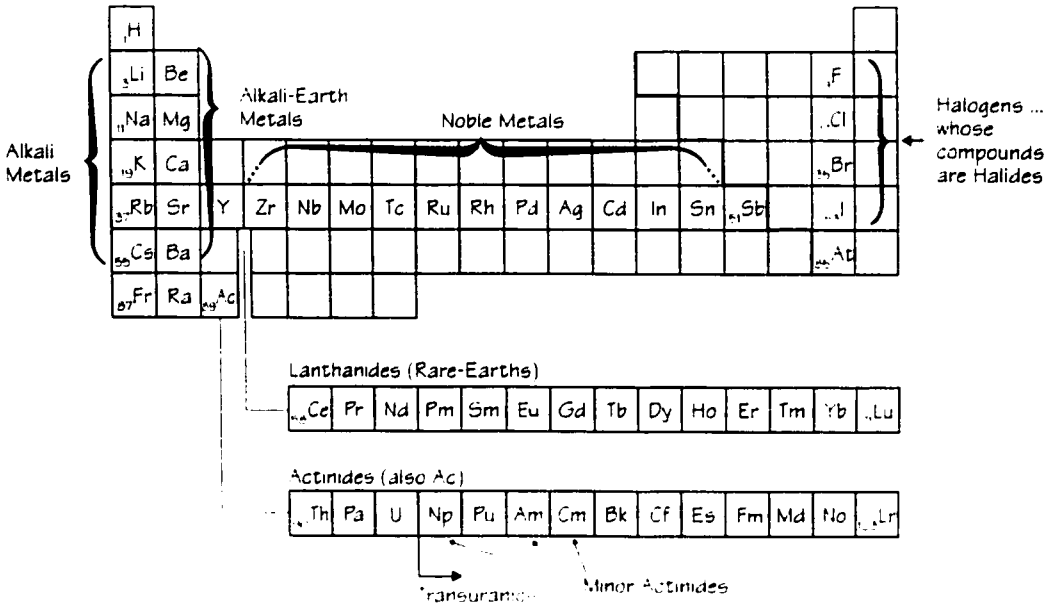

Figure A.1: Terms referring to groups of elements in the Periodic Table used to describe parts of the electro-refining operation for the fuel management scheme of Chapter 5.

Appendix B

Typical SCALE Input Files

The SCALE input file for the first burnup period of case (ii) is given in Figure B.1. It includes a list of the isotopes and elements initially present in the volume being analysed, their atomic densities ($10^{30}\cdot m^{-3}$ -- calculated based on a homogeneous distribution of pellets within the suspension column), and the temperature (K) of each. The fluorine in the ablative material of the pellets (ZrF_4) is not listed as it is of little significance neutronically. Also given are geometric parameters of the suspension column and the surrounding media which form the cell being assessed, and the burnup history data for the three year cycle.

A similar input file for a burnup cycle many years into the calculational assessment of case (ii) in Chapter 5 is given in Figure B.2. Note that it is the same as that in Figure B.1 except for the addition of several neutronically significant actinides and fission products which are now a part of the volume being assessed due to the recycling aspect of the on-site strategy. For each isotope, its mass in grams and a volume correction factor are given which allow the code to calculate the atomic density for each. As in Figure B.1, the temperature for each isotope is also given, along with geometric properties of the cell and data for the three year burnup history.

```
=SAS2      PARM='OLDSAS2,SKIPSHIPDATA'
SAS2 PSR   first start
'
' - - - - - - - - - - - - - - - - - - - - - - - - - - - - - - - -
'
'   MIXTURES OF FUEL-PIN-UNIT-CELL:
'
27BURNUPLIB     LATTICECELL
     C       1 0  3.06e-3      1000 END
     SI      1 0  2.36e-3      1000 END
     ZR      1 0  4.72e-4      1000 END
     U-234   1 0  3.9000e-8    1000 END
     U-235   1 0  1.400e-5     1000 END
     U-238   1 0  6.950e-4     1000 END
     C       2 0  8.8392e-2    800  END
     C       3 0  8.8392e-2    800  END
'
' - - - - - - - - - - - - - - - - - - - - - - - - - - - - - - - -
END COMP
'
' - - - - - - - - - - - - - - - - - - - - - - - - - - - - - - - -
'
'       FUEL-PIN-CELL GEOMETRY:
'
SQUAREPITCH   26.50 20.00  1 3  22.0  2  END
'
' - - - - - - - - - - - - - - - - - - - - - - - - - - - - - - - -
'
'     ASSEMBLY AND CYCLE PARAMETERS:
'
NPIN/ASSM=1  FUELNGTH=500.0  NCYCLES=3  NLIB/CYC=1
PRINTLEVEL=7  LIGHTEL=1 INPLEVEL=1 END
'           ..THESE MIXTURES & RADII
'
POWER=0.93    BURN= 230  DOWN= 15   END
POWER=0.93    BURN= 225  DOWN= 15.5  END
POWER=0.93    BURN= 215  DOWN= 30   END
   TI 0.01

  END
END
```

Figure B.1: SCALE input file for the first burup period of case (ii) of the fuel management scheme assessment in Chapter 5.

```
=SAS2      PARM='OLDSAS2,SKIPSHIPDATA
'          404  YEARS at the begining of the cyc
27BURNUPLIB     LATTICECELL
     PA-233   1 DEN= 5.40000E-05      6.370e-6  1000 END
      U-233   1 DEN= 2.54000E-02      6.370e-6  1000 END
      U-234   1 DEN= 8.05000E+02      6.370e-6  1000 END
      U-236   1 DEN= 1.08000E+04      6.370e-6  1000 END
     NP-237   1 DEN= 1.21000E+03      6.370e-6  1000 END
     PU-238   1 DEN= 2.51000E+03      6.370e-6  1000 END
     PU-239   1 DEN= 8.09000E+02      6.370e-6  1000 END
     PU-240   1 DEN= 3.09000E+02      6.370e-6  1000 END
     PU-241   1 DEN= 2.92000E+02      6.370e-6  1000 END
     PU-242   1 DEN= 8.51000E+01      6.370e-6  1000 END
     AM-241   1 DEN= 1.04000E+02      6.370e-6  1000 END
     AM-243   1 DEN= 1.05000E+02      6.370e-6  1000 END
     CM-244   1 DEN= 1.33000E+02      6.370e-6  1000 END
      C-12    1 DEN= 1.10538E+03      6.370e-6  1000 END
      U-235   1 DEN= 6.39116E+03      6.370e-6  1000 END
      U-238   1 DEN= 3.94000E+03      6.370e-6  1000 END
     ZR-90    1 DEN= 3.28000E+00      6.370e-6  1000 END
     ZR-91    1 DEN= 4.64000E+01      6.370e-6  1000 END
     ZR-92    1 DEN= 4.86000E+01      6.370e-6  1000 END
     ZR-93    1 DEN= 3.53000E+01      6.370e-6  1000 END
     ZR-94    1 DEN= 5.67000E+01      6.370e-6  1000 END
     ZR-95    1 DEN= 1.42000E+00      6.370e-6  1000 END
     ZR-96    1 DEN= 5.79000E+01      6.370e-6  1000 END
     RU-99    1 DEN= 3.06000E-03      6.370e-6  1000 END
     RU-100   1 DEN= 2.16000E+00      6.370e-6  1000 END
     RU-101   1 DEN= 7.72000E+01      6.370e-6  1000 END
     RU-102   1 DEN= 7.82000E+01      6.370e-6  1000 END
     RU-103   1 DEN= 5.23000E-01      6.370e-6  1000 END
     RU-104   1 DEN= 4.73000E+01      6.370e-6  1000 END
     RU-106   1 DEN= 2.98000E+00      6.370e-6  1000 END
     RH-103   1 DEN= 1.12000E+02      6.370e-6  1000 END
     RH-105   1 DEN= 1.60000E-08      6.370e-6  1000 END
     CE-140   1 DEN= 4.60000E+03      6.370e-6  1000 END
     CE-141   1 DEN= 7.63000E-01      6.370e-6  1000 END
     CE-142   1 DEN= 4.06000E+03      6.370e-6  1000 END
     CE-143   1 DEN= 1.69000E-08      6.370e-6  1000 END
     CE-144   1 DEN= 9.99000E+00      6.370e-6  1000 END
     PM-147   1 DEN= 1.08000E+01      6.370e-6  1000 END
```

Figure B.2: SCALE input file for a burnup period many years into the assessment of the fuel management scheme of Chapter 5 for case (ii).

```
    PM-148   1 DEN= 5.82000E-04      6.370e-6   1000 END
    PM-149   1 DEN= 2.02000E-06      6.370e-6   1000 END
    PM-151   1 DEN= 1.20000E-10      6.370e-6   1000 END
     SI      1 0   2.36e-3      1000 END
     ZR      1 0   4.72e-4      1000 END
     C       2 0   8.8392e-2    800  END
     C       3 0   8.8392e-2    800  END
'
' - - - - - - - - - - - - - - - - - - - - - - - - - - - - - - -
END COMP
'
' - - - - - - - - - - - - - - - - - - - - - - - - - - - - - - -
'
'       FUEL-PIN-CELL GEOMETRY:
'
SQUAREPITCH    26.50 20.00   1 3   22.0   2   END
'
' - - - - - - - - - - - - - - - - - - - - - - - - - - - - - - -
'
'     ASSEMBLY AND CYCLE PARAMETERS:
'
NPIN/ASSM=1   FUELNGTH=500.0   NCYCLES=3   NLIB/CYC=1
PRINTLEVEL=7   LIGHTEL=1 INPLEVEL=1 END
'           ..THESE MIXTURES & RADII
'
POWER=0.93    BURN= 230   DOWN= 15   END
POWER=0.93    BURN= 225   DOWN= 15.5   END
POWER=0.93    BURN= 215   DOWN= 30   END
    TI 0.01

  END
END
```

Figure B.2: (continued) SCALE input file for a burnup period may years into the assessment of the fuel management scheme of Chapter 5 for case (ii).

Appendix C

Isotope Listings

The burnup calculations in Chapter 5 -- spanning several hundred years -- which assess the effectiveness of the on-site spent fuel management approach as compared to the once-through fuel strategy take into account ≈2000 isotopes. Listings of all the isotopes remaining in the volume element of case (ii) whose masses are greater than 10^{-10} g are included here for selected times. Table C.1 includes the actinides in decreasing order of mass following the second burnup stage, i.e. after 4 years. The notation 4- refers to the time immediately following the fourth year of burnup calculations, whereas 4+ includes the subsequent process of selected fission product removal and fissile fuel top-up. Thus, all the species in Table C.1 accumulate over time with the exception of ^{235}U and ^{238}U. These fuel species deplete during each burnup stage and are replenished -- to varying degrees due to the changing enrichment -- during the electro-refining and recycling operation. Other fissile isotopes such as ^{239}Pu accumulate less rapidly as they are also depleted due to fission, however this effect is not distinguishable in the reduced data included here.

Table C.2 similarly lists fission products in descending order of abundance following the second burnup cycle. The highlighted isotopes are of elements which are extracted following each burnup campaign (^{139}La), some burnup campaigns (^{106}Ru), and no burnup campaigns (^{148}Pm), respectively. There are, evidently, many examples of each case in Table C.2.

Table C.1: Mass (in grams) of the most abundant actinide species remaining in the volume element of case (ii) at selected times during the burnup calculations of Chapter 5. See page 177 for further explanation.

Isotope	Time (years)										
	0	4-	4+	10-	10+	42-	42+	102-	102+	202-	202+
U238	43087.6	4.1E+4	4.1E+4	4.1E+4	4.1E+4	3.7E+4	3.7E+4	3.2E+4	3.2E+4	2.4E+4	2.4E+4
U235	858.7	7.4E+2	1.4E+3	1.1E+3	1.7E+3	2.4E+3	2.9E+3	4.4E+3	4.9E+3	7.0E+3	7.6E+3
U236	0	2.7E+2	2.7E+2	4.0E+2	4.0E+2	1.4E+3	1.4E+3	3.4E+3	3.4E+3	6.7E+3	6.7E+3
PU239	0	2.6E+2	2.6E+2	3.3E+2	3.3E+2	7.0E+2	7.0E+2	1.2E+3	1.2E+3	1.5E+3	1.5E+3
PU240	0	1.3E+2	1.3E+2	1.5E+2	1.5E+2	2.8E+2	2.8E+2	4.6E+2	4.6E+2	6.4E+2	6.4E+2
PU241	0	9.7E+1	9.7E+1	1.2E+2	1.2E+2	2.6E+2	2.6E+2	3.7E+2	3.7E+2	4.3E+2	4.3E+2
PU242	0	5.1E+1	5.1E+1	6.4E+1	6.4E+1	9.3E+1	9.3E+1	1.1E+2	1.1E+2	1.2E+2	1.2E+2
AM243	0	2.6E+1	2.6E+1	4.5E+1	4.5E+1	9.8E+1	9.8E+1	1.2E+2	1.2E+2	1.4E+2	1.4E+2
NP237	0	2.6E+1	2.6E+1	4.6E+1	4.6E+1	2.2E+2	2.2E+2	5.1E+2	5.1E+2	9.1E+2	9.1E+2
PU238	0	1.6E+1	1.6E+1	3.6E+1	3.6E+1	3.3E+2	3.3E+2	9.7E+2	9.7E+2	1.8E+3	1.8E+3
CM244	0	1.2E+1	1.2E+1	2.9E+1	2.9E+1	1.4E+2	1.4E+2	1.7E+2	1.7E+2	1.6E+2	1.6E+2
AM241	0	6.8E+0	6.8E+0	1.1E+1	1.1E+1	4.6E+1	4.6E+1	1.1E+2	1.1E+2	1.8E+2	1.8E+2
CM242	0	1.5E+0	1.5E+0	2.0E+0	2.0E+0	4.7E+0	4.7E+0	7.0E+0	7.0E+0	7.9E+0	7.9E+0
U234	2.38	1.5E+0	1.5E+0	1.8E+0	1.8E+0	2.5E+1	2.5E+1	1.4E+2	1.4E+2	4.5E+2	4.5E+2
CM245	0	5.6E-1	5.6E-1	2.0E+0	2.0E+0	1.9E+1	1.9E+1	2.8E+1	2.8E+1	2.8E+1	2.8E+1
AM242M	0	2.7E-1	2.7E-1	4.8E-1	4.8E-1	2.5E+0	2.5E+0	5.9E+0	5.9E+0	9.0E+0	9.0E+0
HE 4	0	1.8E-1	1.8E-1	4.3E-1	4.3E-1	6.2E+0	6.2E+0	2.8E+1	2.8E+1	7.8E+1	7.8E+1
CM246	0	1.0E-1	1.0E-1	4.8E-1	4.8E-1	1.3E+1	1.3E+1	3.2E+1	3.2E+1	3.5E+1	3.5E+1
CM243	0	6.2E-2	6.2E-2	9.6E-2	9.6E-2	2.9E-1	2.9E-1	4.7E-1	4.7E-1	5.4E-1	5.4E-1
U237	0	1.2E-2	1.2E-2	1.6E-2	1.6E-2	3.6E-2	3.6E-2	5.4E-2	5.4E-2	6.9E-2	6.9E-2
CM247	0	1.9E-3	1.9E-3	1.4E-2	1.4E-2	8.3E-1	8.3E-1	2.4E+0	2.4E+0	2.7E+0	2.7E+0
NP239	0	3.5E-4	3.5E-4	3.5E-4	3.5E-4	3.4E-4	3.4E-4	3.0E-4	3.0E-4	2.6E-4	2.6E-4
CM248	0	1.9E-4	1.9E-4	2.2E-3	2.2E-3	6.5E-1	6.5E-1	4.5E+0	4.5E+0	7.9E+0	7.9E+0
TH232	0	3.3E-5	3.3E-5	7.1E-5	7.1E-5	8.2E-4	8.2E-4	4.0E-3	4.0E-3	1.3E-2	1.3E-2
U233	0	2.4E-5	2.4E-5	5.4E-5	5.4E-5	7.2E-4	7.2E-4	3.8E-3	3.8E-3	1.4E-2	1.4E-2
NP236	0	2.2E-5	2.2E-5	6.2E-5	6.2E-5	1.4E-3	1.4E-3	7.9E-3	7.9E-3	2.8E-2	2.8E-2
TH230	0	2.2E-5	2.2E-5	2.6E-5	2.6E-5	3.6E-4	3.6E-4	2.6E-3	2.6E-3	9.8E-3	9.8E-3
PU236	0	1.8E-5	1.8E-5	4.1E-5	4.1E-5	3.4E-4	3.4E-4	8.5E-4	8.5E-4	1.5E-3	1.5E-3
PA231	0	1.6E-5	1.6E-5	2.6E-5	2.6E-5	3.6E-4	3.6E-4	3.9E-3	3.9E-3	1.7E-2	1.7E-2
U232	0	1.3E-5	1.3E-5	3.7E-5	3.7E-5	7.3E-4	7.3E-4	4.2E-3	4.2E-3	1.5E-2	1.5E-2
AM242	0	3.4E-6	3.4E-6	6.2E-6	6.2E-6	3.2E-5	3.2E-5	7.7E-5	7.7E-5	1.2E-4	1.2E-4
NP238	0	2.1E-6	2.1E-6	3.3E-6	3.3E-6	1.1E-5	1.1E-5	1.9E-5	1.9E-5	2.5E-5	2.5E-5
BK249	0	2.1E-6	2.1E-6	3.1E-5	3.1E-5	1.4E-2	1.4E-2	9.6E-2	9.6E-2	1.6E-1	1.6E-1
CF249	0	9.7E-7	9.7E-7	2.0E-5	2.0E-5	1.9E-2	1.9E-2	1.8E-1	1.8E-1	3.6E-1	3.6E-1
PA233	0	8.7E-7	8.7E-7	1.6E-6	1.6E-6	7.9E-6	7.9E-6	1.9E-5	1.9E-5	3.6E-5	3.6E-5
TH234	0	6.0E-7	6.0E-7	5.9E-7	5.9E-7	5.4E-7	5.4E-7	4.6E-7	4.6E-7	3.5E-7	3.5E-7
CF250	0	3.9E-7	3.9E-7	5.7E-6	5.7E-6	2.2E-3	2.2E-3	1.3E-2	1.3E-2	2.0E-2	2.0E-2
PU237	0	3.9E-7	3.9E-7	8.5E-7	8.5E-7	7.8E-6	7.8E-6	2.3E-5	2.3E-5	4.3E-5	4.3E-5
CF251	0	2.3E-7	2.3E-7	4.2E-6	4.2E-6	2.7E-3	2.7E-3	1.9E-2	1.9E-2	3.1E-2	3.1E-2
TH228	0	1.7E-7	1.7E-7	5.8E-7	5.8E-7	1.7E-5	1.7E-5	1.1E-4	1.1E-4	3.9E-4	3.9E-4
CF252	0	1.5E-7	1.5E-7	3.1E-6	3.1E-6	2.7E-3	2.7E-3	1.7E-2	1.7E-2	2.4E-2	2.4E-2
NP235	0	1.2E-7	1.2E-7	2.4E-7	2.4E-7	1.5E-6	1.5E-6	3.5E-6	3.5E-6	6.1E-6	6.1E-6
PB208	0	1.1E-7	1.1E-7	5.6E-7	5.6E-7	7.4E-5	7.4E-5	1.2E-3	1.2E-3	9.1E-3	9.1E-3
TH229	0	9.9E-9	9.9E-9	3.8E-8	3.8E-8	1.8E-6	1.8E-6	1.3E-5	1.3E-5	5.4E-5	5.4E-5
TH231	0	3.0E-9	3.0E-9	4.4E-9	4.4E-9	9.8E-9	9.8E-9	1.8E-8	1.8E-8	2.8E-8	2.8E-8
AC227	0	1.1E-9	1.1E-9	2.6E-9	2.6E-9	6.7E-8	6.7E-8	1.3E-6	1.3E-6	8.1E-6	8.1E-6

Table C.1: (continued).

Isotope	Time (years)										
	0	4-	4+	10-	10+	42-	42+	102-	102+	202-	202+
RA226	0	1.0E-9	1.0E-9	1.9E-9	1.9E-9	4.1E-8	4.1E-8	7.6E-7	7.6E-7	6.0E-6	6.0E-6
RA224	0	8.5E-10	8.5E-10	3.0E-9	3.0E-9	8.7E-8	8.7E-8	5.4E-7	5.4E-7	2.0E-6	2.0E-6
PU244	0	3.7E-10	3.7E-10	7.0E-9	7.0E-9	1.2E-5	1.2E-5	2.9E-4	2.9E-4	1.5E-3	1.5E-3
PB212	0	9.7E-11	9.7E-11	3.4E-10	3.4E-10	1.0E-8	1.0E-8	6.2E-8	6.2E-8	2.3E-7	2.3E-7
ES253	0	9.1E-11	9.1E-11	1.8E-9	1.8E-9	1.2E-6	1.2E-6	6.7E-6	6.7E-6	8.6E-6	8.6E-6
PB207	0	7.3E-11	7.3E-11	2.7E-10	2.7E-10	2.1E-8	2.1E-8	9.1E-7	9.1E-7	1.3E-5	1.3E-5
CF253	0	3.7E-11	3.7E-11	7.1E-10	7.1E-10	4.8E-7	4.8E-7	2.6E-6	2.6E-6	3.3E-6	3.3E-6
BI212	0	9.2E-12	9.2E-12	3.2E-11	3.2E-11	9.4E-10	9.4E-10	5.9E-9	5.9E-9	2.2E-8	2.2E-8
BI209	0	6.1E-12	6.1E-12	2.7E-11	2.7E-11	2.7E-9	2.7E-9	4.0E-8	4.0E-8	3.1E-7	3.1E-7
ES254	0	4.3E-12	4.3E-12	7.6E-11	7.6E-11	2.8E-8	2.8E-8	6.8E-8	6.8E-8	4.3E-8	4.3E-8
TH227	0	2.4E-12	2.4E-12	5.9E-12	5.9E-12	1.6E-10	1.6E-10	3.0E-9	3.0E-9	1.9E-8	1.9E-8
PB210	0	1.5E-12	1.5E-12	4.5E-12	4.5E-12	2.2E-10	2.2E-10	5.3E-9	5.3E-9	5.5E-8	5.5E-8
RA223	0	1.5E-12	1.5E-12	3.6E-12	3.6E-12	9.4E-11	9.4E-11	1.8E-9	1.8E-9	1.2E-8	1.2E-8
CM250	0	6.4E-13	6.4E-13	8.6E-12	8.6E-12	5.3E-9	5.3E-9	5.7E-8	5.7E-8	1.6E-7	1.6E-7
PB206	0	7.6E-14	7.6E-14	3.8E-13	3.8E-13	6.7E-11	6.7E-11	3.5E-9	3.5E-9	7.8E-8	7.8E-8

Table C.2: Mass (in grams) of the most abundant fission products remaining in the volume element of case (ii) at selected times during the burnup calculations of Chapter 5. See page 177 for further explanation.

Isotope	Time (years)										
	0	4-	4+	10-	10+	42-	42+	102-	102+	202-	202+
PR141	0	8.1E+1	8.1E+1	1.2E+2	1.2E+2	4.1E+1	0.0E+0	2.0E+1	0.0E+0	1.2E+2	0.0E+0
RU102	0	6.0E+1	6.0E+1	1.4E+1	1.4E+1	8.9E+1	0.0E+0	7.0E+1	7.0E+1	5.3E+1	0.0E+0
RU101	0	5.8E+1	5.8E+1	1.5E+1	1.5E+1	8.1E+1	0.0E+0	6.8E+1	6.8E+1	5.4E+1	0.0E+0
LA139	0	4.5E+1	0.0E+0	4.5E+1	0.0E+0	2.2E+1	0.0E+0	4.4E+1	0.0E+0	2.2E+1	0.0E+0
RU104	0	4.5E+1	4.5E+1	1.1E+1	1.1E+1	6.3E+1	0.0E+0	4.9E+1	4.9E+1	3.5E+1	0.0E+0
XE136	0	3.7E+1	0.0E+0	3.4E+1	0.0E+0	2.8E+1	0.0E+0	2.5E+1	0.0E+0	2.3E+1	0.0E+0
RH103	0	3.1E+1	3.1E+1	3.9E+1	3.9E+1	6.9E+1	6.9E+1	1.0E+2	1.0E+2	1.1E+1	1.1E+1
Y 89	0	3.0E+1	0.0E+0	4.5E+1	0.0E+0	7.8E+0	0.0E+0	3.9E+1	0.0E+0	3.3E+1	0.0E+0
ZR 96	0	2.9E+1	0.0E+0	2.9E+1	0.0E+0	1.4E+1	0.0E+0	2.9E+1	0.0E+0	2.9E+1	0.0E+0
XE134	0	2.8E+1	0.0E+0	2.8E+1	0.0E+0	2.7E+1	0.0E+0	2.7E+1	0.0E+0	2.7E+1	0.0E+0
ZR 94	0	2.7E+1	0.0E+0	2.8E+1	0.0E+0	1.3E+1	0.0E+0	2.7E+1	0.0E+0	2.8E+1	0.0E+0
BA138	0	2.4E+1	0.0E+0	2.4E+1	0.0E+0	2.4E+1	0.0E+0	2.3E+1	0.0E+0	2.3E+1	0.0E+0
CE140	0	2.4E+1	0.0E+0	7.1E+1	0.0E+0	9.2E+1	0.0E+0	6.8E+1	0.0E+0	6.8E+1	0.0E+0
CS137	0	2.4E+1	0.0E+0	2.4E+1	0.0E+0	2.3E+1	0.0E+0	2.3E+1	0.0E+0	2.2E+1	0.0E+0
CS133	0	2.4E+1	0.0E+0	2.4E+1	0.0E+0	2.3E+1	0.0E+0	2.3E+1	0.0E+0	2.3E+1	0.0E+0
ZR 92	0	2.2E+1	0.0E+0	2.2E+1	0.0E+0	1.1E+1	0.0E+0	2.3E+1	0.0E+0	2.4E+1	0.0E+0
CE142	0	2.1E+1	0.0E+0	6.3E+1	0.0E+0	8.2E+1	0.0E+0	6.1E+1	0.0E+0	6.1E+1	0.0E+0
ZR 91	0	2.0E+1	0.0E+0	2.1E+1	0.0E+0	9.3E+0	0.0E+0	2.1E+1	0.0E+0	2.2E+1	0.0E+0
ND143	0	1.9E+1	0.0E+0	1.9E+1	0.0E+0	1.9E+1	0.0E+0	1.9E+1	0.0E+0	2.0E+1	0.0E+0
XE132	0	1.8E+1	0.0E+0	1.8E+1	0.0E+0	1.7E+1	0.0E+0	1.7E+1	0.0E+0	1.6E+1	0.0E+0
SR 90	0	1.8E+1	0.0E+0	9.4E+0	0.0E+0	1.8E+1	0.0E+0	9.8E+0	0.0E+0	1.0E+1	0.0E+0
MO100	0	1.8E+1	0.0E+0	1.7E+1	0.0E+0	1.7E+1	0.0E+0	1.7E+1	0.0E+0	1.6E+1	0.0E+0
ZR 93	0	1.7E+1	0.0E+0	1.7E+1	0.0E+0	8.3E+0	0.0E+0	1.7E+1	0.0E+0	1.7E+1	0.0E+0
TC 99	0	1.6E+1	0.0E+0	1.6E+1	0.0E+0	1.6E+1	0.0E+0	1.5E+1	0.0E+0	1.5E+1	0.0E+0
MO 98	0	1.5E+1	0.0E+0	1.5E+1	0.0E+0	1.5E+1	0.0E+0	1.5E+1	0.0E+0	1.5E+1	0.0E+0
MO 95	0	1.4E+1	0.0E+0	1.4E+1	0.0E+0	1.3E+1	0.0E+0	1.4E+1	0.0E+0	1.4E+1	0.0E+0
MO 97	0	1.4E+1	0.0E+0	1.4E+1	0.0E+0	1.4E+1	0.0E+0	1.4E+1	0.0E+0	1.4E+1	0.0E+0
ND145	0	1.3E+1	0.0E+0	1.4E+1	0.0E+0	1.3E+1	0.0E+0	1.3E+1	0.0E+0	1.3E+1	0.0E+0
CS135	0	1.3E+1	0.0E+0	1.5E+1	0.0E+0	2.0E+1	0.0E+0	2.2E+1	0.0E+0	2.3E+1	0.0E+0
ND144	0	1.2E+1	0.0E+0	1.9E+1	0.0E+0	1.9E+1	0.0E+0	1.8E+1	0.0E+0	1.8E+1	0.0E+0
SR 88	0	1.2E+1	0.0E+0	5.9E+0	0.0E+0	1.2E+1	0.0E+0	6.1E+0	0.0E+0	6.5E+0	0.0E+0
ND146	0	1.1E+1	0.0E+0	1.1E+1	0.0E+0	1.1E+1	0.0E+0	1.1E+1	0.0E+0	1.1E+1	0.0E+0
XE131	0	1.1E+1	0.0E+0	1.1E+1	0.0E+0	1.0E+1	0.0E+0	1.0E+1	0.0E+0	9.9E+0	0.0E+0
PD105	0	9.3E+0	0.0E+0	8.9E+0	0.0E+0	8.6E+0	0.0E+0	7.8E+0	0.0E+0	6.7E+0	0.0E+0
PD104	0	8.8E+0	0.0E+0	9.9E+0	0.0E+0	1.2E+1	0.0E+0	1.1E+1	0.0E+0	4.0E-1	0.0E+0
CE144	0	8.1E+0	0.0E+0	9.8E+0	0.0E+0	9.7E+0	0.0E+0	9.7E+0	0.0E+0	9.8E+0	0.0E+0
PD106	0	7.9E+0	0.0E+0	3.6E+0	0.0E+0	7.0E+0	0.0E+0	6.1E+0	0.0E+0	5.1E+0	0.0E+0
TE130	0	6.9E+0	0.0E+0	6.8E+0	0.0E+0	6.6E+0	0.0E+0	6.5E+0	0.0E+0	6.3E+0	0.0E+0
ND148	0	6.8E+0	0.0E+0	6.8E+0	0.0E+0	6.7E+0	0.0E+0	6.5E+0	0.0E+0	6.5E+0	0.0E+0

Table C.2: (continued)

Isotope	Time (years)										
	0	4-	4+	10-	10+	42-	42+	102-	102+	202-	202+
PD107	0	5.8E+0	0.0E+0	5.5E+0	0.0E+0	5.2E+0	0.0E+0	4.5E+0	0.0E+0	3.7E+0	0.0E+0
PM147	0	5.5E+0	5.5E+0	8.6E+0	8.6E+0	9.8E+0	9.8E+0	1.1E+1	1.1E+1	1.1E+1	1.1E+1
RU106	0	5.5E+0	5.5E+0	8.9E+0	3.9E+0	4.9E+0	0.0E+0	4.3E+0	4.3E+0	3.6E+0	0.0E+0
SM150	0	5.1E+0	0.0E+0	5.8E+0	0.0E+0	5.0E+0	0.0E+0	4.0E+0	0.0E+0	3.0E+0	0.0E+0
RB 87	0	4.1E+0	0.0E+0	4.2E+0	0.0E+0	4.1E+0	0.0E+0	4.3E+0	0.0E+0	4.5E+0	0.0E+0
PD108	0	3.9E+0	0.0E+0	3.8E+0	0.0E+0	3.5E+0	0.0E+0	3.1E+0	0.0E+0	2.5E+0	0.0E+0
I129	0	3.6E+0	0.0E+0	3.5E+0	0.0E+0	3.4E+0	0.0E+0	3.2E+0	0.0E+0	3.1E+0	0.0E+0
ND150	0	3.5E+0	0.0E+0	3.4E+0	0.0E+0	3.3E+0	0.0E+0	3.2E+0	0.0E+0	3.0E+0	0.0E+0
SM152	0	3.2E+0	0.0E+0	3.0E+0	0.0E+0	2.4E+0	0.0E+0	2.0E+0	0.0E+0	1.8E+0	0.0E+0
KR 86	0	3.1E+0	0.0E+0	3.2E+0	0.0E+0	3.2E+0	0.0E+0	3.3E+0	0.0E+0	3.5E+0	0.0E+0
AG109	0	2.7E+0	0.0E+0	2.6E+0	0.0E+0	2.5E+0	0.0E+0	2.1E+0	0.0E+0	1.8E+0	0.0E+0
RU100	0	2.2E+0	2.2E+0	4.9E-1	4.9E-1	2.5E+0	0.0E+0	1.9E+0	1.9E+0	1.4E+0	0.0E+0
KR 84	0	1.8E+0	0.0E+0	1.8E+0	0.0E+0	1.8E+0	0.0E+0	1.8E+0	0.0E+0	1.9E+0	0.0E+0
TE128	0	1.8E+0	0.0E+0	1.7E+0	0.0E+0	1.6E+0	0.0E+0	1.6E+0	0.0E+0	1.5E+0	0.0E+0
EU153	0	1.7E+0	0.0E+0	1.6E+0	0.0E+0	1.4E+0	0.0E+0	1.3E+0	0.0E+0	1.1E+0	0.0E+0
SM147	0	1.6E+0	0.0E+0	4.1E+0	0.0E+0	4.8E+0	0.0E+0	5.2E+0	0.0E+0	5.6E+0	0.0E+0
RB 85	0	1.6E+0	0.0E+0	1.6E+0	0.0E+0	1.6E+0	0.0E+0	1.7E+0	0.0E+0	1.7E+0	0.0E+0
ZR 95	0	1.4E+0	0.0E+0	1.4E+0	0.0E+0	1.4E+0	0.0E+0	1.4E+0	0.0E+0	1.4E+0	0.0E+0
PD110	0	1.2E+0	0.0E+0	1.1E+0	0.0E+0	1.1E+0	0.0E+0	9.1E-1	0.0E+0	7.5E-1	0.0E+0
SM148	0	1.0E+0	0.0E+0	2.7E+0	0.0E+0	2.7E+0	0.0E+0	2.5E+0	0.0E+0	2.2E+0	0.0E+0
ZR 90	0	9.7E-1	0.0E+0	5.6E-1	0.0E+0	7.0E-1	0.0E+0	5.3E-1	0.0E+0	5.6E-1	0.0E+0
NB 95	0	9.6E-1	0.0E+0	9.7E-1	0.0E+0	9.5E-1	0.0E+0	9.6E-1	0.0E+0	9.8E-1	0.0E+0
I127	0	9.0E-1	0.0E+0	8.7E-1	0.0E+0	8.3E-1	0.0E+0	7.6E-1	0.0E+0	6.9E-1	0.0E+0
KR 83	0	8.5E-1	0.0E+0	8.8E-1	0.0E+0	8.8E-1	0.0E+0	9.1E-1	0.0E+0	9.5E-1	0.0E+0
Y 91	0	8.5E-1	0.0E+0	8.7E-1	0.0E+0	8.8E-1	0.0E+0	9.2E-1	0.0E+0	9.7E-1	0.0E+0
CS134	0	8.2E-1	0.0E+0	7.7E-1	0.0E+0	6.1E-1	0.0E+0	4.8E-1	0.0E+0	3.8E-1	0.0E+0
SM154	0	8.0E-1	0.0E+0	7.7E-1	0.0E+0	7.4E-1	0.0E+0	6.7E-1	0.0E+0	5.9E-1	0.0E+0
CE141	0	7.6E-1	0.0E+0	7.7E-1	0.0E+0	7.5E-1	0.0E+0	7.5E-1	0.0E+0	7.5E-1	0.0E+0
RU103	0	7.1E-1	7.1E-1	6.9E-1	6.9E-1	6.5E-1	0.0E+0	6.1E-1	6.1E-1	5.7E-1	0.0E+0
SM151	0	6.6E-1	0.0E+0	8.5E-1	0.0E+0	1.4E+0	0.0E+0	1.6E+0	0.0E+0	1.6E+0	0.0E+0
ND142	0	6.5E-1	0.0E+0	1.1E+0	0.0E+0	1.6E-1	0.0E+0	5.6E-2	0.0E+0	4.0E-1	0.0E+0
GD156	0	6.1E-1	0.0E+0	5.5E-1	0.0E+0	4.3E-1	0.0E+0	3.4E-1	0.0E+0	2.7E-1	0.0E+0
CD111	0	5.9E-1	0.0E+0	5.6E-1	0.0E+0	5.3E-1	0.0E+0	4.7E-1	0.0E+0	3.9E-1	0.0E+0
BA137	0	5.9E-1	0.0E+0	5.8E-1	0.0E+0	5.7E-1	0.0E+0	5.6E-1	0.0E+0	5.5E-1	0.0E+0
SE 82	0	5.7E-1	0.0E+0	5.7E-1	0.0E+0	5.6E-1	0.0E+0	5.7E-1	0.0E+0	5.9E-1	0.0E+0
SR 89	0	5.2E-1	0.0E+0	5.4E-1	0.0E+0	5.5E-1	0.0E+0	5.8E-1	0.0E+0	6.2E-1	0.0E+0
SN126	0	4.1E-1	0.0E+0	4.0E-1	0.0E+0	3.7E-1	0.0E+0	3.4E-1	0.0E+0	3.0E-1	0.0E+0
KR 85	0	4.0E-1	0.0E+0	4.1E-1	0.0E+0	4.1E-1	0.0E+0	4.2E-1	0.0E+0	4.4E-1	0.0E+0
BR 81	0	3.6E-1	0.0E+0	3.6E-1	0.0E+0	3.6E-1	0.0E+0	3.6E-1	0.0E+0	3.7E-1	0.0E+0
CD110	0	3.5E-1	0.0E+0	3.2E-1	0.0E+0	2.7E-1	0.0E+0	2.2E-1	0.0E+0	1.6E-1	0.0E+0
GD158	0	3.4E-1	0.0E+0	3.2E-1	0.0E+0	2.9E-1	0.0E+0	2.4E-1	0.0E+0	1.8E-1	0.0E+0
CD112	0	2.7E-1	0.0E+0	2.6E-1	0.0E+0	2.5E-1	0.0E+0	2.2E-1	0.0E+0	1.8E-1	0.0E+0
CD114	0	2.7E-1	0.0E+0	2.6E-1	0.0E+0	2.3E-1	0.0E+0	1.8E-1	0.0E+0	1.4E-1	0.0E+0
EU154	0	2.6E-1	0.0E+0	2.3E-1	0.0E+0	1.7E-1	0.0E+0	1.4E-1	0.0E+0	1.1E-1	0.0E+0
SE 80	0	2.4E-1	0.0E+0	2.4E-1	0.0E+0	2.4E-1	0.0E+0	2.4E-1	0.0E+0	2.4E-1	0.0E+0
BA136	0	2.3E-1	0.0E+0	2.3E-1	0.0E+0	2.4E-1	0.0E+0	2.2E-1	0.0E+0	2.0E-1	0.0E+0
EU155	0	2.1E-1	0.0E+0	2.4E-1	0.0E+0	2.8E-1	0.0E+0	2.8E-1	0.0E+0	2.5E-1	0.0E+0
BA134	0	2.1E-1	0.0E+0	2.0E-1	0.0E+0	1.6E-1	0.0E+0	1.2E-1	0.0E+0	9.8E-2	0.0E+0
MO 96	0	2.0E-1	0.0E+0	1.9E-1	0.0E+0	1.3E-1	0.0E+0	1.4E-1	0.0E+0	1.3E-1	0.0E+0
SN124	0	1.7E-1	0.0E+0	1.6E-1	0.0E+0	1.5E-1	0.0E+0	1.4E-1	0.0E+0	1.3E-1	0.0E+0
SB125	0	1.6E-1	0.0E+0	1.6E-1	0.0E+0	2.4E-1	0.0E+0	1.4E-1	0.0E+0	1.3E-1	0.0E+0
SM149	0	1.6E-1	0.0E+0	2.4E-1	0.0E+0	5.9E-1	0.0E+0	1.2E+0	0.0E+0	2.0E+0	0.0E+0

Table C.2: (continued)

Isotope	Time (years)										
	0	4-	4+	10-	10+	42-	42+	102-	102+	202-	202+
PR143	0	1.3E-1	1.3E-1	1.4E-1	1.4E-1	1.3E-1	0.0E+0	1.4E-1	0.0E+0	1.4E-1	0.0E+0
BA140	0	1.2E-1	0.0E+0	1.2E-1	0.0E+0	1.2E-1	0.0E+0	1.2E-1	0.0E+0	1.2E-1	0.0E+0
SN122	0	9.9E-2	0.0E+0	9.6E-2	0.0E+0	9.1E-2	0.0E+0	8.5E-2	0.0E+0	7.8E-2	0.0E+0
CD116	0	9.8E-2	0.0E+0	9.5E-2	0.0E+0	9.1E-2	0.0E+0	8.5E-2	0.0E+0	7.8E-2	0.0E+0
SN117	0	9.6E-2	0.0E+0	9.2E-2	0.0E+0	8.7E-2	0.0E+0	7.9E-2	0.0E+0	7.0E-2	0.0E+0
SB123	0	9.0E-2	0.0E+0	8.8E-2	0.0E+0	1.7E-1	0.0E+0	7.9E-2	0.0E+0	7.3E-2	0.0E+0
SE 79	0	8.9E-2	0.0E+0	8.8E-2	0.0E+0	8.6E-2	0.0E+0	8.6E-2	0.0E+0	8.6E-2	0.0E+0
SN119	0	7.8E-2	0.0E+0	7.5E-2	0.0E+0	7.2E-2	0.0E+0	6.7E-2	0.0E+0	6.1E-2	0.0E+0
SB121	0	7.7E-2	0.0E+0	7.5E-2	0.0E+0	1.4E-1	0.0E+0	6.7E-2	0.0E+0	6.2E-2	0.0E+0
SN120	0	7.5E-2	0.0E+0	7.3E-2	0.0E+0	7.0E-2	0.0E+0	6.5E-2	0.0E+0	6.0E-2	0.0E+0
SN118	0	7.2E-2	0.0E+0	7.0E-2	0.0E+0	6.7E-2	0.0E+0	6.2E-2	0.0E+0	5.6E-2	0.0E+0
TB159	0	6.2E-2	0.0E+0	5.9E-2	0.0E+0	5.6E-2	0.0E+0	4.8E-2	0.0E+0	3.9E-2	0.0E+0
IN115	0	5.5E-2	0.0E+0	5.3E-2	0.0E+0	5.2E-2	0.0E+0	4.9E-2	0.0E+0	4.5E-2	0.0E+0
SE 78	0	4.8E-2	0.0E+0	4.8E-2	0.0E+0	4.6E-2	0.0E+0	4.5E-2	0.0E+0	4.5E-2	0.0E+0
TE125	0	4.4E-2	0.0E+0	4.3E-2	0.0E+0	9.9E-2	0.0E+0	3.8E-2	0.0E+0	3.5E-2	0.0E+0
XE130	0	4.3E-2	0.0E+0	3.6E-2	0.0E+0	2.4E-2	0.0E+0	1.9E-2	0.0E+0	1.6E-2	0.0E+0
TE127M	0	3.3E-2	0.0E+0	3.1E-2	0.0E+0	2.9E-2	0.0E+0	2.7E-2	0.0E+0	2.4E-2	0.0E+0
ND147	0	3.1E-2	0.0E+0	3.1E-2	0.0E+0	3.0E-2	0.0E+0	3.0E-2	0.0E+0	3.0E-2	0.0E+0
TE129M	0	2.7E-2	0.0E+0	2.7E-2	0.0E+0	2.5E-2	0.0E+0	2.4E-2	0.0E+0	2.3E-2	0.0E+0
GD160	0	2.7E-2	0.0E+0	2.6E-2	0.0E+0	2.5E-2	0.0E+0	2.1E-2	0.0E+0	1.7E-2	0.0E+0
PM148M	0	2.1E-2	2.1E-2	3.6E-2	3.6E-2	4.1E-2	4.1E-2	3.8E-2	3.8E-2	3.4E-2	3.4E-2
SN116	0	2.1E-2	0.0E+0	2.0E-2	0.0E+0	1.8E-2	0.0E+0	1.5E-2	0.0E+0	1.3E-2	0.0E+0
LA140	0	1.8E-2	0.0E+0	1.8E-2	0.0E+0	1.8E-2	0.0E+0	1.8E-2	0.0E+0	1.8E-2	0.0E+0
I131	0	1.6E-2	0.0E+0	1.5E-2	0.0E+0	1.5E-2	0.0E+0	1.5E-2	0.0E+0	1.4E-2	0.0E+0
SE 77	0	1.5E-2	0.0E+0	1.5E-2	0.0E+0	1.5E-2	0.0E+0	1.5E-2	0.0E+0	1.5E-2	0.0E+0
GD154	0	1.4E-2	0.0E+0	1.3E-2	0.0E+0	9.9E-3	0.0E+0	8.0E-3	0.0E+0	6.6E-3	0.0E+0
XE128	0	1.3E-2	0.0E+0	1.3E-2	0.0E+0	1.1E-2	0.0E+0	9.6E-3	0.0E+0	8.0E-3	0.0E+0
DY161	0	1.1E-2	0.0E+0	1.1E-2	0.0E+0	1.0E-2	0.0E+0	9.2E-3	0.0E+0	7.5E-3	0.0E+0
AG110M	0	7.4E-3	0.0E+0	6.8E-3	0.0E+0	5.7E-3	0.0E+0	4.5E-3	0.0E+0	3.4E-3	0.0E+0
EU156	0	6.9E-3	0.0E+0	6.0E-3	0.0E+0	4.3E-3	0.0E+0	3.3E-3	0.0E+0	2.6E-3	0.0E+0
CD113	0	6.6E-3	0.0E+0	9.3E-3	0.0E+0	2.6E-2	0.0E+0	5.0E-2	0.0E+0	6.6E-2	0.0E+0
DY162	0	6.5E-3	0.0E+0	5.9E-3	0.0E+0	5.1E-3	0.0E+0	4.3E-3	0.0E+0	3.5E-3	0.0E+0
XE133	0	6.4E-3	0.0E+0	6.4E-3	0.0E+0	6.2E-3	0.0E+0	6.1E-3	0.0E+0	6.1E-3	0.0E+0
GE 76	0	6.3E-3	0.0E+0	6.3E-3	0.0E+0	6.2E-3	0.0E+0	6.3E-3	0.0E+0	6.5E-3	0.0E+0
TE126	0	6.2E-3	0.0E+0	5.9E-3	0.0E+0	6.1E-3	0.0E+0	4.8E-3	0.0E+0	4.1E-3	0.0E+0
GD155	0	6.1E-3	0.0E+0	8.3E-3	0.0E+0	2.0E-2	0.0E+0	2.9E-2	0.0E+0	3.2E-2	0.0E+0
KR 82	0	5.0E-3	0.0E+0	4.8E-3	0.0E+0	4.4E-3	0.0E+0	3.9E-3	0.0E+0	3.4E-3	0.0E+0
Y 90	0	4.7E-3	0.0E+0	2.5E-3	0.0E+0	4.8E-3	0.0E+0	2.5E-3	0.0E+0	2.7E-3	0.0E+0
GD157	0	3.9E-3	0.0E+0	5.2E-3	0.0E+0	1.3E-2	0.0E+0	2.7E-2	0.0E+0	4.3E-2	0.0E+0
SN115	0	3.8E-3	0.0E+0	3.7E-3	0.0E+0	3.5E-3	0.0E+0	3.2E-3	0.0E+0	2.9E-3	0.0E+0
DY163	0	3.2E-3	0.0E+0	3.0E-3	0.0E+0	2.6E-3	0.0E+0	2.2E-3	0.0E+0	1.8E-3	0.0E+0
SR 86	0	2.8E-3	0.0E+0	1.4E-3	0.0E+0	2.4E-3	0.0E+0	1.1E-3	0.0E+0	1.1E-3	0.0E+0
CD113M	0	2.6E-3	0.0E+0	2.5E-3	0.0E+0	2.4E-3	0.0E+0	2.1E-3	0.0E+0	1.9E-3	0.0E+0
EU152	0	2.3E-3	0.0E+0	2.7E-3	0.0E+0	3.0E-3	0.0E+0	2.7E-3	0.0E+0	2.4E-3	0.0E+0
EU151	0	2.3E-3	0.0E+0	3.4E-3	0.0E+0	7.3E-3	0.0E+0	9.1E-3	0.0E+0	9.8E-3	0.0E+0
RU 99	0	2.2E-3	2.2E-3	5.8E-4	5.8E-4	3.1E-3	0.0E+0	2.6E-3	2.6E-3	2.1E-3	0.0E+0
AS 75	0	2.2E-3	0.0E+0	2.2E-3	0.0E+0	2.1E-3	0.0E+0	2.1E-3	0.0E+0	2.1E-3	0.0E+0
TE125M	0	2.1E-3	0.0E+0	2.0E-3	0.0E+0	3.2E-3	0.0E+0	1.7E-3	0.0E+0	1.6E-3	0.0E+0
DY160	0	2.0E-3	0.0E+0	1.9E-3	0.0E+0	1.7E-3	0.0E+0	1.4E-3	0.0E+0	1.0E-3	0.0E+0
CS136	0	2.0E-3	0.0E+0	2.1E-3	0.0E+0	2.1E-3	0.0E+0	2.0E-3	0.0E+0	1.8E-3	0.0E+0
SN123	0	1.6E-3	0.0E+0	1.6E-3	0.0E+0	1.5E-3	0.0E+0	1.5E-3	0.0E+0	1.4E-3	0.0E+0
TE122	0	1.4E-3	0.0E+0	1.4E-3	0.0E+0	3.6E-3	0.0E+0	1.0E-3	0.0E+0	8.8E-4	0.0E+0

Table C.2: (continued)

Isotope	Time (years)										
	0	4-	4+	10-	10+	42-	42+	102-	102+	202-	202+
GD152	0	1.4E-3	0.0E+0	1.5E-3	0.0E+0	1.5E-3	0.0E+0	1.3E-3	0.0E+0	1.1E-3	0.0E+0
XE131M	0	1.2E-3	0.0E+0	1.2E-3	0.0E+0	1.2E-3	0.0E+0	1.2E-3	0.0E+0	1.1E-3	0.0E+0
TE124	0	1.0E-3	0.0E+0	1.0E-3	0.0E+0	2.8E-3	0.0E+0	7.9E-4	0.0E+0	6.8E-4	0.0E+0
H 3	0	9.7E-4	0.0E+0	9.6E-4	0.0E+0	9.3E-4	0.0E+0	9.0E-4	0.0E+0	8.8E-4	0.0E+0
SN121M	0	9.3E-4	0.0E+0	8.9E-4	0.0E+0	8.3E-4	0.0E+0	7.5E-4	0.0E+0	6.6E-4	0.0E+0
NB 95M	0	9.1E-4	0.0E+0	9.2E-4	0.0E+0	9.1E-4	0.0E+0	9.2E-4	0.0E+0	9.3E-4	0.0E+0
DY164	0	8.0E-4	0.0E+0	8.4E-4	0.0E+0	9.0E-4	0.0E+0	8.0E-4	0.0E+0	6.4E-4	0.0E+0
RH103M	0	7.0E-4	7.0E-4	6.8E-4	6.8E-4	6.5E-4	6.5E-4	6.0E-4	6.0E-4	5.6E-4	5.6E-4
HO165	0	7.0E-4	0.0E+0	5.7E-4	0.0E+0	3.7E-4	0.0E+0	2.7E-4	0.0E+0	2.0E-4	0.0E+0
AG111	0	6.4E-4	0.0E+0	6.1E-4	0.0E+0	5.5E-4	0.0E+0	4.7E-4	0.0E+0	3.9E-4	0.0E+0
TB160	0	5.6E-4	0.0E+0	5.3E-4	0.0E+0	4.6E-4	0.0E+0	3.6E-4	0.0E+0	2.7E-4	0.0E+0
PM148	0	4.5E-4	4.5E-4	7.0E-4	7.0E-4	6.9E-4	6.9E-4	6.2E-4	6.2E-4	5.3E-4	5.3E-4
PR144	0	3.4E-4	3.4E-4	4.1E-4	4.1E-4	4.1E-4	0.0E+0	4.1E-4	0.0E+0	4.1E-4	0.0E+0
BA135	0	3.3E-4	0.0E+0	3.1E-4	0.0E+0	2.2E-4	0.0E+0	1.7E-4	0.0E+0	1.2E-4	0.0E+0
LA138	0	3.1E-4	0.0E+0	3.0E-4	0.0E+0	1.4E-4	0.0E+0	2.8E-4	0.0E+0	1.4E-4	0.0E+0
GE 73	0	3.0E-4	0.0E+0	2.9E-4	0.0E+0	2.8E-4	0.0E+0	2.7E-4	0.0E+0	2.6E-4	0.0E+0
GE 74	0	2.4E-4	0.0E+0	2.3E-4	0.0E+0	2.2E-4	0.0E+0	2.2E-4	0.0E+0	2.1E-4	0.0E+0
CD115M	0	2.2E-4	0.0E+0	2.1E-4	0.0E+0	1.9E-4	0.0E+0	1.7E-4	0.0E+0	1.5E-4	0.0E+0
TE132	0	2.0E-4	0.0E+0	2.0E-4	0.0E+0	1.9E-4	0.0E+0	1.9E-4	0.0E+0	1.8E-4	0.0E+0
SB124	0	2.0E-4	0.0E+0	1.9E-4	0.0E+0	3.4E-4	0.0E+0	1.4E-4	0.0E+0	1.2E-4	0.0E+0
SN119M	0	1.8E-4	0.0E+0	1.8E-4	0.0E+0	1.7E-4	0.0E+0	1.5E-4	0.0E+0	1.3E-4	0.0E+0
SN125	0	1.4E-4	0.0E+0	1.4E-4	0.0E+0	1.3E-4	0.0E+0	1.2E-4	0.0E+0	1.1E-4	0.0E+0
IN113	0	1.3E-4	0.0E+0	1.3E-4	0.0E+0	1.2E-4	0.0E+0	1.1E-4	0.0E+0	9.4E-5	0.0E+0
TE127	0	1.2E-4	0.0E+0	1.1E-4	0.0E+0	1.1E-4	0.0E+0	9.7E-5	0.0E+0	8.8E-5	0.0E+0
GE 72	0	1.0E-4	0.0E+0	1.0E-4	0.0E+0	9.5E-5	0.0E+0	8.9E-5	0.0E+0	8.1E-5	0.0E+0
ER166	0	8.6E-5	0.0E+0	7.5E-5	0.0E+0	5.8E-5	0.0E+0	4.7E-5	0.0E+0	3.7E-5	0.0E+0
MO 99	0	5.0E-5	0.0E+0	5.0E-5	0.0E+0	4.9E-5	0.0E+0	4.8E-5	0.0E+0	4.8E-5	0.0E+0
NB 94	0	4.1E-5	0.0E+0	5.8E-5	0.0E+0	1.7E-4	0.0E+0	3.0E-4	0.0E+0	4.2E-4	0.0E+0
SB127	0	3.8E-5	0.0E+0	3.6E-5	0.0E+0	3.3E-5	0.0E+0	3.1E-5	0.0E+0	2.8E-5	0.0E+0
RB 86	0	3.5E-5	0.0E+0	3.5E-5	0.0E+0	3.1E-5	0.0E+0	2.9E-5	0.0E+0	2.7E-5	0.0E+0
SR 87	0	3.4E-5	0.0E+0	1.5E-5	0.0E+0	2.9E-5	0.0E+0	1.3E-5	0.0E+0	1.2E-5	0.0E+0
TE129	0	2.5E-5	0.0E+0	2.5E-5	0.0E+0	2.3E-5	0.0E+0	2.2E-5	0.0E+0	2.1E-5	0.0E+0
GD153	0	2.4E-5	0.0E+0	1.7E-5	0.0E+0	5.3E-6	0.0E+0	1.8E-6	0.0E+0	7.5E-7	0.0E+0
NB 93M	0	2.1E-5	0.0E+0	3.3E-5	0.0E+0	7.8E-5	0.0E+0	1.0E-4	0.0E+0	1.1E-4	0.0E+0
XE129	0	1.8E-5	0.0E+0	1.6E-5	0.0E+0	1.1E-5	0.0E+0	7.9E-6	0.0E+0	5.9E-6	0.0E+0
SE 76	0	1.6E-5	0.0E+0	1.6E-5	0.0E+0	1.4E-5	0.0E+0	1.3E-5	0.0E+0	1.2E-5	0.0E+0
SB126	0	1.6E-5	0.0E+0	1.5E-5	0.0E+0	1.5E-5	0.0E+0	1.2E-5	0.0E+0	1.0E-5	0.0E+0
RH102	0	1.5E-5	1.5E-5	2.2E-5	2.2E-5	5.1E-5	5.1E-5	7.7E-5	7.7E-5	2.0E-6	2.0E-6
TC 98	0	1.4E-5	0.0E+0	1.4E-5	0.0E+0	1.5E-5	0.0E+0	1.5E-5	0.0E+0	1.5E-5	0.0E+0
PM146	0	1.4E-5	1.4E-5	8.0E-5	8.0E-5	1.7E-4	1.7E-4	2.1E-4	2.1E-4	1.8E-4	1.8E-4
LI 6	0	1.2E-5	0.0E+0	1.7E-5	0.0E+0	3.9E-5	0.0E+0	6.4E-5	0.0E+0	8.4E-5	0.0E+0
SM146	0	1.2E-5	0.0E+0	4.9E-5	0.0E+0	6.7E-5	0.0E+0	7.6E-5	0.0E+0	7.6E-5	0.0E+0
TB161	0	1.1E-5	0.0E+0	1.0E-5	0.0E+0	9.0E-6	0.0E+0	7.6E-6	0.0E+0	6.1E-6	0.0E+0
I132	0	5.9E-6	0.0E+0	5.9E-6	0.0E+0	5.7E-6	0.0E+0	5.6E-6	0.0E+0	5.5E-6	0.0E+0
RH106	0	5.1E-6	5.1E-6	3.6E-6	3.6E-6	4.5E-6	4.5E-6	4.0E-6	4.0E-6	3.3E-6	3.3E-6
TE123	0	4.8E-6	0.0E+0	4.7E-6	0.0E+0	1.5E-5	0.0E+0	3.2E-6	0.0E+0	2.5E-6	0.0E+0
TC 99M	0	4.4E-6	0.0E+0	4.4E-6	0.0E+0	4.3E-6	0.0E+0	4.2E-6	0.0E+0	4.2E-6	0.0E+0
NB 93	0	3.6E-6	0.0E+0	8.3E-6	0.0E+0	9.8E-5	0.0E+0	3.4E-4	0.0E+0	7.6E-4	0.0E+0
BA137M	0	3.6E-6	0.0E+0	3.6E-6	0.0E+0	3.5E-6	0.0E+0	3.4E-6	0.0E+0	3.4E-6	0.0E+0
BE 10	0	2.4E-6	0.0E+0	2.4E-6	0.0E+0	2.4E-6	0.0E+0	2.3E-6	0.0E+0	2.3E-6	0.0E+0
PM149	0	2.4E-6	2.4E-6	2.6E-6	2.6E-6	2.3E-6	2.3E-6	2.2E-6	2.2E-6	2.0E-6	2.0E-6
PR144M	0	2.0E-6	2.0E-6	2.4E-6	2.4E-6	2.4E-6	0.0E+0	2.4E-6	0.0E+0	2.4E-6	0.0E+0

Table C.2: (continued)

Isotope	Time (years)										
	0	4-	4+	10-	10+	42-	42+	102-	102+	202-	202+
GA 71	0	1.7E-6	0.0E+0	1.7E-6	0.0E+0	1.5E-6	0.0E+0	1.4E-6	0.0E+0	1.2E-6	0.0E+0
SN114	0	1.6E-6	0.0E+0	1.6E-6	0.0E+0	1.4E-6	0.0E+0	1.1E-6	0.0E+0	8.9E-7	0.0E+0
SN117M	0	1.6E-6	0.0E+0	1.5E-6	0.0E+0	1.4E-6	0.0E+0	1.2E-6	0.0E+0	1.1E-6	0.0E+0
KR 80	0	1.3E-6	0.0E+0	1.2E-6	0.0E+0	1.1E-6	0.0E+0	9.9E-7	0.0E+0	8.4E-7	0.0E+0
HO166M	0	1.3E-6	0.0E+0	1.1E-6	0.0E+0	8.5E-7	0.0E+0	6.8E-7	0.0E+0	5.3E-7	0.0E+0
CD108	0	1.1E-6	0.0E+0	1.1E-6	0.0E+0	1.1E-6	0.0E+0	9.2E-7	0.0E+0	7.5E-7	0.0E+0
ER167	0	9.9E-7	0.0E+0	8.2E-7	0.0E+0	5.7E-7	0.0E+0	4.2E-7	0.0E+0	3.1E-7	0.0E+0
TE123M	0	9.8E-7	0.0E+0	9.4E-7	0.0E+0	2.6E-6	0.0E+0	6.1E-7	0.0E+0	4.7E-7	0.0E+0
AG108M	0	8.8E-7	0.0E+0	8.9E-7	0.0E+0	8.9E-7	0.0E+0	7.9E-7	0.0E+0	6.4E-7	0.0E+0
LI 7	0	7.6E-7	0.0E+0	1.1E-6	0.0E+0	4.1E-6	0.0E+0	9.6E-6	0.0E+0	1.9E-5	0.0E+0
SM145	0	6.9E-7	0.0E+0	2.4E-6	0.0E+0	3.0E-6	0.0E+0	3.2E-6	0.0E+0	3.4E-6	0.0E+0
AG107	0	6.2E-7	0.0E+0	5.9E-7	0.0E+0	5.7E-7	0.0E+0	5.0E-7	0.0E+0	4.1E-7	0.0E+0
C 14	0	4.9E-7	0.0E+0	4.9E-7	0.0E+0	4.8E-7	0.0E+0	4.7E-7	0.0E+0	4.7E-7	0.0E+0
ER168	0	4.6E-7	0.0E+0	3.5E-7	0.0E+0	2.0E-7	0.0E+0	1.4E-7	0.0E+0	9.5E-8	0.0E+0
XE133M	0	4.4E-7	0.0E+0	4.3E-7	0.0E+0	4.2E-7	0.0E+0	4.1E-7	0.0E+0	4.1E-7	0.0E+0
PM145	0	3.8E-7	3.8E-7	3.1E-6	3.1E-6	1.1E-5	1.1E-5	1.9E-5	1.9E-5	1.1E-5	1.1E-5
BE 9	0	3.7E-7	0.0E+0	3.7E-7	0.0E+0	3.6E-7	0.0E+0	3.5E-7	0.0E+0	3.5E-7	0.0E+0
YB172	0	2.9E-7	0.0E+0	4.3E-7	0.0E+0	1.5E-6	0.0E+0	3.3E-6	0.0E+0	5.8E-6	0.0E+0
BA132	0	2.9E-7	0.0E+0	3.0E-7	0.0E+0	3.0E-7	0.0E+0	3.0E-7	0.0E+0	2.9E-7	0.0E+0
SM153	0	2.6E-7	0.0E+0	2.4E-7	0.0E+0	1.9E-7	0.0E+0	1.6E-7	0.0E+0	1.4E-7	0.0E+0
IN114M	0	2.4E-7	0.0E+0	2.3E-7	0.0E+0	2.0E-7	0.0E+0	1.6E-7	0.0E+0	1.3E-7	0.0E+0
BR 79	0	2.3E-7	0.0E+0	2.3E-7	0.0E+0	2.2E-7	0.0E+0	2.2E-7	0.0E+0	2.2E-7	0.0E+0
CE139	0	2.0E-7	0.0E+0	1.9E-7	0.0E+0	1.7E-7	0.0E+0	1.5E-7	0.0E+0	1.5E-7	0.0E+0
ZN 70	0	1.8E-7	0.0E+0	1.7E-7	0.0E+0	1.6E-7	0.0E+0	1.4E-7	0.0E+0	1.2E-7	0.0E+0
YB171	0	1.2E-7	0.0E+0	1.8E-7	0.0E+0	6.4E-7	0.0E+0	1.4E-6	0.0E+0	2.5E-6	0.0E+0
ER170	0	8.5E-8	0.0E+0	8.0E-8	0.0E+0	7.5E-8	0.0E+0	6.5E-8	0.0E+0	5.3E-8	0.0E+0
TM171	0	7.8E-8	0.0E+0	7.3E-8	0.0E+0	6.7E-8	0.0E+0	5.8E-8	0.0E+0	4.8E-8	0.0E+0
TM169	0	7.5E-8	0.0E+0	7.1E-8	0.0E+0	6.5E-8	0.0E+0	5.7E-8	0.0E+0	4.6E-8	0.0E+0
XE129M	0	5.2E-8	0.0E+0	4.4E-8	0.0E+0	2.9E-8	0.0E+0	2.1E-8	0.0E+0	1.6E-8	0.0E+0
KR 81	0	4.1E-8	0.0E+0	3.8E-8	0.0E+0	3.4E-8	0.0E+0	2.9E-8	0.0E+0	2.5E-8	0.0E+0
SN121	0	4.0E-8	0.0E+0	3.9E-8	0.0E+0	3.6E-8	0.0E+0	3.3E-8	0.0E+0	2.9E-8	0.0E+0
CD115	0	3.4E-8	0.0E+0	3.3E-8	0.0E+0	3.1E-8	0.0E+0	2.8E-8	0.0E+0	2.5E-8	0.0E+0
RH105	0	2.7E-8	2.7E-8	2.6E-8	2.6E-8	2.4E-8	2.4E-8	2.2E-8	2.2E-8	1.9E-8	1.9E-8
CS132	0	1.7E-8	0.0E+0	1.8E-8	0.0E+0	1.8E-8	0.0E+0	1.8E-8	0.0E+0	1.7E-8	0.0E+0
CE143	0	1.6E-8	0.0E+0	1.6E-8	0.0E+0	1.6E-8	0.0E+0	1.6E-8	0.0E+0	1.6E-8	0.0E+0
ZN 66	0	1.5E-8	0.0E+0	1.4E-8	0.0E+0	1.3E-8	0.0E+0	1.2E-8	0.0E+0	1.1E-8	0.0E+0
NB 92	0	1.1E-8	0.0E+0	1.7E-8	0.0E+0	5.8E-8	0.0E+0	1.4E-7	0.0E+0	2.8E-7	0.0E+0
SB122	0	7.9E-9	0.0E+0	7.6E-9	0.0E+0	1.3E-8	0.0E+0	5.6E-9	0.0E+0	4.8E-9	0.0E+0
GA 69	0	6.8E-9	0.0E+0	6.4E-9	0.0E+0	6.0E-9	0.0E+0	5.4E-9	0.0E+0	4.6E-9	0.0E+0
EU150	0	3.3E-9	0.0E+0	4.9E-9	0.0E+0	9.1E-9	0.0E+0	1.1E-8	0.0E+0	1.1E-8	0.0E+0
IN115M	0	3.3E-9	0.0E+0	3.1E-9	0.0E+0	2.9E-9	0.0E+0	2.6E-9	0.0E+0	2.4E-9	0.0E+0
BA133	0	2.4E-9	0.0E+0	2.3E-9	0.0E+0	2.1E-9	0.0E+0	1.8E-9	0.0E+0	1.5E-9	0.0E+0
ZN 67	0	1.8E-9	0.0E+0	1.7E-9	0.0E+0	1.6E-9	0.0E+0	1.5E-9	0.0E+0	1.4E-9	0.0E+0
YB170	0	1.4E-9	0.0E+0	2.0E-9	0.0E+0	7.1E-9	0.0E+0	1.5E-8	0.0E+0	2.7E-8	0.0E+0
NB 91	0	9.2E-11	0.0E+0	1.4E-10	0.0E+0	4.6E-10	0.0E+0	9.9E-10	0.0E+0	1.7E-9	0.0E+0

REFERENCES

Ackerman, J.P., T.R. Johnson, L.S.H. Chow, E.L. Carls, W.H. Hannum, and J.J. Laidler. 1997. Treatment of Wastes in the IFR Fuel Cycle. Progress in Nuclear Energy 31: 141-154.

Ahlf, J., R. Conrad, M. Cundy, and H. Scheurer. 1990. Irradiation Experiments on High Temperature Gas-Cooled Reactor Fuels and Graphites at the High Flux Reactor Petten. Journal of Nuclear Materials 171: 31-36.

Aithal, S.M., T. Aldemir, and K. Vafai. 1994. Assessment of the Impact of Neutronic/ Thermal-Hydraulic Coupling on the Design and Performance of Nuclear Reactors for Space Propulsion. Nuclear Technology 106: 15-29.

Baetson, C. 1993. private communication. Department of Engineering Physics, McMaster University, Hamilton, Ontario, Canada.

Balakrishnan, A.R., and D.C.T. Pei. 1975. Fluid-Particle Heat Transfer in Gas Fluidized Beds. Canadian Journal of Chemical Engineering 53: 231-233.

Barin, I., O. Knacke, and O. Kubaschewski. 1977. Thermochemical Properties of Inorganic Substances Supplements. Berlin: Springer-Verlag.

Basalla, G. 1988. The Evolution of Technology. Cambridge, UK: Cambridge University Press.

Bayazitoğlu, Y., and M.N. Özişik. 1988. Elements of Heat Transfer. New York: McGraw Hill.

Benedict, R.P. 1980. Fundamentals of Pipe Flow. Toronto: Wiley and Sons.

Bisio, A., and R.L. Kabel. 1985. Scale up of Chemical Processes - Conversion from

Laboratory Scale Tests to Successful Commercial Size Design. New York: Wiley and Sons.

Bleeker, G., J. Moody, and M. Kesaree. 1993. The Space Nuclear Thermal Propulsion Program: Propulsion for the Twenty First Century. In Proceedings of the 28th Intersociety Energy Conversion Engineering Conference, Atlanta, GA, 8-13 August 1993, American Chemical Society. Warrendale, PA: SAE, 1.587-1.592.

Blix, H. 1997. Nuclear Energy in the 21st Century. Nuclear News 40: September 1997, 34-39.

Boothroyd, R.G. 1971. Flowing Gas-Solids Suspensions. London: Chapman and Hall.

Borges, V., and M.T. Vilhena. 1995. Dynamic Stability of a Fluidized-Bed Nuclear Reactor. Nuclear Technology 111: 251-258.

Botterill, J.S.M. 1975. Fluid-Bed Heat Transfer. London: Academic Press.

Burke, S.P., and W.B. Plummer. 1928. Gas Flow Through Packed Columns. Industrial Engineering Chemistry 20: 1196-1200.

Cameron, I.R. 1982. Nuclear Fission Reactors. New York: Plenum Press.

Caveny, L.H., ed. 1984. See Summerfield, M., ed. 1984.

Chase Jr., M.W., C.A. Davies, J.R. Downey Jr., D.J. Frurip, R.A. McDonald, and A.N. Syverud. 1985. JANAF Thermochemical Tables. 3rd ed. Journal of Physical and Chemical Reference Data 14: Supplement 1.

Cheremisinoff, N.P., and P.N. Cheremisinoff. 1984. Hydrodynamics of Gas-Solids Fluidization. Houston: Gulf Publishing.

Chow, L.S., J.K. Basco, J.P. Ackerman, and T.R. Johnson. 1993. Continuous Extraction of Molten Chloride Salts with Liquid Cadmium Alloys. In Proceedings of the International Conference on Future Nuclear Systems: Emerging Fuel Cycles and Waste Disposal Options, Seattle, 12-17 September 1993. American Nuclear Society, La Grange Park, IL: 1080-1085.

Clift, R., J.R. Grace, and M.E. Weber. 1978. Bubbles, Drops and Particles. San Diego: Academic Press.

Colakyan, M., and O. Levenspiel. 1934. Elutriation from Fluidized Beds. Powder Technology 38: 223-232.

Cowan, R. 1990. Nuclear Power Reactors: A Study in Technological Lock-in. Journal of Economic History Vol. L: 541-567.

Dalle Donne, M., and G. Sordon. 1990. Heat Transfer in Pebble Beds for Fusion Blankets. Fusion Technology 17: 597-635.

Davidson, J.F., R. Clift, and D. Harrison, eds. 1985. Fluidization. 2nd ed. London: Academic Press.

Dobranich, D., and M.S. El-Genk. 1991. Thermal Stress Analysis of the Multilayered Fuel Particles of a Particle-Bed Reactor. Nuclear Technology 94: 372-382.

Duderstadt, J.J., and L.J. Hamilton. 1976. Nuclear Reactor Analysis. New York: Wiley and Sons.

Ergun, S. 1952. Fluid Flow Through Packed Columns. Chemical Engineering Progress 48: 89-94.

Ergun, S., and A.A. Orning. 1949. Fluid Flow Through Randomly Packed Columns and Fluidized Beds. Industrial and Engineering Chemistry 14: 1179-1184.

Ertas, A., and J.C. Jones. 1996. The Engineering Design Process. 2nd ed. New York: Wiley and Sons.

Eskandari, M.R., and A. Ghasemi-zad. 1995. Dynamics of Intrinsically Safe Pellet Suspension Reactors. Department of Physics, Shiraz University, Shirz, Iran.

Felix, F. 1997. State of the Nuclear Economy. IEEE Spectrum November 1997: 29-32.

Figuerido, J.L., et. al. 1990. Carbon Fibre Filaments and Composites. Boston: Kluwer Academic Publishers.

Geldart, D. 1986. Gas Fluidization Technology. Chichester, GB: Wiley and Sons.

Glasstone, S., and A. Sesonske. 1981. Nuclear Reactor Engineering. 3rd ed. Malabar, FL: Krieger Publishing.

Goltsev, A.O., N.E. Kuharkin, I.S. Mosevitsky, N.N. Ponomarev-Stepnoy, S.V. Popov, Y.N. Udyansky, and V.F. Tsybulsky. 1994. Concept of a Safe Tank-Type Water-Water Reactor with HTGR Micro-Particle Fuel Blocks. Annals of Nuclear Energy 21: 513-518.

Gupta, S.N., R.B. Chaube, and S.N. Upadhyay. 1974. Fluid-Particle Heat Transfer in Fixed and Fluidized Beds. Chemical Engineering Science 29: 839-843.

Hannerz, K. (date unknown). ASEA-Atom, Sweden.

Harms, A.A., ed. 1993. On the Technology of Benign Fission Reactor Systems. Department of Engineering Physics, McMaster University, Hamilton, Ontario, Canada.

Harms, A.A. 1996. Civilian Nuclear Energy: Towards the 21st Century. Department of Engineering Physics, McMaster University, Hamilton, Ontario, Canada. Presented at the 4th Annual Scientific Symposium of the Interfaculty Reactor Institute, Delft University of Technology, Delft, The Netherlands, 7 November 1996.

Harms, A.A., and W.R. Fundamenski. 1993. Fail-Safe Decay-Heat Removal in a Pellet Suspension Fission Reactor. In Proceedings of the 7th International Conference on Emerging Nuclear Energy Systems, Chiba, Japan, 20-24 September 1993. Singapore: World Scientific Publishing, 377-380.

Harms, A.A., and D.R. Kingdon. 1993. Passively Fail-Safe Fission Reactor Based on Pellet Suspension Technology. In Proceedings of the International Joint Power Generation Conference, Kansas City, MO, 17-21 October 1993, J.M. Yedidia and J. Kunze, ed. Status of Advanced Reactors and Developments in Advanced

Reactor Instrumentation and Control, ASME Nuclear Engineering Division, NE Vol. 12. New York: ASME.

Harms, A.A., and D.R. Kingdon. 1994. A Gravity-Removable Suspended Fuel-Core for Passive Coolability of a Reactor. American Nuclear Society Transactions 71: 329-330.

Hejzlar, P., N.E. Todreas, and M.J. Driscoll. 1996. Passive Pressure Tube Light Water Reactors. Nuclear Technology 113: 123-133.

Henry, A.F. 1975. Nuclear Reactor Analysis. Cambridge, MA: MIT Press.

Holman, R.R., and B.L. Pierce. 1986. Development of NERVA Reactor for Space Nuclear Propulsion. In Proceedings of the 22nd Joint Propulsion Conference, Huntsville, AL, 16-18 June, 1986, AIAA. New York: AIAA paper 86-1582.

IAEA. See International Atomic Energy Agency.

International Atomic Energy Agency. 1991. Safety Related Terms For Advanced Nuclear Plants. Vienna: International Atomic Energy Agency - TECDOC-626.

International Atomic Energy Agency. 1993. Objectives For the Development of Advanced Nuclear Plants. Vienna: International Atomic Energy Agency - TECDOC-682.

Juhn, P.E., and J. Kupitz. 1996. Nuclear Power Beyond Chernobyl: A Changing International Perspective. IAEA Bulletin n.s. 1: 2-9.

Karassik, I.J., ed. 1986. Pump Handbook. Toronto: McGraw-Hill.

Khotylev, V.A., J.E. Hoogenboom, D.R. Kingdon, and A.A. Harms. 1997. Study of Nuclide Field Behaviour in Reactors with Continuously Changing Core Parameters. In Proceedings of the 20th CNS Nuclear Simulation Symposium, Niagara-on-the-Lake, Canada, 7-9 September 1997.

Khotylev, V.A., D.R. Kingdon, and A.A. Harms. 1997. A Viable Alternative to Permanent Nuclear Waste Disposal. McMaster University, Hamilton, Ontario,

Canada.

Khotylev, V.A., D.R. Kingdon, A.A. Harms, and J.E. Hoogenboom. 1997a. On-Site Spent Fuel Management Based on Electrorefining. In Proceedings of the NATO Advanced Research Workshop on Safety Issues Associated with Plutonium Involvement in Nuclear Fuel Cycles, Volga 97, Volga, Russia, 2-6 September, 1997.

Khotylev, V.A., D.R. Kingdon, A.A. Harms, and J.E. Hoogenboom. 1997b. On-Site Spent Fuel Management. In press: Proceedings of 9th International Conference on Emerging Nuclear Energy Systems, Tel Aviv, Israel, June 28 - July 2, 1998.

Kingdon, D.R. 1994. Particle Suspension in a Constriction-Expansion Bound Vertical Tube via Fluidization and Related Concepts. Department of Engineering Physics, McMaster University, Hamilton, Ontario, Canada.

Kingdon, D.R., and A.A. Harms. 1996. Pellet Power Ratio in a Pellet-Suspension Fission Core. Nuclear Technology 116: 1-8.

Kingdon, D.R., A.N. Kornilovsky, and A.A. Harms. 1996. Fuel Energetics and Pellet Dynamics of Pellet Suspension Reactors. In Proceedings of 8th International Conference on Emerging Nuclear Energy Systems, Obninsk, Russia, 24-28 June, 1996, Vol. 1, Institute of Physics and Power Engineering. Obninsk, Russia, 213-220.

Kirchsteiger, C., B. Reusens, and H. Böck. 1995. Some Probabilistic Considerations on Future Serious Power Reactor Accidents. Nuclear Energy 34: 271-275.

Kloosterman, J.L., and J.E. Hoogenboom. 1995. New Data Libraries for Transmutation Studies. In Proceedings of the International Conference on Emerging Nuclear Fuel Cycle Systems, Versailles, France, 11- 14 September, 1995.

Kornilovsky, A.N. 1996. private communication. Department of Engineering Physics,

McMaster University, Hamilton, Ontario, Canada.

Kornilovsky, A.N., and A.A. Harms. 1996. Pellet Dynamics in a Gas-Filled Vertical Column. International Journal of Multiphase Flow 23: 183-192.

Kornilovsky, A.N., D.R. Kingdon, and A.A. Harms. 1996. On the Dynamics of Fuel Pellets in Suspension. Annals of Nuclear Energy 23: 171-182.

Kosolapova, T.Y. 1971. Carbides - Properties, Production, and Applications. New York: Plenum Press.

Kovan, D. 1992. 2nd December 1942 - The Birth of the First Reactor. Nuclear Engineering International 37: November, 42-46.

Koyama, T., R. Fujita, M. Iizuka, M. Fujie, Y. Sumida, and M. Tokiwai. 1993. Pyrometallurgical Reprocessing of Metallic Fuel of Fast Breeder Reactor - Development of New Electrorefiner with Ceramic Partition. In Proceedings of the International Conference on Future Nuclear Systems: Emerging Fuel Cycles and Waste Disposal Options, Seattle, 12-17 September 1993, American Nuclear Society. La Grange Park, IL: 197-200.

Koyama, T., M. Iizuka, Y. Shoji, R. Fujita, H. Tanaka, T. Kobayashi, and M. Tokiwai. 1997. An Experimental Study of Molten Salt Electrorefining of Uranium Using Solid Iron Cathode and Liquid Cadmium Cathode for Development of Pyrometallurgical Reprocessing. Journal of Nuclear Science and Technology 34: 384-393.

Kreyger, P.J., Th. van der Plas, B.L.A. van der Schee, J.J. Went, and J.J. van Zolingen. 1958. Development of a 250 kW Aqueous Homogeneous Single Region Suspension Reactor. In Proceedings of the 2nd International Conference on the Peaceful Uses of Atomic Energy, Geneva, 1-13 September, 1958, Vol 9, United Nations Publication 58.IX.2. Great Britain, 427.

Kugeler, K., and P.-W. Phlippen. 1996. The Potential of the Self-Acting Safety

Features of High Temperature Reactors. Kerntecknik 61: 239-244.

Kunii, D., and O. Levenspiel. 1969. Fluidization Engineering. New York: Wiley and Sons.

Laidler, J.J., J.E. Battles, W.E. Miller, J.P. Ackerman, and E.L. Carls. 1997. Development of Pyroprocessing Technology. Progress in Nuclear Energy 31: 131-140.

Leva, M. 1959. Fluidization. New York: McGraw-Hill.

Lide, D.R., ed. 1995. CRC Handbook of Chemistry and Physics. 76th ed. Boca Ratan, FL: CRC Press.

Lidsky, L.M. 1984. The Reactor of the Future. Technology Review February/March 1984: 52-56.

Liem, P.H. 1996. Design Procedures for Small Pebble-Bed High Temperature Reactors. Annals of Nuclear Energy 23: 207-215.

Ludewig, H., J.R. Powell, M. Todosow, G. Maise, R. Barletta, and G. Schweitzer. 1996. Design of Particle Bed Reactors for the Space Nuclear Thermal Propulsion Program. Progress in Nuclear Energy 30: 1-65.

Lundberg, L.B., and R.R. Hobbins. 1992. Nuclear Fuels for Very High Temperature Applications. In Proceedings of the 27th Intersociety Energy Conversion Engineering Conference, San Diego, 3-7 August, 1992, Society of Automotive Engineers. Piscataway, NJ: IEEE, 1.363-1.369.

Malloy, J., and R. Rochow. 1993. Approach to Hybrid Operation Using Particle Bed Reactor Technology. In Proceedings of the 28th Intersociety Energy Conversion Engineering Conference, Atlanta, 8-13 August, 1993, American Chemical Society. Warrendale, PA: SAE, 1.631-1.635.

Matsumoto, S., S. Ohnishi, and S. Maeda. 1978. Heat Transfer to Vertical Gas-Solid Suspension Flows. Journal of Chemical Engineering of Japan 11: 89-95.

McFarlane, H.F., and M.J. Lineberry. 1997. The IFR Fuel Cycle Demonstration. Progress in Nuclear Energy 31: 155-173.

McPheeters, C.C., R.D. Pierce, and T.P. Mulcahey. 1997. Application of the Pyrochemical Process to Recycle of Actinides from LWR Spent Fuel. Progress in Nuclear Energy 31: 175-186.

Mizuno, T., T. Ito, and K. Ohta. 1990. The Inherently-Safe Fluidized-Bed Boiling Water Reactor Concept. Annals of Nuclear Energy 17: 487-492.

Nishimura, T., T. Koyama, M. Iizuka, and H. Tanaka. 1998. Development of an Environmentally Benign Reprocessing Technology - Pyrometallurgical Reprocessing Technology. Progress in Nuclear Energy 32: 381-387.

Nuclear News 35: September 1992, 65-90.

Nuclear News 41: March 1998, 54.

Pandey, D.K., S.N. Upadhyay, S.N. Gupta, and P. Mishra. 1978. Particle - Fluid Heat Transfer in Fixed and Fluidized Beds. Journal of Scientific and Industrial Research 37: 224-249.

Pell, M. 1990. Gas Fluidization. Amsterdam: Elsevier Scientific Publishers.

Pemberton, S.T., and J.F. Davidson. 1986. Elutriation from Fluidized Beds -- II. Disengagement of Particles From Gas In The Freeboard. Chemical Engineering Science 41: 253-262.

Perrow, C. 1984. Normal Accidents - Livir.; With High-Risk Technologies. New York: Basic Books.

Poulain, M. 1996. private communication. Centre D'Etude des Materiaux Avances, Universite de Rennes, Rennes, France.

Powell, J.R., H. Takahashi, and F.L. Horn. 1986. High Flux Research Reactors Based on Particulate Fuel. Nuclear Instruments and Methods in Physics Research A249: 66-76.

Reynolds, 0. 1900. Papers on Mechanical and Physical Subjects, Vol. 2. Cambridge, UK: Cambridge University Press.

Rothwell, E. 1962. A Precise Determination of the Viscosity of Liquid Tin, Lead, Bismuth, and Aluminum by an Absolute Method. Journal of the Institute of Metals 90: 389-394.

RSICC Computer Code Collection: SCALE 4.3. 1995. Modular Code System for Performing Standardized Computer Analysis for Licensing Evaluation for Workstations and Personal Computers. CCC-545, Martin Marietta Systems, Inc., ORNL.

Sagan, S.D. 1993. The Limits of Safety - Organizations, Accidents, and Nuclear Weapons. Princeton, NJ: Princeton University Press.

Sakamura, Y., T. Hijikata, K. Kinoshita, T. Inoue, T.S. Storvick, C.L. Krueger, L.F. Grantham, S.P. Fusselman, D.L. Grimmett, and J.J. Roy. 1998. Separation of Actinides from Rare Earth Elements by Electrorefining in LiCl-KCl Eutectic Salt. Journal of Nuclear Science and Technology 35: 49-59.

Samsonov, G.V., ed. 1974. Refractory Carbides. New York: Consultants Bureau.

Sawa, K., K. Minato, T. Tobita, and K. Fukuda. 1997. An Investigation of Cesium Release from Coated Particle Fuel of the High-Temperature Gas-Cooled Reactor. Nuclear Technology 118: 123-131.

Sefidvash, F. 1985. A Fluidized-Bed Nuclear Reactor Concept. Nuclear Technology 71: 527-534.

Sefidvash, F. 1996. Status of the Small Modular Fluidized Bed Light Water Nuclear Reactor Concept. Nuclear Engineering and Design 167: 203-214.

Seifritz, W. 1992. A Passively Safe 10 MW(th) Fluidized-Bed Heating Reactor Module. In Proceedings of the 1992 Annual Meeting on Nuclear Technology, Karlsruhe, Germany, 5-7 May, 1992.

Seifritz, W., and F. Sefidvash. 1997. Non-Linear Noise Theory for the Fluidized Bed Light Water Reactor. Kerntechnik 62: 178-183.

Sengers, J.V., and J.T.R. Watson. 1986. Improved International Formulations for the Viscosity and Thermal Conductivity of Water Substance. Journal of Physical and Chemical Reference Data 15: 1291-1314.

Starr, C. 1997. The Future of Nuclear Power. Nuclear News 40: March, 58-60.

Steiner, D., and A.P. Fraas. 1972. Preliminary Observations on the Radiological Implication of Fusion Plant. Nuclear Safety 13: 353.

Storms, E.K. 1967. Refractory Materials Volume 2: The Refractory Carbides. New York: Academic Press.

Summerfield, M., ed. 1984. Progress in Astronautics and Aeronautics. Vol. 89, Orbit Raising and Manoeuvring Propulsion: Research Status and Needs, L.H. Caveny, ed. New York: American Institute of Aeronautics and Astronautics.

Sweet, W. 1997. Advanced Reactor Development Rebounding. IEEE Spectrum November 1997: 41-48.

Taube, M., M. Lanfranchi, T. von Weissenfluh, J. Ligou, G. Yadigaroglu, and P. Taube. 1986. The Inherently-Safe Power Reactor Dyonisos (Dynamic Nuclear Inherently-Safe Reactor Operating With Spheres). Annals of Nuclear Energy 13: 641-648.

Taylor, J.J. 1989. Improved and Safer Nuclear Power. Science 244: 318-325.

Tomlinson, R.H. 1997. private communication. Department of Chemistry, McMaster University, Hamilton, Ontario, Canada.

Tsederberg, N.V., V.N. Popov, and N.A. Morozova. 1971. Thermodynamic and Thermophysical Properties of Helium. Jerusalem: Keter Press.

United Nations. 1954. Proceedings of the [1st] International Conference of the Peaceful Uses of Atomic Energy, Geneva, 8-20 August, 1955, United Nations

Publication 1956.IX.1. New York.

United Nations. 1958. Proceedings of the 2nd International Conference on the Peaceful Uses of Atomic Energy, Geneva, 1-13 September, 1958, United Nations Publication 58.IX.2. Great Britain.

van Dam, H. 1996a. Delayed Neutron Effectiveness in a Fluidized Bed Fission Reactor. Annals of Nuclear Energy 23: 41-46.

van Dam, H. 1996b. Dynamics of Passive Reactor Shutdown. Progress in Nuclear Energy 30: 255-264.

van Dam, H., T.H.J.J. van der Hagen, J.E. Hoogenboom, V.A. Khotylev, P.E.A. Rots, R.F. Muddle, and H.E.A. van den Akker. 1996. Neutronics and Thermal Aspects of a Fluidized Bed Fission Reactor. In Proceedings of the 8th International Conference on Emerging Nuclear Energy Systems, Obninsk, Russia, 24-28 June, 1996, Vol. 1, Institute of Physics and Power Engineering. Obninsk, Russia, 196-204.

Vrillon, B., F. Carre, and E. Proust. 1988. Space Nuclear Power Studies in France -- A New Concept of a Particle Bed Reactor. In Proceedings of the 23rd Intersociety Energy Conversion Engineering Conference, Denver, CO, July 31 - August 5, 1988, Vol. 3, American Society of Mechanical Engineers. Piscataway, NJ: IEEE, 249-254.

Warring, R.H. 1984a. Pumping Manual. Houston: Gulf Publishing.

Warring, R.H. 1984b. Pumps: Selection, Systems and Applications. Houston: Gulf Publishing.

Watanabe, Y., and J. Appelbaum. 1991. Magnetically Stabilized Fluidized Bed Nuclear Fission Reactor. Fusion Technology 20: 615-619.

Went, J.J., and H. de Bruyn. 1954. Fluidized- and Liquid-Fuel Reactors with Uranium Oxides. Nucleonics 12: September 1954, 16-19.

Went, J.J., and M.E.A. Hermans. 1972. The KEMA Suspension Test Reactor. In Proceedings of the 4th International Conference on the Peaceful Uses of Atomic Energy, Geneva, 6-16 September, 1971, Vol. 9, IAEA. Austria, 271.

Whitaker, S. 1981. Introduction to Fluid Mechanics. Malabar, FL: Krieger Publishing Co.

Whitlock, J. 1993. Reactor Neutronic Analysis. See A.A. Harms, ed. 1993.

Wilhelm, R.H., and M. Kwauk. 1948. Fluidization of Solid Particles. Chemical Engineering Progress 44: 201-218.

Zabrodski, S.S. 1966. Hydrodynamics and Heat Transfer in Fluidized Beds, Cambridge, MA: M.I.T. Press.

Zenz, F.A. 1977. How Flow Phenomena Affect Design of Fluidized Beds. Chemical Engineering 84: 19 December, 81-91.

Zenz, F.A. 1983. Particulate solids: The Third Fluid Phase in Chemical Engineering. Chemical Engineering 90: 28 November, 61-67.

Zenz, F.A., and N.A. Weil. 1958. A Theoretical-Empirical Approach to the Mechanism of Particle Entrainment from Fluidized Beds. AIChE Journal 4: 472-479.